Characterisation of Microparticles and Nitro-Oxidative Stress in Cardiometabolic Disease

by

Gareth Rhys Willis
(BSc Hons.)

A thesis submitted for the degree of

DOCTOR OF PHILOSOPHY

Institute of Molecular and Experimental Medicine

Wales Heart Research Institute

Cardiff University – School of Medicine

2015

Declaration

This work has not previously been accepted in substance for any degree and is not concurrently submitted in candidature for any degree.

Signed …… (candidate) Date……

Statement 1

This thesis is being submitted in partial fulfilment of the requirements for the degree of PhD.

Signed …… (candidate) Date ……

Statement 2

This thesis is the result of my own independent work/investigation, except where Otherwise stated. Other sources are acknowledged by explicit references.

Signed …… (candidate) Date ……

Statement 3

I hereby give consent for my thesis, if accepted, to be available for photocopying and for interlibrary loan, and for the title and summary to be made available to outside organisations.

Signed …… (candidate) Date ……

To Sarah,

Thank you for supporting me,

&

To my family,

For always believing in me.

Acknowledgements

First and foremost, I would like to thank both of my supervisors, Dr Philip James and Dr Aled Rees, for all their support throughout my PhD.

A special thank you to my colleagues and friends: Dr Jessica Dada, Dr Ewelina Sagan, Dr Phillip Freeman, Dr Lawrence Thornhill, Ms Katie Connolly, Dr Fairoz Abdul, Ms Jessica Davis, Ms Jessica Williams, Mr Nick Burnley-Hall and Ms Libby Ellins.

I would also like to thank Dr Aled Clayton, Dr Irina Gushina, Prof Maurice Hallett, Dr Maneesh Udiawar, Dr Thomas Davies and Prof Keith Morris for their advice and support.

My PhD was funded by grants from The Wales Heart Research Institute and Mrs John Nixon Scholarship.

Contents

Abstract

Polycystic ovary syndrome (PCOS) is a common condition characterised by hyperandrogenism, oligo/anovulation and defects in insulin secretion and sensitivity. PCOS patients also have an increased prevalence of hypertension, dyslipidaemia and endothelial dysfunction, a state associated with decreased nitric oxide bioavailability and increased oxidative stress. Using women with PCOS as a model of predisposition to cardiovascular disease (CVD), the aim of this thesis was to provide a clearer understanding of mechanisms that may predispose individuals to endothelial dysfunction, and ultimately CVD.

PCOS patients were compared to healthy controls in an observational study, which involved a comprehensive assessment of biochemical nitro-oxidative stress indices and a detailed characterisation of circulating microparticles (MPs). There was little evidence to suggest that women with PCOS have an increased oxidative stress compared to age/BMI-matched controls. However, PCOS patients did display elevated levels of annexin V positive MPs that were predominantly derived from platelets.

In vitro studies investigated the effect of several metabolic stressors akin to those found in PCOS on endothelial-derived MP characteristics and function. Human endothelial (HECV) cells were exposed to oxidative, hypoxic, hyperandrogenic and metabolic stressors. Each metabolic stressor affected MP generation uniquely, suggesting MP characteristics and function reflect parental cell conditions.

In order to determine whether circulating MP levels could be modulated in a clinical cohort, the effect of apheresis on circulating MP levels was investigated in patients with established CVD (familial hypercholesterolaemia). Apheresis decreased circulating levels of MPs and was associated with a decreased thrombin generation capacity in these patients.

The data in this thesis thus provide evidence that young women with PCOS have an elevated concentration of annexin V positive MPs, even though there is little biochemical evidence for nitro-oxidative stress. Further studies are needed to assess the effect of this increase in circulating MPs on cardiovascular clinical end-points. *In vitro* experiments showed that the cellular stress condition is reflected in the MP characteristics, whereby each pathological stressor resulted in a unique MP phenotype. Furthermore, in patients with established CVD, apheresis reduced circulating levels of MPs.

In conclusion, an elevated annexin V positive MP population may represent a novel mechanism by which cardiovascular risk is increased in patients with PCOS. These findings could have future implications for use as biomarkers, in diagnosis and therapeutics.

Abbreviations

AA	Arachidonic acid
AAPH	2,2' Azobia-2-methyl-propanimidamide
ABCA1	Adenosine triphosphate-binding cassette transporter
ACE	Angiotensin converting enzyme
ADP	Adenosine diphosphate
AE-PCOS	Androgen Excess - Polycystic Ovary Syndrome
Alix	ALG-2-interacting protein X
Ang-II	Angiotensin II
APC	Allophycocyanin
AT1	Angiotensin type 1 receptor
AT2	Angiotensin type 2 receptor
ATP	Adenosine triphosphate
AUC	Area-Under-Curve
BH_4	Tetrahydrobiopterin
BMI	Body mass index
BSA	Bovine serum albumin
Ca^{2+}	Calcium
CAD	Coronary artery disease
cDNA	Complementary deoxyribonucleic acid
CFSE	Carboxyfluorescein diacetate succinimidyl
cGMP	Cyclic guanosine 3’-5’monophosphate
CHD	Coronary heart disease
COX	Cyclooxygenase
Cr	Sodium 51Cr-chromate
CT	Computerised tomography
CVD	Cardiovascular disease
Del-1	Developmental endothelial locus-1
DETC	Diethyldithiocarbamate
DMEM	Dulbecco's modified eagle's medium
DTT	Dithiothreitol
E-selectin	Endothelial selectin
EC	Endothelial cell
EPC	Endothelial protein C
EPCR	Endothelial protein C receptor
EDHF	Endothelial derived hyperpolarising factor
EDTA	Ethylenediaminetetraacetic acid
EGTA	Ethylene glycol tetraacetic acid
ELISA	Enzyme-linked immunosorbent assay
EM	Electron microscopy
EMP	Endothelial derived-microparticle
eNOS (NOS-3)	Endothelial nitric oxide synthase
EPR	Electron magnetic resonance spectroscopy
ERK-1	Extracellular-signal-regulated kinase-1

ESCRT	Endosomal sorting complexes required for transport
ET_1	Endothelin-1
FC	Fold change
Fe^{2+}	Reduced iron (ferrous)
Fe^{3+}	Oxidised iron (ferric)
FFA	Free fatty acid
FH	Familial hypercholesterolaemia
FITC	Fluorescein isothiocyanate
FMD	Flow mediated dilatation
FMO	Fluorescence minus one
FLNA	Filamin A
fMLP	Formyl-Methionyl-Leucyl-Phenylalanine
FOX	Ferrous oxidation-xylenol orange
FSC	Forward scatter channel
FSHB	Follicle stimulating hormone β-subunit
FSHR	Follicle stimulating hormone receptor
g	Gravity
G	Gauss
GLUT4	Glucose transporter type 4
GTP	Guanosine-5'-triphosphate
H^+	Hydrogen
H_2O	Water
H_2O_2	Hydrogen peroxide
H6PD	Hexose-6-phosphate dehydrogenase
HCL	Hydrochloric acid
HDL	High-density lipoprotein
HECV	Human endothelial vascular cell
HMDS	Hexamethyldislazane
HOMA-IR	Homeostatic model assessment - Insulin resistance
Hr	Hour
HRS	Hepatocyte growth factor-regulated tyrosine kinase substrate
hsCRP	High sensitivity C-reactive protein
HUVEC	Human umbilical vascular endothelial cell
hv	Photon
I_3^-	Tri-iodide
ICAM-1	Intercellular Adhesion Molecule 1
IGF-1	Insulin-like growth factor-1
IGFBP3	Insulin-like growth factor binding protein
IGT	Impaired glucose tolerance
IHD	Ischaemic heart disease
IL	Interleukin
ILV	Intraluminal vesicles
IMT	Intima media thickness
iNOS (NOS-2)	Inducible nitric oxide synthase
IR	Insulin resistance
IRS	Insulin receptor substrate

ISEV	International society for Extracellular Vesicles
KLF2	Krüppel-like Factor 2
L-NAME	L-Nitro-Arginine Methyl Ester
L-NMMA	NG-monomethyl-L-arginine
LBF	Leg blood flow
LDL	Low-density lipoprotein
LH	Luteinizing hormone
LMP	Leukocyte derived microparticles
LPS	Lipopolysaccharides
m	Metre
M	Molar
MAPK	Mitogen-activated protein kinase
MDA	Malondialdehyde
MFI	Median fluorescence intensity
MHC	Major histocompatibility complex
MI	Myocardial infarction
Min	Minute
miR	Micro-ribonucleic acid
mm	Millimetre
MP	Microparticle
mRNA	Messenger-ribonucleic acid
MUFA	Monounsaturated fatty acids
MV	Microvesicles
mV	Millivolts
MVB	Multivesicular bodies
n/a	Not applicable
Na^+	Sodium
NaCL	Sodium chloride
NaOH	Sodium hydroxide
NADPH	Nicotinamide adenine dinucleotide phosphate
$NaNO_2$	Sodium nitrite
$NaNO_3$	Sodium nitrate
NF-κB	Nuclear factor- κB
NIH	National institutes of health
nm	Nanometre
nM	Nanomolar
nNOS (NOS-1)	Neuronal nitric oxide synthase
NO	Nitric oxide
NO2	Nitrogen dioxide
NO_2^-	Nitrite
NO_3^-	Nitrate
NOA	Nitric oxide analyser
NOS	Nitric oxide synthase
NO_x	Nitric oxide metabolites
NOX	Nicotinamide adenine dinucleotide phosphate oxidase
NTA	Nanoparticle tracking analysis

O_2	Oxygen
O_3	Ozone
OGTT	Oral glucose tolerance test
OH^-	Hydroxyl radical
$OONO^-$	Peroxynitrite
ORACfl	Oxygen radical absorbance capacity - fluorescence
PAD	Peripheral artery disease
PAF	Platelet activating factor
PAGE	Polyacrylamide gel electrophoresis
PAI-1	Plasminogen activator inhibitor-1
PBS	Phosphate buffer saline
PC	Phosphatidylcholine
PCOS	Polycystic ovary syndrome
PCR	Polymerase chain reaction
PE	Phycoerythrin
PE-cy5	Phycoerythrin - Integrin α-chain B2
PECAM-1	Platelet endothelial cell adhesion molecule-1
pg	Picogram
PGI_2	Prostacyclin
PI3K	Phosphoinositide 3-kinase
PKB	Protein kinase B
PMNL	Polymorphonuclear leukocyte
pM	Picomolar
PMP	Platelet derived microparticle
PPARGCA1	Peroxisome proliferator-activated receptor-γ co-activator 1
PPARγ	Peroxisome proliferator-activated receptor-γ
PPP	Platelet poor plasma
PS	Phosphatidylserine
PUFA	Polyunsaturated fatty acid
PWV	Pulse wave velocity
qPCR	Quantitative polymerase chain reaction
RBC	Red blood cell
RLU	Relative light units
RNA	Ribonucleic acid
ROCK	Rho-associated protein kinase
ROOH	Hydroperoxides
ROS	Reactive oxygen species
RPM	Revolutions per minute
RSNO	S-nitrosothiols
RT	Room temperature
SD	Standard deviation
SDS	Sodium dodecyl sulphate
SEM	Standard error of mean
SFM	Serum free medium
sGC	Soluble guanylate cyclase
SHBG	Sex hormone-binding globulin

sICAM-1	Soluble intercellular Adhesion Molecule 1
siRNA	Silencing ribonucleic acid
SMC	Smooth muscle cell
SNARE	Soluble NSF Attachment Protein Receptor
SOD	Superoxide dismutase
SR-B1	Scavenger receptor B1
SSC	Side scatter channel
SSH	Sonic hedgehog
sVCAM-1	Soluble vascular cell adhesion protein 1
T½	Half-life
T2DM	Type 2 diabetes mellitus
TAC	Total antioxidant capacity
TBARS	Thiobarbituric acid reactive substances
TBS	Tris-buffered saline
TBST	Tris-buffered saline + Tween-20
TEM	Transmission electron microscopy
TEMED	Tetramethylethylenediamine
TEMPO	(2,2,6,6-tetramethylpiperidin-1-yl)oxidanyl
TF	Tissue factor
TG	Triglyceride
TGFβ1	Transforming growth factor β1
TM	Thrombomodulin
TNFα	Tumour necrosis factor α
TRAP	Thrombin receptor activating peptide
TRPS	Tunable resistive pulse sensing
TSG 101	Tumour susceptibility gene 101
uPA	Urokinase plasminogen
V	Volts
v/v	Volume/Volume
VCAM-1	Vascular cell adhesion protein 1
VCL_3	Vanadium chloride
VE	Vascular endothelial
VEGF	Vascular endothelial growth factor receptor
Vps	Vacuole protein sorting
VS.	Versus
VSMC	Vascular smooth muscle cell
WHO	World Health Organisation
w/v	Weight in volume
XO	Xanthine oxidase
Yrs	Years
$^{\bullet}O_2^-$	Superoxide anion
°C	Degrees Celsius
µl	Microlitre
µm	Micrometre
µM	Micromolar

Publications

Gareth R. Willis, Maneesh Udiawar, William D. Evans, Helen L. Blundell, Philip E. James* and D. Aled Rees*. Detailed characterisation of circulatory nitric oxide and free radical indices – is there evidence for abnormal cardiovascular homeostasis in young women with polycystic ovary syndrome? 2014. BJOG: International Journal of Obstetrics and Gynaecology. doi: 10.1111/1471-0528.12834.

Gareth R. Willis, Katherine Connolly, Kristin Ladell, Thomas S. Davies, Irina A. Guschina, Dipak Ramji, Kelly Miners, David A. Price, Aled Clayton, Philip E. James & D. Aled Rees. Young women with polycystic ovary syndrome have raised levels of circulating annexin V-positive platelet microparticles. 2014. Human Reproduction. doi:10.1093/humrep/deu281.

Katherine D. Connolly*, Gareth R Willis*, Borunendra N. Datta, Elizabeth A. Ellins, Kristin Ladell, Irina A. Guschina, D Aled. Rees and Philip E. James. LDL-Apheresis reduces the concentration of circulating platelet-derived microparticles in individuals with familial hypercholesterolaemia. 2014. Journal of Lipid Research. doi:10.1194/jlr.M049726.

David J Muggeridge, Nicholas Sculthorpe, Fergal M Grace, Gareth R Willis, Laurence Thornhill, Richard B Weller, Philip James, Chris Easton. Acute whole body UVA irradiation combined with nitrate ingestion enhances time trial performance in trained cyclists. 2014. Nitric Oxide. doi:10.1016/j.niox.2014.09.158.

Philip E. James, Gareth R. Willis, Jason D. Allen, Paul G. Winyard, Andrew M. Jones. Nitrate Pharmacokinetics: Taking Note of the Difference. 2015. Nitric oxide. Submitted.

Published abstracts

Gareth R. Willis, Katherine Connolly, Kristin Ladell, Irina A. Guschina, Kelly Miners, David A. Price, Aled Clayton, Philip E. James, D. Aled Rees. Women with PCOS have increased circulating annexin V positive microparticles, which are predominantly platelet-derived. Endocrine Abstracts. 2014;31:P218.

Gareth R Willis, Maurice Hallet, Kirsty Richardson, D Aled Rees & Philip E James. *In vitro* characterisation of endothelial-derived microparticles stimulated from pathologically relevant insults. Journal of Extracellular Vesicles. 2014;3:24214;P8A-289.

Katie Connolly, Keith Morris, Gareth R. Willis, D A. Rees and Philip E. James. Do conditions of freezing and time-in-freezer really matter? Journal of Extracellular Vesicles. 2014;3:24214;P8B-301.

Gareth R Willis, Rosie Hocking, Maneesh Udiawar, D Aled Rees, Philip E James. Oxidative stress and nitric oxide in polycystic ovary syndrome. Nitric Oxide. 2012;(27):S28.

Presentations, conference proceedings, honours and awards

- Prize: Young endocrinologist (BES, Liverpool, UK. 2014).
- International Society of Extracellular Vesicles (ISEV, Rotterdam, Netherlands. 2014), [Poster presentation].
- Endocrine Society (BES, Liverpool, UK. 2014), [Featured icon presentation].
- Endocrine Society (BES, Liverpool, UK. 2014), [Invited Chair: 'Endocrine Regulation of Cell Behaviour'].
- Welsh Endocrine and Diabetes Society (Newport, UK. 2014), [Poster presentation].
- International Society of Extracellular Vesicles (ISEV), (Boston, MA. 2013).
- IZON Science Research Symposium (Oxford, UK. 2013).
- Cardiovascular Medicine YLS (Queen Marys University, London, UK. 2013), [Poster presentation].
- International Society of Nitric Oxide (Edinburgh, UK. 2012), [Poster presentation].
- Postgraduate Research Conference - Cardiff University (University Hospital of Wales, UK. 2012 - 2014), [Poster presentation].
- Institute of Molecular and Experimental Medicine (Cardiff University, 2014).
- Vascular Biology and Cardiometabolic Research Group Seminar (Cardiff University, 2012, 2013, 2014).
- Centre for Endocrine and Diabetes Sciences, (University Hospital of Wales, 2011 & 2012).
- Institute of Molecular and Experimental Medicine, Postgraduate research, Science symposium (Cardiff University, 2014).

1. GENERAL INTRODUCTION

1.1 Cardiovascular disease

Cardiovascular disease (CVD) or disease of the blood vessels and heart, comprise many pathological conditions that vary in manifestation, prevalence and public health importance. CVD is the leading cause of morbidity and mortality across the globe (1). Since the initial description of heart disease, there has been a burgeoning awareness in the concept of CVD risk factors and an ever-increasing understanding of its pathophysiology.

Preceding a generic overview of CVD, associated entities and its global burden, it would be useful to define CVD. Terminology and definitions vary amongst published studies, as CVD may also refer to cerebrovascular disease; coronary heart disease (CHD); peripheral artery disease (PAD); cardiometabolic disease; coronary artery disease (CAD) and ischaemic heart disease (IHD). Furthermore the definition of CVD has evolved/expanded with increasing awareness and understanding. In essence, the generic term CVD will be employed throughout this thesis, or the terminology utilised will reflect the original manuscript quoted. The present focus is chiefly on CVD entities that predispose individuals to endothelial dysfunction and atherosclerotic diseases.

1.1.1 Epidemiology: The global burden of cardiovascular disease

The World Health Organisation (WHO) declared that CVD kills in excess of 17 million people a year, representing ~30% of total global deaths (1). This trend is set to worsen in the near future, with in excess of 23 million CVD attributed deaths a year are expected by 2030 (2). Of these, ~50% of deaths are from myocardial infarction (MI) and a further 23% from stroke, affecting both men and women equally (2).

Although CVD is a global problem, epidemiological studies have shown mortality rates vary considerably on a geographic and demographic basis. Broadly, the lowest age-adjusted mortality rates are in the developed industrialised countries and parts of Latin America, whereas the worst rates are found in Eastern Europe and several low/middle income countries (3). Specifically, age-standardised mortality rates for CVD are >500 per 100,000 individuals in Russia and Egypt; between 400 and 450 in countries such as South Africa and India and around 300 for Brazil and China. In comparison, Australia, Japan and France have between 100 and

200 CVD attributed deaths per 100,000 individuals. Interestingly, Japan has a three-four fold lower rate of CVD mortality rate than the USA (4). The discrepancies in inter-population CVD morbidity and mortality rates are intrinsically related to CVD risk factors (table 1.1).

Table 1.1 Cardiovascular disease risk factors

1. Smoking
2. Dyslipidaemia (characterised by elevated LDL-cholesterol and low HDL-cholesterol)
3. Diet
4. Hypertension
5. Diabetes mellitus
6. Physical inactivity
7. Obesity
8. Low socioeconomic status
9. Elevated prothrombotic/inflammatory markers
10. Genetic susceptibility

LDL, low density lipoprotein; HDL, high density lipoprotein. Adapted from (3).

Collectively, the spectrum of CVD risk factors are coupled with environmental, geographic and demographic dyanmics which contribute to the global variation in prevalence of CVD (3). In addition to this, the epidemiology of CVD within each specific geographic region differs, in terms of male-female and ethnic risk. For example, Cubbin *et al*, (5) noted higher rates of hypertension and diabetes amongst African American women living in deprived (low socioeconomic) areas compared to female African Americans living in more affluent areas.

Of all CVD entities, the American Heart Association noted CHD was the largest cause of death accounting for 48.2 % of total CVD deaths. Other causes of CVD death included stroke (16.4 %), heart failure (7.3 %), disease of the arteries (3.4%) and hypertension (8 %) (6). In Wales, CVD accounts for 10,341 deaths, out of a total of 31,197 deaths per year, where adult males appear modestly more prone to CVD than their female counterparts (7). Although, CVD still represents the leading cause of death in Wales and the rest of the UK, mortality rates have been steadily declining. The majority of countries in Europe, except Eastern European countries, have all experienced a similar decreased trend in CVD mortality rates over recent decades (4). However, CVD remains the leading cause of death globally and represents a great global health burden.

1.2 Vascular endothelium

1.2.1 Structure and function

The vascular endothelium occupies a unique interface between circulating blood and extravascular tissues. It is a dynamic autocrine and paracrine organ that maintains vascular homeostasis by modulating vascular tone, governing local cellular growth, possessing critical secretory, metabolic and immunological functions whilst regulating inflammatory responses (8, 9). The endothelium is a continuous cellular monolayer that retains a selectively permeable membrane and possesses an array of membrane-associated receptors for numerous molecules including lipid transport particles (such as low-density lipoprotein (LDL)-cholesterol), metabolites (serotonin), proteins (such as growth factors, coagulant/anticoagulant proteins) and hormones (including endothelin-1 (ET_1)). Moreover, the endothelial cell (EC) is equipped with specific junction proteins that aid cell-cell matrix interactions (9).

Structurally, a network of adhesive proteins link ECs together to form the endothelium. Functionally, three junctions have been described, tight, gap and adheren junctions. Tight junctions form close seals between ECs and are often associated with cytosolic proteins such as cingulin. Adheren junctions are formed by cadherins (adhesion molecules with vascular endothelial (VE)-cadherin being the most abundant). These adhesive structures (junctions) are involved in the regulation of membrane permeability. EC permeability is associated with changes/redistribution of surface cadherins in an attempt to meet the functional requirements of the perfused organ. Under physiological conditions, EC permeability permits the transport of plasma molecules (such as drugs, glucose and hormones) via non-specific and receptor mediated endocytosis or transcytosis.

The endothelium plays an integral role in the regulation of vascular tone. ECs regulate vascular tonicity by the release of a spectrum of vasodilatory molecules such as nitric oxide (NO), endothelial-derived hyperpolarising factor (EDHF) and prostacyclin (PGI_2). Conversely, the endothelium is able to secrete vasoconstrictive factors (such as platelet activating factor (PAF), angiotensin-II (Ang-II) and ET_1, (figure 1.1) (10). In addition to their direct effects on vascular tonicity, these vasoactive mediators also influence EC interactions with circulating leukocytes and platelets, playing an important role in EC permeability and vascular homeostasis. Furthermore, the endothelium plays a pivotal role in angiogenesis, a process that is predominantly governed by growth factors, particularly vascular endothelial growth factor (VEGF, figure 1.2) (11, 12). However, the mechanisms governing such modes of action are

complex and the overall vascular responsiveness varies between endothelial 'beds' and the differing pathophysiological circumstances. A summary of the principal regulatory compounds synthesised by the vascular endothelium are described in table 1.2.

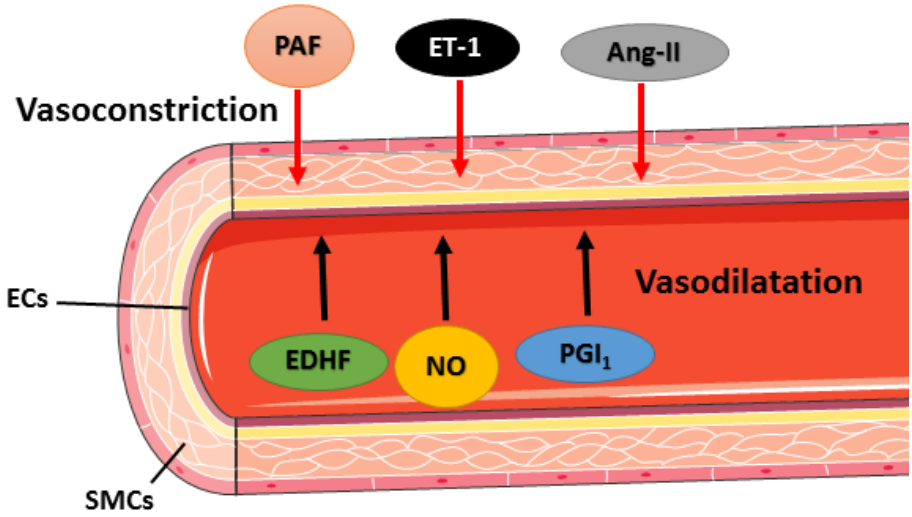

Figure 1.1. Vasoactive agents regulate vascular tone of a blood vessel. Vasoactive substances synergistically regulate vascular tone, (vasodilatation and vasoconstriction). Arrow direction indicates the principle effect of the vasoactive agent (vasoconstriction or vasodilatation). ECs, endothelial cells; SMCs, smooth muscle cells; EDHF, endothelial derived hyperpolarising factor; NO, nitric oxide; PGI_1, prostacyclin; PAF, platelet activating factor; ET-1, endothelin-1; Ang-II, angiotensin-II. Adapted from (12).

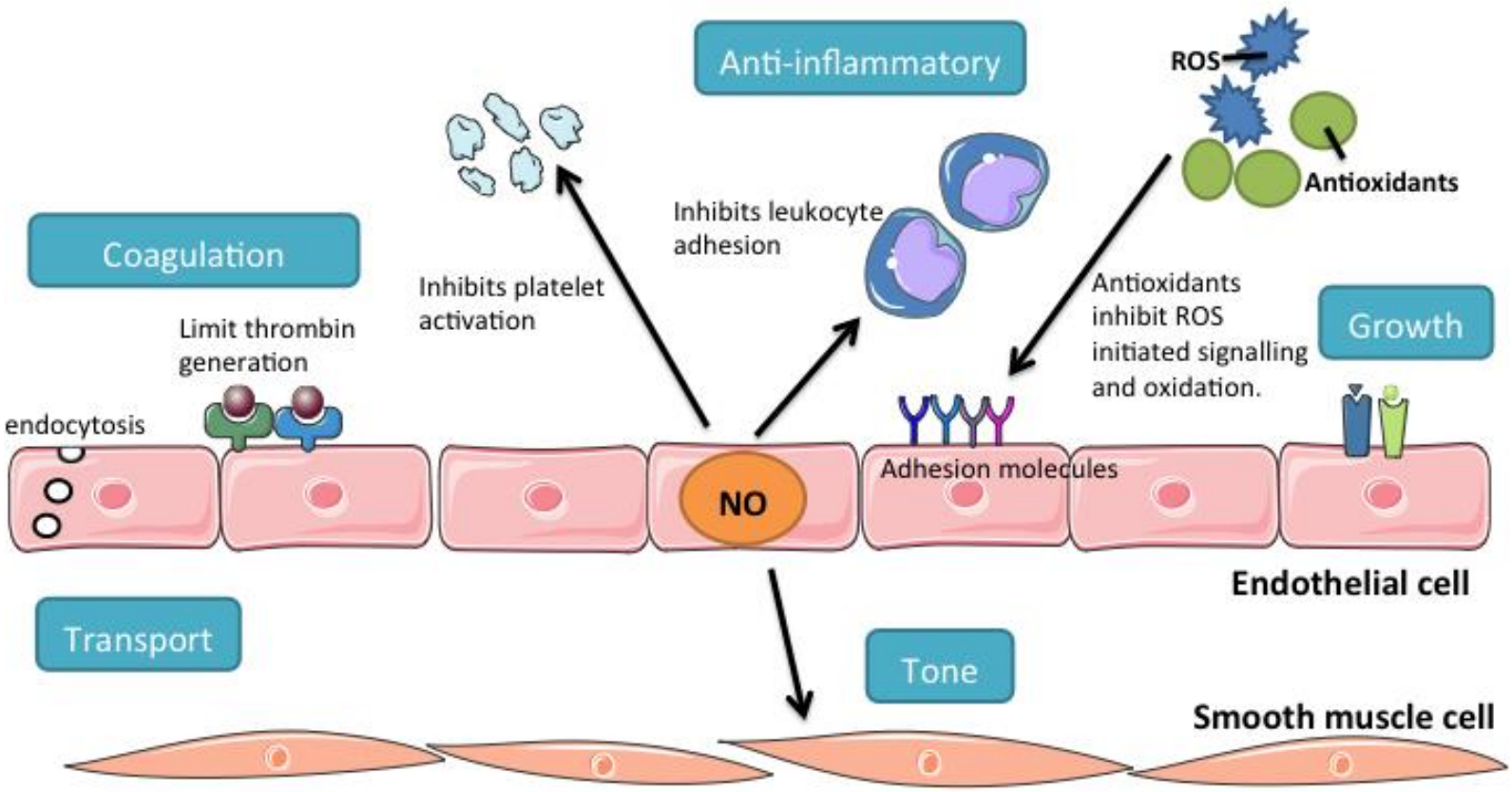

Figure 1.2 Schematic diagram representing key characteristics in vascular endothelial homeostasis. Endothelial cells (ECs) regulate the transport between blood and tissues via the caveolae/vesicle system and the intracellular junctions. The endothelium regulates the vascular tone and blood coagulation by the secretion of vasoactive substances. The endothelium plays an important role in inflammation by facilitating the migration of leukocytes into the sites of vascular injury. ECs can initiate angiogenesis, which is essential for tissue growth and wound repair. Described in detail in text. Adapted from (9).

Table 1.2 **Summary of the principal regulatory compounds synthesised by the vascular endothelium**

Substance	Principle effect	Other effects	Stimulation	Compound
NO	Vasodilatation	Maintains basal tone of vessels, inhibits leukocyte adhesion, inhibits platelet adhesion / activation / aggregation and inhibits SMC migration and proliferation.	Bradykinin, substance P, muscarinic agonists, shear stress, thrombin, ADP.	Diatomic radical
PGI_2	Vasodilatation	Inhibits platelet aggregation and deposition	Induced at sites of vascular perturbation	Eicosanoid
EDHF	Vasodilatation	-	-	-
PAF	Vasoconstriction	Promotes leukocyte adhesion at cell surface Inducement of platelet activation and aggregation	-	Phospholipid
ET_1	Vasoconstriction	Mitosis of SMC. Activation of ACE.	Induced by hypoxia, shear stress, and ischemia	Peptide
VEGF	Angiogenesis	Increases EC migration, mitosis and MMP activity. Vasodilation (indirectly by NO release).	Hypoxia	Peptide
Ang-II	Vasodilatation	Vasoconstriction (via AT1 receptor), Vasodilatation (via AT2 receptor and by stimulation of NO release). Angiogenesis.	-	Peptide

NO, nitric oxide; PGI_2, prostacyclin; EDHF, endothelial derived-hyperpolarising factor; PAF, platelet activating factor; ET_1, endothelin-1; VEGF, vascular endothelial growth factor; Ang-II, angiotensin-II; SMCs, smooth muscle cells; ADP, adenosine diphosphate AT receptor, angiotensin receptor; ACE, angiotensin-converting enzyme; EC, endothelial cell. A muscarinic receptor agonist is a substance that activates the muscarinic acetylcholine receptor. The chemical identity of the EDHF has not been determined. Adapted from (13, 14).

1.2.2 Endothelial dysfunction

Endothelial dysfunction refers to the impaired ability of the endothelium to regulate and maintain vascular homeostasis (15). Under physiological conditions the vascular endothelium maintains an antithrombotic surface. In contrast, under pathological stresses, alterations in the vascular endothelium may shift the pattern towards a prothrombotic state. EC activation is associated with a reduction in anticoagulant surface molecules such as thrombomodulin (TM) and a concomitant elevation in prothrombotic components such as tissue factor (TF) or increased binding of coagulation factors (15). Cellular activation can also promote EC interactions with circulating cells by elevated expression of surface adhesion molecules, including VE-cadherin, intercellular cell adhesion molecule (ICAM)-1, vascular cell adhesion molecule-1 (VCAM-1), platelet endothelial cell adhesion molecule-1 (PECAM-1), endoglin, E-selectin and P-selectin (16). Accordingly, abnormalities in the endothelium (endothelial dysfunction) is characteristically observed in the initial stages of CVD and is often evident before CVD phenotypically manifests itself (17). Of note, the endothelium observes a shift, from NO mediated signalling towards EC activation by altered redox signalling.

There are many cumulative and synergistic causes of endothelial dysfunction. Although decreased NO production, L-arginine depletion and SMC stiffening are known to be important in endothelial dysfunction, NO bioavailability, reactive oxygen species (ROS) and antioxidant levels are considered central to many mechanisms that predispose individuals to endothelial dysfunction (16, 18).

1.2.3 Nitric oxide

1.2.3.1 Nitric oxide synthase

Although there are alternative mechanisms that can generate NO (for example the acidification or reduction of nitrite (NO_2^-)), the majority of mammalian NO is derived enzymatically from NO synthase (NOS) (19). NOS enzymes convert L-arginine to L-citruline and NO in an oxygen (O_2) and NADPH dependent manner. There are three NOS isoforms that have been described, including nNOS (neuronal, NOS-1), iNOS (inducible, NOS-2) and eNOS (endothelial, NOS-3). iNOS and nNOS are found mainly in the cytosol whilst eNOS is predominantly membrane associated. Two of these isoforms are constitutive (eNOS and nNOS) whereas the other is inducible (iNOS) (19). The activity of all NOS isoforms is also dependent on the presence of

several critical co-factors including tetrahydrobiopterin (BH_4), nicotinamide adenine dinucleotide phosphate (NADPH), as well as an optimum supply of the substrates O_2 and L-arginine. A reduction in these cofactors or substrates will limit NO production proportionately.

Of the three NOS isoforms, eNOS is the primary signal generator in the control of vascular tone. The endothelial isoform is activated in response to shear stress and several key endogenous agonists. For example bradykinin and acetylcholine act via endothelial receptors that modulate intracellular calcium (Ca^{2+}), interaction with substrate and protein phosphorylation. Dysregulation of these processes alters eNOS activity and may reduce NO output, a characteristic feature of several pathological disorders including diabetes and atherosclerosis (20).

Several pharmacological agents can inhibit NO production by disrupting eNOS. For example, arginine-derived analogues such as NG-monomethyl-L-arginine (L-NMMA) and NG-nitro-L-arginine methyl ester (L-NAME) inhibit eNOS derived-NO production. Interestingly, the effect of L-NMMA *in vivo* is primarily dependent on the route of administration, whereby Clark and co-workers found that a single intrapleural injection of L-NMMA in a rodent model of inflammation (carrageenin-induced pleurisy) exacerbated the inflammatory status (21). In contrast, administering L-NMMA systemically ameliorated the severity of inflammation (22), exemplifying the complexity of NO biochemistry *in vivo* and demonstrating the route of administration is vital to the clinical outcome.

1.2.3.2 Nitric oxide metabolites

NO is an important signalling molecule that plays an important role in a range of biological activities, including vascular tonicity and vasodilation. NO can rapidly diffuse to smooth muscle (3200 $\mu m^2 s^{-1}$, diffusion coefficient) where it activates soluble guanylate cyclase (sGC) and initiates a downstream signalling cascade resulting in K^+ channel activation and subsequent Ca^{2+} channel inhibition, reducing intracellular Ca^{2+} concentration and inducing vascular relaxation (23). This highly diffusible diatomic radical gives rise to a complex biochemistry. Scavenging reactions with antioxidants, free radicals and haemoglobin limit the diffusion rate and influence NO metabolite formation. NO can be stabilised in blood, most notably in the form of NO_2^- and nitrate (NO_3^-). These metabolites are now considered bioactive endocrine molecules. Other research groups have shown NO can also be stabilised in the form of nitrated fatty acids and S-nitrosothiols (RSNO). However, *in vivo* detection and measurement of these metabolites is difficult, and as such their physiological concentration is highly debated. Traditionally, NO_2^-

and NO_3^- were viewed as undesirable inert end products of NO metabolism. More recently NO_2^- and NO_3^- reduction has been shown to complement the traditional NO/sGC/cGMP pathway, playing a key role in vasodilatation (24) (figure 1.3).

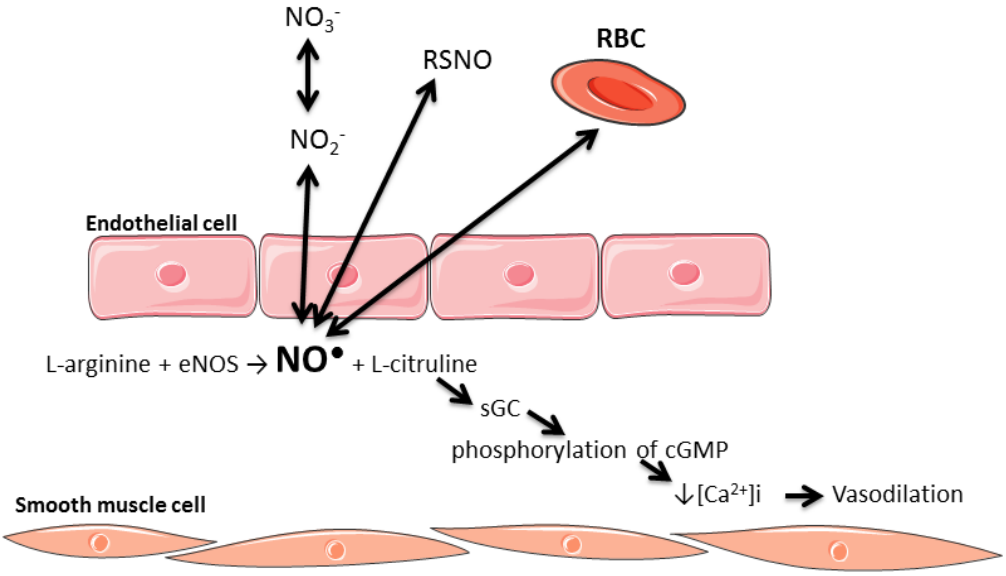

Figure 1.3 Endothelial nitric oxide production. Endothelial derived- nitric oxide (NO) is enzymatically generated via a reaction between endothelial NO synthase (eNOS), L-arginine and molecular oxygen to yield NO and L-citruline. NO can rapidly diffuse to smooth muscle cells (SMCs) where it activates soluble guanylate cyclase (sGC) and initiates a downstream signalling cascade resulting in K^+ channel activation and subsequent Ca^{2+} channel inhibition, reducing intracellular Ca^{2+} concentration ($[Ca^{2+}]_i$) and inducing vascular relaxation. NO in the blood is readily oxidised to nitrite (NO_2^-) and nitrate (NO_3^-). S-nitrosothiols (RSNO) are produced when NO binds to thiols. RBC refers to red blood cell. Adapted from (23).

1.2.3.3 Nitrite

NO_2^- is an ionic compound that represents a bioactive reservoir for NO. *In vivo*, NO_2^- is formed in the body through the oxidation of NO or through the reduction of NO_3^-. Interestingly, L-arginine–NOS generation of NO is O_2 dependent, whereas the NO_2^-–NO pathway is implemented when the O_2 concentration decreases. Thus, the NOS-independent generation of NO (i.e. NO_2^- – NO pathway) may be viewed as a back-up mechanism to ensure that there is copious NO levels when O_2 supply is limited (25). However, the precise physiological O_2 concentration at which NOS dependent NO generation fails is unclear. Previous studies have shown that at low O_2 conditions (ischaemia/reperfusion studies), NO generation in tissues is independent of NOS activity and dependent on NO_2^- (26). The vasoactive properties of NO_2^- at

supra-physiological levels have been known for decades, where Furchgott and Bhadrakom found that $NaNO_2$ induced relaxation of rabbit aortic strips, however the micromolar concentration range used did not reflect endogenous NO_2^- levels (27). A number or research groups (including ours) have shown that the typical plasma NO_2^- range from healthy subjects is between 100 – 500 nM (28, 29). Previous research in our laboratory has shown that intravenous infusion of $NaNO_2$ (1.5 μmol/min for 20 min) protects against vascular ischemia-reperfusion injury only when it is given before the onset of ischemia (30). Furthermore, *ex vivo* studies have shown that the efficacy of NO_2^- (in terms of vasodilatation) is enhanced at lower buffer pH levels in isolated vessel (myography) experiments (31). Moreover, Gladwin and coworkers found that artery-to-vein gradients in NO_2^- across the human forearm (with venous blood exhibiting reduced NO_2^- levels in a study involving 5 healthy subjects), suggesting that NO_2^- is metabolised across the peripheral circulation (32).

1.2.3.4 Nitrate

Several research groups (including ours) have shown that plasma NO_3^- concentration ranges between 20 – 40 μM in healthy subjects (29, 33). *In vivo*, NO_3^- originates from two potential sources: (i) the oxidative metabolism of NO, or (ii) dietary NO_3^-. Foodstuffs contain varying concentrations of NO_3^-, where leafy vegetables and beetroot are a relatively rich source (34). Kapil and coworkers noted that ~66% of the absorbed NO_3^- is excreted (unaltered) in the urine (35). The remaining bioavailable NO_3^- is believed to enter the entero-salivary circulation for subsequent metabolism where NO_3^- is converted to NO_2^- by bacteria in the oral cavity. Located at the posterior, dorsal area of the tongue, several bacterial species (including lactobacillus, micrococcous, corynebacterium and propionibacterium) have been shown to convert NO_3^- to NO_2^- (24). Importantly, several studies have shown that the destruction of the oral micro-flora by antibacterial mouthwashes prevents the conversion of NO_3^- to NO_2^- (36). Furthermore, in a rodent model, Sobko and coworkers showed that the gut micro-flora also participates in the conversion of NO_3^- to NO_2^- (37). Wylie and co-workers showed that NO_3^- administration (4 – 24 mM) elevated plasma NO_2^- in a dose dependent manner (38). There is an increasing awareness of the potential therapeutic applications of the NO_3^- - NO_2^- - NO pathway. Larsen and co-workers showed that $NaNO_3$ (0.1 mmol/kg body weight) administration reduces blood pressure (39). Webb *et al*, (40) showed that a bolus dietary NO_3^- load attenuated endothelial dysfunction caused by an acute ischaemic insult in the human forearm, as well as reduced *ex vivo* platelet aggregation.

1.2.3.5 Nitric oxide bioavailability

A reduction in bioactive NO metabolites (NO_x) is recognised to reflect an overall decreased NO bioavailability. Such pathological environments may lead to abnormalities in endothelial function (41). Moreover, such conditions are an established feature of atherosclerotic vascular disease, where decreased NO bioavailability and a concomitant increase in reactive oxygen species (ROS) may synergistically contribute to endothelial impairment. There are several possible defects that could account for reduced NO bioavailability. These include depletion of NO as a consequence of its reaction with superoxide ($^{\cdot}O_2^-$), diminished NO production due to changes in eNOS activity (i.e. eNOS uncoupling, depletion of L-arginine or other co-factors such as BH_4), or decreased dietary consumption of NO_x (20, 42, 43).

Altered NO production, often coupled with accelerated NO removal (through poorly understood mechanisms) may have detrimental consequences on secondary NO species and overall NO bioavailability. Rubbo *et al*, (44) suggested that the powerful radical peroxynitrite ($OONO^-$) accounts for the major part of accelerated NO removal. Interestingly, $OONO^-$ dissociation yields a hydroxyl radical ($OH^{\cdot}$) and nitrogen dioxide (NO2), which participate in secondary oxidative/nitrative actions (as mentioned in section 1.2.4).

With a short half-life and potent tendency for reactivity, NO is difficult to directly detect *in vivo*. Thus, studies have relied on plasma NO_x levels (in particular plasma NO_2^- and NO_3^-) to reflect NO bioavailability. On assessment of 351 healthy volunteers, Kleinbongard *et al*, (41) found that plasma NO_2^- concentration is a direct measurement of endothelial function. Inhibition of endothelial NO production by L-NMMA infusion can impair endothelial function. Virdis and colleagues showed that L-NMMA decreased endothelial-dependent vasodilatation, as assessed by flow-mediated dilatation (FMD) (45). However in this particular study NO_x levels were not assessed. Interestingly, Rogers *et al*, (46) explored the effect of L-NMMA on cross heart NO_x metabolism. They found that infusion of L-NMMA increased diastolic and systolic blood pressure coupled with the constriction of coronary artery diameter. However, no change in net NOx concentration was observed. This trend was also observed in control subjects not receiving L-NMMA. Thus, it can be concluded that although NO_x metabolites have been shown to be a biomarker for endothelial dysfunction in the chronic setting, because NO redox chemistry is complex *in vivo* these measures can only reflect the net effects of NO production, NO utilisation, and NO inactivation. This also questions whether measurement of venous NO_x can accurately reflect endothelial NO production in the acute setting, a parameter that will be influenced by the changes in flow and O_2 saturation per se. Using physiological parameters to assess endothelial function is practically challenging, is operator dependent, and has relatively

poor repeatability. Often, loosely defined terms for flow and velocity are interchanged, coupled with singular measurement parameters used as physiological/clinical endpoints without considering the synergistic relationship between cardiac output, heart rate, pressure, velocity, flow and function of the vessel.

1.2.3.6 Clinical assessment

Assessment of endothelial function is employed as a diagnostic and prognostic tool in regards to CVD risk. With a diverse pathogenesis endothelial dysfunction can be assessed at a molecular / biochemical and physiological level, where numerous *in vitro*, *ex vivo* and *in vivo* methodologies are routinely employed in research, as highlighted in table 1.3.

Table 1.3 **Common measures / indicators of endothelial dysfunction**

Measure	Type	Interpretation
FMD	Physiological	Impaired responsiveness of NO vasodilatation.
NO metabolites	Biochemical	Decreased NO metabolite levels (accelerated NO removal and/or reduced NO production).
Inflammatory markers / cytokines: inc' (VCAM-1, sICAM-1, E-selectin, TNFα, IL-8)	Biochemical	Enhanced leukocyte adhesion/inflammatory activation / EC activation. ROS production and up regulation of inflammatory genes
PWV	Physiological	Arterial stiffness / impaired responsiveness of NO vasodilation.
Angiogenic growth factors: VEGF	Biochemical	Indication of membrane permeability, migration and angiogenesis.
Nitro-oxidative stress (inc' TBARS, TAC, lipid radicals)	Biochemical	Reflects systemic nitro-oxidative stress.
MPs	Biochemical	Elevated levels are associated with endothelial dysfunction.

FMD, flow mediated dilatation; NO, nitric oxide; sVCAM-1, soluble vascular cell adhesion molecule-1; sICAM-1, soluble intercellular cell adhesion molecule-1; E-selectin, endothelial selectin; TNFα, tumour necrosis factor alpha; IL-8, interleukin 8; PWV, pulse wave velocity; VEGF, vascular endothelial growth factor; TBARS, thiobarbituric acid reactive substances; MPs, microparticles; EC, endothelial cell. Adapted from (47).

1.2.4 Reactive oxygen species

Reactive oxygen species (ROS) play a central role in modulating endothelial function. ROS are produced via numerous oxidase enzymes, including NADPH oxidase, xanthine oxidase, uncoupling of eNOS and mitochondrial electron transport. Common ROS include $^{\cdot}O_2^-$, hydrogen peroxide (H_2O_2), $OH^{\cdot}$, $ONOO^-$ and NO. ROS are generated from numerous cell types, including vascular smooth muscle cells (VSMCs), ECs and mononuclear cells, by a variety of cellular processes. $^{\cdot}O_2^-$ is a common bi-product of the electron transport system in mitochondria.

Notably, $^{\cdot}O_2^-$ rapidly reacts with NO to yield $ONOO^-$ (44). $ONOO^-$ is an established mediator of lipid peroxidation and protein nitration, both of which have downstream proatherogenic capabilities. During vascular homeostasis, $^{\cdot}O_2^-$ is commonly metabolised by superoxide dismutase (SOD) to H_2O_2. H_2O_2 may then be converted to H_2O and O_2 by glutathione peroxidase or catalase (48). Oxidative stress is defined as an imbalance between the production of ROS and their removal by naturally occurring antioxidant defences of cells including the enzymatic catalase and SOD, as well as direct actions of antioxidants like glutathione, vitamin E, β-carotene and ascorbate. Increased cellular production of $^{\cdot}O_2^-$ and H_2O_2 can facilitate the formation of $OH^{\cdot}$ in the presence of metal ions such as iron (Fenton reaction) or copper (figure 1.4). As $OH^{\cdot}$ has a very short half-life (T½) and is highly reactive, it can rapidly damage surrounding macromolecules, including amino acids (potentially leading to protein inactivation/denaturation), carbohydrates (causing degradation), lipids (by interaction with polyunsaturated fatty acids (PUFAs) of membrane phospholipids, leading to lipid peroxidation) and nucleic acids (resulting in possible mutations) (48). In addition to mitochondrial ROS generation, NADPH oxidases (NOX) a multi-subunit complex composed of cytosolic components ($p47^{phox}$, $p67^{phox}$ and Rac 1) and membrane-spanning components ($p22^{phox}$ and $gp91^{phox}$) are also considered an important source of ROS (49).

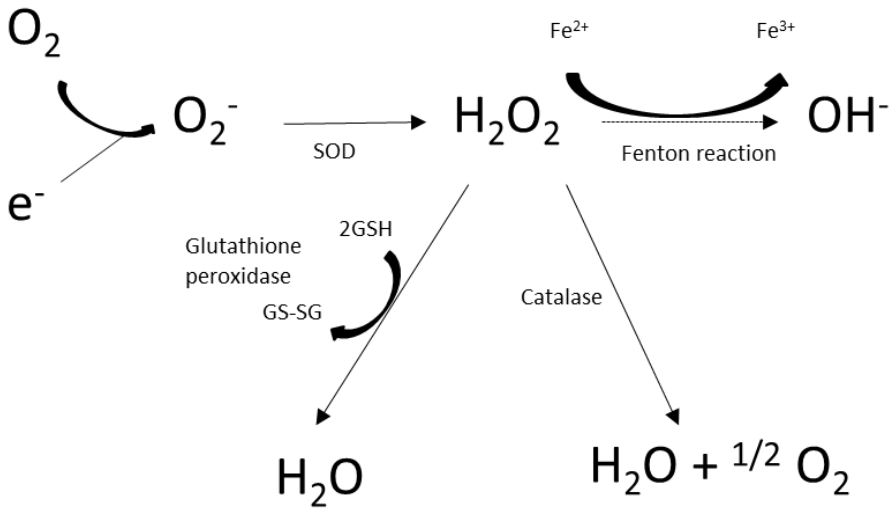

Figure 1.4. Generation and inactivation of reactive oxygen species. Superoxide (O_2^-) is converted to hydrogen peroxide (H_2O_2) by superoxide dismutase (SOD). Fenton style reactions propagate the conversion of H_2O_2 to hydroxyl radicals (OH^-). H_2O_2 can be detoxified by glutathione peroxidase or catalase to H_2O. Adapted from (50).

Numerous studies have shown that cardiovascular risk factors increase the expression / activity of NOX in the vasculature, and consequently elevate levels of ROS. Evidence for NOX activation has been provided in animal models of diabetes mellitus, hypercholesterolaemia and hypertension. In isolated atherosclerotic arteries, Xu and colleagues showed an elevated expression of NOX2 and NOX4 (51). Additionally, Ushio-Fukai *et al*, (52) were the first to report that inhibition of $p22^{phox}$ (NOX subunit) messenger ribonucleic acid (mRNA) (achieved by antisense transfection in VSMCs) resulted in decreased Ang-II-stimulated NADPH dependent $^{\cdot}O_2^-$ production and subsequent H_2O_2 production.

NOX attenuate a plethora of signalling pathways that regulate gene expression. Kunsch and colleagues noted that ROS may influence cell proliferation, apoptosis and inflammation through the activation of redox-sensitive transcriptional factors and signalling cascades which may result in overexpression of redox genes, intracellular calcium overload and DNA fragmentation in ECs (53). Moreover Lu *et al*, (54) found that ROS regulate EC gene expression, including surface adhesion molecules, antioxidant enzymes and vasoactive mediators. Increased expression of adhesion molecules (including VCAM-1 and ICAM-1) by redox reactions may also contribute to endothelial dysfunction. These surface adhesion molecules promote adhesion and migration of leukocytes to the endothelium (54). Conversely, NO has been shown to inhibit the transcriptional induction of surface adhesion molecules by cytokines in a cGMP-independent manner (54).

1.2.4.1 Xanthine oxidase

Xanthine oxidase (XO) is an enzyme that catalyses the oxidation of hypoxanthine to xanthine and ultimately the oxidation of xanthine to uric acid. XO also plays a role in the catabolism of purines and caffeine. XO is also a potential source of ROS generation in states of endothelial dysfunction whereby XO readily donates electrons to O_2, consequently producing $^{\cdot}O_2^-$ and H_2O_2. Previous studies showed that pharmacological inhibition of XO (using XO inhibitor oxypurinol), improved endothelial function in patients with hypercholesterolaemia (55) and diabetes (56). This is supported by *in vitro* studies showing reduced $^{\cdot}O_2^-$ production and improved endothelium-dependent vasorelaxation in isolated hypercholesterolaemia animal vessels (57). In contrast, other studies have reported no improvement in endothelial function with another XO inhibitor, allopurinol (58).

1.2.4.2 Antioxidant defence

The influence of ROS (such as $^{\cdot}O_2^-$and H_2O_2) on the vascular endothelium is regulated by the capacity of the antioxidant defence system. An array of enzymes typically constitute key antioxidant systems, these include SOD, catalase, glutathione peroxidase and glutathione reductase coupled with water and lipid soluble antioxidants, such as ascorbate, glutathione, α-tocopherol and carotenoids (table 1.4).

Table 1.4 Summary of antioxidant defenses in biological systems

System	Remarks
Non-enzymatic	
α-tocopherol	Radical chain breaker
β-carotene	Singlet O_2 quencher
Lycopene	Singlet O_2 quencher
Ubiquinol-10	Radical scavenger
Ascorbate	Diverse functions
GSH	Diverse functions
Urate	Radical scavenger
Flavonoids	Plasma antioxidant
Plasma proteins	Plant antioxidant
Chemical	Food/drugs
Enzymatic	
Superoxide dismutase	Converts $^{\cdot}O_2^-$ into either O_2 or H_2O_2.
GSH peroxidase	Reduces lipid hydroperoxides
Catalase	Decomposition of H_2O_2

GSH, glutathione; $^{\cdot}O_2^-$, superoxide radical; Hydrogen peroxide, H_2O_2. Adapted from (59).

Numerous clinical studies/trials have studied the effects of antioxidants on CVD. Engler *et al*, (60) demonstrated that antioxidant therapy (vitamin C and E supplementation) improved endothelial function (assessed via flow-mediated dilatation) in hyperlipidaemic children. Conversely, in a meta-analysis, Vivekananthan and colleagues assessed the effect of vitamin E or β carotene on long-term cardiovascular mortality. Vitamin E supplementation did not significantly decrease risk of cardiovascular death (>81,000 patients across 7 randomised studies) (61). Also, β carotene supplementation was associated with a modest increase in cardiovascular death. However, supplementation dose did vary across studies. Clinical trial results investigating antioxidant therapy in the setting of preventive CVD, have been, to date, mostly negative. Although there are a number of hypotheses for this, the exact reason remains unknown. Steinhubl *et al*, 2008 speculated that perhaps the single vitamin regimen was not what was needed (i.e. a multi-vitamin supplement would provide a broader range of antioxidants) (62). Additional reasons could include the wrong dosage range, inadequate durations and the wrong subject populations (i.e. testing antioxidant therapy on subjects with depleted antioxidant levels or increased oxidative stress rather than healthy subjects).

Although it is well established ROS may damage proteins, nucleic acids and membrane phospholipids, ROS may also be important in maintaining normal cell function (such as signal transduction, cell proliferation, transcription regulation and phagocytosis) (63).

Interestingly, physical exercise (specifically 200 eccentric muscle actions of the rectus femoris) has been shown to elevate systemic nitro-oxidative stress, oxidatively modify proteins and initiate damage to DNA in skeletal muscle in human and animal models (64). In order to tolerate this exposure to ROS during exercise, previous studies have shown that antioxidant enzymes are up regulated by exercise (65). Thus, exercise-induced oxidative stress appears to be counter balanced by a concomitant increase in endogenous antioxidants, including glutathione.

Although exercise (i.e. cycling until volitional exhaustion) is known to increase ROS production, a known risk for endothelial dysfunction, there is a wealth of evidence supporting the notion that exercise improves endothelial dysfunction and reduces the risk of CVD. Antioxidant supplementation prior to exercise has been reported to blunt exercise induced (interleukin) IL-6 release from contracting human skeletal muscle. However, Ristow *et al*, (66) noted that the additional health benefits of physical exercise such as up regulation of glucose transporter type-4 (GLUT4), plasma adiponectin level and antioxidant enzymes in human skeletal muscle are abolished by administration of vitamin C and E. Therefore, whilst antioxidant supplementation may reduce ROS damage, this protective quenching of ROS may

subsequently inhibit the body's natural antioxidant systems and neutralise any potential benefits.

1.2.5 Clinical significance of endothelial dysfunction - implications in atherosclerosis

Homeostatic alterations in the endothelium can result from a chemical insult (for example, ROS damage). Endothelial dysfunction resulting from insult can often shift the vessel into a prothrombotic state, whereby the endothelium attempts to repair the damage by increasing leukocyte recruitment. Additionally, endothelial injury initiates the secretion of procoagulant factors (including cytokines and growth factors). If this inflammatory cascade is not neutralised back to a non-procoagulant state, it may continue indefinitely, leading to migration and proliferation of lipid and SMCs to the site of damage. If these responses continue unrestricted, they can thicken and stiffen the arterial wall.

Continued inflammation results in increased recruitment of leukocytes (macrophages and lymphocytes), which migrate to the lesion. Activation of these cells results in the release of cytokines, chemokines, and growth factors, which further induce vascular damage and eventually lead to focal necrosis. Fatty streaks are initiated by the adherence of circulating monocytes to activated ECs. Subsequently, adhered monocytes may migrate to the subendothelial space where they differentiate into macrophages, a process governed by chemoattractant molecules (67). Monocyte differentiation is coupled with a substantial up regulation of 'scavenger' receptors. Typically, scavenger receptors are involved in the recognition and internalisation of pathogens however, scavenger receptors also recognise modified low-density-lipoprotein and mediate the formation of lipid peroxides and accumulation of cholesterol in the macrophage to form foam cells (67). Accumulation of mononuclear cells, migration and proliferation of SMCs, and formation of fibrous tissue results in the further enlargement of the lesion. The fibrous cap encapsulates the necrotic tissue and accumulated lipid, to become an advanced atherosclerotic lesion (67).

Concomitantly, endothelial dysfunction has been proposed to be of immense pathophysiological importance in the development of atherosclerosis. The imbalance in NO bioavailability coupled with a concomitant increase in ROS is referred to as nitro-oxidative stress. The pathological mechanisms that oversee endothelial dysfunction are complex. For example, decreased NO bioavailability is associated with increased VCAM-1 expression in ECs. In parallel, elevated

ROS may directly or indirectly (via oxidised LDL) up-regulate EC surface adhesion molecule expression. Consequently, with a decreased NO bioavailability, VCAM-1 binds to leukocytes and initiates their subsequent invasion of the vessel wall. Following foam cell formation oxidised LDL attenuate the damage by reducing eNOS expression and further stimulating surface adhesion molecule expression in ECs (67).

Eventually, compensatory mechanisms (such as vascular dilatation) become exhausted, and consequently atherosclerotic lesions may rupture, intrude into the lumen and alter the flow of blood. The vicious spiral of nitro-oxidative stress may also activate matrix metalloproteinases (MMP, including MMP-2 and MMP-9), which weaken the fibrous cap of atherosclerotic lesions causing plaque ruptures and acute coronary syndrome (67). Summarised in figure 1.5.

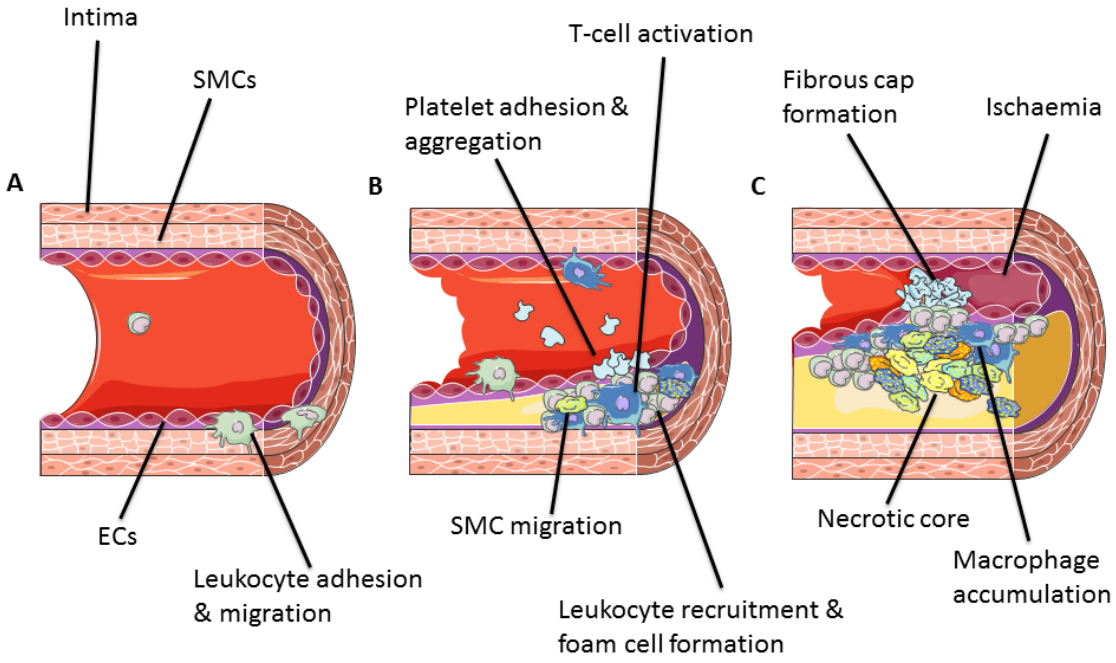

Figure 1.5. The pathology of atherosclerosis. (A) Endothelial dysfunction. Endothelial dysfunction is the earliest manifestation of atherosclerosis to precede the formation of atherosclerotic lesions. (B) Fatty streak formation. The fatty streak involves the recruitment of monocytes, macrophages and T-lymphocytes to initiate foam cell formation. Foam cell formation is accompanied by SMC migration (stimulated by platelet-derived growth factor, fibroblast growth factor 2, and transforming growth factor β). Additionally, T-cell activation is mediated by tumour necrosis factor alpha (TNFα), interleukin-2, and granulocyte–macrophage colony-stimulating factor. Macrophages engulf modified LDL (especially oxLDL) by endocytosis via scavenger receptors to initiate the formation of foam cells. Foam cell formation is associated with oxidised low-density lipoprotein (LDL), macrophage colony-stimulating factor, TNFα, and interleukin-1 (IL-1) and platelet adhesion and aggregation (itself stimulated by integrins, P-selectin, fibrin, thromboxane A2, tissue factor (TF)). (C) Advanced atherosclerosis. A fatty streak can progress to an advanced atherosclerotic lesion. These advanced lesions often form a fibrous cap that walls off the lesion from the lumen (as a healthy blood vessel would respond to a vascular injury). The fibrous cap encapsulates an array of leukocytes, lipid deposits and debris, which in turn form a necrotic core. Lesions may expand via continued leukocyte adhesion and entry. ECs, endothelial cells; SMCs, smooth muscle cells. Adapted from (67).

1.3 Polycystic ovary syndrome

In my thesis, I chose to use patients with Polycystic Ovary Syndrome (PCOS) as a clinical model of early CVD. PCOS is a common endocrine disorder affecting 5-10% of women in reproductive age (68). The syndrome is a complex disorder with environmental and epigenetic factors playing a key role in the phenotypical expression of disease symptoms, of which cardiovascular disease is prevalent. The clinical characteristics of PCOS are highlighted in table 1.5.

Whilst the aetiology of PCOS is largely unknown, studies in families have shown it appears to be heritable in nature, at least in part. In a study looking at 93 patients with PCOS, Kashar-Miller *et al*, (69) found that 35% of patients' mothers and 40% of their sisters also had PCOS, a proportion which is markedly higher than the 5-10% anticipated in the general population. To date, numerous efforts have been made to find candidate genes that influence PCOS pathology. Several possible genes have been suggested including hexose-6-phosphate dehydrogenase (H6PD) (70), a pivotal gene in glucocorticoid and cortisone regulation.

Major endocrine disruption includes enhanced androgen activity coupled with the impaired action of insulin. Endocrine abnormalities affect a variety of physiological processes, resulting in several common health complications, including menstrual dysfunction and infertility, acne, hirsutism, obesity and metabolic syndrome (71).

Table 1.5 Clinical characteristics of polycystic ovary syndrome

1. Oligomenorrhea / amenorrhea
2. Infertility
3. Hirustism
4. Male pattern baldness
5. Acne
6. Obesity
7. Impaired actions of insulin

Adapted from (71).

1.3.1 Diagnosis

The diagnostic traits for PCOS include hyperandrogenism, oligomenorrhea / anovulation, and polycystic ovaries. The disorder was first described by Stein and Leventhal in 1935, reporting a case of several women that presented with amenorrhea, hirsutism and polycystic ovaries, which has now come to be known as PCOS. However, despite the high prevalence of PCOS, diagnosis remains controversial (72). Additionally, since the first description of PCOS in 1935, the importance of different clinical features to the diagnosis of the syndrome has undergone multiple revisions (table 1.6).

Firstly, the National Institute of Health (NIH, 1990) defined PCOS as chronic anovulation with clinical and/or biochemical hyperandrogenism (73). Following this, the European Society for Human Reproduction/American Society of Reproductive Medicine proposed the Rotterdam criteria for diagnosis. This includes any two of the following three criteria: oligomenorrhea and/or anovulation, clinical and/or biochemical hyperandrogenism and polycystic ovaries (assessed via bilateral ultrasound). The Rotterdam criteria is still used in current clinical practice. With the additional diagnostic tool (polycystic ovaries) suggested by the Rotterdam criteria, it expanded the diagnosis of PCOS to women with oligomenorrhea / anovulation and polycystic ovaries (nonhyperandrogenic), as well as women with hyperandrogenism and polycystic ovaries (74). This diagnostic criteria has multiple phenotypes which when coupled to the spectrum of environmental factors, contributes to the diverse pathophysiology and phenotypical manifestations of the syndrome. More recently, the Androgen Excess and PCOS Society reported that PCOS is predominantly a hyperandrogenic disorder and suggested that the criteria should encompass hyperandrogenism and abnormal ovarian function (oligomennorrhea /anovulation and/or polycystic ovaries) (75). This definition makes hyperandrogenism a prerequisite for diagnosis. To date, the Rotterdam criteria is the most widely used. All revisions of the syndrome acknowledge the importance of correct diagnosis with the exclusion of other mimicking etiologies such as Cushing's syndrome, thyroid and adrenal pathologies.

Table 1.6 **Diagnostic criteria for polycystic ovary syndrome**

Criteria	Hyperandrogenism	Oligomenorrhea / amenorrhea	Polycystic ovaries
NIH 1990	+	+	+/-
Rotterdam 2003			
phenotype 1	+	+	-
phenotype 2	+	-	+
phenotype 3	-	+	+
phenotype 4	+	+	+
AE-PCOS 2006			
phenotype 1	+	+	-
phenotype 2	+	-	+
phenotype 3	+	+	+

NIH, National Institute of Health; AE, androgen excess; PCOS, polycystic ovary syndrome. Adapted from (76).

1.3.2 Cardiovascular disease in PCOS

In addition to the well-established reproductive complications, the complexity of the syndrome has widened to encompass an array of cardiovascular health problems including obesity (77), hypertension (78) and dyslipidaemia (79). Reduced insulin sensitivity and impaired insulin secretion are considered the key metabolic deficits within PCOS, subsequently leading to an increased risk of type 2 diabetes (80, 81). Thus, there are a plethora of cardiometabolic derangements, synergistically contributing to the development of CVD risk in PCOS patients.

1.3.3 Hypertension in PCOS

The cardiovascular risk factors associated with PCOS may indeed be responsible for the promotion of hypertension in these patients. Numerous studies have reported an increased occurrence of hypertension in PCOS patients compared to control populations (81, 82). In a study investigating hypertension in 346 Dutch PCOS patients, Elting *et al*, (83) declared women with PCOS had a 2.5 fold greater prevalence of hypertension than women in the corresponding age-matched Dutch female population. However, this study was not adjusted for BMI, thus the additional complication of obesity related hypertension may confound this association. Holte *et al*, (82) found that compared to controls, women with PCOS had higher day-time ambulatory systolic blood pressure and mean arterial blood pressure measurements compared to their non-PCOS counterparts. Groups did not differ in day-time diastolic blood pressure or in night-time measurements. This indication of pre-clinical hypertension was independent of BMI.

In contrast, another study involving small participant numbers (14 PCOS patients and 18 obese controls) found no relationship between PCOS and hypertension (84). Interestingly, Wild *et al*, (85) undertook a long-term (31 year) retrospective analysis of patients with PCOS, finding that women with PCOS had an increased prevalence of hypertension. However, BMI was again not considered, hence the effects of the syndrome, independent of obesity on BP, are yet to be fully established.

Numerous mechanisms are potentially responsible for the development of hypertension in women with PCOS, including obesity, insulin resistance and androgen excess. In a study looking at 40 PCOS patients and 20 age/BMI matched controls, Luque-Ramirez *et al*, (86) found that androgen excess was associated with an increase in carotid intima media thickness (cIMT) in patients with PCOS. Furthermore, increased cIMT has been shown to reflect preclinical atherosclerosis, an established culprit in the development of hypertension (87). Conversely, a study employing the anti-androgen drug cyproterone acetate (2 mg/day) found that it increased systolic, diastolic ambulatory blood pressure measurements in PCOS patients (81).

1.3.4 Dyslipidaemia in PCOS

Dyslipidaemia in PCOS (and metabolic syndrome in general) is typically characterised by high LDL-cholesterol, low HDL- cholesterol levels and raised triglyceride (TG) levels, however various dyslipidaemia patterns have been described. Dyslipidaemia in PCOS appears to be common, yet the pattern and prevalence in PCOS is variable. Notably, the National Cholesterol Education Program reported ~70% of the PCOS population present with abnormal lipid levels (88).

In a recent meta-analysis of dyslipidaemia in PCOS patients (diagnosed against Rotterdam (and NIH criteria) found that on average women with PCOS have a higher TG and lower HDL-cholesterol than their respective counterparts. Moreover, the meta-analysis found that PCOS patients have elevated LDL- cholesterol levels even when matching subjects for age/BMI (89).

An array of dietary, ethnic, genetic and lifestyle factors might play a key role in the pathology of PCOS dyslipidaemia. For example, a small proportion of PCOS patients from the Mediterranean (Italy, $n = 20$) presented with an altered lipid profile compared to their American counterparts ($n = 20$), with USA patients exhibiting significantly higher TG and lower HDL-cholesterol levels, even after adjustment for BMI (90). In addition, Carmina and colleagues also

found USA patients presented with an increased saturated fat intake, hyper-caloric diets and significantly higher BMI compared to Italian PCOS patients (91).

Akin to all other cardiometabolic abnormalities in PCOS, the pathogenesis of dyslipidaemia is multifactorial. Several mechanisms may influence this, with obesity, IR and hyperandrogenism likely playing key roles. For example, within adipocytes, IR and hyperandrogenism result in elevated catecholamine induced lipolysis and subsequent increased free fatty acids (FFAs) in the bloodstream. Elevated FFA flux to the liver may stimulate VLDL assembly and secretion resulting in hypertriglyceridemia. Testosterone has been associated with the regulation of hepatic lipase and scavenger receptor B1 (SR-B1) activity, both of which have been shown to reduce HDL levels in animal models. Moreover, testosterone (via androgen receptor interaction) has been shown to limit the removal of LDL by increasing the oestrogen receptor-mediated inhibition of the LDL-receptor, resulting in elevated LDL levels in the circulation. However the exact mechanism of how this occurs remains unclear (92).

1.3.5 Insulin resistance in PCOS

IR appears to be of paramount importance, not only for PCOS pathology, but for several CVD entities, as evidenced by the finding that IR and atherosclerosis frequently coexist in common proatherogenic disorders. By definition, IR is a common pathologic state where target cells fail to efficiently respond to endogenous insulin and is subsequently linked to the development of type 2 diabetes (93).

In 1980, Burghen and coworkers first described the association of PCOS and IR (94). They found that obese PCOS women had elevated glucose levels and an increased glucose area-under-curve (AUC) following an oral glucose tolerance test (OGTT) compared with age/BMI-matched control women. However, in this study no difference was found between non-obese PCOS patients and their respective counterparts. Apter *et al*, (95) found the prevalence of IR in adolescent PCOS patients was ~20-40%, which was markedly higher than the prevalence rates reported in population-based studies for women of the same age (10.3% by WHO criteria in women aged 20–44 year). Additionally, in a recent cross-sectional study in our own research group involving 84 PCOS patients (diagnosed using Rotterdam criteria) and 95 healthy volunteers, Rees and colleagues found that PCOS subjects had an elevated insulin response (insulin AUC) following a 75g OGTT (96). In another study, Dunaif *et al*, (97) found that PCOS patients showed subnormal insulin action coupled with a reduced glucose effectiveness

(i.e. the ability of glucose per se to stimulate glucose uptake and suppress hepatic glucose production, independently of insulin), compared to controls.

Carmina *et al*, (98) investigated the prevalence of IR in 3 geographically and genetically different populations (PCOS patients from the United States, Italy, and Japan, 25 patients per group). In this study fasting insulin was elevated in all groups when compared to age/BMI matched controls, but was greatest within patients from the United States and Italy compared to Japanese PCOS patients. The study also noted that the prevalence of IR, estimated from the results of an insulin tolerance test, ranged from 68 - 76%, across all ethnic groups.

Although IR is a common feature of PCOS and confers a substantial burden, not all women with PCOS present with IR. As many as 50% of obese women with PCOS may not have documented insulin resistance by intensive testing and this prevalence has been shown to be even lower in non-obese PCOS patients (99-101). On balance, PCOS is a heterogeneous disorder, reflected by the different phenotypes which may or may not present with IR. In a recent review, Christakou and Diamanti-Kandarkis concluded that the reported prevalence of IR in PCOS within the literature was 44-70%, a rate higher than the prevalence for IR in the expected general population (102). It has been suggested that different diagnostic criteria used in the array of studies looking at IR in PCOS may account for some of the discrepancies in the prevalence and severity of IR. With the Rotterdam criteria giving a spectrum of possible phenotypes (four), with each phenotype harbouring differing degrees of IR. It has been suggested that those patients presenting with all three symptoms on the Rotterdam criteria present with the most severe IR (103).

Insulin is a potent endocrine hormone that acts upon insulin sensitive tissues, including adipose tissue, skeletal muscle and the endothelium. Upon binding to its receptor, insulin initiates the phosphorylation of insulin receptor substrate (IRS), which subsequently activates phosphoinositide 3-kinase (PI3K) and mitogen-activated pathway kinase (MAPK) pathways. As IR is a tissue selective complication, the body will compensate for an impaired insulin responsiveness by producing excess insulin (hyperinsulinaemia). Hyperinsulinaemia in unaffected insulin-sensitive tissues will cause an imbalance in P13K mediated insulin signalling. IR in PCOS has been characterised in adipocytes by a post-binding defect in the insulin receptor-mediated signal transduction, which has also been confirmed in clinical studies of skeletal muscle action. In studies taking skeletal muscle biopsies from PCOS patients undergoing a hyperinsulinaemic euglycemic clamp, investigators have shown that women with PCOS have a decreased insulin-induced peroxisome proliferator agonist receptor-γ (PPARγ) co-

activator 1α (PGC-1α) and enhanced IRS-2 expression when compared to controls (104). From subcutaneous adipocytes derived from 9 obese and 7 lean PCOS patients (with BMI matched controls), Rosenbaum *et al*, (105) noted that GLUT-4 expression was decreased in PCOS patients by 36%, independent of obesity. Collectively, these molecular abnormalities may lead to selective resistance to the actions of insulin.

In addition to IR, β-cell dysfunction is a frequent feature in women with PCOS. It is this dual combination of these two metabolic derailments that synergistically contribute to the development of T2DM. Moreover, impaired glucose tolerance (IGT) and type 2 diabetes are both increased in women with PCOS compared to women of similar BMI with regular menses. In fact, in a large study of glucose intolerance among women with PCOS, 38.6% of the PCOS women had either IGT (31.1%) or diabetes (7.5%) by WHO criteria (99).

1.3.5.1 Insulin resistance and PCOS pathology

In patients with PCOS, excess insulin disrupts metabolic homeostasis. Such effects include androgen secretion by the ovarian theca; acanthosis nigricans and abnormal hepatic and peripheral lipid metabolism (103). Specifically, elevated insulin levels directly increase luteinizing hormone (LH)-stimulated androgen secretion from the ovary. Furthermore, in a study looking at 6 obese PCOS patients, elevated insulin levels were shown to decrease circulating sex hormone-binding globulin (SHBG) levels, subsequently yielding higher levels of free androgens (106).

There are a number of studies linking IR with a spectrum of CVD aberrations. Notably, there is a striking association between IR and endothelial dysfunction. Kelly *et al*, (107) demonstrated an elevated pulse wave velocity (PWV, (increased vascular stiffness) and a functional defect in the vascular action of insulin in patients with PCOS (measured via micro-myography *ex vivo*). Several studies have also demonstrated an association between IR and increased carotid IMT and FMD of the brachial artery in women with PCOS, independent of age and obesity (108).

During endothelial homeostasis, insulin binds to IRS and activates downstream MAPK and PI3K pathways. In IR states, as in PCOS, imbalances in these pathways occur, as a result of hyperinsulinaemia, impairment of PI3K pathway leading to decreased eNOS and subsequently NO levels (103). Also, hyperinsulinaemia associated MAPK activation promotes ET_1 expression coupled with increased expression of surface adhesion molecules such as VCAM-1

and E-selectin. Thus, IR is associated with endothelial dysfunction and may contribute to the development of accelerated atherosclerosis (103).

The effects of insulin sensitisers on CVD pathology in PCOS are discussed in sections 1.3.7 and 1.3.8.

1.3.6 Inflammation in PCOS

In an observational study looking at 8 lean and 8 obese PCOS patients and age/BMI matched healthy controls, Gonzalez *et al*, (109) declared that women with PCOS exhibited higher inerleukin-6 (IL-6), sICAM-1, C-reactive protein (CRP) and plasminogen activator inhibitor-1 (PAI-1) levels compared to controls. In agreement, Diamanti-Kandarakis *et al*, (110) found that plasma hsCRP, sICAM-1 and sE-selectin levels were higher in the PCOS group compared to age/BMI matched controls. Interestingly, although soluble (s)VCAM-1 did not differ between the groups at baseline, a significant reduction in hsCRP and sVCAM-1 was noted in PCOS patients following 6 months of metformin administration. Thus, several studies have suggested that PCOS patients suffer from low-grade chronic inflammation which may play a role in atherogenesis and may be intrinsically linked to the development of IR (111).

1.3.7 Obesity in PCOS

With a spectrum of cardiometabolic abnormalities noted in PCOS, obesity is a major aggravator and often presents as a confounder in the interpretation of clinical studies. Clinically, a BMI of 25–29 kg/m^2 is classified as overweight whilst subjects with BMIs ≥30 kg/m^2 are regarded as obese. Obesity prevalence in PCOS varies between studies (38-88% of patients). In a large observational study looking at 1741 PCOS patients, 38.4% were classified as obese, however this was based upon BMI >25 kg/m^2 (112). With multiple studies demonstrating symptomatic improvements in PCOS following even modest weight loss, the marriage between obesity and PCOS appears to be an integral feature in PCOS pathophysiology.

Independent of PCOS per se, obesity is an established risk factor and prerequisite for the array of cardiometabolic abnormalities seen within the syndrome, including hypertension, dyslipidaemia and accelerated atherosclerosis. Adipose tissue is an important endocrine organ that synthesises and secretes a variety of compounds into the bloodstream, playing a key immunomodulatory role. For example, adipocytes are a significant source of TNFα, IL-6, PAI-

1, lipoprotein lipase, oestrogens (through P450 aromatase activity), leptin, adiponectin, insulin-like growth factor-I (IGF-I) and insulin-binding protein 3 (IGFBP3). In addition to mature adipocytes, adipose tissue contains a network of pre-adipocytes, macrophages and vascular constituents. There is growing evidence to suggest that an increased adipose tissue mass directly elevates systemic inflammation. Numerous studies have found that BMI positively correlates with increases in systemic proinflammatory indices, including C-reactice protein (CRP), IL-6, plasminogen activator inhibitor-1 (PAI-1), P-selectin and VCAM-1 (113, 114).

BMI is the most widely used measure of obesity in clinical practice. However, like other anthropometric measures, it is only a surrogate measure of obesity and is fraught with numerous limitations which are often overlooked when considering the associated benefits of BMI. Although BMI is of fundamental importance in predicting numerous pathological conditions including MI, type 2 diabetes, stroke, hypertension and even CVD mortality (115), BMI offers little information in regards to fat distribution or total body fat percentage. However a comprehensive assessment of total body fat distribution can be achieved using more sensitive methodology (for example computerised tomography (CT) scans).

There is much evidence to suggest that the regional distribution of body fat is an important factor in the relationship between obesity, metabolism and the development of CVD. Broadly, visceral adipose tissue appears to show a much stronger association than subcutaneous adipose tissue with CVD risk and mortality (116).

Rosito *et al,* (117) studied the CVD burden attributed by differing regional fat deposits in >1100 subjects, and concluded that visceral and pericardial fat are correlated with CVD mortality. Interestingly, in comparison to subcutaneous or pericardial adipose tissue, visceral fat has the richest accumulation of infiltrated macrophages. In turn, visceral fat is a source of several cytokines which may invoke a proinflammatory state and initiate oxidative damage leading to the propagation of atherosclerosis (118).

In a study investigating 200 overweight PCOS patients and 100 age/BMI matched controls, Cascella *et al*, (119) demonstrated that visceral fat amount (assessed by CT scan) associated with subclinical CVD in PCOS patients. In this study carotid IMT was positively correlated with visceral fat area, whereas an inverse relationship was found between FMD and visceral fat. In contrast, several studies have shown that visceral obesity is positively associated with endothelial dysfunction and premature atherosclerosis (120, 121).

Therapeutically, even modest weight loss achieved via diet and/or physical activity has been shown to improve an array of obesity-related factors. Additionally, weight loss (to achieve a healthy BMI) has been shown to improve PCOS symptoms including ovulatory function (122).

IR may be one of the most important factors linking abdominal visceral adiposity to cardiovascular risk. Impaired suppression of adipocyte lipolysis and elevated fatty acid levels are also associated with excess visceral adiposity, potentially contributing to the impairment of endothelial function (123). Visceral fat is also associated with increased levels of the pro-coagulant PAI-1 and low-grade inflammation (123). Besides these metabolic disorders, visceral fat accumulation is associated with elevated systolic blood pressure in postmenopausal women, and visceral fat reduction was directly associated with lowering of blood pressure.

1.3.8 Endothelial dysfunction in PCOS

Numerous studies have challenged the existence of endothelial dysfunction in PCOS at a physiological (Table 1.7) and biochemical level (Table 1.8).

Several studies have shown that PCOS patients have impaired endothelium-dependent and independent vasodilator responses in the brachial artery (108, 124). However, other studies have failed to detect changes in endothelium-dependent vascular function but have shown that women with PCOS appear to exhibit an impaired endothelium-independent vasodilator response (125). Whereas impaired endothelium-dependent vasodilatation is indicative of eNOS dysfunction endothelium-independent vasodilatation is more complex and may be indicative of smooth muscle dysfunction. In addition, obese women with PCOS show similar basal leg blood flow (LBF), but an impaired metacholine-induced LBF in comparison to age/BMI matched controls (126). Conversely, in a slightly larger study population employing FMD, no vaso-responsive difference was observed between PCOS and healthy controls (125).

On balance, endothelial dysfunction within PCOS remains unclear. Of interest, several studies have noted key relationships between endothelial dysfunction and with metabolic variables in PCOS. Studies have found that endothelium-dependent responses were positively correlated with free testosterone (124, 126) and BMI (126). However Worboys *et al*, (127) found that testosterone implants in post-menopausal women receiving hormone replacement therapy improved both endothelial-dependent and independent brachial artery vasodilation. Tarkun *et al*, (111) found that endothelium-dependent vasodilatation was inversely associated with CRP levels in PCOS patients. In this study, PCOS patients presented with severe endothelial

dysfunction in comparison to age/BMI matched controls. Additionally IR, total testosterone and total cholesterol were all independent predictors of reduced FMD. IR may play a pivotal role in the development of endothelial dysfunction in PCOS patients. In a study involving 10 obese PCOS and 13 age/BMI matched controls, Paradisi *et al*, (128), found that after 3 months of troglitazone therapy (600 mg/day), PCOS patients had improved metacholine induced LBF responses which was similar to their non-PCOS counterparts. Similar results were noted in studies involving metformin (1700 mg/day for 6 months) and rosiglitazone (4 mg /day for 12 months), where PCOS patients showed improved FMD (129, 130) and reduced plasma ET_1 levels (130). Also, in a randomised, placebo-control, cross over trial, previous work in our research group has found that metformin improves aortic and brachial PWV, central blood pressure and both endothelium-dependent and endothelium-independent vascular response in PCOS patients (131).

Table 1.7 **Summary of endothelial dysfunction in patients with polycystic ovary syndrome**

Reference	Methodology	Population	Interpretation
Carmina *et al*, (108)	FMD	50 PCOS patients 50 controls age/BMI matched	PCOS patients showed an impaired endothelial-dependent response and greater carotid ITM compared to controls.
Paradisi *et al*, (126)	LBF	12 obese PCOS patients 13 controls age/BMI matched	PCOS subjects showed a normal endothelial independent but diminished endothelial-dependent vasodilatation compared to controls.
Tarkun *et al*, (111)	FMD	37 PCOS patients 25 controls age/BMI matched	Women with PCOS showed a decreased endothelial independent and endothelial-dependent vasodilatation response compared to controls.
Orio *et al*, (11)	FMD	30 PCOS patients 30 controls age/BMI matched	PCOS patients showed an impaired endothelial-dependent response and greater carotid ITM compared to controls.
Kravariti *et al*, (132)	FMD	62 PCOS patients 17 controls age/BMI matched	PCOS presented with a decreased endothelial independent and endothelial-dependent vasodilatation response compared to controls.
Rajendran *et al*, (133)	PWV	24 PCOS patients: lean (n = 12), obese (n = 12) lean controls (n = 12) age matched	Women with PCOS displayed a greater PWV than controls PCOS patients demonstrated an impaired endothelial-dependent vascular response compared to controls.
Sorensen *et al*, (134)	FMD	44 PCOS patients 13 controls age/BMI matched	PCOS patients showed an impaired endothelial-dependent vasodilatation response compared to controls.
Sprung *et al*, (124)	FMD	19 PCOS patients 16 controls age/BMI matched	PCOS patients showed an impaired endothelial-dependent response compared to controls.
Mather *et al*, (125)	FMD	18 PCOS patients 19 controls age/matched	PCOS patients presented with similar endothelial-dependent and independent vascular response compared to the control group.
Meyer *et al*, (135)	FMD and PWV	100 OW PCOS 20 controls age/BMI matched	Subjects with PCOS showed increased arterial stiffness and an impaired endothelial-dependent vasodilatation response compared to controls.
Diamanti-Kandarakis *et al*, (136)	FMD	25 PCOS patients 25 Controls age/BMI matched	PCOS patients presented with a normal endothelial independent but diminished endothelial-dependent vasodilatation compared to controls.

FMD; flow mediated dilatation; LBF; leg blood flow; PWV, pulse wave velocity; OW, over weight; ITM, intima thickness media.

In addition to physiological indices of endothelial dysfunction, determining NO bioavailability within PCOS patients may reflect preclinical endothelial dysfunction. To date, studies assessing plasma NO bioavailability employed the Griess methodology for NO_x quantification. Several studies have found no difference in total NO bioavailability between PCOS patients and controls. In contrast, Bayram *et al*, and Mohamadin *et al*, (137) both demonstrated that women with PCOS exhibit decreased NO bioavailability. However a caveat of the studies to date is the methodology employed to detect plasma NO_x. In comparison to more sensitive techniques currently available and employed (such as ozone-based chemiluminescence), the Griess reaction is limited to detecting primarily NO_3^-, with NO_2^- detection limited by the poor sensitivity of the assay to measuring baseline plasma levels even in healthy individuals. Furthermore, NO_3^- is >70% derived from dietary sources and unless participants are maintained on a relatively nitrate-free diet prior to measurement, the plasma values are unlikely to reflect vascular NO availability. More recently, with improvements in detection and advances in recognising factors influencing NO_x measurement in blood, a more comprehensive understanding of blood NO_x in PCOS is possible.

Table 1.8 Nitric oxide measurements in women with polycystic ovary syndrome

Study	Methodology	Population	Interpretation
Nacul *et al*, (138)	Griess method	31 PCOS patients 20 controls age matched	NO levels were similar between groups
Kuşçu *et al*, (139)	Griess method	38 PCOS patients 23 controls age/BMI matched	NO levels were similar between groups
Mohamadin *et al*, (137)	Griess method	50 PCOS patients 30 Controls age-matched	Decreased total NO_x in Saudi PCOS patients compared to controls
Dursun *et al*, (140)	Griess method	25 lean PCOS patients 27 Controls age/BMI matched	NO levels were similar between groups
Turkcuoglu *et al*, (141)	Griess method	22 obese and 11 lean PCOS patients 11 obese and 24 lean controls	NO levels were similar between groups
Baskol *et al*, (142)	Griess method	30 PCOS 20 Controls age matched	NO levels were similar between groups
Bayram *et al*, (143)	Griess method	45 PCOS patients 17 Controls	Decreased total NO_x in PCOS patients compared to controls

NO, nitric oxide; NO_x, nitric oxide metabolites.

1.3.9 Oxidative stress in PCOS

Theoretically, elevated indices of oxidative damage would be expected in women with PCOS if oxidative stress had a significant contribution to pathophysiology. However, studies to date have shown conflicting results. Direct detection of ROS is challenging due to their potent reactivity. Thus, most previous studies relied upon more stable indices as biomarkers of oxidative damage to lipids and proteins. However, such oxidative stress biomarkers are associated with a complex biochemistry where the different thermodynamic and kinetic properties may contribute to the over estimation and inconsistent results (144).

Numerous studies have shown that PCOS patients present with an increased oxidative burden in comparison to their non-PCOS counterparts (145). Malondialdehyde (MDA) levels, an end product of polyunsaturated fatty acid (PUFA) oxidation, were commonly employed as an indication of oxidative damage in these studies.

Sabuncu *et al*, (146) found that plasma MDA levels were related to visceral fat, blood pressure and IR. In contrast, Gonzalez and colleagues found that basal plasma MDA levels were similar between women with PCOS and control subjects (147). However, in response to a 75g OGTT, the percent change in plasma thiobarbituric acid reactive substances (TBARS) as a consequence of hyperglycemia was higher in obese women with PCOS compared with lean and obese controls. Mononucelar cells such as macrophages are ubiquitous in adipose tissue and pose a significant threat to an injured endothelium. Mononucelar cells derived from PCOS patients were found to over-produce ROS in response to a 75g OGTT, *ex vivo*. The glucose challenge also increased $p47^{phox}$ expression (a key protein component of NADPH oxidase), in women with PCOS. Moreover, $p47^{phox}$ expression was negatively associated with insulin sensitivity and positively correlated with visceral fat percentage, whilst ROS generation (MDA levels) was positively associated with androgen levels (147).

Of note, Macut *et al*, (148) found that lean women with PCOS showed an increased level of plasma nitro-tyrosine (assessed by enzyme immunoassay). Elevated nitro-tyrosine levels are indicative of nitro-oxidative stress, formed most notably from the reaction between NO and $^{\bullet}O_2^-$ and specifically from $ONOO^-$.

A recent systematic meta-analysis assessing oxidative stress in PCOS (68 studies, involving 4,933 PCOS patients and 3,671 controls), found that compared to their non-PCOS counterparts, patients with PCOS presented with higher circulating concentrations of homocysteine, MDA, and asymmetric dimethylarginine (145). The magnitude of change in these markers was only

modest and the studies that underpinned the meta-analysis were generally limited to measurement of oxidant or antioxidant molecules in isolation and/or measurement of reaction end-products as surrogates of oxidative stress.

1.3.10 Antioxidant status in PCOS

With a growing awareness of oxidative stress in women with PCOS, many studies have also investigated the antioxidant status in these patients. In a study of 27 women with PCOS and 18 age/BMI-matched controls, Sabuncu *et a*l, (146) found that PCOS patients had an increased oxidative burden and reduced glutathione peroxidase activity. Similarly, a decrease was noted in SOD activity in PCOS patients when compared to healthy controls. Plasma and erythrocyte vitamin C and vitamin E levels were lower in PCOS patients compared to controls. However, no difference was observed in vitamin A and β-carotene levels between groups (149, 150).

Several studies have shown, measures of antioxidants in isolation yield conflicting results. Total antioxidant capacity (TAC) is used to assess the net effect on antioxidant defences. Fenki and colleagues found that women with PCOS exhibit a decreased total antioxidant capacity (TAC) (151). However, on assessment of 7 studies (260 PCOS patients and 210 controls), a meta-analysis found that TAC was similar between women with PCOS and respective controls, independent of age and BMI (145).

1.3.11 PCOS and cardiovascular disease: 'the uncertainties'

Since the early diagnoses of PCOS, a number of studies have highlighted the potential relationship between PCOS and CVD. There is considerable literature identifying established CVD risk factors (such as IR, hyperinsulinaemia, dyslipidaemia, hypertension and chronic low-grade inflammation) in patients with PCOS. However, the prevalence of the reported cardiometabolic abnormalities is difficult to predict. Not all PCOS patients present with IR. Furthermore, the clinical quantification of IR is determined by various methods which may further complicate inter-study comparisons. In addition, dyslipidaemia has been reported as a common metabolic abnormality within the syndrome, yet the pattern (type of dyslipidaemia) and prevalence is highly variable (92).

Notably, the various PCOS phenotypes also make inter-study comparisons challenging. Thus, it is not surprising, with such diversity in diagnostic criteria and subsequent PCOS phenotypes that studies yield conflicting results whereby PCOS patients present with differing cardiometabolic severity. The syndrome suffers from an unknown aetiology and has no clear genetic signature. Therefore, ethnic, geographic and demographic differences need to be considered when interpreting studies.

CVD risk in general, regardless of PCOS status is known to increase with age and BMI. Yet, not all studies assessing CVD in patients with PCOS use an appropriately age/BMI matched control group. Furthermore, many studies have used small sample sizes with limited long-term follow up.

The assessment of nitro-oxidative stress in PCOS has produced conflicting results, which may be due to numerous limitations in the methodology. Previous studies assessing NO bioavailability used methodology that fails to distinguish between NO_x metabolites and thus cannot detect any subtle changes in NO_2^- levels. Interpretation of previous results is made difficult by use of non-specific methods coupled with components of this complex biochemistry measured in isolation. This may have heavily influenced prior interpretation.

There is a lack of adequately powered prospective, long-term studies looking at CVD outcome in PCOS cohorts. Wild *et al*, (85) undertook a retrospective study looking at 678 patients diagnosed with PCOS before 1979. They found that women with PCOS had higher levels of hypertension, diabetes, a greater waist-to-hip ratio and hypercholesterolaemia compared to age-matched controls. However, after adjustment for BMI, despite the increased prevalence of several CHD risk factors, there was no difference found between groups with respect to CHD morbidity or mortality in middle aged-women with PCOS. In a 14 yr prospective follow-up study involving 82,439 females, Solomon and colleagues compared women with a regular menstrual cycle to women reporting irregular/very irregular cycles (between 1982-1996). They found that women with irregular/very irregular menstrual cycles had an increased risk of nonfatal or fatal cardiac events, even after adjusting for age and BMI (152). Furthermore, in a retrospective study looking at 21,740 PCOS patients, previous data from our research group showed that women with PCOS were not at increased risk of large-vessel-disease, cancer, or death, but they had increased risk of type 2 diabetes (data extracted from the General Practice Research Database in the United Kingdom, assessing patients with a diagnosis of PCOS between 1990 and 2010 (153)).

1.3.12 Treatment and management of PCOS

The main issues which arise in the management of PCOS include menstrual cycle regulation, control of hirsutism, fertility management and the treatment of cardiometabolic abnormalities. Recently, an expert panel from the Androgen Excess – Polycystic Ovary Syndrome Society published a consensus statement on the assessment and prevention of CVD in women with PCOS (76). With many possible phenotypes, the medical management of PCOS needs to be personalised to the patient. The expert panel stated that the medical community should be made fully aware that PCOS patients with obesity, dyslipidaemia, hypertension and subclinical vascular disease are at increased risk of CHD with those patients presenting with metabolic syndrome and/or type 2 diabetes at the highest risk. BMI, waist circumference, serum lipid/glucose, and blood pressure determinations are recommended for all women with PCOS, as is OGTT in those with obesity, advanced age, personal history of gestational diabetes, or family history of type 2 diabetes. Importantly, lifestyle management is of paramount importance for primary CVD prevention, whilst drugs targeting abnormal lipid profiles and hypertension should be prescribed if symptoms persist. Moreover, the panel also recommended insulin-sensitising drugs if risk factors persist, in agreement with the numerous studies that have highlighted the integral role IR plays in the development of endothelial dysfunction in PCOS (76).

1.4 Microparticles: Mediators of cardiovascular disease

Microparticle (MP) production is a curious and intriguing feature of eukaryotic cells. MPs are small, spherical extracellular vesicles enclosed by a phospholipid bilayer that typically occupy a diameter of ~30-1000 nm. *In vitro* studies have demonstrated that platelets, adipocytes, ECs, leukocytes and erythrocytes release MPs, some of which have been detected in biological fluids *in vivo* (154). Recently, MPs have received increasing attention, where they are not only believed to play a pivotal role in health and disease but are key research themes for potential diagnostic, prognostics and therapeutic applications across multiple disciplines.

1.4.1 History

The first suggestion of MPs was provided by Chargaff and West in 1946 (155). They noted that plasma-clotting time was prolonged if plasma underwent high-speed centrifugation or shortened if the centrifugation pellet was added back to plasma. However the cause of this remained unclear. Following this, in 1967 Wolf and colleagues detected a sub-cellular fraction using electron microscopy, finding small spherical vesicles (20 – 50 nm in diameter) derived from platelets and accordingly termed the discovery as 'platelet dust' (156). There were few observations of vesicles in biological fluids over the next couple of decades. More recently, the isolation of vesicles from cell culture medium gave rise to the terminology exosomes, microvesicles (MVs) and MPs (154).

1.4.2 Nomenclature

As a relatively new and multi-disciplinary research community, the nomenclature, clarification and detection of these vesicles remains abstract. Although the International Society for Extracellular Vesicles (ISEV) are making attempts to clarify these uncertainties, traditionally, cell-derived vesicles have been named according to their cellular origin. For example, dexosomes originated from dendritic cells; adiposomes derived from adipocytes and cardiosomes derived from cardiomyocytes (table 1.9).

More recently, these extracellular vesicles have been categorised into several classes (including exosomes, MVs, shedding MVs, apoptotic bodies/vesicles and MPs). These sub-classes of vesicles were named based on their physiochemical properties, such as size, density, lipid composition, sub-cellular origin (i.e. membrane derived or intracellular) and predominant protein markers. With such a diverse and heterogeneous nature, practically it is increasingly difficult to uphold one terminology over another. Also, despite recent advances, terminology such as exosomes, MVs and MPs have been interchanged in many published studies (154).

Arguably the most common term used in the published literature is MPs. In this thesis, the term MP will be used unless otherwise stated. For clarification, MP is a generic term that encompasses all extracellular vesicles (including exosomes and MVs), which are 30 – 1000 nm in diameter. However, for MP biogenesis, nomenclature will reflect the terminology used in original manuscripts.

Table 1.9 Overview of vesicle nomenclature

Previously, MP classification was often based upon the MPs cellular origin. Alternatively, MPs are now categorised on the basis of their biogenesis pathways.

Cellular origin nomenclature:

- Ectosomes: neutrophil derived MPs
- Cardiosomes: cardiomyocytes derived MPs
- Adiposomes: adipocyte derived MPs

More recently, different biogenesis pathways have driven changes in nomenclature. MP definitions based solely on MP size are not conclusive. Thus, more generalised (‘umbrella’) terminology such as MPs and/or extracellular vesicles is often used.

Terminology	Size	Sub-cellular origin	Markers
Microparticles (MPs)	30 nm – 1 µm	Both intracellular and membrane derived	-
Exosomes	30 – 100 nm	Exosomal classical pathway (intracellular derived)	TSG101, CD9, Alix, CD81, CD63
Microvesicles (MVs)	100 nm – 1 µm	Cell surface (membrane derived)	PS exposure on surface
Apoptotic bodies	1 – 5 µm	Cell surface (membrane derived)	-

TSG 101, tumour susceptibility gene 101; CD, cluster of differentiation; Alix, ALG-2-interacting protein X. Adapted from (154).

1.4.3 Microparticle biogenesis

MPs are released from both eukaryotic and prokaryotic cells. MP production is a natural phenomenon where the precise cytoskeletal events involved in the formation and release of MPs remain relatively unclear. Two cellular processes appear to promote this; cellular activation and apoptosis. Several mechanistic pathways have been implied in the biogenesis of MPs such as the classical exosomal pathway and membrane shedding (figure 1.6) (157).

1.4.3.1 Biogenesis: classical exosomal pathway

Exosomes are a homogeneous class of MPs that are believed to be of endosomal origin. To unravel the mechanisms which govern their formation, several studies have pharmacologically inhibited MP release *in vitro* by using sphingomyelinase, Na^+/H^+ and Na^+/ Ca^{2+} channel inhibitors (158). However, this type of cellular inhibition invokes a spectrum of pleiotropic effects, which makes it difficult to decipher the exact mechanism that governs MP formation. Arguably, the classic exosomal pathway is the most widely studied mechanism for MP formation. It involves the formation of intraluminal vesicles within multivesicular bodies (MVB). MVB are formed by the invagination (reverse – budding) of the membrane. In comparison to other intracellular budding events (i.e. intracellular transport vesicles for the transport of cargo between intracellular compartments), this reverse budding is unique to exosomes and apoptotic bodies (154). However, it remains unclear if all the MPs formed via reverse budding events use common intracellular machinery.

During the formation of the MVB, internalised membrane receptors/proteins are often silenced and degraded, a process which often requires the ubquitination of the receptor/protein. This post-translational modification leads to the subsequent interaction with the endosomal sorting complex required for transport (ESCRT) machinery. Core components of this protein complex include Alix (ALG-2-interacting protein X)/vacuolar protein sorting-31 (Vps31) and tumor susceptibility gene 101 (Tsg101) (154, 159). It is hypothesised that the presence of these proteins in exosomes suggests that exosome secretion could be dependent on the ESCRTs. Few studies have addressed the function of ESCRTs in the biogenesis/secretion of exosomes: one report proposed that HRS (hepatocyte growth factor-regulated tyrosine kinase substrate, an ESCRT-0 member) promotes exosome secretion by dentric cells (159), whereas other studies did not find any role for Tsg101, Alix or Vps4 in exosome formation in oligodendroglial cells (160). Paradoxically, Bobrie and colleagues noted that inhibition of Vps4B increases secretion

of exosomes (but also of soluble proteins) by major histocompatibility complex (MHC) class-II expressing HeLa cells (161).

Buschow *et al*, (162) have shown that dendritic cell derived exosomes express MHC class-II molecules, which do not require ubiquitination (or any ubiquitinated chaperones) and subsequently does not rely on the ESCRT machinery. Instead, targeting of MHC class II to dendritic cell derived exosomes may require their sequestration in lipid domains enriched in the tetraspanin (CD9). Additionally, Trajkovic and colleagues demonstrated the secretion of proteolipid protein within exosomes derived from oligodendroglial cells, a processes which required sphingomyelinase-derived ceramide (160).

On balance, it is fair to suggest that several proteins may play an influential role in MP biogenesis via the classical exosomal pathway. The formation of the intraluminal vesicles within MVBs has been shown to require ESCRT proteins, tetraspanins and ceramide, but the role and importance of all these molecules in exosome biogenesis is unclear and may vary depending on cell. However, the biogenesis of exosomes has been examined in different cell lines of differing maturity.

Mature MVBs fuse with the plasma membrane to release their content / secrete exosomes to the extracellular environment. Intracellular trafficking and fusion of compartments classically involve small GTPases of the Rab family. Different molecules have been described in different cells: Rab11 is required for Ca^{2+} induced exosome secretion by the K562 erythroleukemia cell line (163), Rab35 is involved in secretion of proteolipid protein-enriched exosomes by oligodendroglial cells (160), and Buschow *et al*, (162) have shown that Rab27A and Rab27B play complementary roles in spontaneous secretion of MHC class-II bearing exosomes by HeLa-CIITA cells.

The final step of exosome release involves the fusion of MVBs with the plasma membrane and expulsion of exosomes. This process is likely to involve a specific combination of soluble attachment protein receptor (SNARE) proteins (a membrane bound, multi subunit protein complex) (161, 164). However, the exact SNARE machinery involved remains unclear.

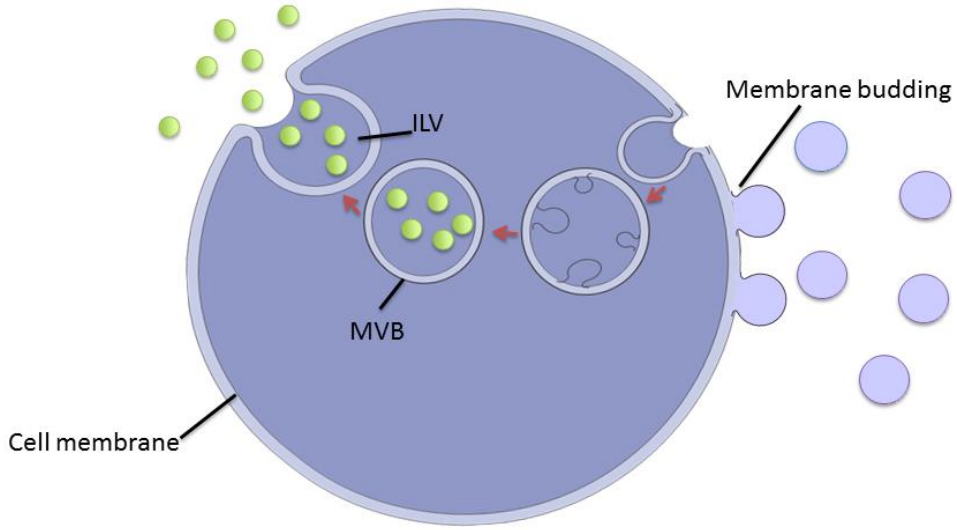

Figure 1.6. Microparticle biogenesis. Cells release microparticles (MPs) via two mechanisms. (i) The classic exosomal pathway involves the formation of intraluminal vesicles (ILVs) within multivesicular bodies (MVBs). In turn, the membrane of MVB fuses with the plasma membrane, resulting in the release of ILVs. When secreted, ILVs are called exosomes or MPs. (ii) The direct (membrane budding) pathway involves the release of vesicles directly from the plasma membrane. Adapted from (161).

1.4.3.2 Biogenesis: membrane budding

Plasma membranes consist of numerous proteins embedded in a double layer of phospholipids. During normal physiological conditions, phospholipids take up an asymmetrical distribution in eukaryotic cells, whereby the outer leaflet is enriched in phosphatidylcholine (PC) and sphingomyelin and the inner leaflet predominantly consists of phosphatidylserine (PS) and phosphatidylethanolamine (PE). Taken together, this serves as a semi-selective permeable membrane.

This alignment of membrane phospholipids is the result of active regulation of phospholipid asymmetry. Floppase, an adenosine triphosphate (ATP)-dependent membrane associated protein, specifically mediates the rapid preclusion of PS to the outer membrane leaflet and is directly responsible for the disruption of membrane asymmetry when cells are activated (165). Concomitantly, flippase, also an ATP-dependent membrane associated protein, mediates the translocation of amino-phospholipids from the outer to the inner plasma membrane leaflet

(166). In addition, scramblase plays an important role in the maintenance of lipid randomisation across the plasma membrane. Scramblase activation results in non-specific, bidirectional movement of membrane phospholipids. In turn, phospholipids on the inner leaflet are readily transferred to the outer plasma membrane leaflet and vice versa (154, 167, 168).

MVs (80-1000 nm) are another sub-class of MPs that are released directly from the plasma membrane during cellular stress. It is assumed that MVs form when the asymmetrical distribution of lipids between the inner and outer plasma membrane leaflets is compromised. When cells are activated or undergo apoptosis, the preclusion of PS to the outer leaflet is one of the first indicators of these processes. The externalisation of PS to outer leaflet of the membrane is the initial event that subsequently leads to the shedding of MVs. The cytoskeletal events that permit MP formation and detachment from the plasma membrane remain uncertain. Although likely to be cell specific, many studies to date have explored mechanisms governing MV biogenesis (membrane shedding) and show cells may share common cellular machinery (169).

The activation of a cell, often initiated by a variety of extracellular stimuli/agonists, is known to promote the formation of MPs. Monocytes, ECs and platelets have been shown to release MPs upon activation from stimuli such as TNFα and lipopolysaccharides (LPS). Cellular activation involves a rapid increase in cytosolic Ca^{2+} concentration, specifically at the membrane shedding microenvironment. This release of activated-cell associated MPs has been shown to be Ca^{2+} dependent. Mechanistically, elevated cytosolic Ca^{2+} activates kinases, inhibits phosphatases and induces calpain activation. Calpain, a Ca^{2+}-dependent thiol protease, is known to play an integral role in platelet MV formation. *Ex vivo* studies show that thrombin-induced platelet MV formation was inhibited when platelets were treated with calpeptin (a known calpain inhibitor) (170). Conversely Wiedmer *et al,* (171) did not see any inhibition of platelet MVs when inhibiting calpain, however this experiment used a different calpain inhibitor (leupeptin) which has been reported to poorly penetrate membrane bilayers. In addition, it has been suggested that MV formation in platelets in a resting state involves glycoprotein IIb/IIIa signalling, subsequently leading to destabilisation of actin filaments and MVs budding off the cellular membrane (172). Once the cellular cytoskeletal structure is destabilised and the budding sequence is initiated, caspases (cytoplasmic proteases) and calpain are responsible for the proteolytic cleavage of the MP from the cytoskeletal proteins (including filamin-1, talin and myosin).

In vitro studies involving a T-lymphocyte cell line have demonstrated that caspase 3 mediates the cleavage of ROCK I, a Rho Kinase protein subunit that induces cell membrane contraction by myosin light chain phosphorylation (168, 173). Moreover, Sapet *et al* (174) have identified

that several cytoskeletal proteins are related to thrombin induced MP release in ECs. These proteins include the Rho kinase subunits; ROCK I and II. These findings are in accordance with previous reports such by Tramontano and co-workers who stated that Rho activation was pivotal in the generation of endothelial MPs (EMPs) during inflammation. Inhibition of Rho kinase activity by lovastatin and the Rho-kinase inhibitor Y26732 also decreased MP formation in ECs (173, 175). Collectively, although the exact mechanism governing MP formation (via membrane budding/shedding) is not fully clear, several proteins are known to play a crucial role in their development.

1.4.4 Annexin V positivity

Most studies support the principle that cells release MPs following the collapse of the plasma membrane asymmetry and subsequent preclusion of PS to outer leaflet of the membrane bilayer. However, the presence of this externalisation of PS on the surface of MPs is a matter of much debate.

Numerous *in vivo* studies have shown that the MPs in the circulation are both PS positive and PS negative. This is commonly measured by the extent of annexin V binding, which indicates PS exposure and to a much lesser extent PE exposure. Connor *et al*, (176) found that, 80% of MPs derived from resting platelets (obtained from healthy subjects) failed to bind annexin V. Furthermore, altering the assay constituents (such as buffer, calcium and annexin V concentration) did not affect the degree of annexin V binding. Interestingly, this study did show that the proportion of annexin V positive MPs was dependent upon the agonist/stimuli, with physiological stimuli such as collagen resulting in fewer annexin V binding MPs than non-physiological stimuli such as Ca^{2+} ionophore. Conversely, other studies have shown that annexin V MPs occupy the vast majority of circulating MPs (>70%) (177).

Uncertainty also exists as to whether MPs formed via the classical exosomal pathway exhibit PS on their surface. Using immunogold labelling electron microscopy (EM), Heijen *et al*, (178) found that annexin V was not detected on the isolated platelet exosomes. In contrast, other studies have shown that exosomes expose PS and fuse with target cells in a PS-dependent manner, a process that was inhibited when exosomes were pretreated with annexin V (179).

Functionally, the extent of annexin V positivity may be great importance in multiple pathological conditions. Of note, Sinauridze and colleagues found that the surface of a platelet derived-MP (PMP) is ~50 - 100-fold more procoagulant than the surface of an activated platelet.

Moreover, other studies have shown circulating annexin V positive MPs is associated with endothelial dysfunction and cardiovascular events (180).

The nature of annexin V negative MP release is poorly understood. It is hypothesised that they represent basal tissue homeostasis. The difference between activated cell derived MPs and MPs derived from resting cells are not only differences in the external phospholipid profiles, but the array of bioactive cargo that is transported in the MPs. However, the methodological approach and pre-analytical protocols may play a crucial role in such discrepancies between studies and may partly account for the confusion as to the extent of annexin V positivity in MPs.

1.4.5 Microparticle isolation and characterisation

Accurate qualitative and quantitative analysis of MPs is of great value, but the current methodologies employed for the isolation, characterisation and quantification of MPs are far from standardised and contain a number of technical hurdles that have been shown to generate/manipulate MP number and function. Thus, the need for a consensus on both MP nomenclature and methods for isolation, identification and quantification has accelerated over the last 5 years and is a major goal for the ISEV. A motion to support this consensus will improve vital aspects for future MP research, as the current lack in methodological clarity obfuscates MP identification, renders inter-study comparisons troublesome and hinders the molecular elucidation of their biogenesis and physiological function.

1.4.5.1 Pre-analytical protocols: Isolation

MPs have been successfully isolated from various biological fluids and cell culture medium. Pre-analytical protocols have been extensively discussed in a review by Théry and colleagues (181). Most published studies have employed ultra-centrifugation based protocols for the isolation of MPs. This procedure is based upon the ability of the centrifugation force to sediment matter based on size and density, where larger and denser components migrate away from the axis of the centrifuge and vice versa for smaller, less dense components. Differential ultra-centrifugation involves sequential centrifugation steps with the aim of separating smaller and less dense constituents at each step. However, there is much variation in ultra-centrifugation protocols and this approach may also isolate a complex assortment of non-MP material. Arguably, this problem is more troublesome in biological fluids (i.e. plasma) than cell culture medium. The removal of cells from biological fluids is also challenging, where apoptotic bodies

and even platelets can often overlap in size with MPs in a viscous and dense fluid such as plasma. Additionally, it has been proposed that ultra-centrifugation itself may activate cells and in turn induce MP production during the isolation protocol. Additionally, the washing of MP pellets has been shown to reduce MP concentration, where studies have shown between 20-60% of PMPs are lost with every wash step (182).

Recently, Boing *et al*, (183) demonstrated that MPs could be purified from platelet poor plasma (PPP, healthy subjects) by sepharose CL-2B size exclusion chromatography. This approach allowed MPs to be separated from proteins and HDL-cholesterol. It is however unclear if this approach has any effect on MP function and needs to be fully explored in differing biological fluids. During the latter stages of my research, MP isolation by size-exclusion chromatography has received increasing attention. However, preliminary data on size-exclusion chromatography from our laboratory and other laboratories (Dr Aled Clayton, Velindre hospital - Cancer Research Wales) have failed to repeat findings described by Boing and colleagues, where in our hands, MPs and protein co-elute with only modest separation (unpublished observations). Table 1.10 summarises MP isolation protocols.

Table 1.10 **Differing pre-analytical protocols**

Blood collection	Plasma processing			Sequential centrifugation steps			Reference
Anticoagulant	**Centrifugation (*g*)**	**Time (Min)**	**Temp (°C)**	**Centrifugation (*g*)**	**Time (Min)**	**Temp (°C)**	
EDTA	1,200	20	4	100,000 x 2	60	4	*(184)*
Citrate	700	15	RT	13,000 x 2	60	RT	*(185)*
Citrate	2,750	10	n/a	-	-	-	*(176)*
n/a	1,500	15	n/a	13,000 18,000	2 20	n/a	*(186)*
Citrate	1,550	15	n/a	1,300	60	n/a	*(187)*
EDTA	1,550	20	20	17,500	60	20	*(188)*
Citrate	1,500	15	n/a	13,400	120	n/a	*(189)*
EDTA	270	20	n/a	1,500 21,000	20 45	n/a	*(190)*
Citrate	11,000	2	n/a	13,000	45	n/a	*(191)*
Cells (*in vitro*)							
Medium	4,300	5	n/a	100,000	90	10	*(187)*
Medium	400	5	n/a	2,000 10,000 100,000 x2	15 40 60 x 2	n/a	*(182)*
Medium	2,000	10	n/a	100,000	120	4	*(192)*
Medium	300	10	n/a	2,000 10,000 100,000	10 30 70	n/a	*(193)*

EDTA, ethylenediaminetetraacetic acid; n/a, not applicable refers to information not stated; RT, room temperature.

1.4.5.2 Pre-analytical protocols: Storage

It is impractical to immediately undertake a comprehensive assessment of MPs from clinical studies in which there may be several time points in succession and a large subject cohort. Thus the storage of MPs is of fundamental importance for clinical studies. To date, several cryo-preservation protocols have been described in the literature. Mobarrez and colleagues demonstrated that the number of PMPs increased 10-fold in frozen/thawed PPP compared to freshly analysed PPP, where phalloidin (binds to actin filaments) was used to detect fragmented cell debris (194).

Furthermore, the number of annexin V positive MPs (MPs bearing PS on their surface) also increased 10-fold with freezing compared to fresh sample, even when various methods of preservation were utilised (such as dimethyl sulfoxide, trehalose and paraformaldehyde) (195). In our laboratory, Connolly *et al,* (196) recently compared different freezing protocols and investigated the effect of time-in-storage on MP size and concentration. Storage time, regardless of method (freezing protocol) significantly increased MP concentration, suggesting samples should be analysed fresh whenever possible.

1.4.5.3 Qualitative and quantitative methods of microparticle analysis

Once the pre-analytical protocols have been chosen, researchers have a growing number of techniques to choose from for quantitation and characterisation of MPs. In contrast to the viewpoint proposed by many who claim one particular technique should be considered the gold-standard, currently there is no gold-standard technique used for the identification of MPs, with each technique harbouring its own advantages and limitations.

Numerous methods for the detection of MPs have been employed including flow cytometry, EM and enzyme linked immunosorbent assay (ELISA). More recently, novel techniques such as nanoparticle tracking analysis (NTA) and tuneable resistive pulse sensing (TRPS) have allowed more accurate quantification of vesicles, which were typically non-detectable by other methods. Each method of detection has certain limitations and advantages, thus the choice of technique used depends on the particular research question. Arguably, the greatest limitation in the MP field is the pre-analytical protocol for isolation and storage, whereas, the techniques employed

for MP quantification reflect advances in current scientific understanding and capabilities of methodology (154).

Van der Pol *et al*, (154) reported the magnitude of this problem and suggested the differing pre-analytical protocols and techniques, each with their own limitations and respective detection limits, that plasma MP concentrations range from 1 x 10^3 /ml to 1 x 10^{14}/ml.

1.4.6 Microparticle composition

MP membranes consist of mainly lipids and proteins. The exact composition is variable and depends upon the cellular origin and cellular stimuli. Numerous MP cell origins have been described in the circulation, including erythrocyte, platelet, endothelial and leukocyte-derived MPs (LMPs). During their biogenesis, MPs engulf an array of bioactive cargo from their parental cell. This cargo includes genetic information in the form of mRNA and microRNA (miRs), bioactive free fatty acids (FFAs) and protein. The bioactive cargo can reflect the stimulus which triggered MP formation (197), suggesting specific packaging of "message" prior to export from the parent cell. Following secretion, MPs may shuttle around this cargo, and can initiate a spectrum of cellular interactions that are now regarded as a novel means of cell-cell communication but also the potential for endocrine communication between organs/tissue locations (198).

1.4.6.1 Microparticle composition reflects stimuli

In vitro studies have demonstrated that the protein and RNA levels in exosomes secreted by ECs reflects the culture and medium conditions and physiological / pharmacological / pathological stimulus that triggers MP release (197). This suggests that ECs may secrete MPs as a means of coping with cellular stress. Moreover, during their biogenesis, MPs become enriched with an array of surface antigens. Identification of such antigens with a cocktail of antibodies is often used to determine the MPs parental cell. However, certain antigens are believed to be constitutively expressed and are not affected by stimuli or apoptotic status of the parental cell. For example, antigens such as CD144 (VE-Cadherin); CD11b and CD41 are commonly used antigens for endothelial, monocyte and platelet-derived MPs, respectively. Additionally, EMPs can be detected using markers against CD54 (ICAM-1), CD106 (VCAM-1), CD61E (E-selectin), CD62P (P-selectin) and TF. The presence of such antigens may dictate their fate, govern target cell interaction and ultimately their biological function. The degree of expression

of such antigens is believed to reflect parental cells activation/apoptotic status. Interestingly, CD54, CD62 and CD106 expression on MPs is known to reflect inflammatory activation of ECs. Additionally, MPs derived from apoptotic ECs have been shown to exhibit CD31 (PECAM-1) and CD62P. In comparison, CD51 (intergrin alpha5) and CD54 are preferentially expressed on activated EMPs (199).

1.4.7 Microparticle-mediated biological effects: cell-cell communication

MP–target cell interaction is likely to be cell and MP specific. Emerging evidence has demonstrated integrin activation, PS-dependent internalisation of MPs, IL-1 receptor activation, sonic hedgehog signalling, FFA transfer and miR transfer as possible mediators of MP-induced biological effects (169). However the precise mechanisms by which MPs interact with cells and induce functional responses remain unclear.

Terrisse *et al*, (200) found that fluorescently labelled human umbilical vein endothelial cells (HUVEC)-derived MPs were internalised as intact vesicles in HUVECs. Furthermore, confocal microscopy images suggested that MPs did not localise with markers of early or late endosomes.

Diehl *et al*, (201) demonstrated a different mode of action for MP–target cell interaction. They reported that MPs fuse with target cells and off load their bioactive cargo (miRs), which in turn alters the transcriptome potential of the target cell. In accordance, Hergenreider *et al* (202) recently demonstrated that ECs and SMCs communicate via exosomes that are enriched with miR – 143 / 145. These miRs regulate Krüppel-like factor 2 (KLF2), a transcription factor involved in a cardio-protective phenotype within ECs. They showed that these miRs are transferred to SMCs acting on miR targets and prevent SMC differentiation. In contrast, another study investigating the physical interaction between MPs and ECs, found that MP–target cell interactions is restricted to phospholipid surface interaction only. Furthermore, Burger and colleagues loaded HUVEC derived-MPs with carboxyfluorescein diacetate succinimidyl ester (CFSE, a non-fluorescent cell permeable compound that fluoresces when exposed to intracellular esterases). They found little evidence to suggest that CFSE labelled-MPs fuse with target cells to offload their bioactive cargo, as CFSE was undetectable in target cells (203).

Collectively there are many schools of thought regarding MP-cell communication. Thus, with

such variation, MP-cell interaction is likely to be MP and cell specific.

1.4.8 Microparticle clearance

In contrast to their biogenesis, much less is known about the mechanisms of MP removal. On the basis that MPs have been found to be engulfed by phagocytic cells *in vitro* (204), it is postulated that phagocytosis is the principle mechanisms governing MP elimination *in vivo*. In this regard, Willekens *et al*, (205) injected chromate (Cr)-labeled erythrocyte-derived MP into the inferior vena cava in rats and demonstrated that MPs are taken up by cells of the reticulo-endothelial system *in vivo*. The phagocytosis and interaction of MPs is thought to be chiefly governed by externalised PS, which may signal scavenger receptors, to promote endocytosis of MPs (200, 205). PMPs have been shown to be endocytosed and internalised in HUVECs, suggesting a role for EC clearance of MPs (206). In accordance with this, Dasgupta and colleagues noted that developmental endothelial locus-1 (Del-1), an EC membrane associated protein, was pivotal in this process. Inhibition of Del-1 prevented MP uptake/endocytosis in ECs *in vitro* and *in vivo* in mice deficient in Del-1 (207).

1.4.9 Cellular functions of microparticles

MPs, by mechanisms that remain controversial, can transfer biological information between cells, in turn acting as potent endocrine signalling vectors. MPs have been reported to play a pivotal role in several pathological conditions, such as inflammation, metastasis, thrombosis and endothelial dysfunction. The cellular effects of these biological vectors depend on their composition – (both membrane and cytoplasmic) and of course, the nature of the target cell.

MPs, being encased in a phospholipid bilayer themselves, provide an additional procoagulant surface for the assembly of the clotting enzyme complexes promoting thrombin generation. It has been proposed that their catalytic property relies on the exposure of the negatively charged PS on the outer bilayer, arguably a key characteristic for MP identification, which increases the potency of target cell interactions. For example, increased exposure of PS on the surface of PMPs renders their surface ~50 – 100 fold more procoagulant than the surface of activated platelet membranes (180) (figure 1.7).

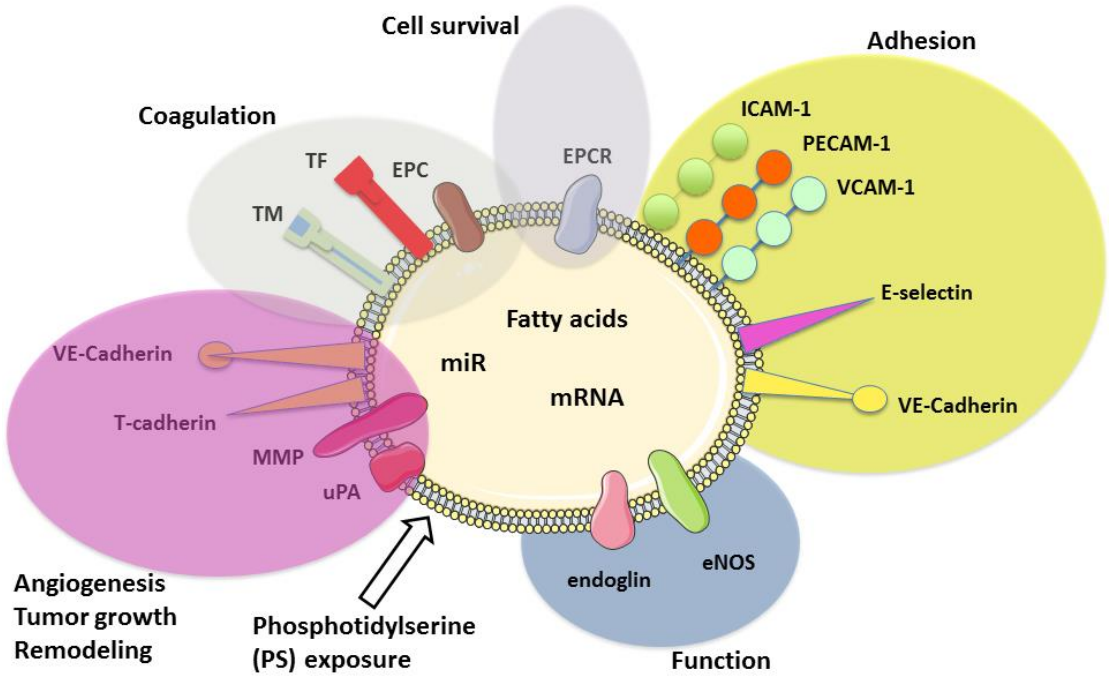

Figure 1.6. Schematic representation of an endothelial derived-MP and the associated biological effects. EPCR indicates endothelial protein C receptor; PECAM-1, platelet endothelial cell adhesion molecule-1; VCAM-1, vascular cell adhesion molecule-1; ICAM-1, intercellular cell adhesion molecule-1; E-selectin, endothelial selectin; VE-cadherin, vascular endothelial cadherin; eNOS, endothelial NO synthase; MMP, matrix metalloproteases; uPA, urokinase plasminogen activator; EPC, endothelial protein C; TM, thrombomodulin; TF, tissue factor; mRNA, messenger ribonucleic acid; miR, micro ribonucleic acid. Adapted from (167).

1.4.9.1 Inflammation and adhesion

MPs are involved in a variety of proinflammatory activities that may contribute to the pathophysiology of CVD. Notably, MPs have been shown to promote the adhesion, rolling and migration of leukocytes, harbour proinflammatory cytokines and initiate the further release of MPs in target cells *in vitro* (187, 208-211).

Forlow *et al*, (212) found that PMPs can enhance the binding of neutrophils to other neutrophils pre-bound to the surface of a flow chamber. The molecular mechanism for this phenomenon appears to be an interaction between P-selectin on PMPs and P-selectin glycoprotein ligand-1 on neutrophils, since administration of blocking antibodies against these surface molecules abrogates the effects of PMPs. Furthermore, PMPs have been shown to promote cell–cell contact by inducing adhesion molecule expression (209).

Membrane associated receptors and surface adhesion molecules enable crosstalk between MPs and target cells. *In vitro* studies indicate that MPs can fuse and pass this fatty acid biosignature into target cells, where it can alter cellular lipid metabolism and subsequent lipid-mediated cell signalling. Barry and co-workers (213)found that PMPs induce platelet activation through the transfer of arachidonic acid (C20: 4n6) (213). Arachidonic acid was shown to propagate pro-inflammatory effects by its subsequent metabolism to thromboxane. Moreover, in these studies, the transfer of arachidonic acid also stimulated the expression of cyclooxygenase-2 (COX-2) and the production of prostaglandins in ECs, a state which was mimicked by the direct treatment of arachidonic acid. To date, little is known about the lipid content of circulating MPs, although Fourcade *et al* (214) found differences in lipid composition between synovial fluid MPs from patients with arthritis compared to MPs from healthy controls.

In addition to PMPs, MPs released from various cell types can demonstrate proinflammatory properties. EMPs have been shown to harbour tissue factor (TF), a potent initiator of the coagulation pathway (187). The thrombin generating capacity of EMPs was first demonstrated using primary HUVECs, by the reduction of the clotting time of normal plasma incubated with increasing amounts of EMP released *in vitro*. The thrombogenic capacity of EMPs was confirmed via a thrombin generation assay where EMPs initiated TF-dependent thrombin formation i*n vitro* and thrombus formation *in vivo* (rat thrombosis model) (215).

Moreover, TF-positive EMPs expressing endothelial adhesive molecules can bind to other cell types, such as monocytes, and transfer their bioactive TF *in vitro (216)*. EMPs have been demonstrated to express surface adhesive molecule profiles similar to those expressed by activated ECs (216). Expression of endothelial antigens by THP-1 (monocyte) cells incubated with EMP was shown by immunoperoxidase staining and flow cytometry using antibodies directed against E-selectin, VCAM-1, and endoglin. EMP binding to THP-1 cells following a 4 hour EMP treatment, (50:1, EMP:THP-1) led to an increase in THP-1 procoagulant activity (determined by a clotting assay). Concomitantly, THP-1 exhibited elevated TF antigen levels and TF mRNA compared to control cells. Interestingly, the ability of EMPs to promote THP-1 procoagulant activity was restricted when THP-1 cells were incubated with ICAM-1 and β2 integrin blocking agents. This, suggests that EMPs interact with THP-1 cells *in vitro* and stimulate TF-mediated procoagulant activity that is partially dependent on the interaction of ICAM-1 on EMP and its counter receptor, β2 integrins on THP-1 cells (216).

In human aortic ECs, Curtis and colleagues found that EMP release was positively correlated with IL-6 release, thus postulating a relationship between MP generation and cytokine

production (217). Additionally, this interaction triggers elevated ICAM-1 mRNA expression and increased secretion of sICAM-1 in targeted unstimulated ECs. Interestingly, the functional effects of EMPs was influenced by conditions of generation (the stimulus), whereby non-TNF induced MPs exerted no effect.

In vitro studies have shown that polymorphonuclear leukocyte (PMNL)-derived MPs modulate EC activation and IL-6 release (208). In contrast to other studies, Mesri and coworkers observed that in response to blockage of adhesion molecules to β2 integrin, ICAM-1 or TNFα did not reduce IL-6 release. Furthermore, MPs did not activate nuclear factor- κB (NF-κB) or extracellular-signal-regulated kinases (ERK-1) signalling pathways (208).

Contrary to the bulk of MP literature, other studies have shown that MPs may have either no impact on target cell inflammation or even exhibit anti-inflammatory effects. Neutrophil-derived MPs exerted no pro-inflammatory activity on human macrophages as assessed by the release of IL-8 and TNFα. Furthermore, Gasser and Schifferli, (218) noted that LPS-induced pro-inflammatory cytokine secretion (TNFα, IL-8, and IL-10) was significantly reduced in ECs pre-treated with neutrophil-derived MPs. This effect was observed in a dose-dependent manner. In addition, MPs derived from formyl-methionine-leucine-phenylalanine (fMLP) stimulated neutrophils up-regulated the expression of the anti-inflammatory cytokine transforming growth factor β1 (TGFβ1) in macrophages (218), in turn suggesting that MPs down-regulate cellular activation in macrophages. Methodologically, several notable differences between this study and others might have influenced the results. For example, Gasser and Schifferli (218), stimulated their neutrophils for 20 minutes, whereas in other studies, stimulation periods have been for 24 hours. Furthermore, by collecting and using the MPs generated from a short stimulation period, Gasser and Schifferli may have selected MPs released early after stimulation, which might differ (compositionally / functionally) from MPs released at later time points. However, this remains unconfirmed. Additionally, all these studies have all employed different pre-analytical protocols and quantitatively determined MP amount using different techniques, making inter-study comparisons difficult.

1.4.9.2 Microparticles and endothelial dysfunction

In vitro studies have shown that EMPs impair acetylcholine-induced vasodilatation and decrease NO production by aortic rat vessels in a concentration-dependent manner. Concomitantly, the reduction in NO was coupled with an increase in $^{\bullet}O_2^-$ production. Moreover, Brodsky *et al*, (219) noted the presence of the $p22^{phox}$ subunit of NADPH-oxidase in EMPs. Interestingly,

when EMPs were pre-incubated with SOD, endothelial function was improved, in turn suggesting that EMPs induce EC dysfunction via ROS (203).

Ex vivo studies provide evidence that MPs isolated from patients with acute MI can cause significant endothelial-dependent impairment of rat aorta vessels. This impairment was not affected by diclofenac or the SOD mimetic Mn(III)tetra(4-benzoic acid) porphyrin chloride. No difference was noted in endothelial-independent relaxation (to sodium nitroprusside) or in EC eNOS expression (191). These data indicate that circulating MPs from patients with an acute MI selectively impair the endothelial NO transduction pathway.

Similarly, *ex vivo* treatment of ECs with MPs from patients with metabolic syndrome resulted in decreased eNOS expression and consequently decreased NO production. Interestingly, a reduction in $^{\bullet}O_2^-$ and an increase in protein tyrosine nitration were also noted in ECs treated with MPs from patients with metabolic syndrome, but not from MPs from healthy controls. MPs from both groups did not affect the inflammatory status of ECs. However, *in vivo* injection of metabolic syndrome patient-derived MPs into mice impaired endothelium-dependent relaxation and decreased eNOS expression (220).

In contrast to the majority of studies, Agouni *et al* (221) found that MPs derived from human lymphoid T cells harboured the morphogen sonic hedgehog (Shh). Previously, Shh has been shown to be involved in erectile dysfunction, a state associated with a reduced NO production. Moreover, eNOS and VEGF are established downstream targets of exogenous Shh signalling. In this study, treatment of HUVECs with T cell-derived MPs resulted in increased NO release and triggered increased phosphorylation of eNOS enzymes and reduced ROS production. In addition, *in vivo* injection of T cell-derived MPs in mice (10 µg/ml blood) was also able to improve endothelial function. Mouse blood, aorta, and lung tissue exhibited a greater NO-Fe^{2+} diethyldithiocarbamate Fe(DETC)2 electron paramagnetic resonance (EPR) signal in mice treated with MPs than in control mice. This enhanced NO production by MPs provided cardio-protective properties. Endothelial dysfunction, initiated by an ischaemia reperfusion insult, was entirely reversed by the administration of MPs 24 hours prior to ischaemia, showing that MPs may serve as cardio-protective vectors against endothelial injury. These findings were also abolished when Shh was silenced, suggesting Shh was central to this protective mechanism (221). Supporting this, other studies have investigated chronic (21 days) *in vivo* treatment with Shh bearing MPs in mice. Following an ischaemic insult, Benameur and colleagues showed that the recovery of the blood flow was 1.4 fold higher in MPs^{Shh+} treated mice than in controls and that this was associated with an increase in NO production in both aorta and muscles (222).

A later study from the same research group, also looking at T cell-derived MPs displayed conflicting results (223). In contrast to Agouni and colleagues (221), this more recent study demonstrated that ECs treated with MPs demonstrated a decreased NO production. Furthermore, MPs enhanced ROS production by a mechanism sensitive to xanthine oxidase. Also, *in vivo* injection of MPs (10 μg/ml) in mice impaired endothelial function.

On balance, there is a burgeoning awareness that MPs may play an important role in the pathogenesis of endothelial dysfunction and a spectrum of CVD entities. Studies have shown that MPs not only harbour ROS but can induce an oxidative burden in target cells. However, when interpreting the above studies it is important to consider that the studies mentioned used different MP-target cell/vessel incubation times, ranging from 3-24 hours. Additionally, pre-analytical protocols and cellular stimuli also differed between studies.

1.4.10 Apportion of circulating microparticles *in vivo*

MPs have been detected from a variety of biological fluids, including urine, seminal fluid and synovial fluid. By far the greatest research has focused on circulating MPs, where erythrocyte, leukocyte, platelet and endothelial-derived MPs have been detected. However, there is much variation in the reported origin and apportion of circulating MPs in plasma.

Methodologically, although ELISA, immunofluorescence and immunogold labelling (EM) have been employed, arguably the most established means of determining MP origin is by flow cytometry, using antibodies against specific parental cell markers. This presents several limitations. It is well established that cytometric analysis of MPs struggles to capture the entire MP spectrum, whereby many circulating MPs fall below the detection limit of conventional flow cytometers (limitations of flow cytometry furthered discussed in chapter 7).

In a recent study looking at 6 healthy volunteers, the majority of circulating MPs were observed to be of erythrocyte origin (37.5%), whilst PMPs occupied 24.3%, LMPs occupied 12% (of which 3.4% were monocyte derived) and 6.6% of circulating MPs were from endothelial origin. Additionally, in this study the MP concentration for platelet poor plasma (PPP)-derived MPs was ~2.5×10^6 / ml (224). Conversely, Shah *et al* (225) found higher percentages of endothelial and monocyte-derived MPs in healthy subjects (43% and 10.4%, respectively), which may reflect different methodologies and pre-analytic protocols. However, most studies report that MPs derived from platelets are the most abundant.

1.4.11 Microparticles in disease

In addition to playing a fundamental role in CVD, MPs have been implicated in a diverse spectrum of pathological conditions. Arguably, the most widely researched discipline of MPs falls within cancer. In cancer, MPs have been shown to play an important role in tumor metastasis and tumor angiogenesis. Tumour derived MPs have been shown to harbour and off-load oncogenic cargo in non-cancerous cells, propagating the cancer's pathology (226). Increased levels of EMPs and PMPs have been detected in the serum of patients with multiple sclerosis (227). Also, circulating MPs have been found to be increased in several infectious diseases including sepsis regardless of the causative pathogen. Of interest, in highly contagious disorders such as Ebola, the overexpression of TF from monocytes/macrophages is recognised as a primary event in the haemorrhagic and thrombotic complications. In non-human primate models, TF-bearing MP production was increased following Ebola infection (228). MPs derived from T cells are elevated in other infectious diseases such as HIV (229). Also, MPs have been shown to be pivotal in malaria, where the knockdown of ATP-binding cassette transporter-1 (ABCA1), a lipid transporter implicated in MP biogenesis in transgenic mice, protects from severe malaria and is associated with lower MP levels in plasma (230, 231). Table 1.11 highlights diseases where circulating MPs levels are elevated.

Table 1.11 Diseases where circulating microparticles are increased

Disease	MP population increased
Acute coronary syndrome	Total, EMPs, PMPs
T2DM	Total, PMPs
Hypertension	PMPs, EMPs
Inflammatory disorders	PMPs
Pre-eclampsia	LMPs
Lupus anticoagulant	EMPs
PCOS	Total, PMPs
Stroke	EMPs
Metabolic syndrome	Total

Total, total microparticle (MP level); EMPs, endothelial derived-MPs; PMPs, platelet derived-MPs (PMPs); LMPs, leukocyte derived-MPs. Adapted from (157).

1.4.12 Microparticles in cardiovascular disease

The multifactorial nature and complex pathophysiology of CVD and the development of endothelial dysfunction and atherothrombotic complications involves numerous interactions between multiple cell types and tissues. A recent focus in the field is on the role of circulating MPs in EC damage, hypercoagulability and inflammation.

MPs appear to play an important role in the pathogenesis of CAD, where MPs derived from monocytes and lymphocytes have been found in atherosclerotic plaques (232). Also, in addition to acute coronary syndromes and stable CAD (233, 234) increased number of MPs have been identified in risk states for CVD, such as diabetes mellitus (234) and hypertension (235). Specifically, EMPs (CD144/CD31/CD51 and annexin V positive) were increased in diabetic patients. Furthermore, circulating EMPs have been correlated with the presence of non-calcified coronary plaques in diabetic patients (236). Several studies have also demonstrated that diabetic patients have increased circulating LMP and PMP levels. Studies in type 1 diabetics found that patients present with increased levels of PMPs and EMPs, whilst patients with type 2 diabetes have increased levels of PMPs (237).

Additionally, EMPs appear to be sensitive to even modest haemodynamic changes in hypertension, where increases in EMPs rise in proportion to elevations in pressure (238). Interestingly, TF-bearing MPs are increased in patients with hypertension (239). Notably, pulmonary hypertension is associated with an increase in circulating MPs derived from platelets, leukocytes and ECs (240). However, Amabile and colleagues found that increased EMPs (CD62P positive) but not LMPs predicted adverse clinical events in patients with

pulmonary hypertension in a prospective 12 month follow up study. Also, PMPs have been correlated with diastolic blood pressure (241).

Further evidence for a potential role in CVD pathogenesis comes from observations of increased numbers of MPs during inflammatory states *in vivo* (240). To date, the question of whether antithrombotic therapy has any impact on plasma MP levels in hypercoagulable conditions has not been answered. One study examining PMPs in atrial fibrillation, reported that treatment with aspirin and/or warfarin had no effect on MP count or function (242). However whether antithrombotic therapy has an effect on MP levels in other hypercoagulative states remains unclear. Current US based clinical trials are on-going, investigating the impact of ticagrelor, an anti-coagulant drug on circulating MPs in patients with heart disease (243).

Circulating MPs harbor eNOS. In patients with CAD, endothelial dysfunction was associated with an increase in the total number of circulating MPs as well as a significant decrease in the expression and activity of eNOS in MPs (244). However, no difference in ROS was noted in MPs isolated from CAD patients and the control group. In one study looking at 44 patients with end-stage renal failure, Amabile and colleagues noted that circulating levels of annexin V positive MPs were increased compared with 32 healthy subjects (245). However, only EMPs correlated with elevated FMD, increased aortic and increased carotid artery augmentation index. Interestingly, PMPs, erythrocyte-derived MPs and annexin V positive MP levels did not correlate with measures of endothelial dysfunction. Furthermore, *in vitro* studies have shown that MPs derived from patients with end-stage renal failure, impaired endothelium-dependent relaxation and cGMP generation, whereas MPs from healthy control subjects did not (245).

In another study, increased MP levels were positively correlated with impairment of coronary endothelial function. Moreover, increased MP counts were able to predict severe endothelial dysfunction independent of classic CVD risk factors, such as hypertension, hypercholesterolaemia, diabetes, age and sex (246).

1.4.13 Scott syndrome

There is a vast amount of literature suggesting MPs play a detrimental role in disease pathology. However, MP biogenesis remains a natural phenomenon and is a process that happens in virtually all prokaryotic and eukaryotic cells. The physiological importance of MPs is perhaps best illustrated by Scott syndrome, a rare autosomal recessive disorder of platelet coagulant activity. It is characterised by a rare inherited defect of lipid scramblase within the membrane of

platelets. Consequently, the underlying defect is an inability to generate scramblase and regulate membrane symmetry. In turn, this results in reduced PS expression/externalisation and reduced MP production. The ability to activate prothrombin is impaired and patients with the syndrome exhibit severe bleeding (169).

1.4.14 Microparticles in polycystic ovary syndrome

MPs have been implicated in several CVD entities, which are linked to PCOS. However, to date, little is known about circulating MPs in PCOS. Koiou *et al* (186) found that circulating PMP levels were increased in patients with 'severe' PCOS compared to healthy controls. Specifically, patients diagnosed against the NIH 1990 criteria, where patients exhibit anovulation and hyperandrogenism presented with elevated levels of PMPs, however those diagnosed according to the more recent Rotterdam criteria did not (hyperandrogenism and PCO or anovulation and PCO phenotypes). However, the distribution and content of circulating MPs was not assessed. PMPs were also detected and quantified using flow cytometry. Koiou and colleagues did use calibration beads 0.5, 0.9 and 3.0 μm, but did not comment on the sensitivity of the cytometric analysis. Moreover, Van der Pol *et al*, (247) previously noted that on conventional flow cytometers, determining sensitivity and detection limits based upon calibration beads (often carboxylated polystyrene) does not truly reflect the refractive index characteristic of a heterogeneous MP population. This would over-estimate the detection limit, as the refractive index of a polystyrene bead is typically greater than that of an unknown, lipid enclosed cell/endogenous MP. In addition, Van der Pol *et al*, (248) introduced the concept of 'swarm theory' when employing flow cytometry for MP detection. Briefly, this refers to coincidence, whereby instead of a single MPs passing through the laser interception point at a given time point, multiple MPs may pass and be qualitatively and quantitatively assessed as one MP (as discussed in chapter 7).

Of interest, Koiou *et al*, (186) also found that plasma PMPs correlated with serum testosterone levels across all PCOS categories. Thus, PMPs, either as a cause or consequence, may be associated with hyperandrogenism in PCOS patients. Additionally, in a follow up study, Koiou *et al*, (249), assessed the status of plasma PMPs in overweight/obese women with PCOS. As previously noted, this study also found elevated plasma PMPs in women with PCOS than in age/BMI-matched controls. Furthermore, PMPs correlated with the mean number of ovarian follicles in PCOS patients. In turn, this suggests that independent of obesity, PCOS subjects have elevated PMPs in the circulation (186).

1.4.15 Biomarkers, therapeutics and diagnostics

As a growing field, to date, the majority of published studies have been observational in nature, trying to detect, measure, characterise and understand the function of MPs in numerous disease states. *In vitro* and more recently *in vivo* experiments have begun challenging MPs as diagnostic and therapeutic targets for the management of several disorders.

Much research has focused on MPs as potential biomarkers for CVD entities such as endothelial dysfunction as well as other pathological conditions. MPs released into blood, urine and other body fluids offer a unique opportunity to noninvasively access important biological information which could be potentially applicable to several disease states. In a 30 month prospective follow-up study looking at heart failure patients, Nozaki and colleagues (2010) found that endothelial dysfunction (as assessed by plasma levels of EMPs) was able to independently predict future cardiovascular events (250). Similarly, in CHD patients (n = 154), increased CD31/annexin V positive MPs were predictors of CHD related death and increased risk of recurrent hospitalisation due to CHF (251).

1.4.15.1 Potential role of microparticles as biomarkers in personalised medicine

If MPs truly reflect disease states (i.e. endothelial damage), it may be possible to use them as biomarkers in clinical practice. The ability to detect alterations in MPs, before the disease manifests (i.e. pre-disease stage), raises the exciting possibility of early intervention and potentially reversing certain pathologies.

MPs have already been used in diagnostics and therapeutics in cancer (specifically prostate cancer). Caris Life Sciences, a US based diagnostic, prognostic and therapeutic service company have developed Carisome technology. This patented technology has the ability to detect, identify and profile circulating MPs. Areas of diagnostic clinical practice include early diagnostic testing where circulating MPs shuttle a unique biosignature useful in the early detection of several types of cancer. Additionally, the bioactive cargo can be extensively profiled, generating valuable molecular information from diseased cells so that clinicians can tailor a therapeutic intervention. Also, the biosignature carried by diseased MPs could be used

to assess an individual's response to therapy. The prospect of utilising circulating MPs as biomarkers or as therapeutic targets is an exciting challenge with potential beneficial implications across several disorders.

1.4.16 Microparticles: cause or consequence of disease?

In the process of furthering the current understanding of MPs, paradoxical biological actions have surfaced in numerous disease pathologies. Firstly, it has been demonstrated that MPs shuttle an array of bioactive cargo including genetic information (mRNA, miRs) as well as bioactive fatty acids and surface cell receptors. Collectively they have been shown to represent a novel endocrine network playing a crucial role in cell-cell communication. Their influence on the target cells sometimes evokes paradoxical physiologic processes.

Although the literature is heavily influenced by studies highlighting the damaging nature of MPs in CVD and other disease states, there have also been numerous studies demonstrating cardio-protective roles of MPs. Interestingly, Nieuwland *et al*, (185) identified procoagulant MPs in patients undergoing cardiac bypass operations. The procoagulant nature of MPs seemed to provide beneficial intrinsic and extrinsic clotting in patients post cardiopulmonary bypass.

Considering the diverse functions of MPs and potential applications across several disciplines, our general understanding of MPs is accelerating rapidly. It remains a great challenge to decipher whether MP production is a cause or consequence of disease. However, understanding and characterising MPs in different diseases, such as PCOS, will potentially enable identification of new cellular pathways that are amenable to clinical intervention and therapeutic manipulation.

1.5 Thesis Aims and Objectives

The overall aim of this thesis was to provide a clearer understanding of mechanisms that may predispose young patients with metabolic risk factors to cardiovascular disease (CVD).

Hypothesis

Nitro-oxidative stress is central to the development of endothelial dysfunction in CVD and may play an important role in releasing pathologically relevant MP populations into the blood stream.

In order to achieve the aim of this thesis and challenge the hypothesis, the work was split into several themes, presented in individual result chapters, each with their own specific aims and objectives (a specific aims section is given in each results chapter).

Overall aims were:

- Using a phenotypically detailed PCOS cohort as a model of metabolic disease where patients appear to be prone to developing endothelial dysfunction, I chose to undertake a comprehensive characterisation of nitro-oxidative stress.
- The characterisation of circulating MP populations in PCOS patients and healthy controls.
- To translate the findings of the clinical investigations in order to explore the effect of pathologically relevant insults (akin to those featured in PCOS) by establishing *in vitro* models to study EC MP production.
- To examine the functional characteristic of EMPs formed in the *in vitro* models.
- To assess the effect of LDL-apheresis on circulating levels of MPs in patients with familial hypercholesterolaemia (FH).

2. METHODS

2.1 Details of ethical approval

The clinical studies were approved by Cardiff University (study sponsors), Cardiff & Vale University Health Board and the South East Wales research ethics committee. All subjects gave written informed consent before study commencement (Date awarded: 26/09/08; ethical approval: ref 08/WSE04/53). Ethical approval was sought by Dr Aled Rees (Institute of Molecular and Experimental Medicine – Cardiff University).

2.2 Subjects

Seventeen patients with PCOS (age 16-45 years) were recruited from the endocrine clinic at the University Hospital of Wales (UHW). Studies were carried out in a quiet, temperature controlled room where subjects were required to rest for 10 min before measurements. A diagnosis of PCOS was based on the Rotterdam criteria. Congenital adrenal hyperplasia, Cushing's syndrome, hyperprolactinaemia, androgen-secreting tumours and thyroid disease were excluded by biochemical testing. Subjects were excluded from participation if they were pregnant, breastfeeding, had a history of hypertension, hyperlipidaemia or diabetes, or had a history of current or recent (within 3 months) use of antidiabetics, lipid lowering agents, antioxidant medication, antihypertensives and/or antiandrogens. Healthy volunteers (n = 18; age 16-45 years) were recruited among medical students and staff within our institution. Volunteers had regular menstrual cycles (every 27-32 days). Their healthy state was established by history, physical examination and hormonal evaluation (thyroid function, prolactin, testosterone and 17-hydroxyprogesterone); those with features of hirsutism or a family history of PCOS were excluded. Patient recruitment was co-ordinated by Dr Maneesh Udiawar (Centre for endocrine and diabetes sciences – University Hospital of Wales).

2.3 Body composition assessment

Subjects attended the University Hospital of Wales Clinical Research Facility at 0800h after an overnight fast. Height, weight, hip and waist circumference were measured as per our research group's published protocols (252). Abdominal subcutaneous and visceral fat areas were measured by CT (Hawkeye, GE Medical Systems) on one cross-sectional scan obtained at the level of L4-L5. Scans were performed with subjects in the supine position using standard acquisition parameters (140 kV, 2.5 mA, 10 mm slice width, 13.6 second rotation time, 256^2 pixel matrix). CT images were segmented into fat and non-fat areas according to our previously published protocol (252). CT scans were co-ordinated by Dr Maneesh Udiawar and performed by Dr Helen Blundell (Dept. medical physics - University Hospital of Wales).

2.4 Biochemical measurements

Serum total cholesterol (TC), HDL-cholesterol, and TG were assayed using an Aeroset automated analyser (Abbott Diagnostics, Berkshire, UK); LDL-cholesterol was calculated using Friedewald's formula. Insulin was measured using an immunometric assay specific for human insulin (Invitron, Monmouth, UK) and glucose was measured using the Aeroset chemistry system (Abbott Diagnostics, Berkshire, UK). High sensitivity C-reactive protein (hsCRP) was assayed by nephelometry (BN™ II system, Dade Behring, Milton Keynes, UK) and total testosterone was measured by liquid chromatography-tandem mass spectrometry (Quattro™ Premier XE triple quadruple tandem mass spectrometer, Waters Ltd, Watford, UK). The intra- and inter-assay coefficients of variation were all less than 9%. Biochemical and testosterone measurements were carried out at the University Hospital of Wales [Department of Medical Biochemistry]. After basal sampling, subjects underwent a standard 75g oral glucose tolerance test (OGTT). Glucose and insulin was measured at 0, 30, 60, 90 and 120 minutes. The area under the curve (AUC) for insulin and glucose was calculated using the trapezoid method: where AUC = 15 X (C_0 + C_{120}) + 30 X (C_{30} + C_{60} + C_{120}).

2.5 Blood sampling

Fasting blood samples were drawn from an antecubital vein into EDTA, citrate or hirudin vacutainers. Samples were promptly centrifuged (1,024g x 10 min, 4 °C) to yield PPP. *Ex-vivo* oxidative stress measurements (lipid-derived radicals, described in section 2.7.1) were performed immediately whilst the remaining samples were stored at -80 °C for no longer than 2 months before analysis. For use, samples were thawed in a preheated (37 °C) thermostatically-regulated water bath for 3 min.

2.6 Plasma nitric oxide metabolites: Ozone-based chemiluminescence

2.6.1 Theory

NO metabolites (NO_2^- and NO_3^-) were assessed using well-established ozone-based chemiluminescence techniques, as previously described by our lab (247). Specifically, plasma NO_2^- and NO_3^- levels were measured using a NO analyser, ((NOA), Sievers NOA 280i, Analytix, UK) following cleavage from the species of interest by the use of specific cleavage reagents. NO in a flow of inert gas is passed via a NaOH trap to the NOA, where it reacts with ozone (O_3) in a reaction cell. This reaction forms NO_2*, an excitable form of NO_2 which dissipates energy in the form of photons (*hv*) as they move back to their ground state. These photons are then amplified by a photomultiplier tube (PMT) and converted to an electrical signal (mV) where the potential difference was recorded in real time (Sievers, Liquid NO analysis software) (28). The area-under-curve (AUC) for each peak is calculated and compared to a set of relevant reference standards to obtain a concentration. This is summarised below:

- $NO + O_3 \rightarrow O_2 + NO_2$*
- NO_2* $\rightarrow NO_2 + hv$

2.6.2 Plasma nitrite

For plasma NO_2^- analysis, 5ml tri-iodide reagent (I_3^-, consisting of KI 70 mM, iodine crystals 29 mM in 13.5 M glacial acetic acid) was placed in a glass purge vessel and heated at 50˚C via a water bath thermostatically controlled by a hotplate. The carrier gas (O_2-free N_2) purging I_3^- was linked to a sodium hydroxide (NaOH) trap (1M), connected to an NO analyser. Samples (200 µl) were injected directly into the purge vessel through a rubber septum injection inlet (figure 2.1). Results were compared to a $NaNO_2$ standard curve performed daily to account for temperature and other performance variation (figure 2.2). Room temperature was typically 18±2 ˚C. The limit of sensitivity for plasma NO_2^- is >10nM and the intra-assay coefficient of variation was <5%.

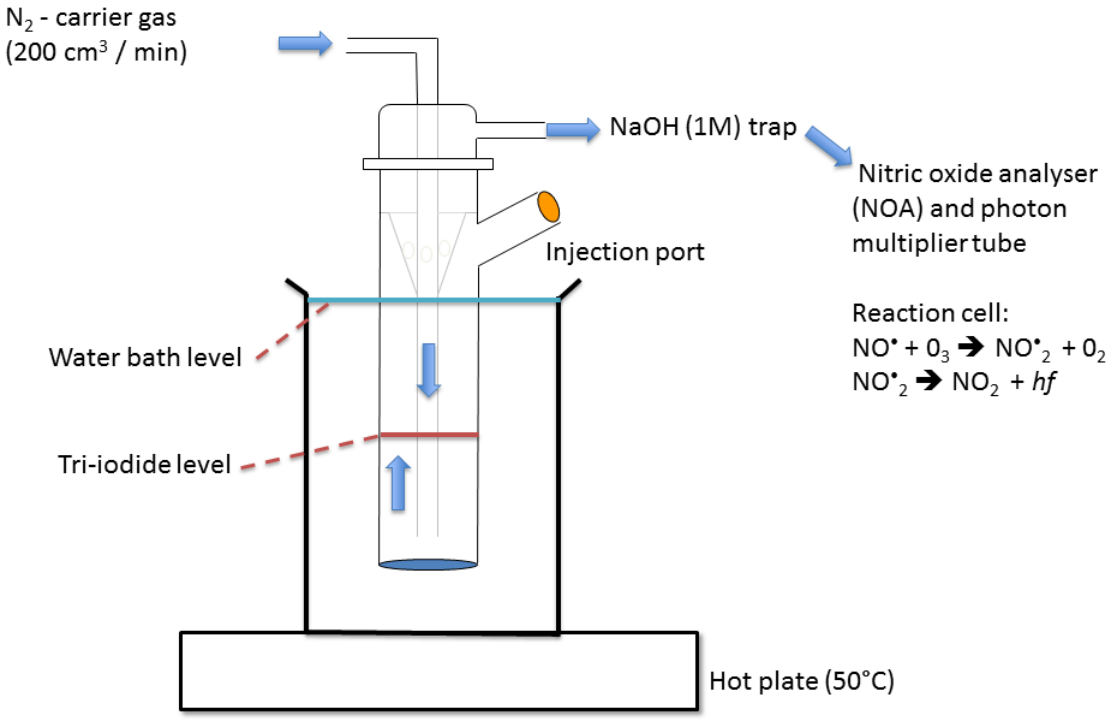

Figure 2.1. Schematic representation of ozone-based chemiluminescence set up. Typically, a 200 µl sample is injected through the rubber septum directly into the purge vessel containing 5 ml tri-iodide reagent heated to 50 °C by a thermostatically regulated water beaker. Cleaved NO is carried in an inert N_2 gas stream (regulated to 200 cm^3/min) to a sodium hydroxide (NaOH) trap (10 ml, 1M). NaOH inhibits hot acid vapour reaching the NOA and ensures that N-oxide contaminants are not converted to NO (no false positives). NO is directed to the NOA where it reacts with ozone (O_3) in the reaction cell; photons released from this reaction are amplified via a photo-multiplier tube (PMT) and recorded as a potential difference (mV).

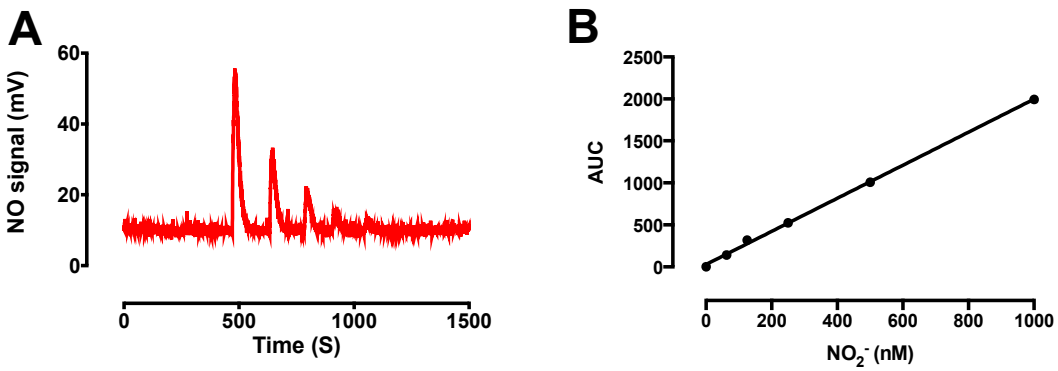

Figure 2.2. Representative $NaNO_2$ standard curve. Typical $NaNO_2$ trace signals (A). A standard curve was undertaken using multiple $NaNO_2$ concentrations (62.5 nM, 125 nM, 250 nM, 500 nM and 1000 nM, diluted in deionised H_2O), [R^2 = 0.999, Y = 1.0382X]. Peak AUC was determined using NOA Liquid analysis software. (B) The AUC was then plotted against known standard $NaNO_2^-$ concentrations.

2.6.3 Plasma nitrate

For NO_3^- analysis, plasma (30 µl) was injected into vanadium chloride (30 ml; 49.9 mM vanadium chloride (VCl_3) in 0.8 M hydrochloric acid (HCl)) heated at 80 °C prior to detection via an NO analyser (Sievers NOA 280i, Analytix, UK, figure 2.3). Vanadium chloride is capable of measuring the same NO metabolites as tri- iodide, coupled with the additional reductive capacity to reduce NO_3^- to NO. In this sense values obtained from vanadium analysis represent the total NO_x- in the sample. To obtain true NO_3^- values, the AUC obtained from tri-iodide analysis is subtracted from the AUC from vanadium analysis.

Results were compared to a $NaNO_3^-$ standard curve performed daily to account for temperature and performance variation (figure 2.4). Room temperature was 18±2 ˚C. The limit of sensitivity for plasma NO_3^- is >500nM and the intra-assay coefficient of variation was <8%.

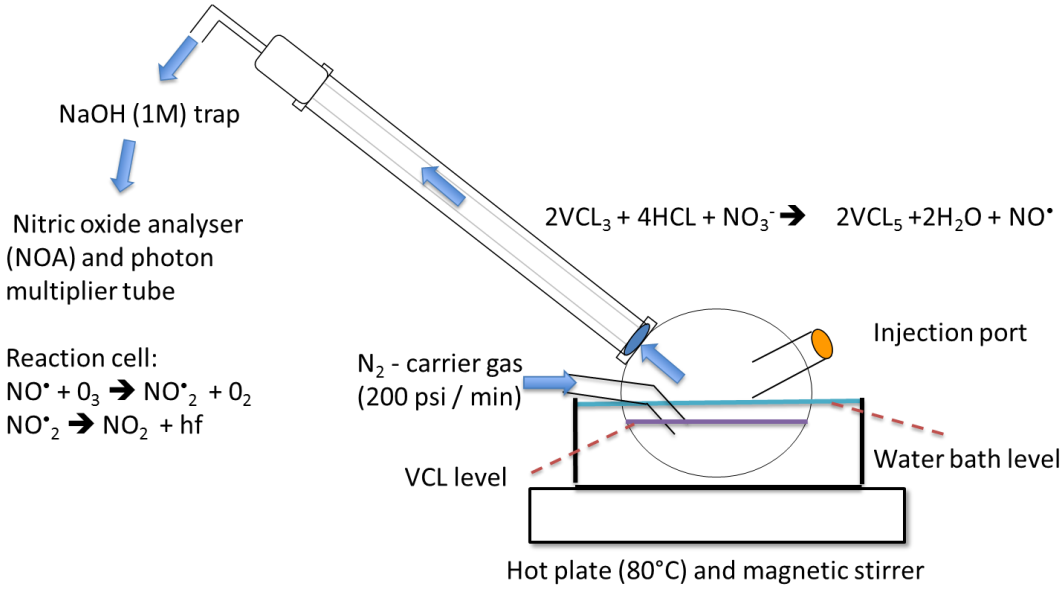

Figure 2.3. Schematic representation of NO_3^- analysis. Typically, a 30 µl sample is injected through the rubber septum into a round bottomed flask containing 30 ml vanadium chloride reagent, thermostatically maintained at 80 °C. Released NO is carried in an inert N_2 gas stream (200 cm^3/min) and directed through a water cooled condenser to a NaOH trap (1 M, 10 ml).

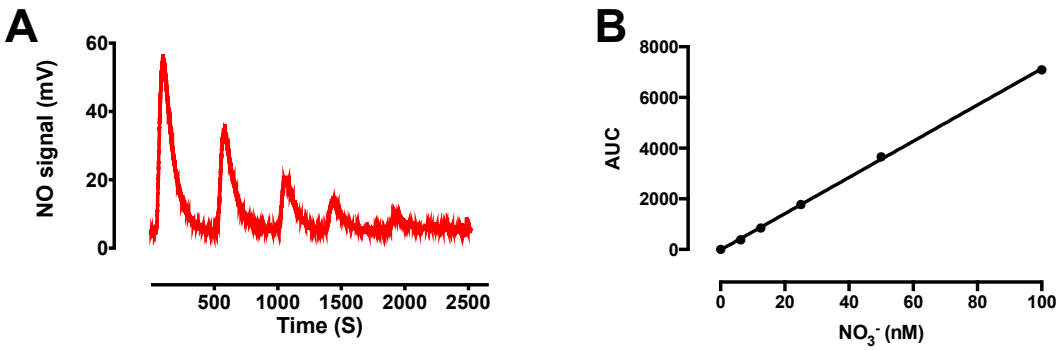

Figure 2.4. Representative $NaNO_3$ standard curve. Typical $NaNO_3$ trace signals (A). A standard curve of known $NaNO_3$ concentrations (6.25 µM, 12.5 µM, 25 µM, 50 µM and 100 µM), was undertaken on a daily basis to account for variations in temperature [$R^2 = 0.995$, $Y = 68.585X$]. (B) Corresponding AUC was plotted against known standard NO_3^- concentrations.

2.7 Electron paramagnetic resonance spectroscopy – spin trapping

Electron paramagnetic resonance (EPR) is a technique employed to detect species with an incomplete outer electron shell (i.e. a free electron or free radicals). Due to the high reactivity and short half-life of free radicals, specific spin traps (i.e. α-phenyl-N-tert-butyl nitrone (PBN)) are utilised to stabilise the free radical for detection. Akin to all other forms of spectroscopy, EPR detects changes during promotion between energy levels (absorption/emission). The two energy states are caused by the application of an external magnetic field and the spectrum recorded relates to the absorption of microwave energy as the unpaired electron is promoted between these two states. Only species with an unpaired electron exhibit EPR signals due to the electron inducing a spin orientation in the magnetic field, which is then flipped on introduction of the appropriate amount of microwave energy. This is usually recorded as the first derivative of the absorption and the signal is split depending on the molecules immediately adjacent/linked to the electron. The extent of this splitting is dependent on the interaction of neighbouring species and in this way detailed information is provided on the chemical structure of the free radical detected.

Numerous studies have used nitrone based probes to investigate lipid radical formation, where resulting EPR spectra typically yield a triplet of doublets (hyperfine coupling constant characteristics). This is due to the free radical interaction with a neighbouring nitrogen atom and an additional hydrogen atom within the chemical structure on the PBN probe (figure 2.7). A typical EPR spectrum is given in section 3.4.3.

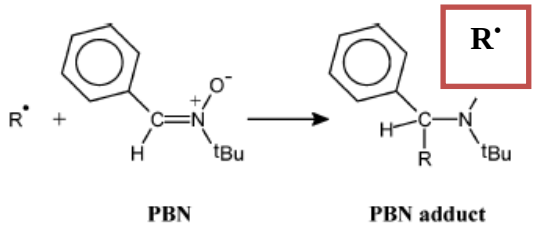

Figure 2.5. PBN/Radical adduct species. PBN/ R• adduct formation, where the extracted lipid hydrogen forms a hydroxyl radical. R• represents a radical.

2.7.1 Free radical spin trapping in blood (*ex vivo*): oxidative stress

EPR spectroscopy coupled with spin trapping was used as a direct measure of *ex-vivo* oxidative burden (circulating lipid radicals). Briefly, the nitrone-based spin trap on interaction with a free radical forms a stable spin adduct, detectable via EPR spectroscopy and exhibiting unique spectral characteristics associated with a particular species. Blood samples were collected directly into a 6 ml EDTA vacutainer containing 2 ml PBN (200 mM, Sigma-Aldrich, UK). Lipid-radical/PBN adducts underwent repeated toluene (Sigma-Aldrich, UK) extraction followed by reconstitution in 100 µl of chloroform (Sigma-Aldrich, UK) before EPR analysis (e-scan, Bruker, Coventry, UK). In order to test *in vitro* radical generating capacity ferrous sulphate (100 mM, Sigma-Aldrich, UK) was added to plasma and PBN (125 mM, 1:1:1, v/v) before lipid extraction and EPR analysis as above. Typical measurement conditions were: modulation amplitude 1.43 G, power 48.1 mW, time constant 40.96 seconds, sweep time 41.94 seconds. EPR signals generated are proportional to radical amount, thus peak height was used to reflect relative spin adduct concentration. A typical EPR spectrum is shown in section 3.4.3, figure 3.2.

2.7.2 Oximetry

EPR oximetry was used to investigate the amount of O_2 present in cell medium, as previously described Dada *et al*, (253). Briefly, N15 per-deuterated tempone (PDT) is a stable nitroxyl spin probe that is sensitive to the presence of molecular oxygen. The extent of this interaction will be a function of the amount of O_2 present. This amount of O_2 present is assessed by the extent of broadening of the EPR spectral peak (253). The spectral line width (peak-to-peak splitting along the magnetic field axis) is measured and converted to PO_2 or concentration of O_2 using an appropriate calibration curve. Briefly, PDT (5 mM) was diluted in distilled water (500 µM). Cell medium (RPMI), exposed to a known O_2 concentration was used as standards (0%, 21% and 95% O_2). Cell medium exposed to 21% oxygen was achieved by equilibration at atmospheric O_2 prior to analysis. Following this, 2 µl of probe (500 µM) was added per 100 µl of cell medium and used for each standard. The 0% and 95% standards were achieved by assessing the probe in gas permeable tygon tubing placed in a narrow hollow quartz tube used for EPR spectroscopy. The tube was then perfused with N_2 or 95% O_2 to equilibrate to 0% or 95% O_2, respectively. The point at which the spectral line width no longer changed was taken as the equilibration point for each standard.

2.8 Plasma hydroperoxides: Ferrous oxidation-xylenol orange assay

Hydroperoxides (ROOH) are well-established ROS associated with oxidative stress. Total plasma ROOH concentrations were determined using the ferrous iron/xylenol orange (FOX) assay, as previously described (254). The FOX assay is a colorimetric method of ROOH estimation, based on the oxidation of Fe^{2+} (ferrous) to Fe^{3+} (ferric) by ROOH, which binds to xylenol orange to give a distinctive dark purple colour, detected by measuring absorbance at 560 nm. Briefly, sample (90 µl, PPP) was transferred into 1.5 ml Eppendorf tubes with 10 µl of methanol. The samples were then vortexed and incubated for 30 min at room temperature. The FOX reagent (FOX2, 900 µl, consisting of 250 µM ammonium sulphate; 100 µM xylenol orange, 25 mM sulphuric acid and 4 mM butylated hydroxyl-toluene in 90 v/v methanol) was added to the samples, vortexed and incubated for 30 minutes. Samples were then centrifuged at 12,000 *g* for 10 min prior to determination of the absorbance of the supernatants at 560 nm. Samples were compared to a H_2O_2 standard curve (0 – 250 µM, figure 2.6).

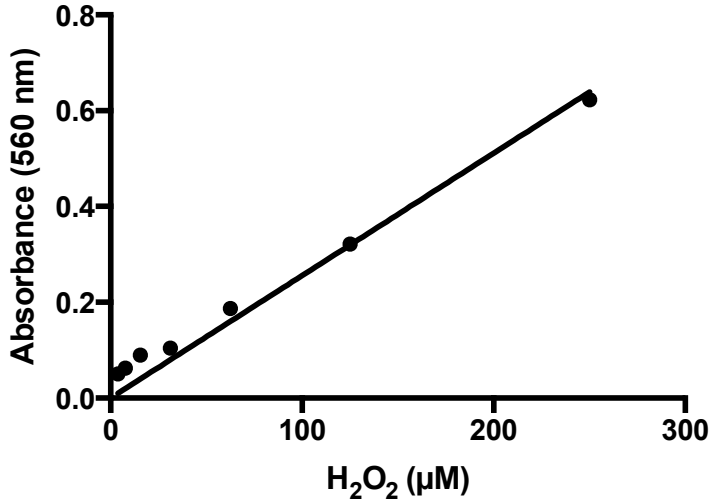

Figure 2.6. FOX assay - H_2O_2 standard curve. A standard curve of known H_2O_2 concentrations (0.9 µM, 1.95 µM, 4 µM, 7.8 µM, 15.6 µM, 31 µM, 62.5 µM, 125 µM, 250 µM), [R^2 = 0.9708, Y = 0.0026X]. H_2O_2 concentration was confirmed by absorbance at 560 nm (spectrometer), checking against the manufacturer's excitation co-efficient (H_2O_2 concentration = absorbance / excitation co-efficient).

2.9 Antioxidant capacity: oxygen radical absorbance capacity – fluorescence

Total plasma antioxidant capacity was assessed by oxygen radical absorbance capacity (ORACfl) whereas lipophilic antioxidant capacity was assessed using a modified extraction process as previously described (255). ORACfl assesses the ability of plasma antioxidants to buffer an insult from a thermally activated peroxyl radical generator. This inhibition is conceptualized by the preservation of the fluorescent probe intensity over time. Results are often calculated by the resultant difference in AUC and are usually reported in comparison to an established antioxidant equivalent (figure. 2.7).

For total plasma antioxidant capacity, samples were diluted (1:500) in PBS and added in triplicate to a 96-well plate (25 µl) loaded with 150 µl sodium fluorescein (10 nM). Following this, 25 µl of 70 µM 4-hydroxy-TEMPO (tempol; Sigma) was used as a standard antioxidant on each plate. Just prior to analysis, either 25 µl of phosphate buffer saline (PBS) (blank) or 2,2'-azobis-2-methyl- propanimidamide (AAPH, 240 mM) were added prior to measurement. AAPH is a thermally activated peroxyl radical generator.

Lipophilic antioxidant capacity was assessed using a modified extraction procedure. Briefly, 100 µl of plasma sample was transferred to a 5 ml glass tube, 200 µl of ethanol and 100 µl of water was added and vortexed, followed by the addition of 400 µl of hexane. The mixture was vortexed and left to settle until two layers appeared (~ 2 minutes), followed by centrifugation at 12,000 *g* for 10 min. The hexane layer was removed and added to a 2.5 ml amber tube. This extraction step was repeated. The two-hexane layers were combined. The combined hexane extracts were dried down under a gentle N_2 flow, and resuspended in 100 µl PBS. Following this, 25 µl of resuspended lipophilic antioxidant sample was assessed as described above. Fluorescence measurement was performed on the FLUOstar OPTIMA for 90 min at 37 °C with 485 nm excitation and 520 nm emission. Fluorescence readings were measured every minute. Samples were run in triplicate and results were expressed in arbitrary units compared to a standard anti-oxidant, tempo (Sigma-Aldrich, UK) equivalent.

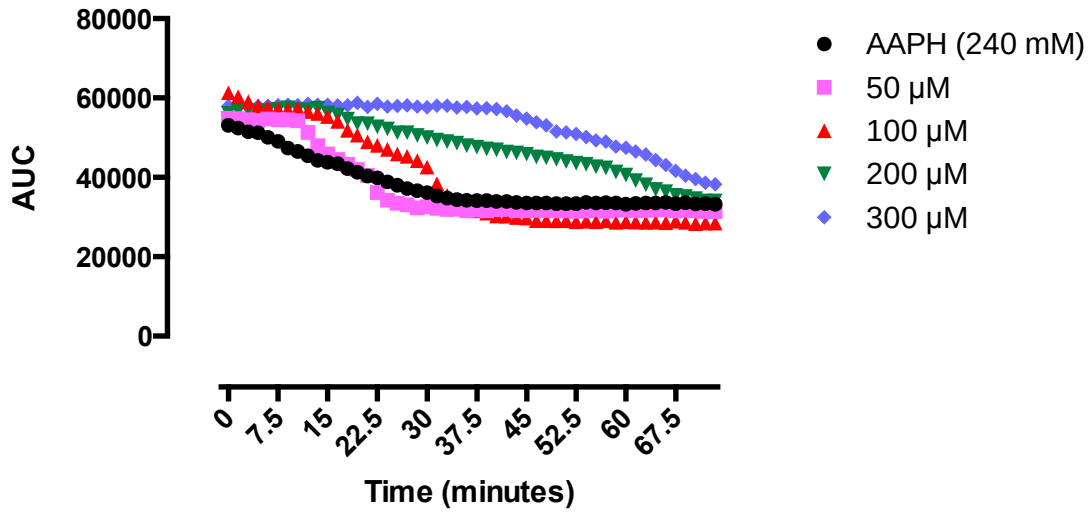

Figure 2.9. The effect of antioxidant concentration on free radical induced fluorescent probe degradation. AAPH 240 mM (Black). Tempo 50 µM (pink). Tempo 100 µM (red). Tempo 200 µM (green). Tempo 300 µM (blue).

2.10 Isolation of plasma derived microparticles

Fasting blood samples were drawn from an antecubital vein into ethylenediaminetetraacetic acid (EDTA) vacutainers. Blood samples were promptly centrifuged (1,024g × 10 min at 4 °C) to yield platelet-poor plasma. Plasma-derived MPs were isolated via differential ultracentrifugation. Briefly, plasma (1 ml) was ultracentrifuged (100,000g × 1 hr at 4 °C; Beckman Coulter, UK). The supernatant was discarded and the remaining pellet was resuspended in 250 ml of RNAase-free phosphate- buffered saline (Fisher Scientific, UK) which had been filtered using a 0.22 µm Millipore (MerckMillipore, UK). Isolated MPs were stored at -80 °C, for no longer than 6 months before analysis. For use, samples were thawed in a preheated (37 °C) thermostatically regulated water bath for 3 min.

2.11 Nanoparticle tracking analysis

NanoSight (LM10) uses NTA technology. NTA determines the size, concentration and distribution of nano-sized particles based upon their light scattering and Brownian motion in a controlled liquid suspension. Briefly, a laser beam (405 nm) is passed through a sample chamber where it illuminates all particles in the suspension, rendering them detectable by a x20 magnification microscope (figure 2.8). The microscope, equipped with a camera captures a video of the particles moving under Brownian motion. NTA software in turn tracks each particle individually and calculates their hydrodynamic diameters (256).

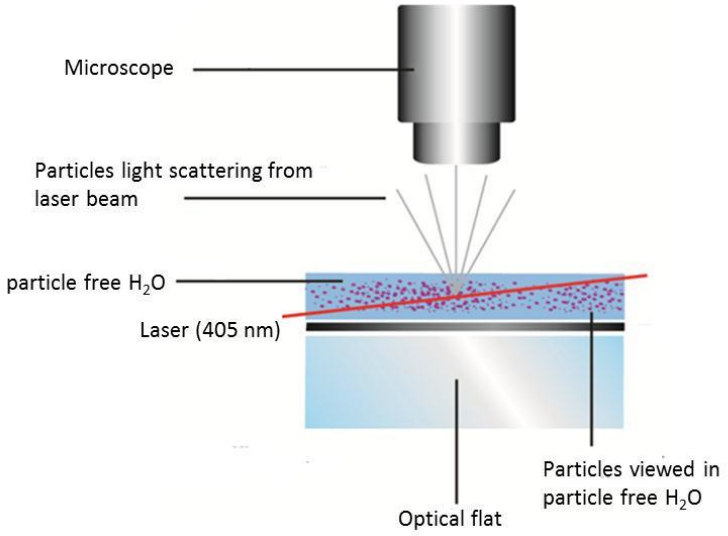

Figure 2.8. Nanoparticle tracking analysis. A schematic diagram illustrating nanoparticle tracking analysis (NTA) technology. Firstly, the particles are diluted in particle-free sterile H_2O. The samples are then loaded across the optical flat using a 1 ml syringe, taking care not to introduce bubbles. Particles are illuminated by a 405 nm laser (50 nm beam diameter), allowing particle visualisation by eye/camera, and consequently quantification by assessment of Brownian motion. Adapted from (256).

Within the microscopic field of view, particles are simultaneously identified and tracked for a set time period on a frame-by-frame basis. The NTA analysis software calculates the distance moved (two dimensional) over a set period of time, allowing the particle diffusion coefficient (Dt) to be determined when coupled with recorded temperature (T) and solvent viscosity (η). The sphere-equivalent hydrodynamic diameter (d) of the particles can be identified using the Stokes-Einstein equation (figure 2.9).

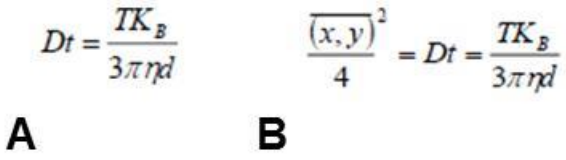

Fig. 2.9. Stokes-Einstein equation. Particle diffusion coefficient (Dt). Temperature (T). Solvent viscosity (η). Sphere-equivalent hydrodynamic diameter (d). Boltzmann's constant (K_B). Equation (A) accounts for the Brownian motion of particles across two dimensions, however, in a suspension the Brownian motion occurs in three dimensions, thus NTA analysis uses a modified equation (B) to account for three dimensional Brownian motion. Adapted from (256).

2.11.1 Nanoparticle tracking analysis methodology

MP size and concentration were determined using NTA (NanoSight LM10 system, UK) as described previously (182). Briefly, NTA is a laser illuminated microscopic technique equipped with a 405 nm laser and a high sensitivity digital camera system (OrcaFlash2.8, Hamamatsu, NanoSight Ltd) that determines the Brownian motion of nanoparticles in real-time to assess size and concentration. Sixty-second videos were recorded and particle movement was analysed using NTA software (version 2.3). Camera shutter speed was fixed at 30.01 milliseconds. Camera gain was fixed to 500. Camera sensitivity and detection threshold were (14–16) and (4–5), respectively. MP samples were diluted in MP-free sterile water (Fresenius Kabi, Runcorn, UK). Samples were run in quintuplicate, from which MP distribution, average concentration and MP size was calculated.

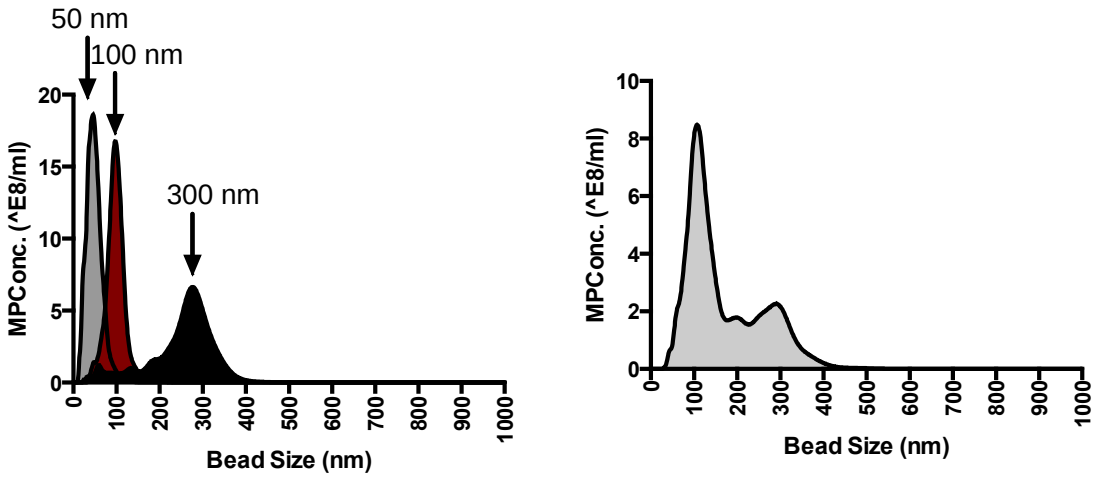

Figure 2.10. Carboxylated polystyrene bead standardisation. Sub-micron diameter beads of known size were used daily to check the machine's functional parameters. Standardized beads were used for validation experiments. NTA results were in good accordance with 50 nm, 100 nm and 300 nm beads in mono-dispersed samples. In biological samples, the particle size, concentration and distribution are unknown. Thus, a poly-dispersed bead sample containing 50 nm, 100 nm and 300 nm beads was used to assess the ability of NTA to measure complex samples [right graph]. Peak broadening and poor clarity (especially between 50 and 100 nm beads) were apparent in the polydispersed bead sample.

2.12 Tunable resistive pulse sensing

TRPS was carried out using the qNano (Izon Science, New Zealand), which uses an electrophoresis-based method to determine the size and concentration of MPs on a particle-by-particle basis. Particles pass through a tunable nanopore which detects particles within a specific size range. Therefore, in order to analyse MP size and concentration across a full spectrum, nanopore 100 (np100) and nanopore 200 (np200) were used. TRPS was performed by Ms Katie Connolly (Cardiff University).

Table 2.1 **Common methods used to detect microparticles**

Method	Detection limit	Size	Concentration	Morphology	ζ-potential	Measurement time
DLS	1 nm	+/-	+/-	-	+	S
NTA	30 nm	+	+/-	-	+/-	M
Flow cytometry	~>400 nm	+	+/-	-	-	S
Cryo-EM	~ 1 nm	+	-	+	-	H
TEM	~ 1 nm	+	-	+	-	H
AFM	< 1 nm	+	+/-	+	-	H
TRPS	70 nm	+	+/-	-	+/-	M

A method which is capable of (+), capable of but is subject to limitations (+/-) or not capable of (-) providing information on MP size, concentration, morphology, zeta potential. The measurement time (S, M or H) reflects the measurement time is < 1 min (S), minutes (M) or hours (H). DLS, dynamic light scattering; NTA, nanoparticle tracking analysis; EM, electron microscopy; TEM, transmission electron microscopy; AFM, atomic force microscopy; TRPS, tunable resistive pulse sensing. Adapted from (257).

2.13 Gas chromatography

Fatty acid profiles (both plasma and plasma derived MPs) were analysed using gas chromatography (GC) with a flame ionisation detector (FID) as described previously (258). Briefly, lipids were extracted from either 100 µl of plasma or 250 µl of re-suspended MPs, using the method of Garbus *et al* (259). Fatty acid methyl esters (FAME) were prepared by incubation for 2 hr with 2.5% H_2SO_4 in dry methanol:toluene (2:1, v/v) at 70 °C. A known amount of C17:0 (margaric acid, Nu-Chek Prep. Inc, MN, USA) was added as an internal standard. FAME were analysed by gas chromatography (GC) using a Clarus 500 gas chromatograph (Perkin-Elmer 8500, CT, USA), fitted with a 30 m × 0.25 mm inner diameter (i.d), 0.25 µm film thickness capillary column (Elite 225, Perkin Elmer). The column temperature was held at 170 °C for 3 min and then temperature-programmed to 220 °C at 4 °C / min. Nitrogen was the carrier gas at a flow rate 2 ml / min. FAME were identified routinely by comparing retention times of peaks with those of standards (figure 2.11, Supelco 37 Component FAME Mix, Sigma-Aldrich, UK). Negative controls included hexane alone, where no fatty acids were detected.

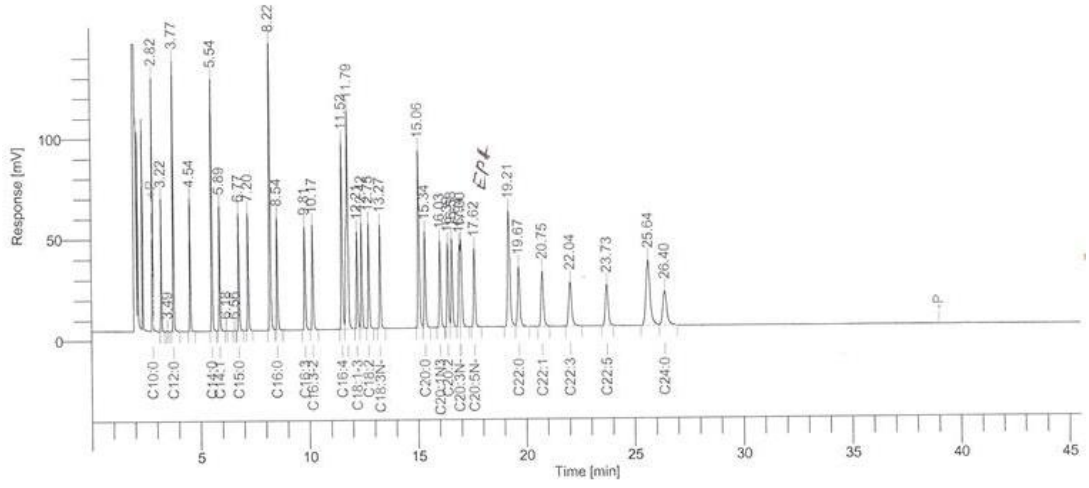

Figure 2.11 An example GC-FID chromatogram: External FAME (Supelco 37) standard (scanned image of raw chromatogram). External FAME standards were used routinely to qualitatively assess the fatty acid profile of plasma and plasma derived MPs. No peaks (fatty acids) were retained on the column >30 minutes. Internal standards (C17:0) were used to quantify the amount of fatty acids.

2.14 Analysis of microRNA expression within circulating microparticles

MP miR expression was analysed on a small subset of PCOS patients (n = 6, age: 33.8 ± 5 years, BMI: 28 ± 5 kg/m^2) and healthy controls (n = 6, age: 29.3 ± 5 years, BMI: 28 ± 6 kg/m^2). Total RNA was extracted from equal volumes of isolated MPs with TRIzol LS Reagent (Ambion, Austin, TX, USA) according to the manufacturer's instructions. miR profile analysis was performed using Toray 3D-Gene™ DNA Chip microarrays (Toray Industries Inc, Tokyo, Japan) according to the manufacturer's protocol. Briefly, total MP RNA was labelled with a mercury LNA microRNA Array Power Labelling kit (Exiqon, Vedbaek, Denmark). Labelled miRNAs were hybridized onto 3D-Gene miRNA oligo chips containing more than 1,600 antisense probe spots (Toray Industries Inc). The annotation and oligonucleotide sequences of the probes correspond to miR Base database version 16. The chips were washed stringently, and fluorescent signals were scanned and analysed with a 3D-Gene™ Scanner 3000 (Toray Industries Inc). Hybridised probe spots with signal intensity greater than the mean intensity plus two standard deviations of the background signal were considered valid. The background average was subtracted from the signal intensity, which was then multiplied by the normalisation factor (25 divided by the median signal intensity of all the subtracted background data) to generate the normalised data. Additionally, miR 4700-5p was selected for validation by standard quantitative PCR (qPCR, PCOS patients (n = 12, age: 30 ± 6 years, BMI: 30 ± 6 kg/m^2) and healthy controls (n = 9, age: 25 ± 2 years, BMI: 26 ± 6 kg/m^2)). MP RNA fraction (25 ng), isolated as described for the microarray, was converted into miR 4700-5p complementary (c)DNA (and RNU48 housekeeping control cDNA) using miR 4700-5p and RNU48 probes (Life Tech) in a reverse transcriptase reaction. 7.5 ng cDNA was used in each PCR reaction following the manufacturer's instructions. miR 4700-5p MP levels were expressed as fold changes compared to healthy volunteers. I undertook sample preparation and interpretation whilst the TORAY micro-array was performed by Central Biotechnology Services - Cardiff University, and qPCR was performed by Dr Thomas Davies - Cardiff University.

2.15 Cell culture

The HECV cell line (obtained from human umbilical vein endothelial cells, IST, Italy) were maintained in Dulbecco's Modified Eagle Medium (DMEM, PAA Laboratories Ltd, UK) supplemented with 10% fetal bovine serum (PAA Laboratories Ltd, UK), penicillin, and streptomycin (Invitrogen, UK). The cells were maintained in an incubator at 37 °C and 5% CO_2. Cells were sub-cultured using Trypsin/EDTA (Invitrogen).

Primary HUVECs (Cell Applications Inc, CA, USA) were cultured in endothelial cell growth medium (Cell Applications Inc) as recommended by the manufacturers. The cells were maintained in an incubator at 37 °C and 5% CO_2. Cells were sub-cultured using a specialised sub-culture reagent kit (Cell applications Inc) and all experiments were carried out prior to 16 population doublings. All cells were counted using Cellometer® (Nexlon Biosciences Auto T4) and expressed as cells/ml.

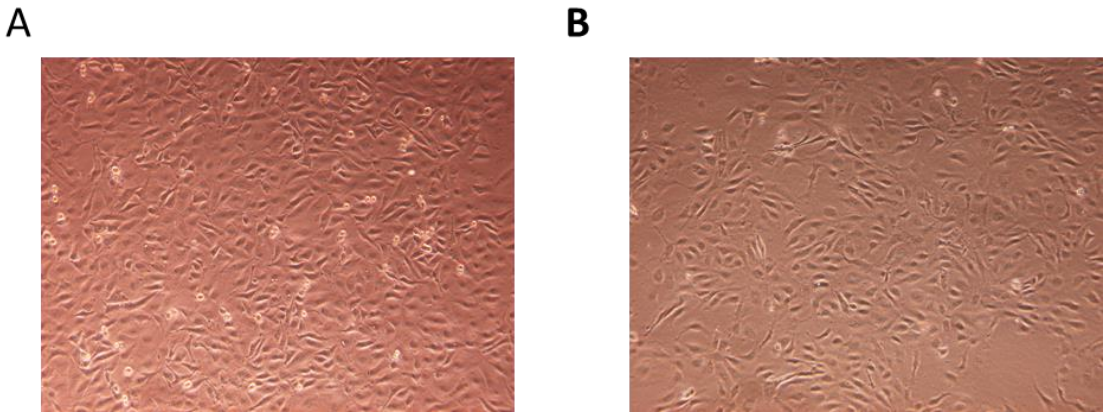

Figure 2.12. Cell images. (A) HECV cells. (B) HUVECS. Both images were captured at x20 magnification.

2.16 Cellular treatments

HECV and HUVEC cultures were treated with several pathological stressors. Upon cells reaching ~80% confluence, cell culture medium was removed (all experiments were undertaken when cells reached ~80% confluence, unless indicated). Cells were washed with PBS and incubated with 10 ml MP-free serum free medium (SFM) for 24-hours (37 °C and 5% CO_2) containing either SFM alone (non-stimulated/control) or with addition of a cellular insult (hydrogen peroxide [H_2O_2 0.1 – 20 mM]; hypoxia [1 – 21% O_2]; glucose [0 – 22.5 mM]; insulin [0 - 2.5 nM] or testosterone [0 -1 μM]). For detailed characterisation and functional analysis, experiments were carried out on MPs subjected to; H_2O_2 (10 mM); testosterone (1 μM); glucose depleted (thus no glucose present); insulin (2.5 nM) or hypoxia (1 % O_2) insults.

2.17 Isolation of cell derived microparticles

MPs were isolated direct from cell culture as previously described (182). Cells were cultured in serum-free medium (SFM) for 24 hours before MP isolation. Cell culture medium was extracted direct from the culture flask and subjected to differential ultra-centrifugation, (300 × *g* for 10 min, 2,000 × *g* for 15 min, and 100,000 × *g* for 60 min). The resulting MP pellet was resuspended in sterile PBS (Fisher Scientific, UK).

2.18 Confocal microscopy: cell and microparticle morphology

Confocal microscopy was utilised in several 'proof of concept' experiments to support NTA observations, visualise cellular MP release in real-time, visualise MP-EC adhesion, MP annexin positivity and HECV morphology. HECV cells were grown on a 35 mm glass bottom dish (In Vitro Scientific, CA, USA), maintained in ~250 µl of DMEM medium in tissue culture conditions previously described in section 2.16. Fluorescent labelling and phase-contrast images were visualised using a Leica SP2 confocal microscope. Images were captured and analysed using Leica Application Suite Advanced Fluorescence (LAS AF).

EMP Morphology: Cells were gently washed with 1 ml PBS followed by the addition of 250 µl of MP-free SFM. Cells were incubated with 250 µl Cell-Trace Red-Orange (dilution 1:1000, Invitrogen) for 30 minutes at 37 °C and 5% CO_2. Post incubation, free Cell-Trace was removed by 2 x 1 ml PBS washes and maintained in 250 µl of MP-free SFM (or pathologically relevant stressor, as indicated) until visualised under confocal microscopy. Following Cell-Trace labelling, cells were treated with 250 µl annexin V (dilution 1:200, FITC, Biolegend) for 15 minutes (37 °C and 5% CO_2). Free annexin V was removed by 2 x 1 ml PBS washes and maintained in 250 µl of MP-free SFM until visualised by confocal microscopy.

EMP Adhesion: Cell-Traced EMPs (red-orange) were derived from cells treated with 8 ml Cell-Trace Red-Orange (dilution 1:1000 in DMEM) for 30 minutes incubation at 37 °C and 5% CO_2. Post incubation, free Cell-Trace was removed by 2 x 10 ml PBS washes and maintained in 10 ml of MP-free SFM for 24 hours. After 24 hours, cell culture supernatant was taken and subjected to differential ultra-centrifugation to isolate EMPs (as described previously in section 2.18. The supernatant from the last wash stage in the differential ultra-centrifugation step was kept and used as a control, to eliminate Cell-Trace contamination. HECV cells grown to 75% confluence were then treated with Cell-Traced EMPs for 3 hours (37 °C and 5% CO_2). To remove non-adherent EMPs, 2 x 10 ml PBS washes were performed. Cells and adhered EMPs were maintained in growth medium until confocal microscopy.

2.19 Electron Microscopy

EM was used to visualise MPs shedding from stimulated and non-stimulated HECV cells. EM was also used to assess isolated MP sample morphology and purity. EM work was carried out in collaboration with Dr Christopher Von Ruhland (Central Biotechnology Services - Cardiff University).

2.19.1 Scanning electron microscopy

HECV cells were grown on a 35 mm glass bottom dish (In Vitro Scientific, USA), maintained in ~250 µl of DMEM medium in tissue culture conditions previously described in section 2.14. Cells were washed twice in PBS and then fixed in 1% glutaraldehyde in Sorensen's phosphate buffer (v/v) for 1 hour. Following fixation, cells were kept in PBS until imaging. Cell samples were then dehydrated in graded isopropanol (IPA) at 50, 70, 90 and 100% (10 minutes each grade) followed by hexamethyldisilazane (HMDS, 3 x 5 minutes; Sigma-Aldrich, UK). Surplus HMDS was removed and remaining residue was allowed to evaporate. A 12mm diameter adhesive carbon disc was then attached to the underside of the glass window. A diamond pen was used to break / release the glass before the sample was sputtered in gold. Specimens were viewed using a JEOL 840A scanning electron microscope (Joel UK, Hertfordshire, UK). Images were acquired using analySIS (Munster, Germany) and processed using Photoshop (Adobe, USA).

2.19.2 Transmission electron microscopy

MPs derived from unstimulated HECV cells were isolated via differential ultra-centrifugation as described in section 2.18. Post final ultra-centrifugation, MPs were resuspended in 100 µl particle-free PBS. Isolated MPs were then fixed in 1% glutaraldehyde in Sorensen's phosphate buffer (1:1 v/v for 1 hr). Negative staining was carried out on 80 nm thick sections on a 400 mesh / carbon-coated grid floated on 50 µl drops of the fixed isolated MP Sample (30 min), followed by 100 mM phosphate buffer pH 7.4 (3 x 1 min), H_2O (6 x 10 min) and finally 2% uranyl acetate (20 min). Residual surplus was allowed to air dry. Isolated MPs were examined in a Philips CM12 TEM (FEI UK Ltd) at 80 kV. Images were captured with a Megaview III camera and presented using Photoshop (Adobe, USA).

2.20 Cell viability and apoptosis

2.20.1 Trypan blue exclusion

For trypan blue exclusion, HECV cells were stained with trypan blue (1:1 v/v) and assessed using a Cellometer Auto T4 (Nexlon Biosciences, USA).

2.20.2 The CellTiter 96® AQueous one solution cell proliferation assay

The CellTiter 96® AQueous one solution cell proliferation assay (Promega, Southampton, UK) is a colorimetric technique used to ascertain cell viability. Briefly, 100 µl of 1 x 10^6 cells was incubated with 20 µl of reagent for 1 hr (37 °C, 5% CO2). During this incubation period the formation of a coloured product named formazan is achieved by dehydrogenase enzymes, which are only located in metabolically active cells. This facilitates the bio-reduction of 3-(4,5-dimethylthiazol-2-yl)-5-(3-carboxymethoxyphenyl)-2-(4-sulfophenyl)-2H-tetrazolium.

Following incubation, absorbance was measured at 490 nm using a FLUOstar OPTIMA (BMG Labtech, USA). The quantity of formazan product as measured by the amount of 490 nm absorbance is directly proportional to the number of living cells in culture, as previously described (260).

2.20.3 Caspase-Glo® 3/7 assay

The Caspase-Glo® 3/7 assay (Promega, Southampton, UK) was undertaken to assess apoptosis, as previously described (260). This assay measures caspase-3 and -7 activity using luminescence. These members of the cysteine aspartic acid-specific protease (caspase) family play key effector roles in apoptosis in mammalian cells. Briefly, cells were added to Caspase-Glo® 3/7 assay reagent (1:1, v/v) prior to incubation for 3 hrs at 37 °C, 5% CO2. Luminescence of the test samples was measured using a FLUORstar OPTIMA.

2.21 Multiple electrode aggregometry

To assess the potential coagulability of EMPs, aggregation assays were undertaken using a Multiplate® analyser (Roche, Switzerland). Briefly, bioelectrical impedance aggregometry measures the ability of blood cells (typically platelets) to adhere to an artificial surface. The assay requires measurement of impedance of an alternating current applied across electrodes. The magnitude of adhesion from platelets/MPs to an artificial electrode is determined by quantifying the change in impedance over a set time. This quantification of adhesion is expressed as area-under-curve (AUC) of electrical impedance over the set time (expressed as arbitrary aggregation units).

As an indication of MP coaguability, the multiplate analyser was used to investigate the ability of EMPs to adhere to the surface of an artificial electrode. Briefly, MPs (300 µl, 1 $x10^9$/ml) were mixed 1:1 v/v with 0.9% NaCl preheated to 37 °C in a Multiplate® electrode aggregometer cell. Samples were continuously mixed using a Teflon coated stirring bar (micro-flea) at 1000 rpm. Following three minutes incubation, aggregation was assessed after either: 20 µl of 0.9% NaCl preheated to 37 °C (non-stimulated) or H_2O_2 (20 µl, final concentration 10 mM) initiated aggregation. An increase in electrical impedance from the electrode pairs within a test cell was recorded for 6 minutes and expressed as a mean of the areas under curve (AUC, arbitrary aggregation units of AU*min).

2.22 Whole blood aggregometry: electrical impedance

To assess the effect of MPs on whole blood platelet aggregation, blood samples were taken from 8 healthy volunteers. Blood was collected from a vein in the antecubital fossa with a 21 G butterfly needle into a Hirudin vacutainer (3 ml). A tourniquet was lightly applied proximal to the site of blood sample acquisition. The first 3 ml was discarded, the sampling blood was then slowly inverted two / three times for optimal mixing.

The blood (300 µl) was first mixed 1:1 v/v with 0.9% NaCl preheated to 37 °C in a Multiplate® electrode aggregometer. Samples were continuously mixed using a Teflon coated stirring bar (micro-flea) at 1000 revolutions per minute (rpm). Following a 3-min incubation, platelet activation was initiated by the addition of ADP (20 µl, Multiplate® ADP-test reagent; final

concentration 6.5 μM) or thrombin receptor activating peptide (20 μl, Multiplate® TRAP-test reagent; final concentration 32 μM). An increase in electrical impedance from the electrode pairs within a test cell was recorded for 6 min and expressed as a mean of the areas under curve (arbitrary aggregation units of AU*min).

Pre-conditioning: Endothelial microparticles. To assess the effect of EMPs on whole blood platelet aggregation, blood (300 μl) was first mixed 1:1 v/v with EMPs (1 $x10^2$/ml - 1 $x10^{10}$/ml) derived from pathologically relevant stressors, constituted in 0.9% NaCl preheated to 37 °C in a Multiplate® electrode aggregometer. As previously described, following a 3-min incubation, platelet activation was initiated by the addition of the ADPtest or TRAPtest. Electrical impedance from the electrode pairs was recorded for 6 min.

2.23 Flow cytometry

2.23.1 Theory

Flow cytometry is a laser-based technique, which is employed across a range of scientific disciplines. Briefly, a MP/cell suspension is injected into the machine and enters the flow cell. The flow cell consists of a central core containing the cell sample surrounded by an outer core of sheath fluid. The pressure of the sheath fluid against the cell/MP sample in the narrowing flow cell creates a laminar sheath flow that transports the cells (or MPs) upward in single file through the centre of the flow cell where they are intercepted by multiple lasers, this is referred to as hydrodynamic focusing. Light scattered in a forward direction, is collected by the forward scatter channel (FSC) lens, and is indicative of cell size and can distinguish between cellular debris and viable cells. Light deflected from cell organelles is detected perpendicular to the laser beam and is measured by the side scatter channel (SSC). This provides information regarding the cytoplasmic complexity or granularity of a cell/MP (figure 2.13). A number of fluorescence channels are used to detect any light emitted by the cells or MPs. The specificity of detection is controlled by several optical filters that only permit the passage of light at specific bandwidths (261). Limitations of flow cytometry for the detection of MPs are discussed in chapter 7.

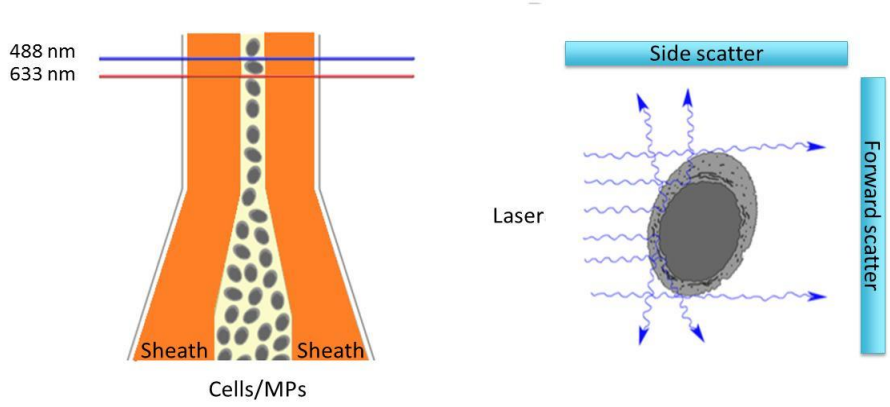

Figure 2.13. Flow cytometer – flow cell and detectors. Cells are hydrodynamically focussed within the flow cell (left) to yield a singular single stream of cells (or MPs) for interrogation by multiple lasers. Light scattered in a forward direction is detected by the forward scatter channel (FSC) and is often indicative of size, whereas the side scatter channel (SSC) provides information about the granularity of each cell (or MP) (right). Adapted from (261).

2.23.2 Cytometric applications within this thesis

Within this thesis, cytometric techniques were used to characterise:

- Cellular origin of circulating MPs (described in section 1.22.3)
- HECV cell and MP surface adhesion molecule profiles (described in section 1.22.4)
- MP annexin V positivity (described in section 1.22.4)
- Platelet activation (P-selectin) - (described in section 1.22.5)

Cytometric measurement of plasma derived MPs was undertaken by Ms Katherine Connolly and Dr Kristin Ladell (Stem Cell and Flow Cytometry Unit, Cardiff University). I undertook all the necessary sample preparation and data analysis.

Antibodies used for cytometric analysis were obtained from Biolegend® (BioLegend, San Diego, CA, USA). They include; mouse anti-human CD62P- allophycocyanin (APC) conjugated (clone AK-4) [P-selectin], mouse anti-human CD144- phycoerythrin (PE) conjugated antibody (clone BV9) [VE-Cadherin], mouse anti-human CD41 – PE-Cy7 [Integrin alpha chain 2B], annexin V-FITC, mouse anti-human αCD41-PECy5, mouse anti-human αCD11b-PECy7 and mouse anti-human αCD144-APC (fluorescent spectra are shown in figure 2.17). All samples were run against non-stained controls and fluorescence minus one.

2.23.3 Cellular origin of circulating microparticles

Flow cytometric measurements were performed using a custom-built FACSAria II (BD Biosciences, San Jose, CA, USA). Forward scatter area and side scatter area were set to log scale. Plasma-derived MPs were resuspended in 100 µl of 0.22 µm-filtered annexin V binding buffer (BD Biosciences). MPs were then stained for 15 min in the dark at room temperature with annexin V-FITC (1.57 µg/ml), αCD41-PECy5 (0.12 µg/ml), αCD11b-PECy7 (7.9 µg/ml) and αCD144-APC (4.1 µg/ml). Fluorescent calibration beads of sizes 200, 500 and 800 nm were detected and distinguishable as three distinct populations (Submicron bead calibration kit, Bangs Laboratories, Inc., IN, USA). The MP gating strategy was based on their forward scatter versus side scatter profile and in relation to platelets in fresh plasma. The MP gate was tested for annexin V positivity and subsequently for monocyte (CD11b), platelet (CD41) and endothelial (CD144) antigens to determine PS exposure and the cellular origin of MPs. FSC-A threshold was set to 1000 to minimize recording of debris. Fluorescence minus one (FMO) stains were used to set the positive gates for each antibody. Data were exported from

FACSDiva™ software version 6.0 (BD Biosciences) and subsequently analysed with FlowJo software version 9.6.4 (Tree Star, Inc., Ashland, OR, USA).

2.23.4 Surface adhesion molecule profiling of HECV cells and microparticles

Flow cytometry was used to determine the surface adhesion molecule profiles of HECV cells (both unstimulated and HECV cells treated with pathological stressors) and their corresponding MPs. Additionally, flow cytometry was used to investigate the effect of MPs on HECV surface adhesion molecule profiles.

HECV cells were grown in T25 flasks as previously described. The medium was carefully removed from the cells and Acutase® (4 ml, Sigma-Aldrich, UK) or trypsin (4 ml, Invitrogen, UK) was added to the cells and incubated at 37 °C for 3 min. Flasks were gently 'tapped' to encourage cell detachment. Detached cells were transferred to 15 ml tubes, and topped up to a 15 ml final volume with medium. The flasks were washed with 10 ml medium to ensure all cells had been obtained and the medium was aspirated to the relevant 15 ml tube. The cells were centrifuged (1,200g x 3 min at RT) and supernatant removed. Cells were re-suspended in 1ml PBS/annexin V binding buffer (Sigma-Aldrich, UK).

Cells were re-suspended at 1 x 10^6 cells / ml and 1 ml of the cell suspension was transferred to 1.5 ml Eppendorfs; the cells were centrifuged and the supernatant aspirated. Conjugated primary antibody was added to each tube, re-suspended and incubated for 15 min at room temperature (in the dark). Following incubation the cells were centrifuged, and washed in PBS. Finally, cells were re-suspended in 0.2 ml PBS/annexin V binding buffer into 12 mm FACS tubes (Falcon, BD Biosciences, UK) and viewed on a BD FACS Canto flow cytometer (BD Biosciences).

Flow cytometry was performed using a BD Canto dual laser bench top flow cytometer, equipped with 488 nm and 633 nm lasers and BD FACS Diva software (v 5.0.3). Single colour analysis was performed using primary antibodies conjugated to FITC, PE, PE-Cy7 or APC, excitation and emission spectra for these fluorophores can be seen in figure 2.15. Carboxylated polysterene beads (200, 500 and 1000 nm in diameter) were used to set the MP gate (figure 2.14. IZON Science, NZ).

HECV cells were analysed for forward scatter area and side scatter area whilst MPs were run on forward scatter area and side scatter area that were set to logarithmic (log) scale. Firstly, density dot-plots were used to show the distribution of cells using the forward scatter and side scatter parameters. The voltage was adjusted accordingly so that all the cells were optimally aligned. A dense area of concentrated pixels (cells/MPs) was selected using a gate. For antibody enabled cytometric analysis, single parameter histograms were used (i.e. relative fluorescence intensity on the x-axis and the cell count of the y-axis). The voltages were adjusted for individual fluorophores so that the negative controls (unstained samples) were set to the first log decade. Instrument settings were adjusted using unstained cell/MP samples. Acquisition was terminated upon recording 10,000 events, gated based on their forward scatter and side scatter characteristics. Fluorescence minus one (FMO) stains were used to set the positive gates for each antibody (gates shown in figure. 2.16).

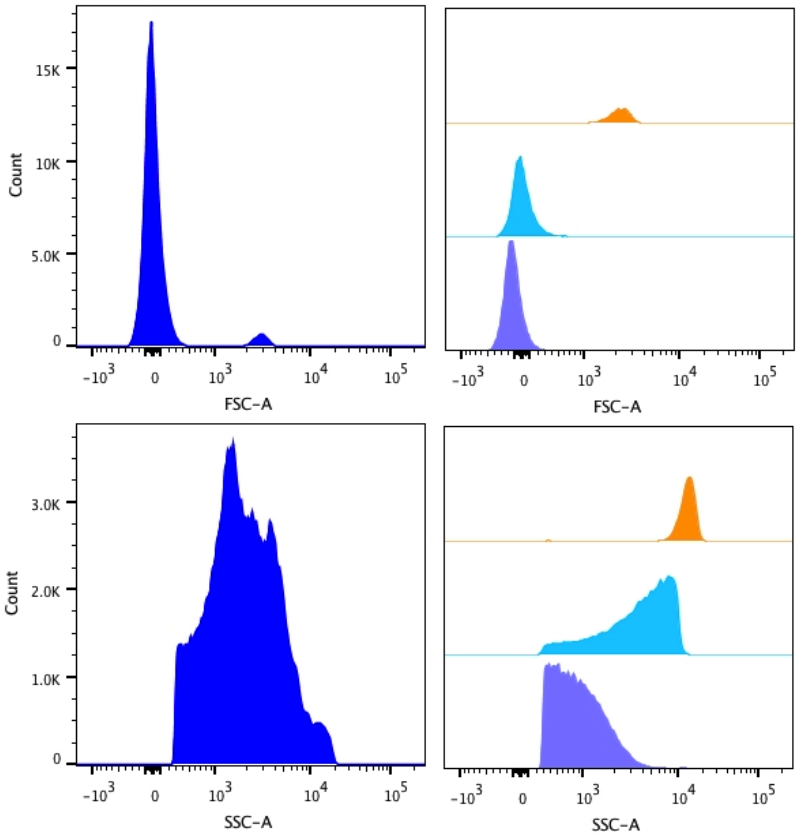

Figure 2.14. Cytometry analysis of < 1 µm diameter carboxylated polystyrene beads. Top graphs represent forward scatter histograms. Bottom graphs represent side scatter histograms. Beads were obtained from Izon Science Ltd. [Orange] - 1 µm beads. [Aqua] – 500 nm beads. [Purple] – 200 nm beads. [Dark blue] – Polydispersed bead sample.

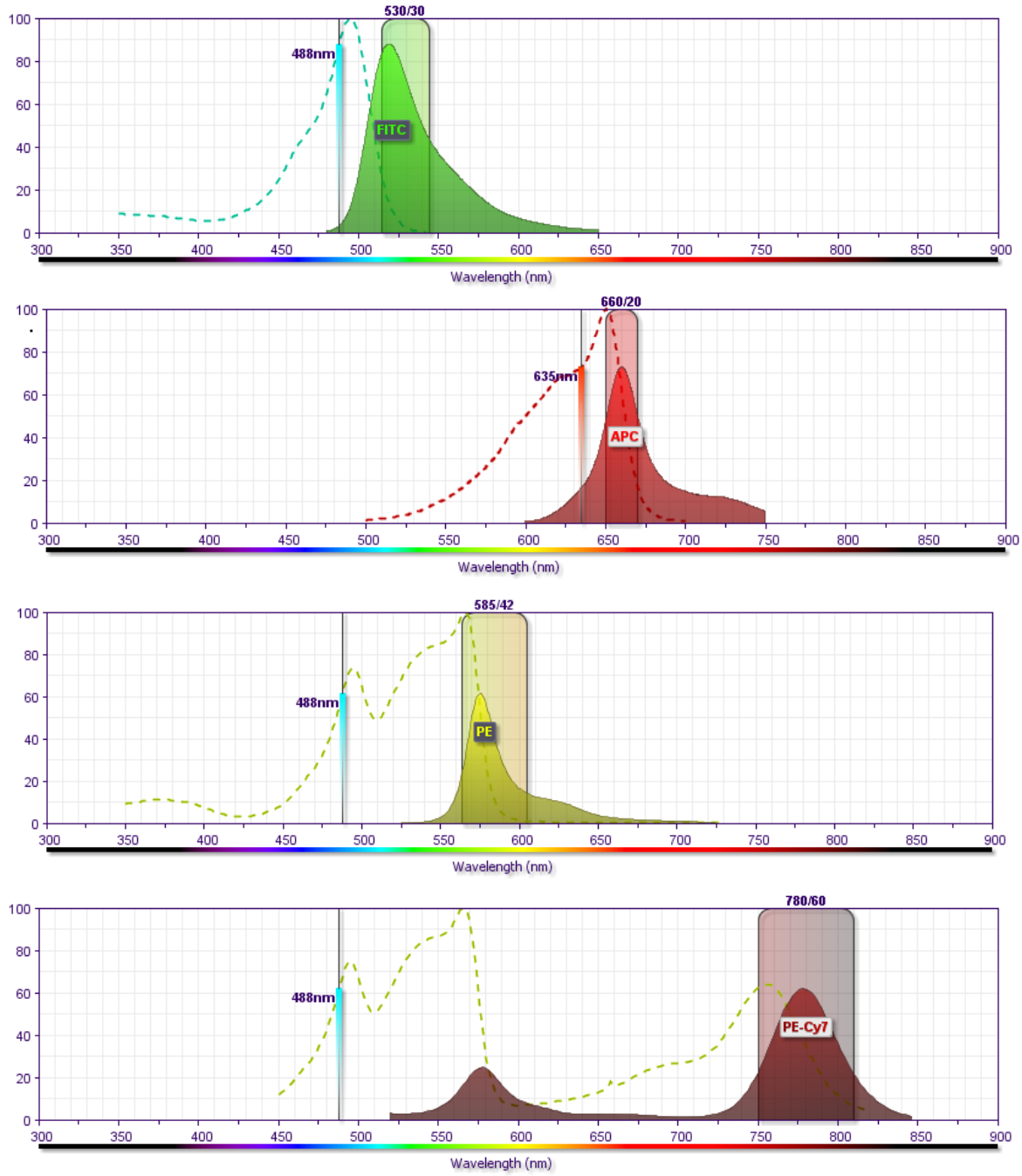

Figure 2.15. Fluorophore spectra: Spectra illustrating the excitation spectrum (dotted/dashed lines) and emission spectra profile (coloured histogram) of (A) FITC (green); (B) APC (red); (C) PE (yellow) and (D) PE-Cy7 (Brown). The shaded areas demonstrate the band pass filter used for each fluorophore (adapted from BD Biosciences 2014).

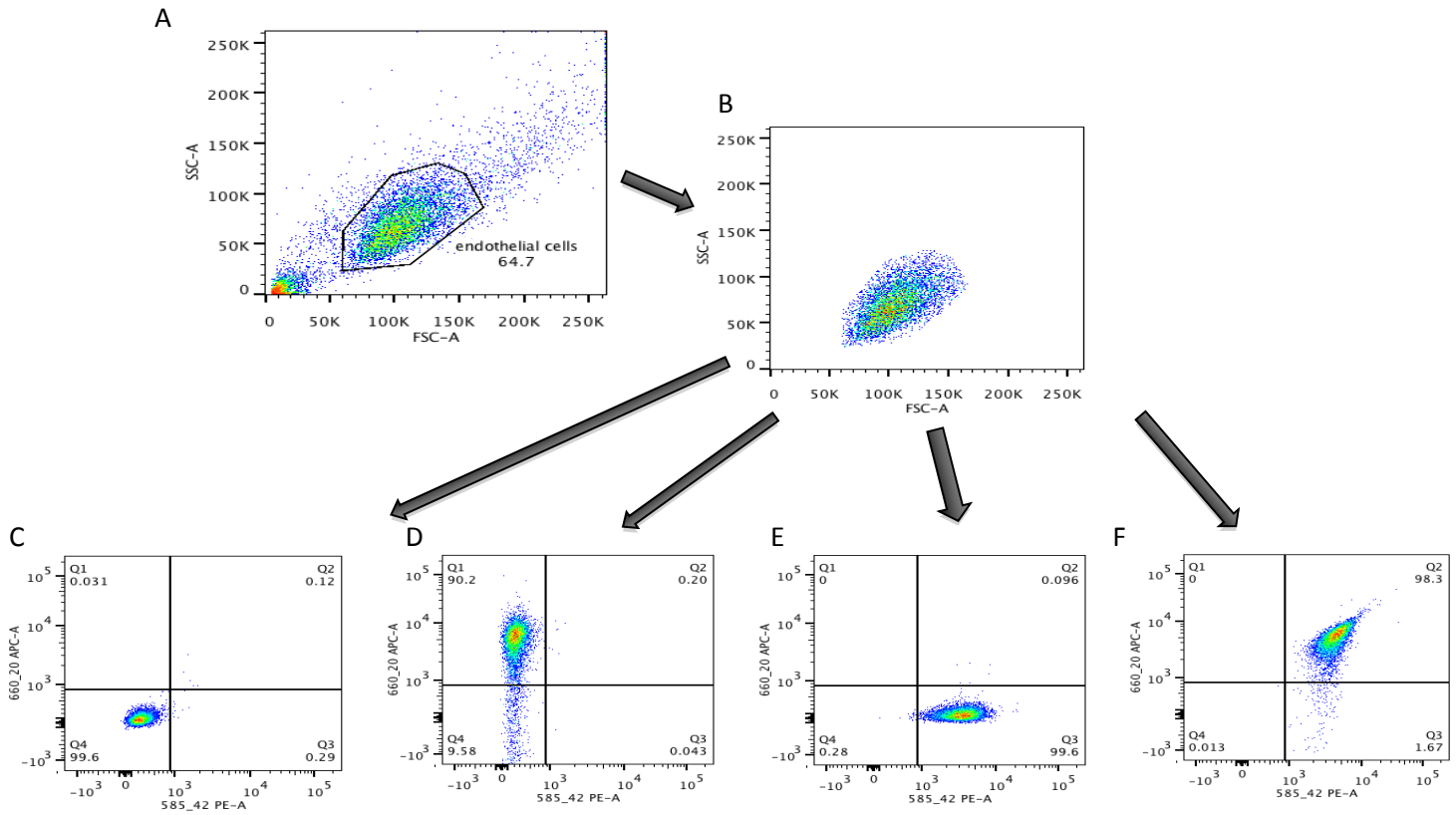

Figure 2.16. Cytometry gating pathway for HECV cell surface adhesion molecule profile. (A) Represents HECV cell gate, excluding cell aggregates and potential debris. (B). Accounts for the CD144+ positive population. (C). HECV control (unstained) in quadrant 4. (D). HECV cells stained for APC (CD54) only, quadrant 1. (E). HECV cells stained with PE (CD144+) only, quadrant 3. (F). Combined staining of CD144+ and CD54 on HECV cells in quadrant 2. FSC, forward scatter channel; SSC, side scatter channel; APC, allophycocyanin; PE, phycoerythrin; A, area.

2.23.5 Flow cytometry: Effect of MPs on whole blood platelet activation

Blood sample collection and preparation: To assess the effect of MPs on whole blood platelet electrical impedance aggregometry, blood samples were taken from 4 healthy volunteers (*n* = 4). Blood was collected from antecubital fossa veins with a 21 G butterfly needle into a citrate vacutainer (3 ml) for platelet activation analysis and into an EDTA vacutainer (4 ml) for a full blood count. A tourniquet was lightly applied proximal to the site of blood sample acquisition. As previously described, the first 3 ml was discarded, the sampling blood was then slowly inverted two / three times for optimal mixing.

Platelet counts were derived from a full blood count preformed on an ABX Pentra X120 haematology blood analyser (Horiba UK Ltd, Northampton, UK). Whole blood was diluted with saline (37 °C) to yield a final platelet count of 150 $x10^3/mm^3$. Whole blood (containing 150 $x10^3/mm^3$, 300 µl) was mixed with MPs (MP conc. 1 x 10^9/ml, 250 µl) for 3 minutes (using a Teflon coated stirring bar (micro-flea) at 1000 rpm). Post incubation, platelet activation was initiated by the addition of ADP (50 µl, Multiplate® ADP-test reagent; final concentration 13 µM), thrombin receptor activating peptide (50 µl, Multiplate® TRAP-test reagent; final concentration 64 µM) or equivalent volume of saline. 200 µl of sample was then fixed with paraformaldehyde 1% v/v for 15 minutes. Following fixation, 40 µl sample was mixed with CD41 (5 µl), CD62P (5 µl) and CD144 (5 µl), reconstituted to a final volume of 150 µl in HEPES buffer solution and stored at 4 °C until analysis. Incubation was terminated by diluting the sample (40 µl) in 960 µl HEPES buffer.

Platelet activation was assessed using a dual laser Canto flow cytometer (BD) within two hours of incubation. Data collection and analysis was performed using FACS DIVA and FlowJo, respectively. Acquisition was terminated upon recoding 10,000 platelets (gated based on their forward scatter and side scatter characteristics).

2.23.6 Thrombin generation assay (microparticles)

To provide a working reservoir of plasma in which to test thrombin generation of MP, blood was drawn gently from healthy volunteers into a syringe containing 6 mM trisodium citrate (Sigma-Aldrich) and 20 μg/ml corn trypsin inhibitor (Cambridge BioScience, UK) and centrifuged (1,024 *g*, 10 min, 4 °C) to yield "vehicle" PPP. Samples were then stored at −80 °C until analysis.

To asses MP thrombin generation, calibrated automated thrombography was used, as described previously (262), with minor modifications. Samples were measured in duplicate using 96-well plates (round-bottomed, Immulon 2HB, Thermo Scientific). Eighty microliters of vehicle PPP (containing endogenous clotting factors) were added to each well with 20 μl of diluted HEPES/NaCl buffer (NaCl 280 mM, KCl 10 mM, Na_2HPO_4 1.5 mM, Glucose 12 mM, HEPES 50 mM, pH 7.4) tissue factor (TF) solution to yield a final concentration of 1 pM (Innovin, Sysmex UK Ltd, UK). Familial hypercholesterolaemia patient MP samples were assayed for thrombin generation both with and without exogenous TF addition. MPs (20 μl) were added to sample wells with the addition of either saline (20 μl, 0.9% w/v NaCl) or TF (20 μl, 1 pM final). Each sample was calibrated to a well containing 80 μl of PPP and 40 μl of thrombin calibrator (600 nM, Synapse BV, Netherlands). The plate was then warmed to 37 °C for 5 min before addition of fluorogenic substrate (20 μl, Z-Gly-Gly-Arg-AMC, Bachem, UK). The fluorescent signal was then measured using a Fluoroskan Ascent plate reader (ThermoLabsystems, Finland) equipped with a 390/460 nm filter set (excitation/emission) at 15 second intervals until the thrombin generation reaction was complete. Data were analysed using Thrombinoscope™ software (Synapse BV, Netherlands) and correlated with MP concentration data.

2.24 Silencing RNA / transfection

In an attempt to decipher the role of hypoxia-inducible factor-1α (HIF-1α), in hypoxia mediated MP formation, silencing RNA (siRNA) targeting HIF-1α expression in HECV was used. Briefly, HECV cells were seeded on a T25 flask and grown as previously described in section 1.14. When cells reached 50 % confluency, the cell medium was discarded and incubated with 4 ml antibiotic free medium (DMEM, 10 % FCS) for 1 hr. Then 20 μl of SMARTpool HIF-1α siRNA (taken from a 20 μM stock solution made up in sterile Dharmacon RNase free siRNA buffer (Dharmacon, USA)) was placed in a sterile polymerase chain reaction (PCR) Eppendorf to which 1 μl of Dharmafect reagent was added, gently mixed and left at room temperature for

20 minutes. Cell medium was again discarded and replaced with 4 ml of fresh antibiotic free medium (DMEM, 10% FCS), to which the transfection reagent mix was added, to yield a final siRNA concentration of 100 nM per flask. Control experiments consisted of medium alone and Dharmafect transfection reagent with non-targeting scrambled siRNA (also 100 nM per flask (Dharmacon, USA)).

2.25 Western blot

A western blot was carried out on HECV cells to detect the presence of HIF-1α protein. The multiple stages of the Western blot and associated methods are detailed below.

2.25.1 Cell lysis

HECV cell culture medium was discarded and cells were washed with sterile PBS (Fischer-scientific) three times. Immediately, 200 µl of ice cold lysis buffer (containing protease/phosphatase inhibitors detailed in table 2.2) was added to the cells. A cell scraper was used to distribute the lysis buffer and detach cells from the flask. Following this, samples were transferred to sterile Eppendorfs and centrifuged at 21,913g x 20 min at 4 °C. The resulting supernatant was carefully transferred to Eppendorf tubes and stored at -20 °C until use.

Table 2.2 Lysis buffer

Constituent (pH 7.5)	
Tris buffer 50 mM	Phenylmethylsulfonylflouride 1 mM
EGTA 5 mM	Sodium flurodioxide 50 mM
NaCl 150 mM	Phenylarsine oxide 20 µM
Triton 1 %	Sodium molybdate 10 mM
Sodium orthovanadate 2 mM	Leupeptin 10 µg/ml
Aprotinin 10 µg/ml	

EGTA, ethylene glycol tetraacetic acid; NaCl, sodium chloride.

2.25.2 Bio-Rad (Bradford) assay

The Bio-Rad protein assay is a colorimetric assay that was used for measuring total protein concentration. It is based upon the established Bradford assay where Coomassie dye binds to protein and is associated with a colour change from brown to blue. Briefly, bovine serum albumin (BSA) standards or samples (100 µl) were added to 400 µl of Bio-rad reagent, vortexed and left to settle for 10 min. After this, the absorbance was analysed at 590 nm. Samples were compared to a standard curve of known protein concentration, (0 – 25 µg/ml BSA). Standards and samples were run in triplicate on a 96-well plate.

2.25.3 Sample preparation

Once the protein content of the cells had been quantified, the protein in the samples had to be denatured. Briefly, 20 µg of sample was diluted 1:1 with dithiothreitol (DTT), followed by heating for 5 min at 95 °C.

2.25.4 Polyacrylamide gels

Polyacrylamide gels (running buffer and stacking gel) were assembled in blotting cassettes using the constituents detailed in table 2.3. Samples (20 µg) were loaded on to wells within the stacking gel to ensure each sample contained an equivalent protein concentration. Also, a broad range molecular weight indicator was loaded as a positive molecular weight standard. The gels were placed in a tank and the reservoir between the blotting cassettes was filled with running buffer (0.25 M Tris buffer, 1.92M glycine and 0.1 % sodium dodecyl sulfate (SDS); pH 8.3). The gel was run at 180 volts (V) for 45 min (or until the bands migrated to the base of the gel).

Table 2.3 **Gel constituents**

Constituent	Resolving gel	Stacking gel
Deionised H_2O	4.8 ml	6.1 ml
Tris Buffer	2.5 ml	2.5 ml
Acrylamide solution	2.5 ml	1.3 ml
10 % (w/v) SDS page	0.1 ml	0.1 ml
10 % (w/v) ammonium persulphate	0.1 ml	0.1 ml
TEMED	6 µl	10 µl

Values based on a 10 ml loading volume. Resolving gel - 7.5%, MW range 70-200 kDa. Stacking gel – 4%gel. Tris buffer, pH 8.8 – resolving buffer or pH 6.8 for stacking buffer. Acrylamide solution consists of: Acrylamide/Bis-acrylamide 30 % solution (37.5:1 ratio).

2.25.5 Transfer

After SDS-PAGE, the resulting gel was transferred to a nitrocellulose membrane. The gel-nitrocellulose membrane was embedded within blotting paper and foam pads, all encased within blotting cassettes. The gel was run at 180 V for 45 min (or until the bands migrated to the base of the gel). The transfer cassette and transfer tank was filled up with cold transfer buffer (0.25M Tris, 1.92 M glycine, methanol 20%; pH 8.3) and run at 100 V for 1 hr. This process encourages the movement of protein from the gel to the membrane. Following transfer, the membrane was placed in Ponceau stain (10 ml), to assess even bands / loading, and the presence of any air bubbles.

2.25.6 Incubation of antibodies

Following Ponceau stain inspection, the membrane was washed in tris-buffer saline (TBS)/tween (10 mM Tris, 150 mM NaCl, tween 0.05 %; pH 7.6) three times. Blocking of non-specific sites of antibody binding was achieved by soaking the membrane in TBS/tween containing 5% w/v non-fat dried milk, with an agitation rocker for 1 hr. The membrane was then incubated with the primary antibody (HIF-1α, mouse monoclonal or β-actin, 1 in 200 in 1% milk-TBS/Tween; GE healthcare, Dharmacon, Germany) overnight at room temperature. After overnight incubation, the membrane was washed 3 x 10 min in TBS/Tween. The secondary antibody (horseradish peroxidase, goat anti-mouse, Sigma-Aldrich) was added at a

concentration of 1 in 1000 made up in 1% milk-TBS/Tween and incubated on the rocker for 1 hour at room temperature. Following this, the membrane was washed (5 x 5 min washes in TBS/Tween).

.

2.25.7 Developing

To detect protein bands, equal volumes (1:1 v/v) of Western blot detection agents (Sigma-Aldrich, UK) were mixed and 100 µl of Western Blot detection reagent (Sigma-Aldrich, UK) was applied to the membrane. GeneSys was used to develop and detect blots. The membrane was exposed to ultraviolet (UV) radiation for 5 min in the GeneSys, after which the image was captured and recorded using GeneSys analysis software.

2.26 Statistics

Statistics are described in each results chapter.

3. RESULTS CHAPTER

Detailed characterisation of circulatory nitric oxide and free radical indices – is there evidence of nitro-oxidative stress in young women with polycystic ovary syndrome?

3.1 Introduction

PCOS is a common condition characterised by hyperandrogenism, oligo/anovulation and defects in insulin secretion and sensitivity (263), leading to an increased risk of type 2 diabetes (153). Patients also have an increased prevalence of hypertension (78), dyslipidaemia (79) and premature atherosclerosis (264) although it is not yet clear whether this translates into an increased risk of cardiovascular mortality (153).

Endothelial dysfunction, an early marker of vascular disease in the general population, is a state linked to reduced NO bioavailability and increased oxidative stress. A recent meta-analysis of 21 studies comparing FMD, a non-invasive measure of endothelial function, in PCOS and healthy women, concluded that endothelial dysfunction was evident in women with PCOS even if they are young and non-obese (265). Few studies have examined NO biochemistry in women with PCOS but these have all used insensitive methodologies that fail to directly resolve total NO into its major component fractions, NO_2^- and NO_3^- (138, 139, 142, 266-269). All failed to show any differences in total NO levels between PCOS subjects and controls, although two studies did note an inverse relationship between total NO and fasting insulin (138, 267), implying that insulin resistance may be mechanistically important in altering NO bioavailability in PCOS. Given that plasma NO_3^- is largely governed by dietary intake (~75%) and plasma NO_2^- is taken to reflect endothelial NO bioavailability, analytical techniques based on colorimetric or fluorometric analysis do not provide sufficient sensitivity for accurate plasma NO_2^- analysis and may contribute to uncertainty regarding NO bioavailability in PCOS.

Oxidative stress, an imbalance arising from excess production of oxidants in the presence of reduced antioxidant capacity, can also reduce NO bioavailability and induce endothelial dysfunction. A recent meta-analysis found evidence of altered antioxidant capacity (increased SOD and reduced glutathione levels) and indices of oxidative stress in PCOS subjects compared to controls (145). However, the studies that underpinned the meta-analysis were generally limited to measurement of oxidant or antioxidant molecules in isolation and/or measurement of reaction end-products as surrogates of oxidative stress. Direct detection of ROS is challenging due to their potent reactivity but is essential if over-estimation of oxidative burden is to be avoided.

3.2 Aims

The aim of this chapter was to establish whether NO bioavailability and oxidant status is altered in a cohort of carefully characterised young women with PCOS free of overt cardiovascular disease, using sensitive, validated methodologies to directly assess plasma NO_2^- / NO_3^-, plasma antioxidant capacity and lipid-derived free radicals.

3.3 Methods

3.3.1 Clinical study design

Ethical approval is detailed in section 2.1 (General Methods). Subject characteristics, anthropometric measurements and blood sampling are described in sections 2.2, 2.3 and 2.5, respectively. Biochemical measurements were carried out at the Department of Medical Biochemistry at the University Hospital of Wales, as noted in section 2.4.

3.3.2 Determination of NO metabolites

Plasma NO_x was measured using ozone-based chemiluminescence, as detailed in section 2.6. Specifically, plasma NO_3^- was assessed using VaCl/HCL cleaving reagent, as described in section 2.6.3. This reagent reduces all plasma NOx (total plasma NO_x apart from nitrated fatty acids). Plasma NO_2^- concentration was determined using I_3^- reducing reagent as described in section 2.6.2. This cleaves NO from non-NO_3^- associated NO metabolites (i.e. NO_2^- and RSNO). To distinguish between these two metabolites, acidified sulphanilamide is used to remove NO_2^-, and allows detection of RSNO alone. Plasma NO_3^- level was calculated by: NO_x concentration (determined by VaCl) minus NO concentration determined by I_3^-. Plasma NO_2^- was calculated by: NO concentration determined by I_3^- minus NO level following acidic sulphanilamide pre-treatment.

3.3.3 Assessment of circulating free radicals and systemic oxidative burden

Circulating lipid-derived radicals were qualitatively and quantitatively assessed using EPR – spin trapping and the FOX assay, respectively, as described in sections 2.7.1 and 2.8. Computer simulations were carried out using Bruker WIN-EPR (Simfonia, Coventry, UK) computer simulation software (version 1.25). Plasma antioxidant capacity was determined using ORACfl, as described in section 2.9.

3.3.4 Statistics

Data were analysed using SPSS version 18.0 (SPSS Inc., Chicago, IL, USA) and Graphpad prism 5 (Graphpad software, CA, USA). The Kolmogorov–Smirnov test was used to check the data for normality. Analysis between groups was performed using the independent t-test or Mann–Whitney U-test for normally or non-normally distributed data, respectively. Age-adjusted correlation coefficients were used to explore the strength of the relationships between *in vitro*/*ex vivo* oxidation and testosterone, regional fat area and insulin sensitivity. Multiple regression analysis was performed to explore the dependence of *in vitro* and *ex vivo* oxidation on age, regional fat area, testosterone and insulin AUC. Results are expressed as mean ± SD or median (range), unless otherwise stated. A *p*-value <0.05 was regarded as statistically significant. Sample size calculations were based on previous published data (within our research group), which demonstrated a 0.28-fold shift in SD in lipid-derived radicals in women with type 2 diabetes compared with controls (270). To detect a similar shift in SD with >90% power at the 5% α level, we sought to recruit at least 14 women in each group. A shift in SD of this magnitude was deemed clinically significant, because this has previously been associated with endothelial dysfunction (270).

3.4 Results

3.4.1 Clinical and metabolic characteristics

Table 3.1 shows the baseline clinical and metabolic characteristics of the PCOS subjects and healthy volunteers. There were no significant differences observed between the groups in age, BMI, waist/hip circumference, subcutaneous/visceral/total fat area, lipids, hsCRP or glucose area under the curve (AUC). As anticipated, insulin AUC and total testosterone were higher in PCOS subjects.

Table 3.1 **Anthropometric and metabolic characteristics of study population**

	PCOS (*n* = 17)	**Healthy volunteers (*n* = 18)**	***p* value**
Age (years)	31 ± 6	31 ± 7	0.9
Weight (kg)	78 ± 21	76 ± 15	0.68
BMI (kg/m^2)	30 ± 6	29 ± 6	0.61
Waist circumference (cm)	91 ± 15	86 ± 13	0.31
Hip circumference (cm)	111 ± 16	106 ± 12	0.24
Waist–hip ratio	0.82 ± 0.05	0.82 ± 0.01	0.94
Visceral fat area (cm^2)	31 ± 23	26 ± 14	0.46
Subcutaneous fat area (cm^2)	287 ± 119	298 ± 114	0.78
Total fat area (cm^2)	318 ± 133	324 ± 124	0.89
Testosterone (nmol/l)	1.4 ± 0.6	0.9 ± 0.6	0.02
hsCRP (mg/l)	1.25 (0.24 - 21.8)	0.9 (0.17 - 16.73)	0.73
Total cholesterol (mmol/l)	4.6 ± 1.3	4.8 ± 1.1	0.67
Triglycerides (mmol/l)	1.2 ± 1.4	1.0 ± 0.5	0.52
LDL cholesterol (mmol/l)	2.4 ± 1.4	2.5 ± 1.3	0.79
HDL cholesterol (mmol/l)	1.2 ± 0.5	1.3 ± 0.6	0.65
Insulin AUC (pmol min/l)	80 ± 46	52 ± 29	0.04
Glucose AUC (nmol min/l)	764 ± 217	692 ± 133	0.24
HOMA-IR	1.9 ± 0.9	2.5 ± 2.4	0.37

Data are presented as mean ± SD or median (range). BMI, body mass index; hsCRP, high sensitivity C-reactive protein; LDL, low density lipoprotein; HDL, high density lipoprotein; HOMA-IR, homeostatic model assessment – insulin resistance; AUC: area under the curve.

3.4.2 Plasma NO metabolites

No significant differences were found between PCOS subjects and healthy volunteers in plasma NO_2^- (257 ± 116 nM versus 261 ± 135 nM, respectively, $p = 0.93$) (figure 3.1. A) or NO_3^- levels (27 ± 7 μM versus 26 ± 6 μM respectively, $p = 0.89$, figure 3.1. B). Plasma RSNO levels were also similar between PCOS patients and healthy volunteers (40 ± 34 nM versus 42 ± 39 nM, respectively, $p = 0.88$, figure 3.1. C). These values are within the expected range for healthy adult individuals, as previously reported by our laboratory and other research groups (28, 33).

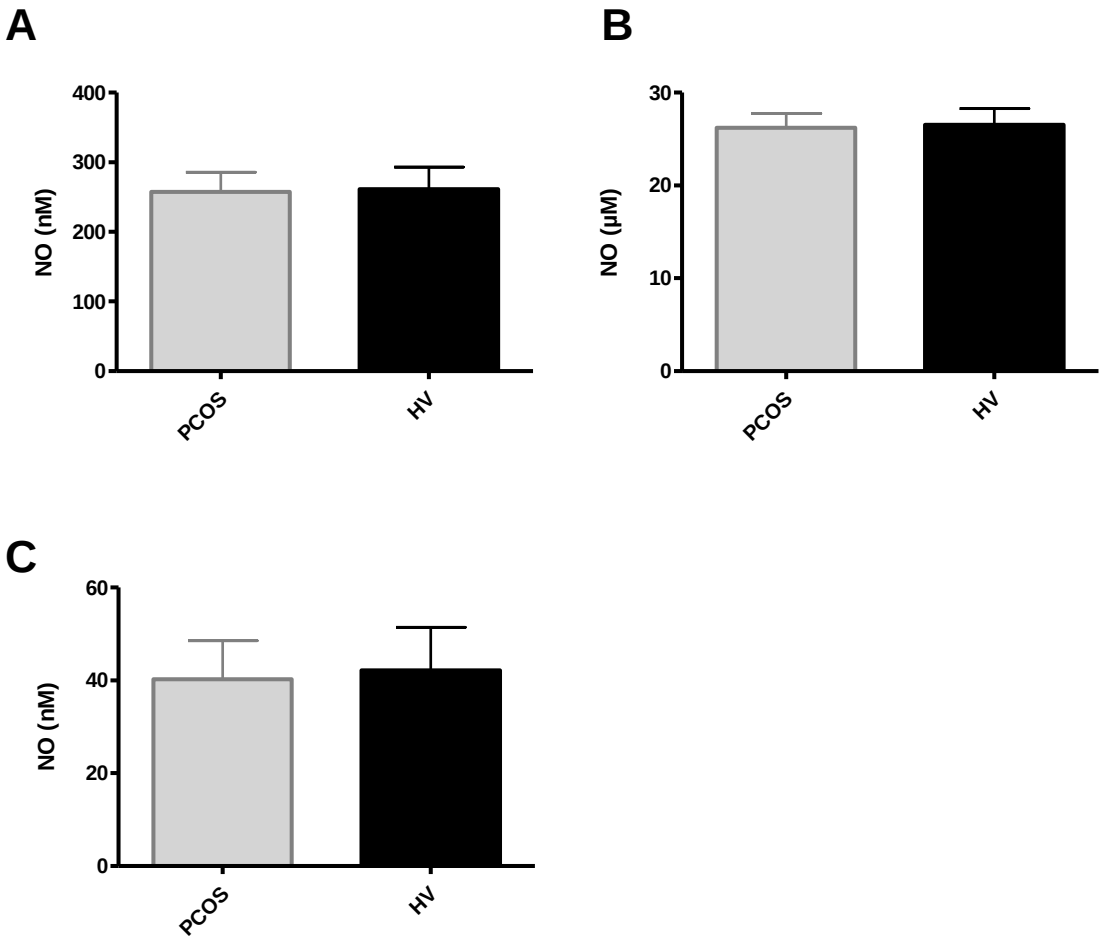

Figure 3.1. Plasma NO metabolite levels: (A), (B) and (C) show plasma NO_2^-, NO_3^- and RSNO concentrations, respectively. [PCOS: $n = 17$, HV: $n = 18$]. Each sample was analysed in duplicate and the mean was used in further analysis. Data is expressed as the group mean ± SEM. The intra-assay coefficient of variation was <5 % for NO_2^- (A) and RSNO (C) measurements, and <8 % for NO_3^- measurements (C).

3.4.3 Free radical determination in blood

Qualitatively, the spectral characteristics (hyperfine coupling constants) were used to specifically identify radical species against reference/standard values (270). The radicals trapped were identified as lipid-alkoxyl radicals (LO^{-}, characterised by coupling constants α^{N} = 14 Gauss (G), α^{H} = 2.3 G, figure 3.2). The EPR spectra also revealed the presence of a PBN radical artefact (α^{N} = 15 G; α^{H} = 5 G) which has been recognised in the literature and is not considered to adversely affect radical detection. To control for possible experimental initiation of radical/PBN adducts, blood was collected directly into EDTA vacutainers containing 200mM PBN covered in foil which limited transient extracellular leakage of Fe^{3+} and photolytic degradation of PBN. No species were detected from PBN alone. In addition, no species were detected when blood was taken into a syringe and transferred to an EDTA vacutainer containing PBN (figure 3.3).

Quantitatively, circulating lipid-derived radicals were similar between PCOS subjects (7.2 (0.17 – 16.73) x 10^{6} arbitrary units (a.u.) and healthy volunteers (7.2 (1.7 – 11.9) x 10^{6} a.u, p = 0.57, figure 3.4 A). Ferrous sulphate-oxidised plasma was used as a measure of *in vitro* lipid radical formation potential. No difference in susceptibility to form lipid-derived radicals was observed between PCOS subjects and healthy volunteers (1.23 (0.3 – 5.62) x 10^{7} a.u. and 1.1 (0.48 – 15.7) x 10^{7} a.u. respectively, p = 0.71, figure 3.4 B).

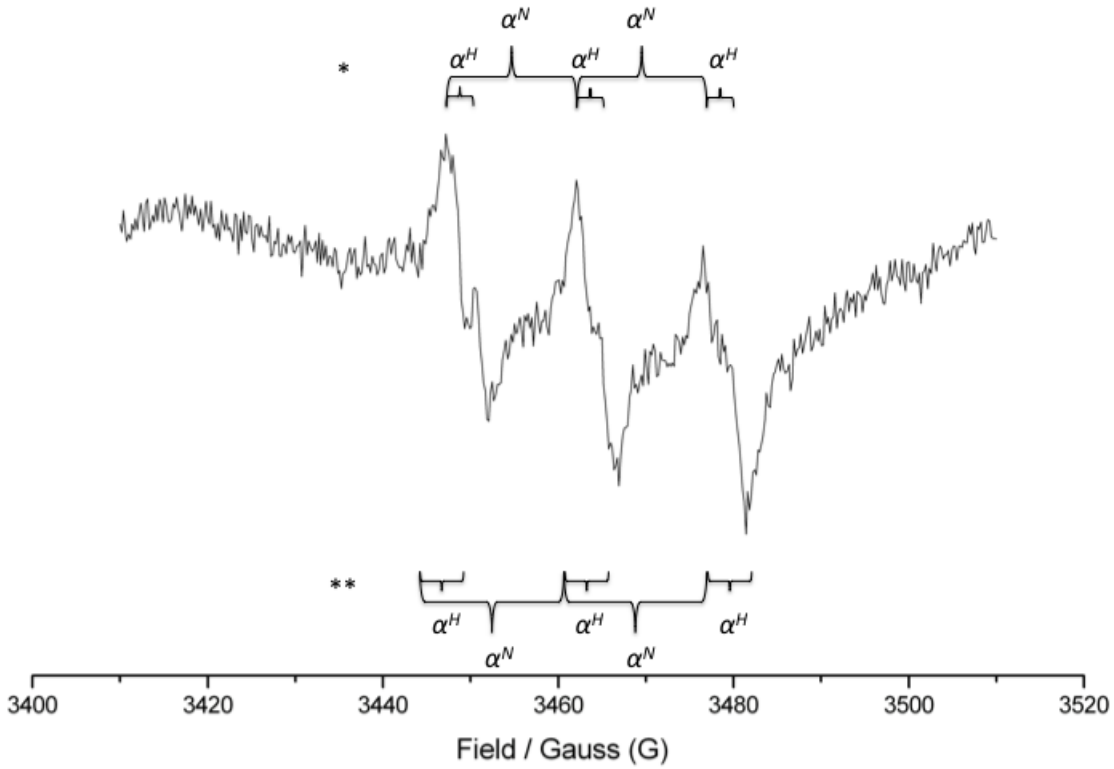

Figure 3.2. Typical EPR spectrum obtained by *ex vivo* free radical measurement. The PBN/radical adducts measured herein yield a six line ('triplet of doublets') spectrum. The six line spectra is the result of the interaction between the free electron and the probe (PBN, which possess a nitrogen (αN) and hydrogen nucleus (αH)). Hyperfine coupling constants (shown in brackets, * and **) of the paramagnetic species are an intrinsic and unique property of the trapped radical and is thus utilised for identification. (*) Indicates the primary alkoxyl (LO^-) radical, αN = 14 Gauss (large bracket) αH = 2.3 Gauss small bracket, (**) indicates PBN/artifact, αN = 15 Gauss αH = 5 Gauss.

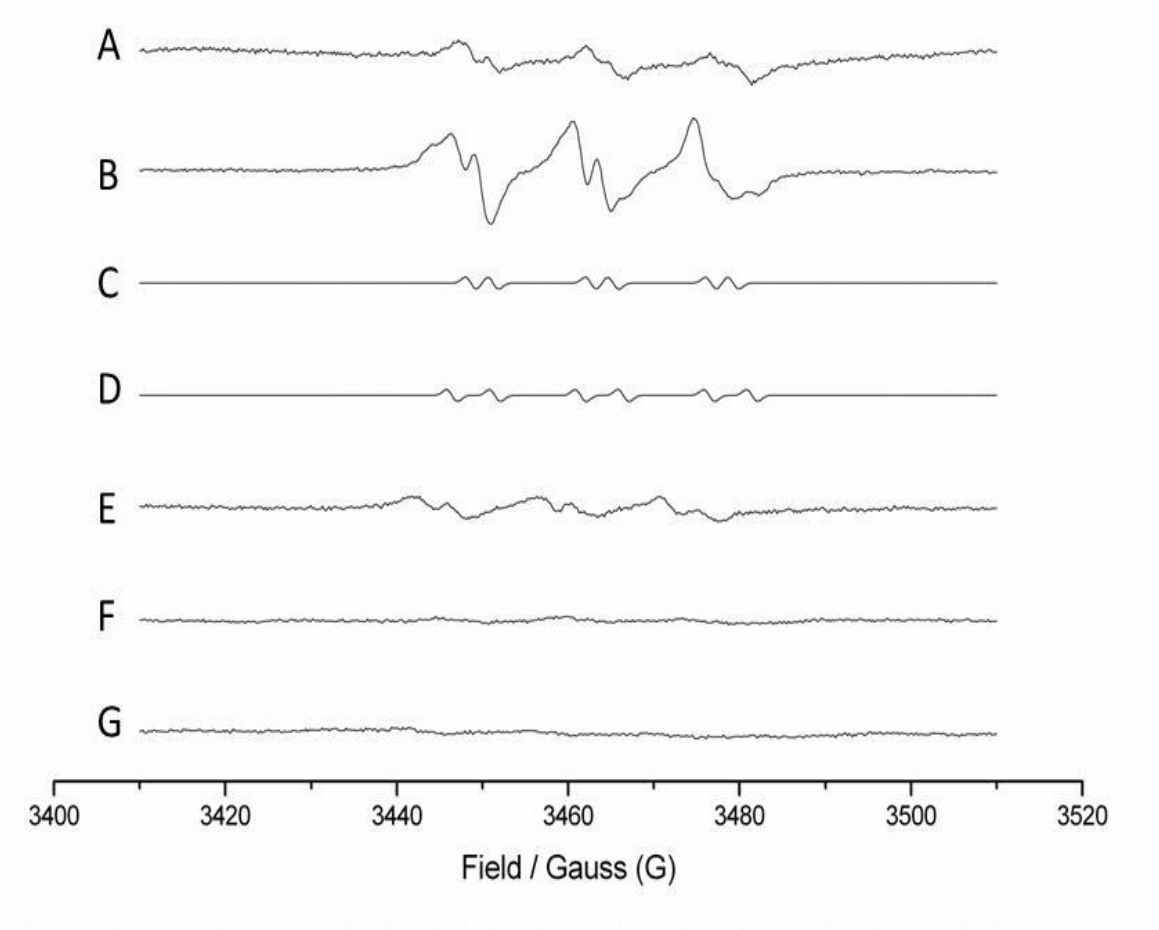

Figure 3.3. Representative EPR spectrum: Plasma lipid-derived radicals and experimental controls. (A) Example *ex-vivo* spectrum. (B) Example *in vitro* spectrum. Computer programming (Simfonia©) was used for qualitative confirmation of radical species identified in (A) and (B). (C) Simulation of the primary alkoxyl radical ($LO^{\cdot}$, αN = 14 Gauss, αH = 2.3 Gauss). (D) Simulation of an established PBN artefact detected within the experimental spectra (αN = 15 G; αH = 5 G). Ferrous sulphate/PBN generated an additional PBN artifact that was subtracted from the *in vitro* oxidation spectrum (E). No signal was generated from blood drawn into a syringe and then transferred directly to an EDTA vacutainer containing PBN, eliminating experimental initiation of radicals as an artifact (F). (G) PBN and saline alone produced no signal. Ordinates for all the spectra are plotted normalised to the same scale.

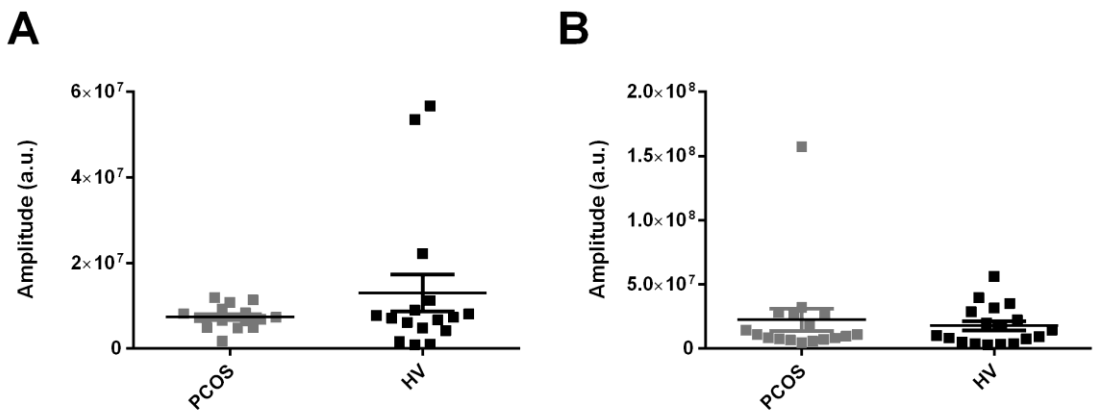

Figure 3.4. EPR measurements – Oxidative burden. Figure. (A) and (B) show the results of EPR analysis (*ex vivo* oxidative stress and *in vitro* oxidative potential, respectively) where the peak height was considered proportional to the amount of relative spin adduct concentration. [PCOS: n = 17, HV: n = 18]. Results are expressed as mean ± SEM.

The FOX assay was used to provide a marker of gross oxidative stress. Plasma hydroperoxide (ROOH) levels were similar between PCOS subjects and healthy volunteers (7.5 ± 4 µM and 6.7 ± 5 µM, respectively, p = 0.21, figure 3.5).

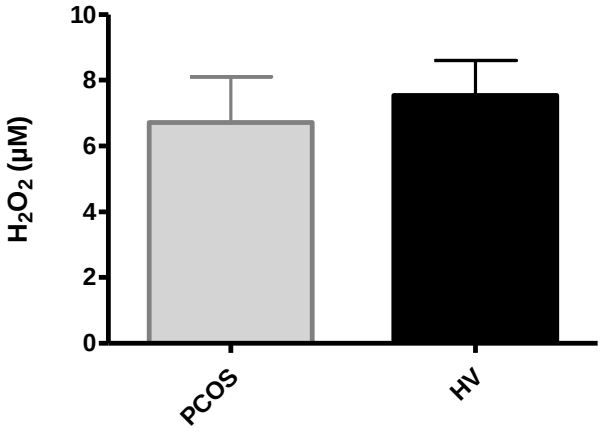

Figure 3.5. FOX assay – total plasma hydroperoxides (ROOH). Total plasma hydroperoxide (ROOH) concentration was measured by the FOX assay, a colorimetric method that involves the selective oxidation of ferrous to ferric ions by plasma ROOH. [PCOS: n = 17, HV: n = 18]. Results are expressed as mean ± SEM.

3.4.4 Antioxidant capacity

Total plasma antioxidant capacity and the lipophilic antioxidant capacity was assessed using ORACfl. Results reflect the ability of plasma (or selectively the lipophilic components of plasma) to buffer against AAPH, a thermally activated peroxyl-radical insult. Total plasma antioxidant capacity was similar between the PCOS group and healthy volunteers (94 ± 30 % and 79 ± 24 % respectively, p = 0.09, figure 3.6 A). However, PCOS subjects displayed a reduced lipophilic antioxidant capacity in comparison to healthy volunteers (92 ± 32 % and 125 ± 48 % respectively, p = 0.02, figure 3.6 B).

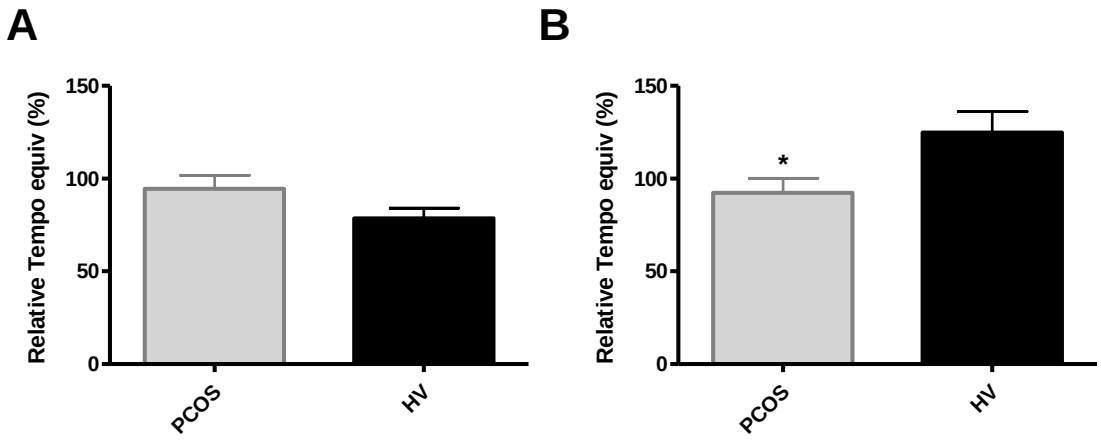

Figure 3.6 Plasma antioxidant measurements: (A) and (B) show plasma (total) antioxidant capacity and lipophilic antioxidant capacity, respectively. Antioxidant measurements represent the ability to buffer an insult from a thermo-activated peroxyl radical insult. [PCOS: n = 17, HV: n = 18]. Results are expressed as a percentage of 100 µM Tempo equivalents, a validated antioxidant. Each sample was analysed in triplicate and the mean was used in further analysis. Data is expressed as the group mean ± SEM.. * p<0.05.

3.4.5 Relationship of oxidative burden with insulin sensitivity, hyperandrogenism and regional adiposity

In PCOS subjects, after adjustment for age, *in vitro* oxidative capacity correlated moderately with testosterone (r = 0.64, *p* = 0.07) and insulin AUC (r = 0.51, *p* = 0.04), and strongly with visceral fat area (r = 0.76, *p* = 001). No significant relationships were noted with *ex vivo* radical generation in PCOS subjects. In control women, *in vitro* oxidative capacity correlated moderately with subcutaneous fat area (r = 0.53, *p* = 0.03) and visceral fat area (r = 0.58, *p* = 0.01), and negatively with testosterone (r = -0.55, *p* = 0.02). *Ex vivo* radical generation correlated moderately with visceral fat area (r = 0.49, *p* = 0.046). When PCOS and control women were analysed together, *in vitro* oxidative capacity correlated moderately with insulin AUC (r = 0.42, *p* = 0.01) and strongly with visceral fat area (r = 0.72, p <0.001) but in multiple linear regression analysis, only visceral fat area remained significant in the model (β = 0.6, *p* = 0.002).

3.5 Discussion

3.5.1 Main Findings

Previous studies have measured indices of global NO metabolism and oxidant status in subjects with PCOS with mixed results. To my knowledge this is the first study to specifically assess plasma NO_2^- (reflecting endothelial NO bioavailability), and directly measure circulating ROS levels (lipid-derived free radicals) in blood, in patients with PCOS using a series of sensitive, 'gold standard' methodologies. There was no evidence for altered NO bioavailability or stressed nitrosative/oxidative metabolism in these patients, other than PCOS subjects did show reduced lipophilic antioxidant capacity compared with healthy volunteers.

3.5.2 Interpretation

Plasma NO_2^- and NO_3^- levels were unaltered in PCOS subjects compared to age- and BMI-matched controls. These findings are consistent with previous reports (138, 139, 142, 266-269) but contrast with observations from many studies of endothelial function in patients with PCOS which have shown reduced FMD compared to healthy volunteers (265). These discrepancies may relate to the difficulties in measuring local, endothelial-derived NO that has an extremely short circulatory half-life estimated at less than 1 second. Researchers are thus reliant on measurement of NO_2^- and NO_3^-, the major metabolites of NO generated by stepwise oxidation, which are widely used as an index of endothelial NO synthase activity (41, 271). However, plasma NO_2^- and particularly NO_3^- reflect not only endogenous NO production but also dietary NO_3^- ingestion. I was careful to minimise the influence of dietary variation by fasting subjects overnight prior to measurement, however I cannot entirely rule out the possibility that dietary factors might have impacted upon my findings. Furthermore, in some instances plasma NO status may not reflect tissue NO status (272). Notwithstanding these limitations, my observations do not support a major alteration in NO bioavailability in women with PCOS, with values measured in the control and PCOS group similar to those measured across a broad range of healthy subjects (30).

Oxidative stress was also unaltered in PCOS patients compared with healthy volunteers. This is in contrast to most previous studies in women with PCOS which have shown an increased oxidative burden but have relied upon measurement of reaction end-products as biomarkers of damage to lipids and proteins (145). These measures are associated with a complex

biochemistry where the different thermodynamic and kinetic properties may contribute to overestimation of oxidative burden and inconsistent results. To my knowledge, this study is the only one to directly assess oxidative burden by EPR spectroscopy, the only analytical technique capable of direct detection of free radical species. Analysis of EPR spectra identified alkoxyl free radicals ($LO^{\cdot}$) as the dominant species present in the circulation of both subject groups. Previous studies have suggested that alkoxyl radicals evolve during a reaction catalysed by Fe^{2+} reductive decomposition of extracellular lipid hydroperoxides formed subsequent to primary radical-mediated damage to membrane phospholipids (144). Lipid-derived radical concentrations, whether measured directly *ex vivo* or *in vitro*, and plasma hydroperoxide levels were not different in women with PCOS compared to controls. However, the strongest implication of an oxidative burden from the observed relationship between visceral fat area and insulin AUC, implying that oxidative stress is linked predominantly with central adiposity and insulin resistance rather than PCOS *per se*. This may reflect accelerated adipocyte lipolysis in the pro-inflammatory obese state, leading to increased non-esterified fatty acids and subsequently increased ROS generation in mononuclear cells (123).

Interestingly, lipophilic but not total antioxidant capacity was reduced in PCOS subjects compared to healthy volunteers. Previous studies have noted reduced total antioxidant capacity in women with PCOS, independent of BMI or insulin resistance (151, 273). In contrast, a meta-analysis of six studies of total antioxidant capacity, including 470 women, found no significant difference between women with PCOS and controls (145). This is in agreement with our findings, although a trend towards an increased total antioxidant capacity in PCOS subjects was noted, but this did not quite achieve statistical significance, suggesting that antioxidant activity in the hydrophilic compartment may have undergone a compensatory increase to maintain homeostasis. The antioxidant capacity of the aqueous compartment is accounted for by proteins (including albumin) and ascorbic acid whereas fat-soluble antioxidants such as carotenoids and α-tocopherol are located in the lipoprotein core. Individual carotenoids may reflect dietary intake of fruits and vegetables, whereas plasma tocopherol concentrations correlate with vitamin E intake. Circulating vitamin E concentrations may be lower in women with PCOS compared with controls but vitamin A and β-carotene levels appear to be unchanged (149).

A depletion of antioxidant defences, accompanied by increased ROS production, is a hallmark of other diseases characterised by insulin resistance, notably type 2 diabetes (149). This redox imbalance leads to increased production of free radicals such as $^{\bullet}O_2^-$, which promote vascular smooth muscle contraction via inhibition of endothelial-dependent relaxation. Lipophilic antioxidant capacity may be especially important in regulating oxidation of LDL-cholesterol. LDL oxidation induces an inflammatory cascade and binding to scavenger receptors on the

surface of macrophages leading to foam cell generation and atherosclerotic plaque formation. Whilst oxidised LDL was not measured in this study, others have found that circulating concentrations are increased in women with PCOS (148, 274) although this is not a consistent finding (275).

3.5.3 Limitations

This study is the first to employ a series of sensitive methodologies to specifically assess plasma NO metabolites and directly detect free radical formation in the circulation of patients with PCOS. A detailed metabolic and anthropometric characterisation was also undertaken in order to understand the relationships of NO/oxidative status with insulin sensitivity and body fat distribution. However, although the well-established Rotterdam criteria was used to classify the PCOS population in this study, this may be associated with a less severe metabolic phenotype than other definitions of the syndrome (276). Hence it is possible that patients defined by NIH or Androgen Excess Society criteria might have more significant disturbances in cardiovascular homeostasis and oxidative burden. This particular cohort were also relatively young and it is tempting to speculate that disturbances in vascular NO metabolism and oxidative stress may not emerge until later in the disease course, in line with findings from studies of carotid intima media thickness where meaningful differences in atheroma burden were not apparent until middle age (264). Long-term dietary influences on antioxidant status are also difficult to adjust for, but we sought to minimise these effects by asking subjects to abstain from antioxidant medication prior to participation.

3.5.4 Conclusion

Further studies are needed to establish the causes and consequences of altered antioxidant capacity in women with PCOS but in the meantime our study confirms there is little evidence of abnormal NO/oxidative metabolism in young, overweight women with PCOS. This is in agreement with a recent finding within our research group, from a large population-based study in which Morgan *et al* (153) found no evidence for an increased incidence of cardiovascular events in young women with PCOS. Whilst these data may reassure clinicians treating young patients with PCOS that cardiovascular risk is not increased at this age, young women with PCOS are at increased risk of type 2 diabetes which is worsened by weight gain (153). Since a strong association of visceral fat with oxidative capacity was found, I speculate that weight loss

may be the most important measure in reducing oxidative stress and cardiometabolic risk in women with PCOS, although further trials are still needed to confirm if this is the case.

3.5.5 Key findings

- There was no evidence for altered NO bioavailability (plasma NO_2^- and NO_3^-) in PCOS patients when compared to age/BMI matched healthy volunteers.
- Indices of oxidative stress were also unaltered in PCOS patients.
- The total antioxidant capacity of plasma was similar between women with PCOS and healthy volunteers.
- PCOS patients presented with a decreased lipophilic antioxidant capacity compared to healthy volunteers.
- Within the PCOS group, *in vitro* oxidative capacity correlated with testosterone, insulin AUC and visceral fat area. Across both group's, *in vitro* oxidative capacity was independently associated with visceral fat.

4. RESULTS CHAPTER

Comprehensive characterisation of circulating microparticles in women with polycystic ovary syndrome

4.1 Introduction

Even though there is little biochemical evidence of nitro-oxidative stress in women with PCOS, there remains significant evidence suggesting that PCOS patients may be at increased risk of CVD, including hypertension (78) and endothelial dysfunction (11, 92, 277) but the mechanisms by which these occur are not yet fully established. Endothelial dysfunction, an early marker of vascular disease, is associated with reduced NO bioavailability and increased oxidative stress. However, in the PCOS patients (cohort studied and described in chapter 3), there was little direct evidence to suggest the presence of an increase in nitro-oxidative stress. More recently, elevated circulating MP levels has been associated with endothelial dysfunction (245, 278), however little is known about MPs in PCOS.

MPs are small (30-1000 nm diameter) membrane-enclosed vesicles released from a variety of prokaryotic and eukaryotic cells including platelets, monocytes and endothelial cells (154). They represent a homeostatic communication network between source and target cells, but may also play a role in disease pathology. Marked elevations in MP concentration have been reported in patients with cancer (279), diabetes (280), sepsis (188), hypertension (235) and myocardial ischaemia (191). Furthermore, elevations in PMPs have been observed in patients with CAD (233, 280).

MPs are formed during cell activation by a range of stimuli including apoptosis, inflammation and cellular differentiation (154). During formation, the phospholipid membrane asymmetry of the parental cell is altered causing translocation of PS moieties from the inner to the outer membrane bilayer. This exposure of negatively charged phospholipids to the outer bilayer, a key characteristic for MP identification, increases the potency of target cell interactions. For example, increased exposure of PS on the surface of PMPs renders their surface approximately 50 to 100 fold more procoagulant than the surface of activated platelet membranes (180).

Communication between MPs and target cells occurs via membrane-anchored receptors and surface adhesion molecules. Additionally, MPs are enriched with bioactive cargo from the parent cell including cytokines, chemokines, growth factors, fatty acids, mRNA and miR (281). *In vitro* studies indicate that MPs can pass this cargo into target cells, leading to alteration of cellular lipid metabolism, cell signalling and transduction. Barry and colleagues (282, 283) found that PMPs induce platelet activation through the transfer of arachidonic acid (C20:4n6, AA), which propagates pro-inflammatory effects via metabolism to thromboxane.

These observations suggest that MPs may play an important role in the pathogenesis of vascular dysfunction in 'at risk' populations. In this sense, MPs may play a critical role in the progression of PCOS pathology. The characteristics of circulating MPs in patients with PCOS is poorly described. Koiou *et al* (186) reported increased PMP concentrations in patients with hyperandrogenic PCOS, but the MP cell-of-origin, fatty acid composition and cellular cargo were not assessed in their study.

4.2 Aims

In light of these considerations, the aim of this chapter was to undertake a detailed characterisation of circulating MP populations in patients with PCOS, hypothesising that PCOS patients would carry an adverse MP profile, which might represent an early marker of disease progression that contributes to increased vascular risk leading to the eventual clinical sequelae.

4.3 Methods

4.3.1 Subjects and protocol

Details of ethical approval are detailed in section 2.1. Subject characteristics and anthropometric measurements are described in sections 2.2 and 2.5, respectively. Biochemical measurements were carried out by the Department of Medical Biochemistry at the University Hospital of Wales, as noted in section 2.4.

4.3.2 Isolation and storage of microparticles

Blood sampling is described in section 2.5. Plasma derived MPs were isolated by differential ultra-centrifugation as detailed in section 2.10.

4.3.3 Microparticle size, concentration and distribution

Plasma derived MP size, concentration and distribution was assessed using NTA as described in section 2.11. Following ultracentrifugation sample pellets were resuspended in MP-free PBS. For NTA, the isolated MP fraction was diluted to achieve an optimum concentration of 2-10 MPs $x10^8$/ml in MP-free sterile H_2O. NTA detection and analysis settings were modestly optimised for each sample. Specifically, camera sensitivity and detection threshold were (14–16) and (4–5), respectively. Samples were run in quintuplicate.

4.3.4 Cellular origin of microparticles

Antibody enabled flow cytometry was used to determine the cellular origin and extent of annexin V positivity of plasma derived MPs, as described in section 2.23.3. Results are expressed as a percentage of total events (MPs).

4.3.5 Lipid extraction and fatty acid analysis: microparticle and plasma

MP and plasma lipid extraction details are described in section 2.13. GC-FID was used to generate detailed fatty acid profiles of plasma and corresponding plasma-derived MPs, as noted in section 2.13. For plasma fatty acid concentration, results are expressed as µg/100µl of plasma. MP fatty acid concentration is normalised to MP count (determined by NTA) and expressed as pg / $1x10^6$ MPs. MP and plasma fatty acid composition represents the proportion (%) of individual fatty acids in relation to the total concentration.

4.3.6 Analysis of microRNA expression within plasma derived microparticles

Comprehensive miR expression profiling of plasma derived MPs was undertaken on a small subset of PCOS patients (n = 6, age: 33.8 ± 5 yrs, BMI: 28 ± 5 kg/m^2) and healthy controls (n = 6, age: 29.3 ± 5 yrs, 28 ± 6 BMI kg/m^2). miR profile analysis was performed using Toray 3D-Gene™ DNA Chip microarrays (Toray Industries Inc, Tokyo, Japan) as described in section 2.13. Additionally, miR 4700-5p was selected for validation by standard quantitative PCR (qPCR, PCOS patients (n = 12, age: 30 ± 6 yrs, BMI: 30 ± 6 kg/m^2) and healthy controls (n = 9, age: 25 ± 2 yrs, BMI: 26 ± 6 kg/m^2)), detailed in section 2.14.

4.3.7 Statistics

Data were analysed using GraphPad Prism version 5.0 (GraphPad Software, San Diego, CA, USA). D'Agostino's K-squared test was used to check data for normality. Analysis between groups was performed using the independent *t*-test or the Mann-Whitney *U*-test for normally or non-normally distributed data, respectively. Spearman's rank correlation coefficients were used to explore the strength of the relationship between MP concentration and biochemical parameters. The normalised microarray data were subjected to a Quantile-Quantile normalisation, $\log^2$ transformed then analysed using an unpaired Student's *t*-test. Results are expressed as mean ± SD unless indicated. A p-value <0.05 was considered statistically significant. Sample size calculations were based on previous data, which demonstrated a 0.55 fold shift in mean circulating MP concentration in women with hyperandrogenic PCOS compared to control subjects (186). Thus, to detect a similar shift in MP concentration, with >90% power at the 5% α level, a minimum of 15 subjects were recruited in each group.

4.4 Results

4.4.1 Clinical and metabolic characteristics

The metabolic and clinical characteristics of the PCOS and healthy volunteer groups are previously described in table 3.1 and section 3.4.1. Briefly, PCOS subjects (n = 17, 31 ± 6 and 30 ± 6 age (yrs) / BMI kg/m^2) had higher testosterone levels and a greater insulin response to an oral glucose challenge, indicating reduced insulin sensitivity compared to healthy volunteers (n = 18, 31 ± 7 and 29 ± 6 age (yrs) / BMI kg/m^2). No significant differences were observed between groups with respect to age, BMI, waist/hip circumference, lipid profile, hsCRP or glucose AUC.

4.4.2 Circulating microparticle concentration and size

PCOS subjects had increased total circulating MP concentration compared to healthy volunteers (11.45 ± 5 x10^{12}/ml vs. 9.98 ± 4 x10^{12}/ml, respectively; p = 0.03; figure. 4.1 A). In PCOS subjects, total MP concentration correlated significantly with HOMA-IR (r = 0.53, p = 0.03). MP size was similar in both groups (123 ± 7 nm vs. 114 ± 4 nm, respectively; p = 0.18; figure 4.1 B). To assess MP distribution, MP concentrations were grouped in 50 nm bin sizes (figure 4.1 C). PCOS subjects displayed an elevated concentration of small MPs (in the exosomal range, <150 nm in diameter) only, compared to healthy volunteers (as highlighted in table 4.1).

Table 4.1 **Distribution of plasma derived-MPs: PCOS versus HV.**

MP size (nm)	PCOS (*n* = 17)	HV (*n* = 18)	*p* value
0-50	4.27 ± 1.08 x10^8/ml	2.8 ± 1.48 x10^8/ml	0.002
51-100	3.71 ± 1.08 x10^9/ml	2.52 ± 1.07 x10^9/ml	0.002
101-150	4.71 ± 1.92 x10^9/ml	3.38 ± 0.9 x10^9/ml	0.001
151-200	2.04 ± 1.12 x10^9/ml	1.51 ± 0.36 x10^9/ml	0.07
201-250	5.34 ± 4 x10^8/ml	3.91 ± 1.25 x10^8/ml	0.17
251-300	1.3 ± 1.07 x10^7/ml	9.55 ± 5.1 x10^7/ml	0.24
301-350	3.58 ± 2.57 x10^7/ml	3.34 ± 2.68 x10^7/ml	0.79
351-400	1.31 ± 0.9 x10^7/ml	1.34 ± 1.3 x10^7/ml	0.93
401-450	1.89 ± 1.1 x10^7/ml	2.04 ± 1.62 x10^7/ml	0.75
451-500	1.91 ± 1.56 x10^6/ml	2.91 ± 2.5 x10^6/ml	0.18
501-550	2.83 ± 2.3 x10^5/ml	4.56 ± 3.93 x10^5/ml	0.13
551-600	5.86 ± 6.3 x10^3/ml	1.27 ± 2.56 x10^4/ml	0.28
600-1000	-	-	-

[PCOS: *n* = 17, HV: *n* = 18]. MPs with a diameter of 600 – 1000 nm were infrequent. MP, microparticle; PCOS, polycystic ovary syndrome. Each sample was analysed in quintuplicate and the mean was used in further analysis. Data is expressed as the group mean ± SEM.

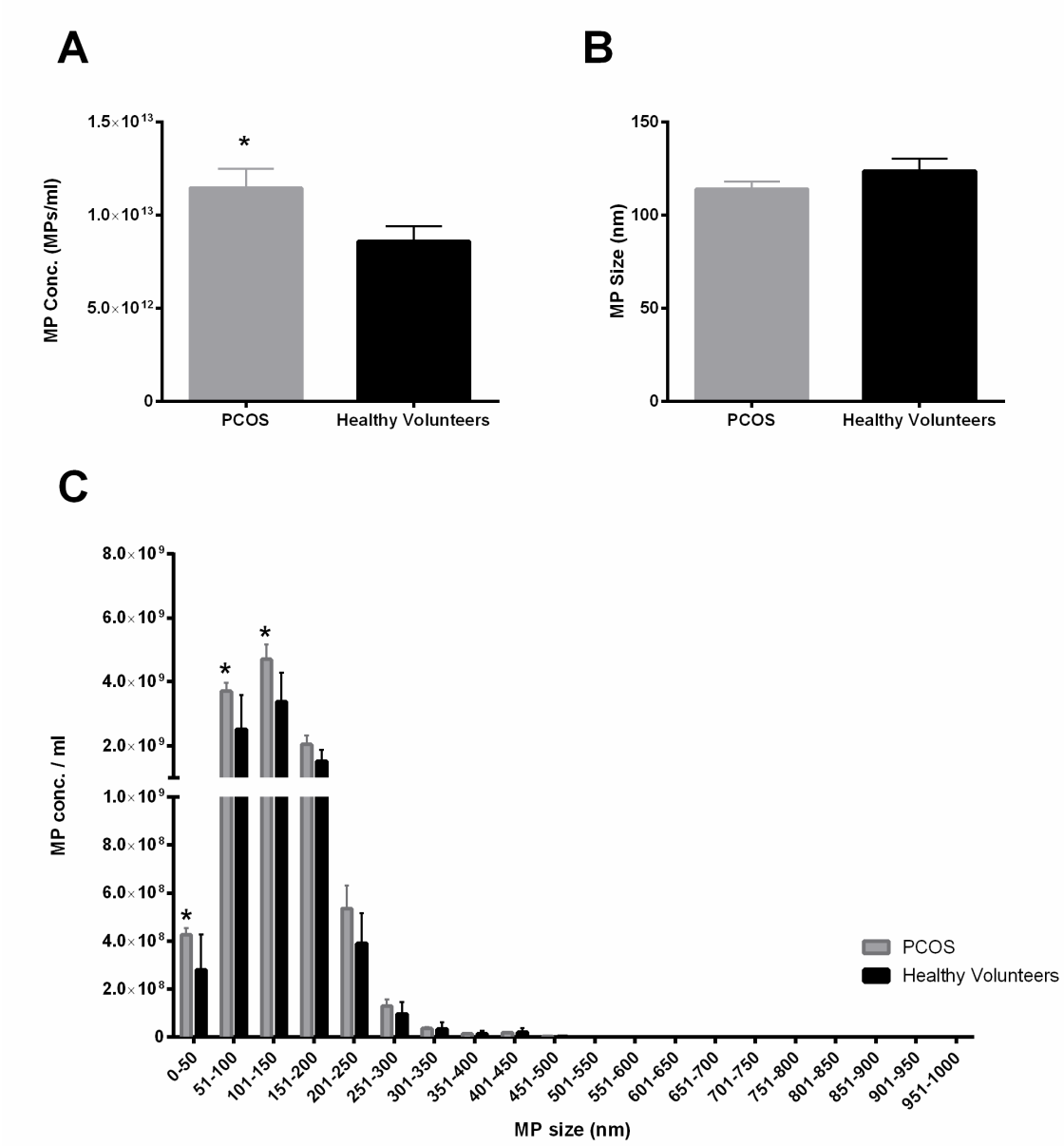

Figure 4.1. Quantification of circulating microparticles. (A) Plasma MP concentration in PCOS patients and healthy volunteers determined by NTA. (B) MP size. (C) Size distribution of plasma-derived MPs (presented in 50 nm bin sizes). [PCOS: n = 17, HV: n = 18]. Each sample was analysed in quintuplicate and the mean was used in further analysis. Data is expressed as the group mean ± SEM. * denotes p <0.05.

4.4.3 Cellular origin of circulating microparticles

MP cellular origin was determined by flow cytometry using monoclonal antibodies specific for the lineage markers CD41 (platelet), CD144 (endothelium) and CD11b (monocyte). In order to adhere to standard definitions, MPs were defined as annexin V positive MPs <1 μm in diameter. A greater percentage of annexin V^+ MPs was detected in PCOS subjects compared to healthy controls (83.6 ± 18 % vs. 74 ± 24 %, respectively; p = 0.05; Figure 4.2 A). PMPs (CD41 positive MPs) occupied by far the greatest proportion of annexin V positive circulating MPs in both PCOS subjects and healthy volunteers (99.3 ± 0.9 % vs. 98.6 ± 2.5 %, respectively; p = 0.27; figure 4.2 A). Annexin V and CD144 or CD11b positive MPs (endothelial and monocyte-derived MPs, respectively) were infrequent (figure 4.2 B). A similar trend was observed in the annexin V negative MP population. PMPs occupied the largest proportion of circulating MPs in both PCOS subjects and healthy volunteers (94 ± 4% vs. 94 ± 9%, respectively; p = 0.8). Annexin V negative but CD144 or CD11b positive MPs were infrequent.

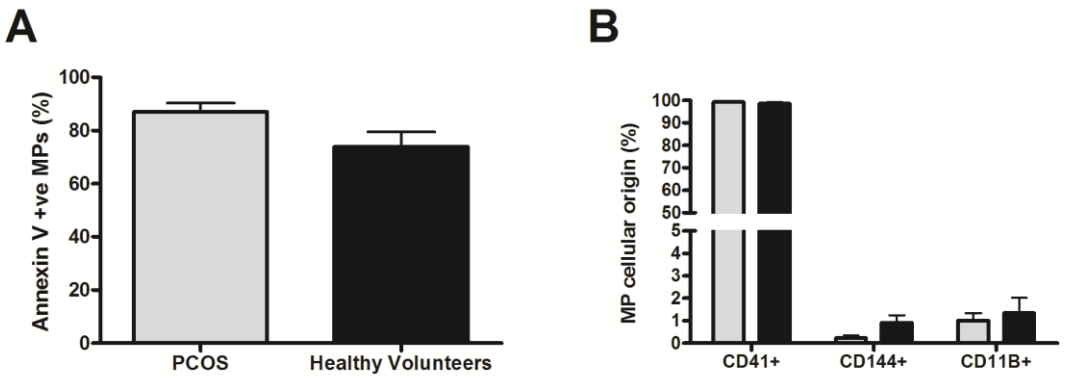

Figure 4.2. **Annexin positivity and cellular origin of annexin V positive plasma-derived MPs.** (A) The percentage of annexin V positive MPs in PCOS patients and healthy controls determined by flow cytometric analysis. (B) Plasma MP cellular origin, determined by flow cytometric analysis of the lineage-specific markers CD41 (platelet), CD144 (endothelium) and CD11b (monocyte) of annexin V positive MPs <1 μm in diameter. [PCOS: n = 17, HV: n = 18]. Data are presented as mean ± SEM.

4.4.4 Fatty acid analysis

Since an altered lipid metabolism may be a feature of PCOS, I explored if MPs similarly exhibited an altered fatty acid profile. Using GC-FID, the total fatty acid concentration of MPs was similar in PCOS subjects and healthy volunteers (9 ± 9 pg/10^6 MPs vs. 12 ± 11 pg/10^6 MPs, respectively; p = 0.39; figure. 4.3 A). No differences in individual MP fatty acid composition were found between PCOS patients and healthy controls (figure. 4.3 B).

To assess whether MP fatty acid composition was unique to MPs and not simply reflecting plasma fatty acid distribution, I also undertook an analysis of plasma fatty acids (figures 4.3 C and D). In an analysis of all PCOS and healthy volunteer samples, MP fatty acid composition was found to be different from the fatty acid composition of plasma, whereby 14 fatty acids were differentially enriched (p <0.05, table 4.2). No differences were found between PCOS patients and healthy volunteers with respect to total plasma fatty acid concentrations (426 ± 99 µg / 100 µl and 335 ± 51 µg / 100 µl, respectively, p = 0.65, figure. 4.3 C) but individually, several plasma fatty acid concentrations were elevated in PCOS subjects including C14: 1 (myristoleic acid), C16: 1n9 (hexadecenoic acid), C22: 3n6 (docosatrienoic acid) and C22: 5n3 (docosapentaenoic acid, all p<0.05).

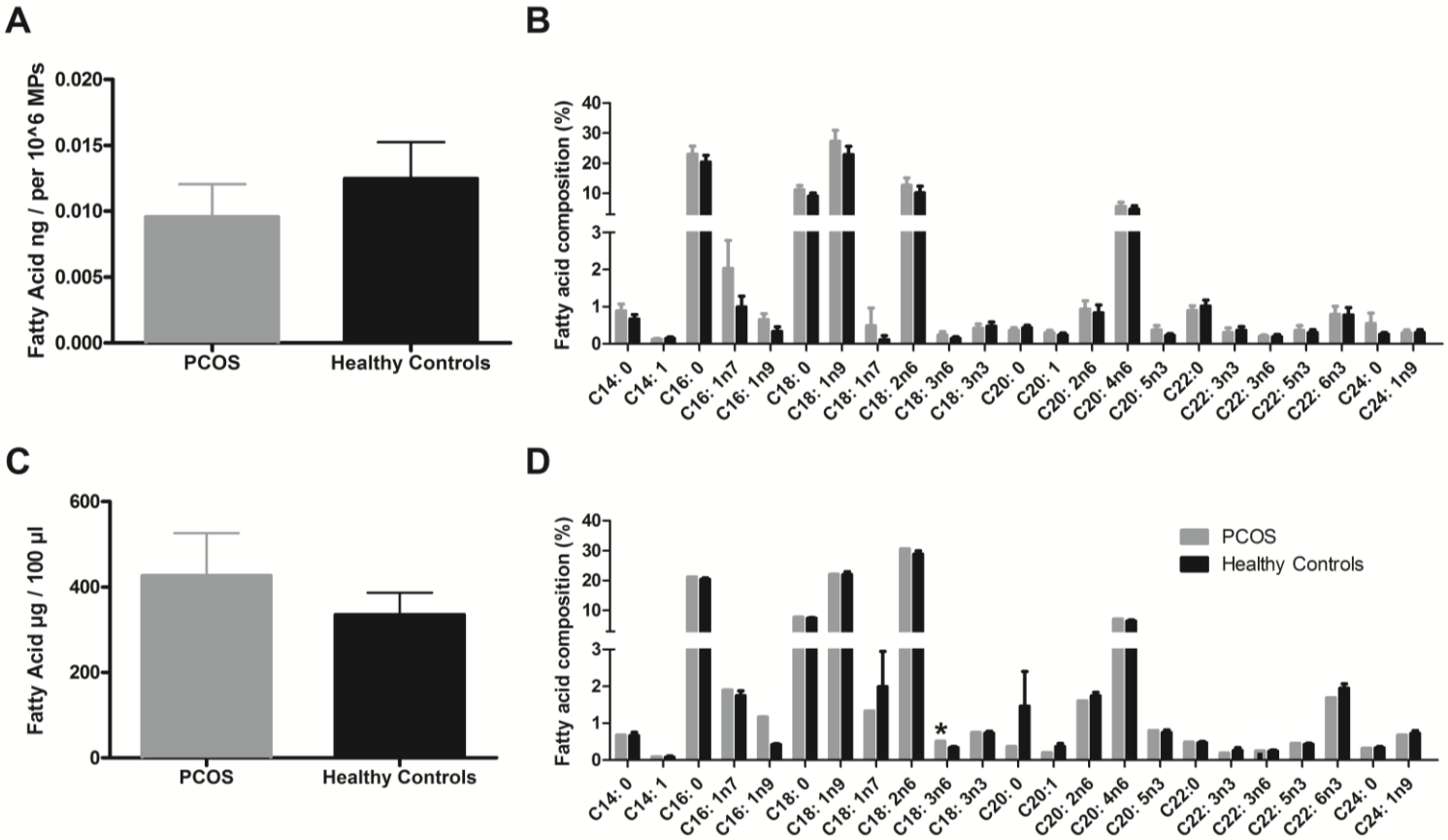

Figure 4.3. Fatty acid analysis. GC-FID was used to measure fatty acids in plasma and circulating MPs. (A) Fatty acid concentration in circulating MPs. (B) Fatty acid composition of plasma derived MPs. (C) Total fatty acid concentration in plasma, reflecting fatty acid concentration per 100 µl of plasma (D) Fatty acid composition of plasma (%). [PCOS: n = 17, HV: n = 18]. Data are presented as mean ± SEM. * denotes p <0.05.

Table 4.2 **Comparison between microparticle and plasma fatty acid composition**

	MP		Plasma		
Fatty Acid	**Mean**	**SD**	**Mean**	**SD**	***p* value**
C14 :0	0.93 %	0.60%	0.67%	0.35%	0.038
C14: 1	0.20 %	0.21 %	0.09 %	0.11 %	0.012
C16: 0	27.32 %	5.82 %	20.80 %	3.27 %	<0.001
C16: 1	0.56 %	0.64 %	0.78 %	1.94 %	0.519
C16: 1n7	1.59 %	2.15 %	1.82 %	0.68 %	0.562
C18: 0	12.95 %	4.07 %	7.59 %	1.24 %	<0.001
C18: 1n9	30.69 %	5.58 %	22.07 %	3.32 %	<0.001
C18 1n7	0.36 %	1.73 %	1.67 %	2.94 %	0.028
C18 2n6	12.72 %	6.04 %	28.20 %	4.05 %	<0.001
C18 3n6	0.20 %	0.20 %	0.42 %	0.20 %	<0.001
C18: 3n3	0.51 %	0.43 %	0.74 %	0.24 %	0.008
C20: 0	0.56 %	0.53 %	0.93 %	2.91 %	0.466
C20: 2n6	0.95 %	0.61 %	1.67 %	0.41 %	<0.001
C20: 4n6	5.74 %	3.85 %	6.83 %	1.61 %	0.139
C20: 5n3	0.31 %	0.25 %	0.77 %	0.30%	<0.001
C22:0	1.40 %	0.95 %	0.48 %	0.20 %	<0.001
C22: 3n3	0.39 %	0.55 %	0.23 %	0.27 %	0.137
C22: 3n6	0.23 %	0.25 %	0.25 %	0.13 %	0.743
C22: 5n3	0.34 %	0.32 %	0.44 %	0.13 %	0.114
C22: 6n3	0.86 %	0.68 %	1.83 %	0.54 %	<0.001
C24: 0	0.51 %	1.06 %	0.33 %	0.13 %	0.346
C24: 1n9	0.33 %	0.27 %	0.70 %	0.27 %	<0.001

MP, microparticle. Mean and SD values represent data from across both subject groups [n = 37].

4.4.5 Analysis of microRNA expression

Toray 3D-Gene™ chip analysis was employed to profile the miR content of circulating MPs in a subpopulation of PCOS patients and healthy controls. In excess of 1,600 antisense probes were plated onto the miR chip. All subjects analysed had a total miR count of >500. Similar miR expression profiles were observed between groups for the most highly expressed miRs. However, among the lowly expressed miRs, 16 were differentially expressed between groups (figure 4.4, table 4.3). qPCR was used to validate the differentially expressed miR 4700-5p. Women with PCOS displayed a threefold-elevated expression of miR 4700-5p compared to healthy volunteers, but this did not quite reach significance ($p = 0.1$).

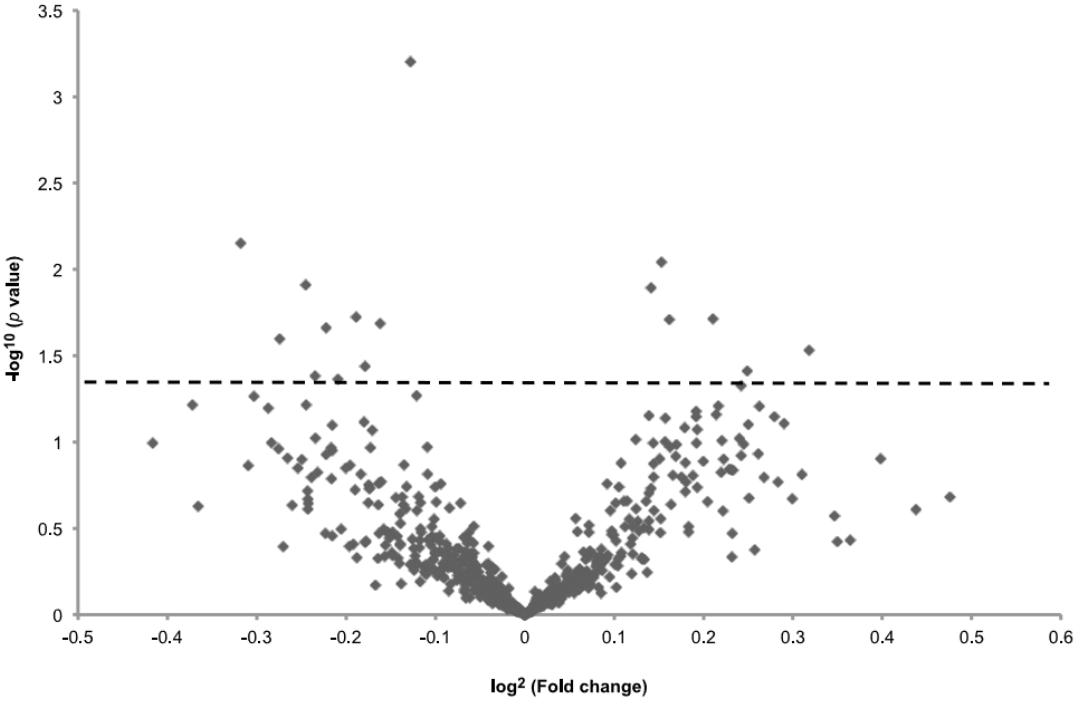

Figure 4.4. microRNA (miR) expression in plasma-derived microparticles. In excess of >1,600 miRs were analysed using the Toray 3D-Gene™ microarray platform. The volcano plot depicts differentially expressed miRs between PCOS patients and healthy volunteers. A -log10 *p*-value >1.3 equates to $p < 0.05$. 16 miRs were differentially expressed at this threshold. [PCOS patients ($n = 6$), healthy controls ($n = 6$)].

Table 4.3 **Differentially expressed miRs in circulating microparticles**

microRNA (miR)	Expression ratio	*p* value
hsa-miR-551a	0.91	<0.001
hsa-miR-4324	0.80	0.007
hsa-miR-3689b, hsa-miR-3689c	1.11	0.009
hsa-miR-1293	0.84	0.012
hsa-miR-3936	1.10	0.012
hsa-miR-4481	0.88	0.019
hsa-miR-629	1.16	0.019
hsa-miR-4425	1.19	0.019
hsa-miR-30b	0.89	0.021
hsa-miR-3622a-3p	0.86	0.022
hsa-miR-514b-5p	0.83	0.025
hsa-miR-4700-5p	1.25	0.029
hsa-miR-4708-3p	0.88	0.037
hsa-miR-574-3p	1.19	0.038
hsa-miR-4283	0.85	0.041
hsa-miR-23a	0.86	0.043
hsa-miR-3156-5p	1.18	0.047

[PCOS patients (n = 6), healthy controls (n = 6)]. Expression ratio was calculated as average PCOS miR expression / average healthy control miR expression. All samples tested had total miR counts >500.

4.5 Discussion

4.5.1 Main findings

This study shows that patients with PCOS have increased concentrations of circulating annexin-V positive MPs compared with age- and BMI-matched healthy volunteers. This study also found that these MPs are predominantly platelet-derived. Thus, it is tempting to speculate that these alterations may contribute to an increased cardiovascular risk. The findings in this chapter are consistent with those found in two previous studies in which PMPs were found to be elevated in lean (186) and overweight/obese (186, 284) hyperandrogenic patients with PCOS. However, this study extended these observations to characterise the fatty acid and miR profile of circulating MPs, and show an association between MP concentration and insulin resistance in this patient population.

4.5.2 Interpretation

A similar proportion of MPs derived from platelets, monocytes and ECs were detected in PCOS patients and healthy volunteers. In accordance with previous reports, we found that PMPs occupied the greatest percentage of circulating MPs (188). In contrast, others have found higher percentages of endothelial- and monocyte-derived MPs in healthy subjects (43% and 10.4%, respectively) (225) which may reflect different methodologies and pre-analytic protocols. Previous studies have shown that PMP concentrations are elevated in lean and overweight/obese women with PCOS compared to controls (186, 284). These studies used CD41-directed flow cytometry to assess PMPs only, hence they were unable to compare MP cellular origin. Using NTA I found that the increases in MP concentration in subjects with PCOS were largely due to an increased concentration of MPs in the small (<150 nm), exosomal range. This may suggest selective stimulation of the intracellular classical exosomal pathway compared to larger MPs (150-1000 nm diameter) formed via cell membrane shedding. The clinical significance of this elevated MP population remains unclear. Flow cytometry and sorting methodologies typically struggle to detect MPs that are <200 nm in diameter, however sucrose density gradients have isolated MPs (within the exosomal range) based on their density. Future studies could attempt to isolate the MPs in the exosomal range via sucrose density gradients and explore their functional characteristics (for example in isolated vessel experiments).

Koiou *et al.*, (186) found a weak, but significant correlation between PMPs and serum testosterone levels in their study of lean patients with PCOS. In contrast, I noted a moderately strong correlation of MP concentration with homeostatic model assessment (HOMA)-IR in PCOS subjects, suggesting that elevated MP levels may be attributable, at least in part, to increased insulin resistance. This is in line with several reports of increased MP concentrations in patients with type 2 diabetes (175) including those with end-organ damage (285). Metabolic syndrome, a disorder underpinned by insulin insensitivity, is also characterised by an increased circulating MP concentration compared to healthy controls (190, 220, 286), where they may contribute to endothelial dysfunction via increased oxidative stress (190) and reduced NOS expression (220), although there is no evidence of this, as yet in this study. Hyperglycaemia (200), inflammation and stress (287) might also contribute to MP production. PCOS patients presented with a greater percentage of annexin V positive MPs. The extent of annexin V staining is largely taken to reflect binding to PS which increases the potency for target cell interactions and may contribute to enhanced pro-coagulant activity (180).

Fatty acids are recognised as potent endocrine signalling molecules, which play an important role in MP function, via the direct transfer of bioactive fatty acids to induce pro-inflammatory responses in target cells (282). No differences were observed in MP fatty acid composition between PCOS patients and healthy controls. However, MP fatty acid composition was significantly different from that of plasma, perhaps indicating that MPs are 'packaged' with a unique fatty acid signature rather than merely reflecting the fatty acid composition of their environment.

This is the first study to investigate the miR content of circulating MPs in patients with PCOS. In an exploratory sub-population, miR expression profiles were similar amongst women with PCOS and healthy volunteers for the most highly expressed miRs. However, 16 lowly-expressed miRs were found to be differentially expressed. Of these, miR-1293, miR-551a and miR-574-3p may be particularly noteworthy, as these target cellular functions of relevance to PCOS pathology. miR-1293 targets peroxisome proliferator-activated receptor gamma (PPAR-γ) co-activator (PPARGCA1), a pivotal regulator of glucose homeostasis. miR-551a regulates H6PD, mutations of which are recognised as a cause of hyperandrogenic PCOS (288), whilst mir-574-3p targets the follicle-stimulating hormone beta-subunit (FSHB) and follicle-stimulating hormone receptor (FSHR) as previously noted in ovarian follicle fluid of PCOS patients (289). Previous studies have shown that MPs harbour a spectrum of miRs, and can offload their genetic content in target cells, altering their biological activity. Thus, data in this chapter suggests a novel mechanism by which PCOS may affect cardiometabolic risk.

4.5.3 Limitations

There are a number of potential limitations to this study. Firstly, PCOS patients were classified by the Rotterdam criteria, which describes a less severe metabolic phenotype than other definitions of the syndrome (276). Thus, these findings may not necessarily be generalisable to all patients with PCOS, but the presence of an altered MP profile in this young, mildly insulin resistant population suggests that changes in MP expression may occur early in the disease course. Secondly, miR expression analysis was only undertaken in an exploratory subset of the overall study population, hence validation of these findings in a larger cohort is mandatory. Furthermore, miR levels were unaltered for the highly expressed miRs and it is unclear whether differences in the lowly expressed miRs carries pathological relevance. Finally, methodological variability at both the sample preparation and analysis stage may make inter-study comparisons difficult. Whilst attempts were made to minimise the number of centrifugation steps, it is conceivable that platelet contamination might generate PMPs in the freeze-thaw process. Additionally, whilst flow cytometry is acknowledged as the current gold standard for the determination of MP origin, the detection of smaller MPs (30-400 nm, representing ~80% of the MP range) is imperfect and it cannot observe the entire spectrum of MPs assessed using NTA. Retrospectively, with the majority of circulating MPs derived from platelets, platelet activity and functional pro-thrombotic analysis (for example via Multiplate and/or thrombinoscope experiments) would perhaps provide information/associations with PMP levels.

4.5.4 Conclusion

In summary, this study suggests that patients with PCOS have an elevated concentration of circulating MPs compared with healthy volunteers. These MPs are predominantly platelet-derived, are associated with increased annexin V binding and an altered miR expression profile. Further studies are needed to confirm these findings, to explore the relevance of such changes to cardiovascular risk in women with PCOS and to establish whether therapies that improve insulin sensitivity are able to reduce circulating MP concentrations.

4.5.5 Key points

- PCOS subjects presented with an elevated concentration of annexin V positive plasma derived MPs compared to age/BMI matched healthy volunteers.
- The increase in MP concentration in women with PCOS was related to an increased concentration of MPs in the small (<150nm) exosomal range. This may suggest selective stimulation of the intracellular classical exosomal pathway compared to larger MPs (150-1000 nm diameter) formed via cell membrane shedding.
- PMPs occupied by far the greatest proportion of plasma derived MPs in both PCOS subjects and healthy volunteers. EMPs and monocyte-derived MPs were infrequent.
- MP miR expression profiles were similar between women with PCOS and healthy volunteers amongst the most highly expressed miRs. However, 16 lowly-expressed miRs were found to be differentially expressed.

5. RESULTS CHAPTER

The effects of metabolic stressors on endothelial cell microparticle production

5.1 Introduction

In the previous chapter, PCOS patients presented with an elevated circulating concentration of annexin V positive MPs compared to healthy volunteers. Mechanisms by which this occurs remain unclear. This chapter seeks to establish a series of *in vitro* models that mimic the key features of PCOS, using pathologically relevant stressors, with the goal of assessing their effect on EC MP production.

The vascular endothelium occupies a unique interface between circulating blood and extravascular tissues. It is a dynamic autocrine and paracrine organ that maintains vascular homeostasis by modulating vascular tone, governing local cellular growth and regulating inflammatory responses (8). Under physiological conditions the vascular endothelium maintains an anti-thrombotic surface. In contrast, under pathological stresses, alterations in the vascular endothelium may shift the pattern towards a pro-thrombotic state. EC activation can also promote cellular interactions with circulating cells by elevated expression of surface adhesion molecules. Moreover, EC activation is associated with a reduction in anticoagulant surface molecules such as TM and a concomitant elevation in prothrombotic components such as TF (8, 9).

An additional feature of an activated EC is the elevated secretion of MPs into the extracellular space (167). MPs derived from the endothelium harbour an array of adhesion molecules including VE cadherin, ICAM-1, VCAM-1, PE-CAM-1, endoglin, E-selectin and P-selectin. Moreover, EMPs have been shown to posess eNOS, vascular endothelial growth factor receptor (VEGF-R2) and NADPH oxidase (167). MPs derived from the endothelium externalise PS to the outer membrane bilayer rendering them annexin V positive. This exposure of negatively charged phospholipids to the outer bilayer may increase the potency of target cell interactions. However, *in vivo* studies have found that annexin V negative MPs expressing endothelial markers are present in human plasma, suggesting that not all EMPs externalise PS (199). The mechanisms governing the release of EMPs remain unclear. *In vitro* experiments have shown that MP release is associated with μ-calpain activation and increased protein tyrosine phosphatase activity (170). However, the protein composition and functional characteristics of EMPs is hypothesised to depend on the stimulus triggering their release (197).

The vascular endothelium, which forms the barrier between blood and the surrounding tissues, is known to efficiently respond to stress signals such as hypoxia by adaptation of cellular physiology, secretion of growth factors and modulation of vascular tone (9). ECs can secrete MPs and have the ability to also be targeted by MPs from multiple cellular origins (200). Thus, with the endothelium playing a crucial role in regulating vascular homeostasis, as a first line blood-tissue defensive barrier against a spectrum of acute and chronic stressors, this study compared MPs secreted by EC's following exposure to pathologically relevant stressors. Building on the human PCOS model (as outlined in chapters 3 and 4), which is characterised by hyperinsulinaemia and hyperandrogenism, ECs were exposed to: testosterone (hyperandrogenism stressor); hypoxia (ischaemia model stressor); insulin (metabolic stressor); glucose (metabolic stressor) and H_2O_2 (oxidative stress stressor).

5.2 Aims

The aim of this study was to assess the effect of metabolic stressors on EC MP production *in vitro*. Specifically, the aims of this work were to:

- Examine the production and characteristics of MPs following exposure to stressors akin to those featured in patients with PCOS.
- Characterise the distribution of surface adhesion molecules on ECs and their corresponding MPs.
- Examine the pro-coagulant activity of EC derived-MPs in response to metabolic stress.

5.3 Methods

5.3.1 Cell culture

The HECV cell line was maintained as described in section 2.15. Primary HUVECs were cultured in Endothelial Cell Growth Medium as detailed in section 2.15. All cells were counted using Cellometer® (Nexlon Biosciences Auto T4) and expressed as cells/ml.

5.3.2 Cell treatments (metabolic stressors)

HECV and HUVEC cultures were treated with metabolic stressors as described in section 2.16 (pathologically relevant stressors: hypoxia, glucose, insulin, H_2O_2, and testosterone). All stressors were diluted in SFM as described in section 2.16. Control ECs were treated with SFM only.

5.3.3 Microparticle isolation

MPs were isolated using differential ultra-centrifugation as detailed in section 2.17. MPs were analysed fresh.

5.3.4 Microparticle size, concentration and distribution

MP size and concentration was determined using the NanoSight LM10 system, as previously described in section 2.11. Specifically, 60-second videos were recorded. Camera sensitivity and detection threshold were (14-16 arbitrary units) and (4-5 arbitrary units), respectively.

5.3.5 Confocal microscopy

Confocal microscopy was employed in several 'proof of concept' experiments. Specifically, confocal microscopy was used to:

- Visualise MP production in real-time
- Assess annexin V positive/negative MPs
- Examine MP adhesion / cell-interaction

- Visually support NTA data

Cell / MP staining and confocal microscopy is detailed in section 2.18.

5.3.6 Electron Microscopy

SEM was used to visualise MPs shedding of stimulated and un-stimulated HECV cells, as noted in section 2.19.1. TEM was also used to assess isolated MP morphology and purity, as detailed in section 2.19.2.

5.3.7 Cell viability and apoptosis

To assess the effect of such pathological insults on cell viability and apoptosis, CellTiter 96® AQueous cell proliferation assay (Promega, UK), Caspase-Glo® 3/7 assay (Promega, UK) and trypan blue exclusion (Sigma-Aldrich, UK) were undertaken. Methods are described in section 2.20.1, 2.20.2 and 2.20.3, respectively.

5.3.8 Flow cytometry

Antibody enabled flow cytometry was used to measure the proportion of MPs that were annexin V positive/negative as well as to characterise the surface adhesion molecule profile of:

- HECV cells following exposure to a pathological stressor.
- EMPs from HECV cells exposed to stressors.
- Unstimulated HECV cells treated with EMPs derived from HECV cells treated with stressors.

Methods are described in section 2.23.4.

5.3.9 Microparticle coagulability

As an indication of MP coagulability, the multiplate analyser was used to investigate the ability of EMPs to adhere to an artificial surface electrode, as detailed in section 2.21.

5.3.10 The effect of MPs on platelet function

Two methods were used to assess the effect of MPs on whole blood (platelet) aggregation, including a Multiplate® multiple electrode aggregometer as described in section 2.22 and cytometric analysis of platelet activation, as detailed in section 2.23.5.

5.3.11 Oximetry

EPR-spin trapping was used to measure the O_2 concentration in cell culture medium following exposure to 1 % O_2 (hypoxia), as described in section 2.7.2.

5.3.12 siRNA and Western blot

To determine the role of HIF-1α in hypoxia-induced MP release, cells were transfected with HIF-1α siRNA as noted in section 2.26. Western blotting was used to compare the protein expression of HIF-1α, as detailed in section 2.27.

5.3.13 Statistics

Data were analysed using GraphPad Prism V6.0. The D'Agostino's K-squared test was used to check data for normality. Analysis between groups was performed using an ordinary one-way ANOVA coupled with a Dunnett's or Tukeys post-analysis test. Results are expressed as mean ± SD unless indicated. A *p*-value of <0.05 was regarded as statistically significant.

5.4 Results

5.4.1 MP production - 'proof-of-principle'

Proof of principle experiments were undertaken to provide evidence that HECV cells produce extracellular MPs and to assess whether these EMPs can interact with other ECs. Firstly, to ensure confocal microscopy could visualise <1 μm MPs, FITC was conjugated to 100 nm carboxylated beads. These were clearly visualised under FITC fluorescence channels (Figure 5.1 B, D). HECVs were seen to produce intact extracellular vesicles (figure 5.1 A, C), however not all MPs were annexin V positive (Figure 5.2). MP-EC interaction and adhesion was visualised by treating an 80 % confluent monolayer of unstimulated HECVs with Cell Trace stained EMPs (figure 5.3 A, B). MPs appeared to internalise as intact vesicles suggesting that EMPs are taken-up by neighbouring ECs and may reflect an important model by which MPs and ECs interact (figure 5.3 C). Of particular interest, MP formation and secretion appeared to originate from nanotubes/micro-spikes protruding from the cell membrane.

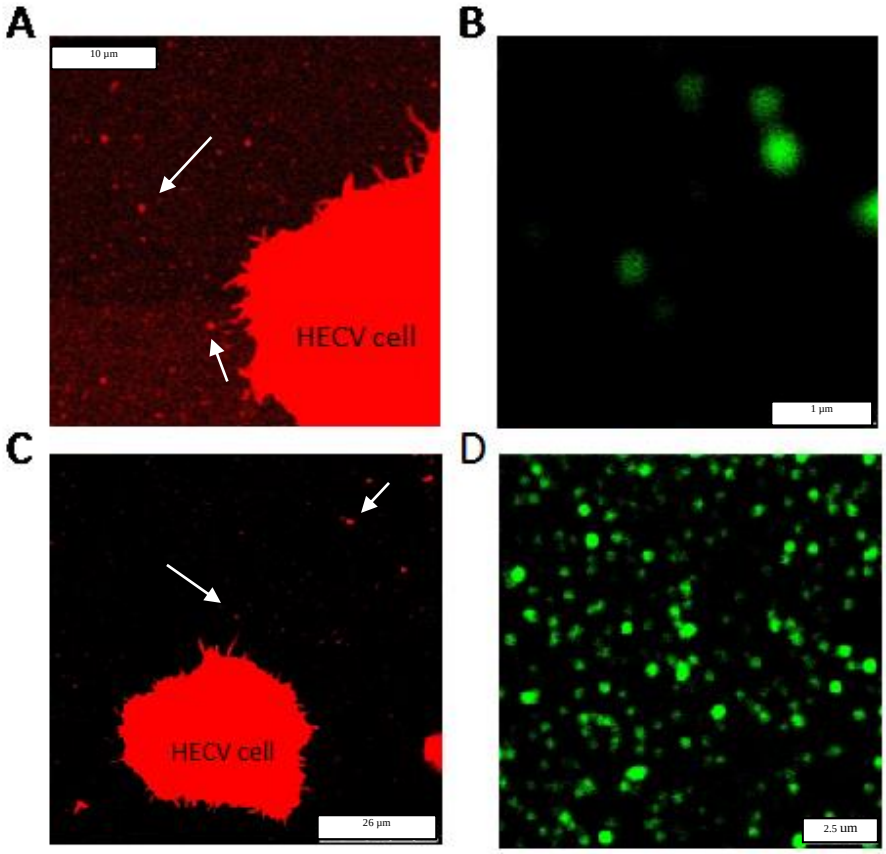

Figure 5.1 HECV-derived microparticles. (A, C). Images showing intact MPs (stained with Cell Trace Red/Orange). (B, D). FITC bound 100 nm polystyrene beads. Arrows = selective MPs. Scale bars: 10 μm (A), 1 μm (B), 26 μm (C) and 2.5 μm (D).

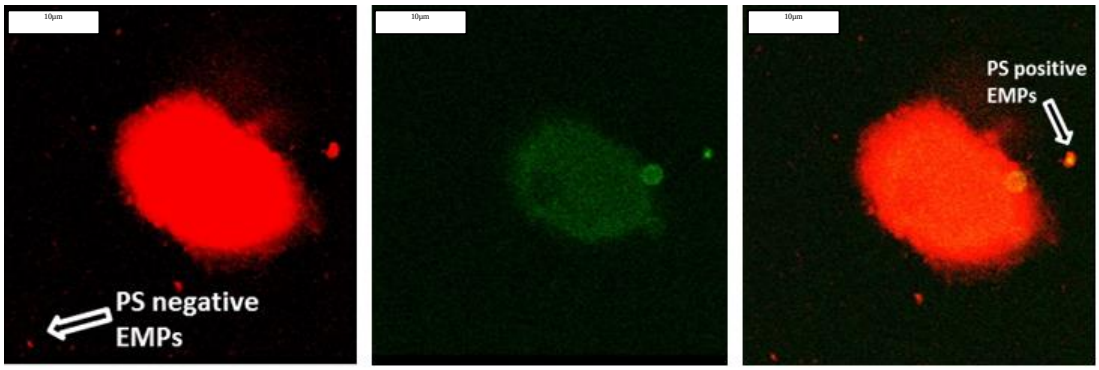

Figure 5.2 Annexin V positive/negative MPs. [Left] HECV cell (stained with Cell Trace Red/Orange) secreting 'intact' spherical MPs. [Middle] Green represents annexin V positive-FITC staining. [Right] Overlay image demonstrating annexin V positivity MPs. Scale bars: 10 μm.

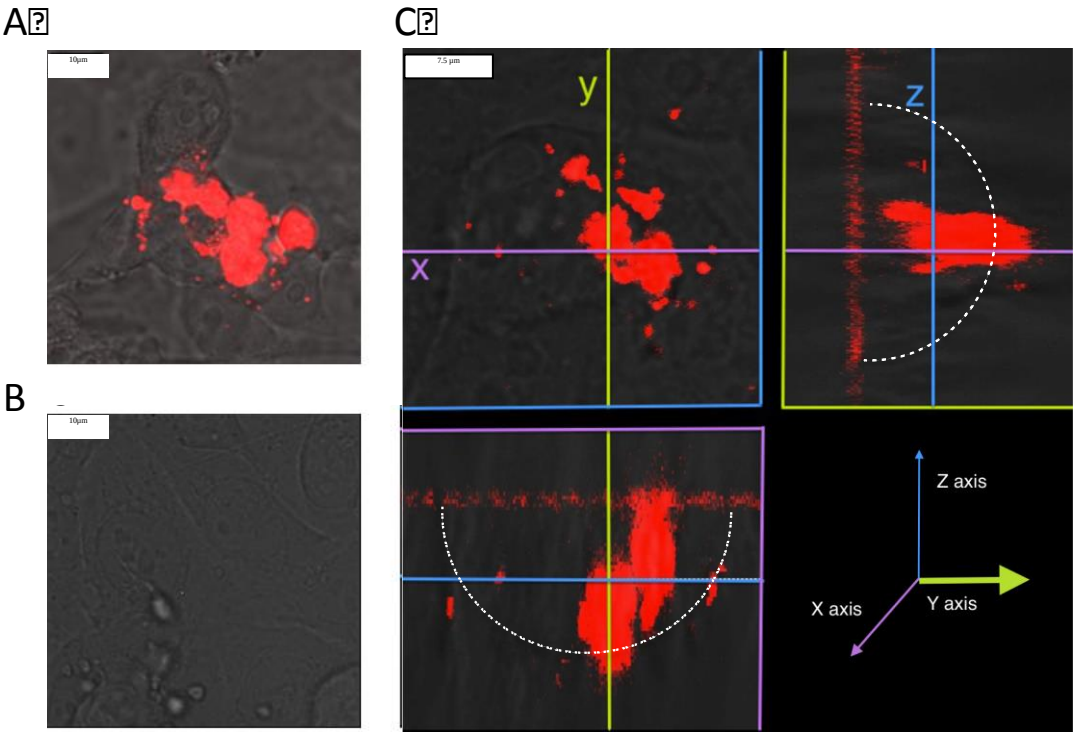

Figure 5.3. EC-MP interaction/adhesion. (A). Confocal microscopy image showing intact MPs (derived from cell traced HECV cells) adhere to an unstimulated HECV monolayer (Red indicates MP stained with Cell Trace Red/Orange). (B). A 3D reconstruction of MPs (stained with Cell Trace) internalised in a HECV cell. MPs appear to endocytose / internalise as intact MPs in target HECV cells. The white dotted line represents the cell membrane (approximation). [Bottom right] schematic demonstrating the confocal viewing planes for figure C (X, Y and Z axis). (C). Control, showing no Cell Trace contamination from the supernatant from the last wash step. Scale bars: 10 μm (A, B) and 7.5 μm (C).

5.4.2 The effect of metabolic stressors on microparticle production

A range of physiological and supra-pharmacological concentrations of metabolic stressors was investigated to assess their effect on MP production. HECV cells were exposed to a metabolic stressor for 24 hours.

5.4.2.1 H_2O_2

H_2O_2 (10 mM) [n = 4] significantly increased MP production (control: 194 ± 125 MPs/cell vs. H_2O_2 (10 mM): 2036 ± 1605 MPs/cell p = 0.03), however, 125 μM, 500 μM and 1 mM H_2O_2 concentrations did not alter MP release (612 ± 314 MPs/cell; 892 ± 738 MPs/cell and 756 ± 756 MPs/cell, respectively, p >0.05, figure 5.4 A). H_2O_2 treatment did not affect MP size. H_2O_2: [n = 4]: control (134 ± 8 nm); H_2O_2 125 μM, (144 ± 40 nm); H_2O_2 500 μM, (140 ± 9 nm), H_2O_2 1 mM, (139 ± 20 nm) and H_2O_2 10 mM, (168 ± 31 nm, p = 0.21, figure 5.4 B).

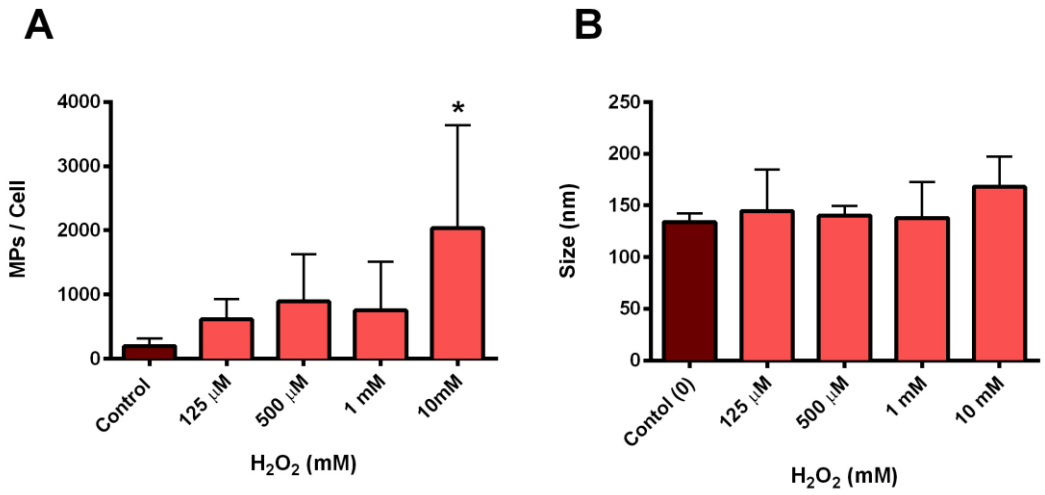

Figure 5.4. The effect of H_2O_2 on microparticle production. (A) The amount of MPs produced per viable cell. (B) MP size. Control reflects H_2O_2 naïve treatment. Each sample was analysed in quintuplicate and the mean was used in further analysis. Data is expressed as the group mean ± SEM. * reflects p < 0.05.

5.4.2.2 Testosterone

Treatment of HECV cells with testosterone (control [testosterone naïve], 3 nM, 30 nM, 300 nM and 1 μM) had no effect on MP production, $p = 0.15$ (figure 5.5 A). Testosterone treatments had no effect on MP size. Testosterone control; (134 ± 8 nm); 3 nM; (194 ± 125 nm); 30 nM; (212 ± 31 nm); 300 nM; (210 ± 9 nm) and 1 μM; (166 ± 61 nm, $p = 0.164$, figure 5.5 B).

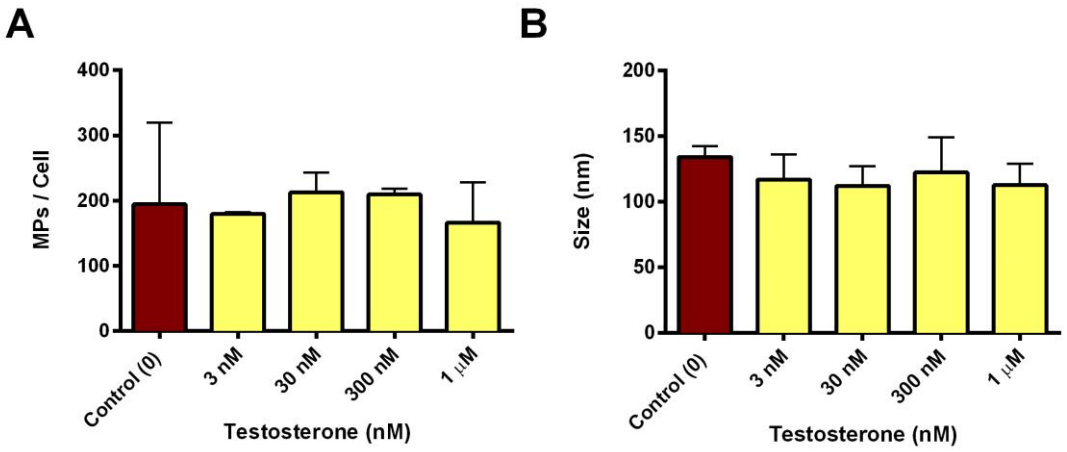

Figure 5.5. The effect of testosterone on microparticle production. (A) The amount of MPs produced per viable cell ($p = 0.15$). (B) MP size. Control = no testosterone. Results represent [$n = 4$]. Each sample was analysed in quintuplicate and the mean was used in further analysis. Data is expressed as the group mean ± SEM.

5.4.2.3 Insulin

Insulin had no effect on HECV MP concentration; control [no insulin] (194 ± 125 MPs/cell), 0.15 nM (280 ± 217 MPs/cell), 0.6 nM (280 ± 217 MPs/cell), 1.25 nM (328 ± 218 MPs/cell), 2.5 nM (419 ± 332 MPs/cell, p = 0.21, figure 5.6 A). Additionally, insulin treatment had no effect on MP size. Insulin: control (134 ± 8 nm); 0.15 nM (134 ± 8 nm); 0.6 nM (184 ± 27 nm); 1.25 nM (158 ± 59 nm); 2.5 nM (168 ± 50 nm, p = 0.21, figure 5.6 B).

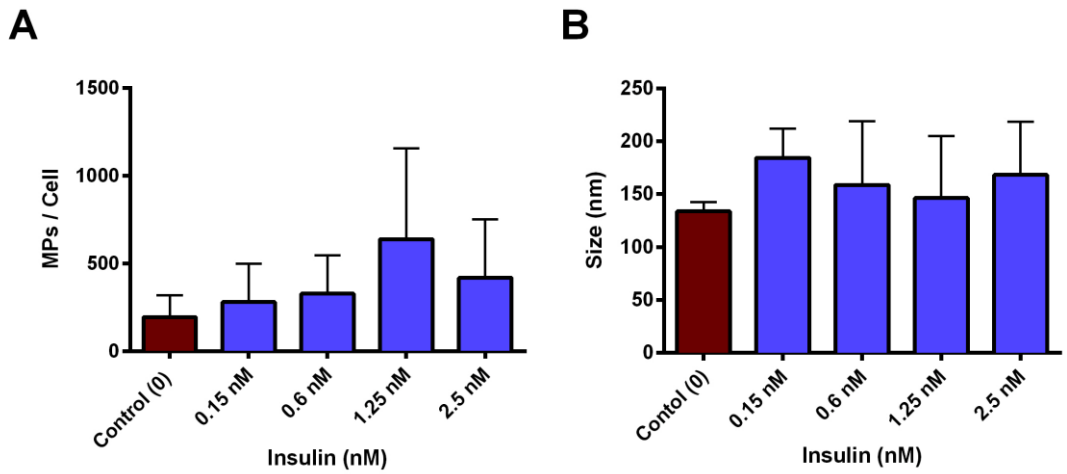

Figure 5.6. The effect of insulin on microparticle production. (A) MPs produced per viable cell. (B) MP size. Control represents no insulin treatment. Results represent [n = 4]. Each sample was analysed in quintuplicate and the mean was used in further analysis. Data is expressed as the group mean ± SEM.

5.4.2.4 Glucose

Glucose-depletion (0mM) [*n* = 4] significantly increased HECV cell MP production compared to HECV cells grown according to the manufacturers recommendations in medium containing 22.5 mM glucose. Control (22.5 mM): 194 ± 125 MPs/cell vs. glucose depleted (0 mM): 2158 ± 1168 MPs/cell $p = 0.002$, figure 5.7 A). However, 5, 10 and 20 mM glucose concentrations did not alter HECV MP release (892 ± 620 MPs/cell; 704 ± 560 MPs/cell and 376 ± 169 MPs/cell, respectively). Glucose treatment did not affect MP size. Glucose: [*n* = 4]: control (22.5 mM, 134 ± 8 nm); glucose-depleted (0mM) (119 ± 18 nm); 5 mM (117 ± 11 nm); 10 mM (172 ± 180 nm); 20 mM (148 ± 61 nm, $p = 0.16$ figure 5.7 B).

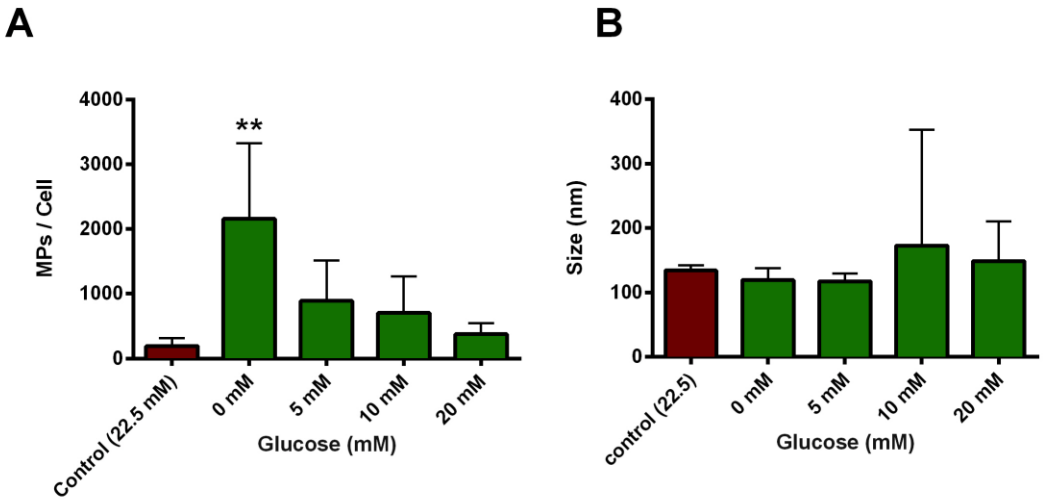

Figure 5.7. The effect of glucose concentration on microparticle production. (A) MPs per viable cell ($p = 0.002$). (B) MP size ($p = 0.65$). Control refers to the HECV culture medium recommendations of 22.5mM glucose. Results represent [*n* = 4]. Each sample was analysed in quintuplicate and the mean was used in further analysis. Data is expressed as the group mean ± SEM. . ** represents $p < 0.01$.

5.4.2.5 Hypoxia

Hypoxia (1% O_2) [n = 4] enhanced HECV cell MP production in comparison to HECV cells grown in normoxia (95% air, control: 194 ± 125 MPs/cell vs. 1% O_2: 409 ± 20 MPs/cell p = 0.04). However 2, 5, 10 and 20% O_2 did not change HECV MP production (279 ± 26 MPs/cell; 290 ± 104 MPs/cell; 218 ± 79 MPs/cell; and 217 ± 98 MPs/cell, respectively, p >0.05, figure 5.8 A). Hypoxic conditions did not affect MP size; [n = 4]: normoxic control (95% air, 134 ± 8 nm); 1% O_2 (131 ± 27 nm); 2% O_2 (133 ± 33 nm); 5% O_2 (143 ± 38 nm); 10% O_2 (133 ± 38 nm), 20% O_2 (132 ± 30 nm, p > 0.05, figure 5.8 B).

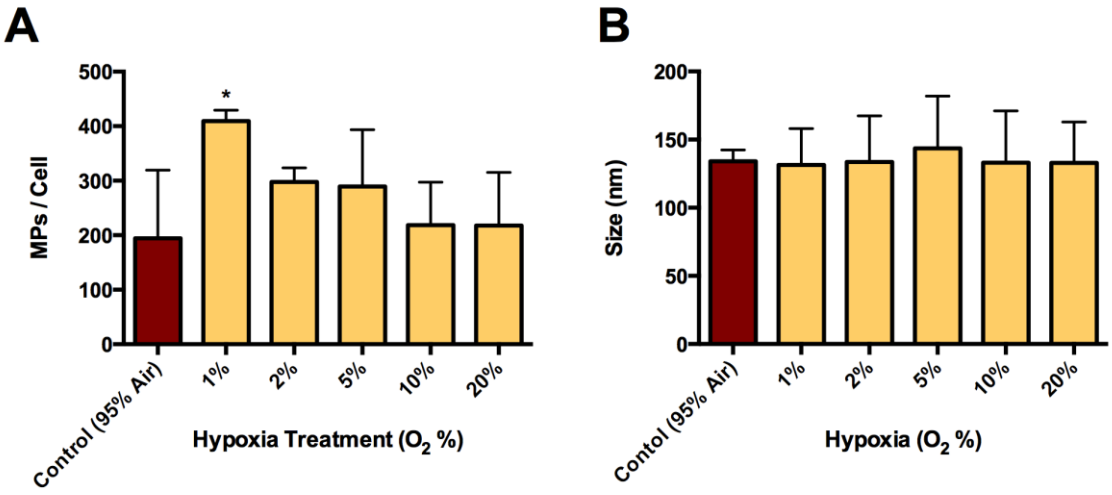

Figure 5.8. The effect of hypoxia (1% O_2) on microparticle production. (A) MPs produced per viable cell. (B) MP size. Control refers to cells grown in normoxia (95% air, which equates to 21% O_2). Results represent [n = 4]. Each sample was analysed in quintuplicate and the mean was used in further analysis. Data is expressed as the group mean ± SEM. * reflects p <0.05.

5.4.3 Microparticle size distribution following metabolic stressors

Following these initial experiments, subsequent *in vitro* comparisons were all carried out at a single concentration: un-stimulated (control); H_2O_2 (10 mM); testosterone (1 μM), glucose-depletion, insulin (2.5 nM) and hypoxia (1% O_2). These concentrations were chosen because they either provoked the largest difference in MP production or, for cases where MP production was not affected, the highest concentration was used.

On assessment of MP size distribution, no differences were observed for MPs derived following testosterone (1 μM), insulin (2.5 nM) and hypoxia (1% O_2) cellular treatments (figure 5.9). H_2O_2 (10 mM) and glucose depletion produced an altered MP distribution compared to unstimulated/control MPs, displaying an elevated concentration of MPs within a diameter range of 51 – 300 nm and 51 – 200 nm, respectively (as highlighted in table 5.1).

Table 5.1 **Distribution of endothelial cell (HECV) derived-MPs**

	Control	H_2O_2 (10 mM)	Testosterone (1 µM)	Glucose depleted	Insulin (2.5 nM)	Hypoxia (1% O_2)	*p*
MP size (nm)			*MPs / cell*				
0-50	11 ± 2	28 ± 20	3 ± 3	62 ± 45	47 ± 22	15 ± 4	>0.05
51-100	74 ± 11	296 ± 110*	34 ± 14	442 ± 112****	73 ± 20	64 ± 17	0.005
101-150	136 ± 20	637 ± 268****	52 ± 15	656 ± 103****	82 ± 58	102 ± 20	0.01
151-200	104 ± 14	665 ± 280****	33 ± 8	370 ± 9**	59 ± 61	84 ± 10	0.03
201-250	64 ± 6	457 ± 213****	20 ± 8	189 ± 28	55 ± 39	57 ± 11	<0.01
251-300	40 ± 5	274 ± 135**	11 ± 5	119 ± 29	26 ± 16	30 ± 9	<0.01
301-350	20 ± 4	164 ± 172	5 ± 4	54 ± 15	8 ± 8	13 ± 7	>0.05
351-400	11 ± 2	132 ± 150	3 ± 2	24 ± 12	6 ± 4	8 ± 5	>0.05
401-450	10 ± 2	107 ± 150	2 ± 2	12 ± 8	6 ± 4	4 ± 2	>0.05
451-500	6 ± 1	80 ± 120	1 ± 1	7 ± 5	4 ± 5	3 ± 2	>0.05
501-550	3 ± 0.3	52 ± 71	1 ± 1	5 ± 3	2 ± 3	2 ± 1	>0.05
551-600	2 ± 1	35 ± 52	0..5 ± 0.6	4 ± 2	2 ± 3	1 ± 0.6	>0.05
601-650	2 ± 1	19 ± 32	0.4 ± 0.5	3 ± 3	2 ± 3	1 ± 0.3	>0.05
651-700	2 ± 1	10 ± 18	0.2 ± 0.3	2 ± 2	2 ± 2	0.3 ± 0.3	>0.05
701-750	2 ± 1	6 ± 11	0.1 ± 0.2	1 ± 2	1 ± 1	0.2 ± 0.3	>0.05
751-800	2 ± 1	5 ± 9	0.06 ± 0.1	1 ± 1	1 ± 1	0.2 ± 0.2	>0.05
801-850	1 ± 1	6 ± 11	0.07 ± 0.1	0.4 ± 1	1 ± 1	0.2 ± 0.2	>0.05
851-900	1 ± 1	5 ± 10	0.1 ± 0.2	0.2 ± 0.3	1 ± 1	0.1 ± 0.1	>0.05
901-950	0.3 ± 0.3	4 ± 7	0.1 ± 0.2	0.04 ± 0.07	0.4 ± 1	0.08 ± 0.06	>0.05
951-1000	0.2 ± 0.1	3 ± 5	0.09 ± 0.2	0.01 ± 0.01	0.1 ± 0.2	0.05 ± 0.01	>0.05

The effect of cardiometabolic insults on HECV derived-MP distribution. NTA was used to assess the size distribution of MPs (normalised to cell count, presented in 50 nm bin sizes). Samples were measured in quintuplicate. SEM. Results represent [$n = 4$]. Each sample was analysed in quintuplicate and the mean was used in further analysis. Data is expressed as the group mean ± SEM. *, ** and **** reflects significance ($p < 0.05$, $p < 0.01$, $p < 0.0001$, respectively). MP; microparticle.

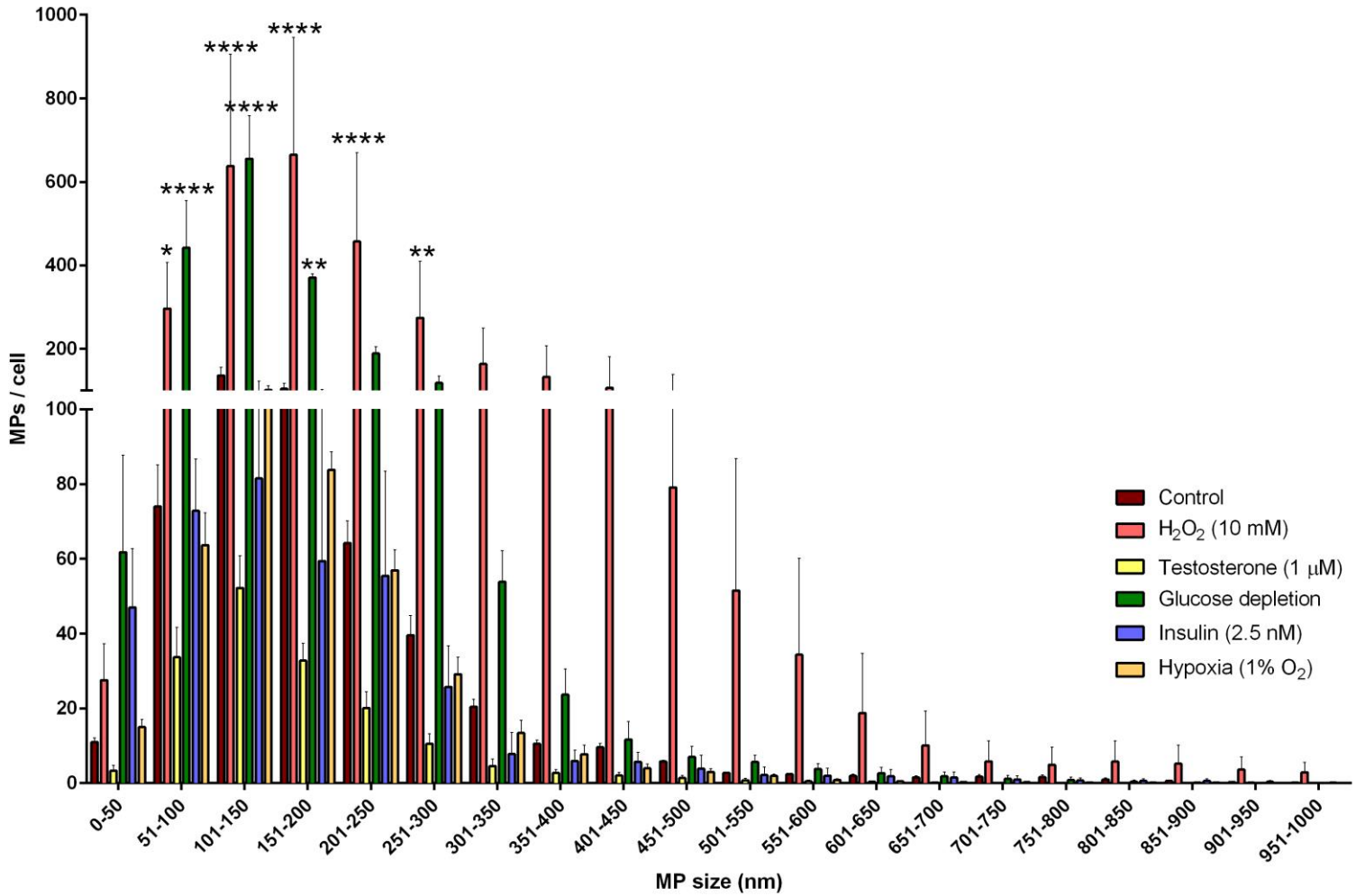

Figure 5.9. The effect of cardiometabolic insults on HECV derived MP distribution. NTA was used to assess the size distribution of MPs (normalised to cell count). Results represent [n = 4]. Each sample was analysed in quintuplicate and the mean was used in further analysis. Data is expressed as the group mean ± SEM. *, ** and **** reflects significance (p <0.05, p <0.01, p <0.0001, respectively).

5.4.4 The effect of pathologically relevant insults on cell viability and apoptosis

Some MP production may relate to apoptosis. Thus, cell viability and apoptosis assays were undertaken on HECV cells. Cell viability was determined using a colourimetric method. Viable cells with active metabolism convert tetrazolium compounds into a formazan dye (purple colour). Cell death diminishes the ability of cells to convert tetrazolium compounds into formazan. Thus, results represent the absorbance of formazan at 490 nm. Improved cell viability was shown in HECV cells treated with testosterone (1 μM), insulin (2.5 nM) and glucose depletion compared to control HECV cells, [testosterone 1 μM]: 2.18 ± 0.17, [insulin 2.5 nM]: 2.18 ± 0.12, [glucose depletion]: 2.4 ± 0.04 vs. control: 1.7 ± 0.22, $p = 0.001$, $p = 0.001$ and $p = 0.0001$, respectively). H_2O_2 (10 mM): 1.8 ± 0.17, and hypoxia (1% O_2): 1.9 ± 0.04 did not alter cell viability (figure 5.10 A).

Apoptosis was determined by measuring caspase-3 and -7 activity via luminescence. Values represent relative luminescence (RLU) units. Testosterone (1 μM) enhanced caspase 3/7 activity in HECV cells compared to control HECV cells (testosterone (1 μM): 920 ± 73, Control: 612 ± 75, $p < 0.0001$). H_2O_2 (10 mM): 535 ± 129, glucose depletion: 758 ± 121, insulin (2.5 nM): 672 ± 7 and hypoxia (1% O_2): 672 ± 79, had no effect on caspase 3/7 activity in cells ($p > 0.05$, Figure 5.10 B).

H_2O_2 (10 mM) increased the proportion of trypan blue stained HECV cells compared to control HECV cells (H_2O_2 (10 mM): 78 ± 14% vs. Control: 89 ± 1%, p 0.02). Testosterone (1 μM): 92 ± 0.5%, glucose depletion: 87 ± 1%, insulin (2.5 nM): 88 ± 1% and hypoxia (1% O_2): 87 ± 1%, had no significant effect on HECV trypan blue exclusion ($p > 0.05$, figure 5.10 C). Again, HECV cells were exposed to metabolic stressors for 24 hours for all apoptosis and cell viability experiments.

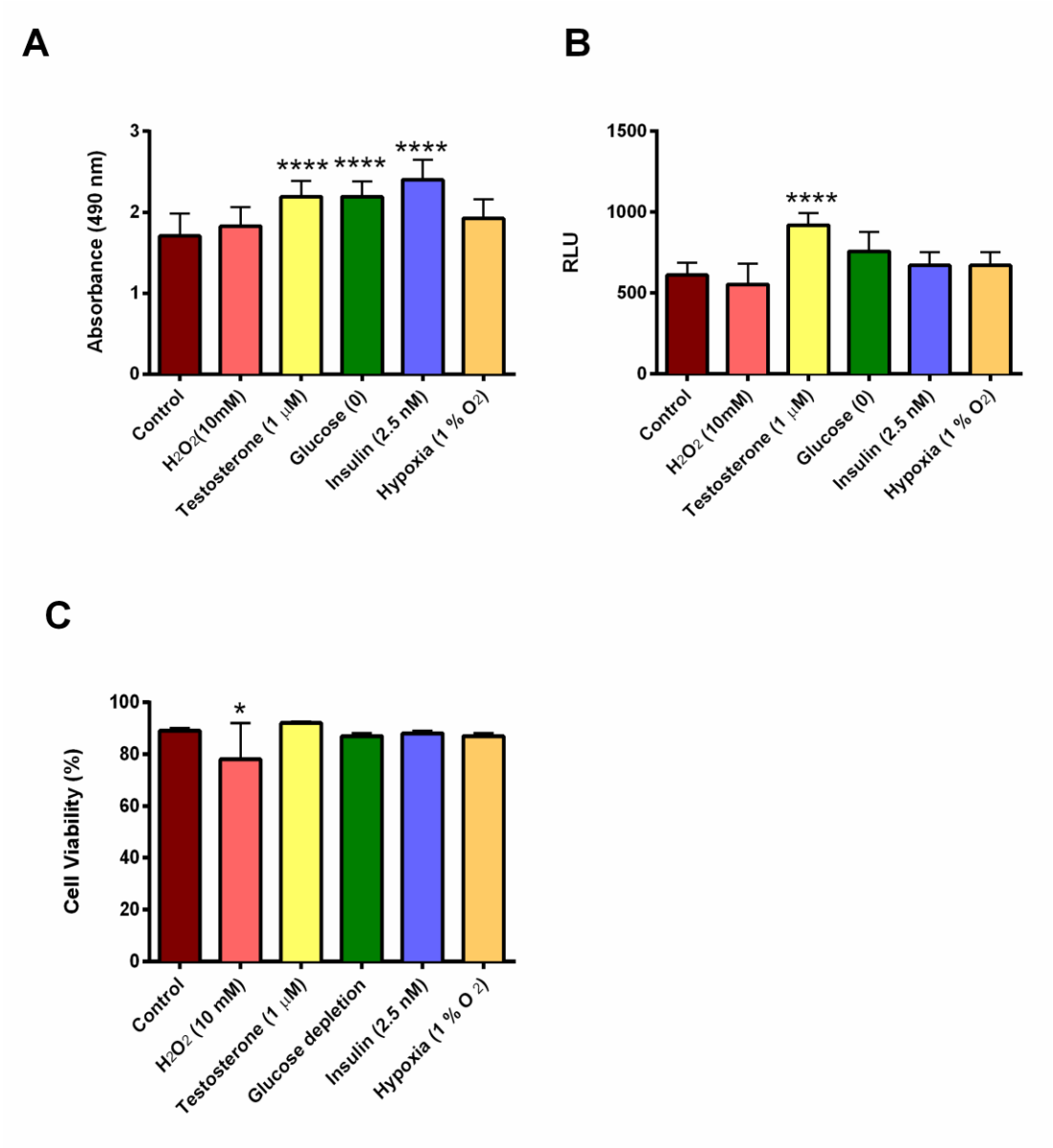

Figure 5.10. The effect of metabolic stressors on cell viability and apoptosis. (A). CellTiter 96® AQ_{ueous} one solution cell proliferation assay. Relative MTS activity obtained from 80 µl of control HECV cells and treated HECV cells at 1 x 10^6/ml, p = 0.0007. (B). Caspase-glo 3/7 apoptosis assay. Relative caspase-glo 3/7 activity obtained from 50 µl control HECV cells and treated HECV cells at 1 x 10^6/ml, p = 0.0012. (C). Trypan blue exclusion. Percentage of viable cells (identified by the intracellular exclusion of trypan blue) in treated HECV and control HECV cells (p = 0.02). All samples were analysed in triplicate for the CellTiter96® AQueous one solution cell proliferation assay [n = 4] (A), caspase 3/7 assay [n = 4] (B) and trypan blue exclusion experiments [n = 4] (C), and the mean was used in further analysis. Data is expressed as the group mean ± SEM. p values reflect one-way ANOVA analysis, * and **** reflect post-hoc analysis (Dunnetts multi-comparisons), p <0.05 and p <0.0001, respectively. RLU, relative light units.

5.4.5 The effect of metabolic stressors on HUVEC microparticle production

HUVECs were sourced to compare how pathologically relevant stressors affected MP production in primary ECs compared to HECV cells. The HUVEC medium recommended by the manufacturers contained 5 mM glucose and a proprietary blend of growth nutrients. Thus, glucose depleted treatments were not possible. Moreover, the HUVEC medium contained MPs (which are likely to be FBS derived-MPs), therefore results are presented as actual MP concentration minus MPs in growth medium, normalised to cell count. Hypoxia and H_2O_2 appeared to enhance HUVEC MP production, a similar trend observed in HECV cells (figure 5.11). However, results were obtained from two experiments (n = 2), thus no statistical analysis was performed.

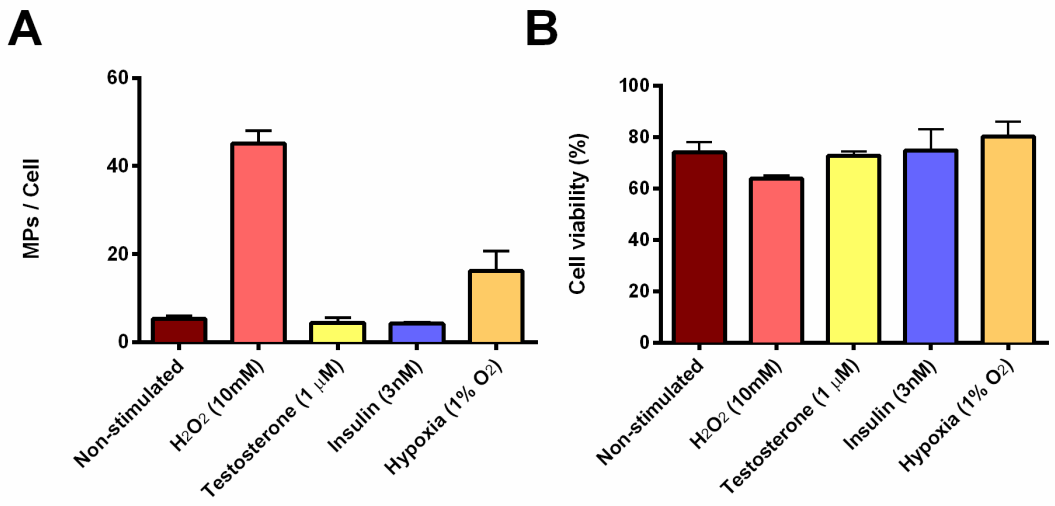

Figure 5.11. The effect of metabolic stressors on HUVEC MP production. (A) MPs produced per viable cell. (B) Trypan blue exclusion – cell viability (%). Results were obtained from two experiments (n = 2). Each sample was analysed in quintuplicate and the mean was used in further analysis. Data is expressed as the group mean ± SEM..

5.4.6 Microscopy

Confocal and electron microscopy was used to visually support the NTA data (figures 5.12 and 5.13, respectively). For confocal microscopy, prior to exposure to pathologically relevant stressors, HECVs were stained with Cell Trace red/orange and visualised 3 hours post exposure. Confocal and electron microscopy were also used to confirm the diameter of MPs. Both techniques confirmed MP diameters were <1 μm.

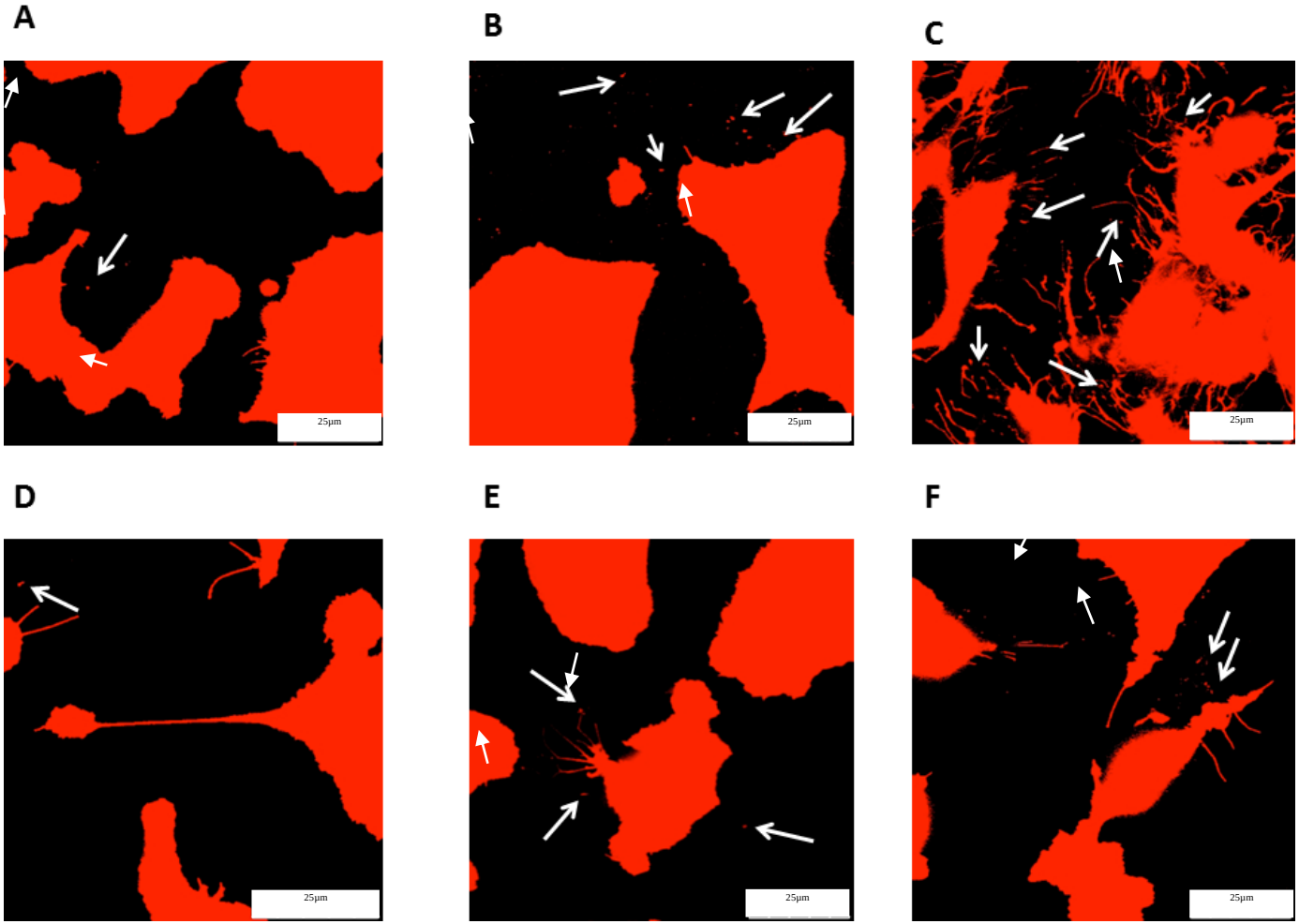

Figure 5.12. Representative images of microparticle generation following exposure to pathological stressors. (A) Control. (B) Hypoxia (1 % O_2). (C) H_2O_2 (10 mM). (D) Testosterone (1 µM). (E) Insulin (2.5 nM). (F) Glucose depleted. White arrows identify select MPs. Scale bar represents 25 µM.

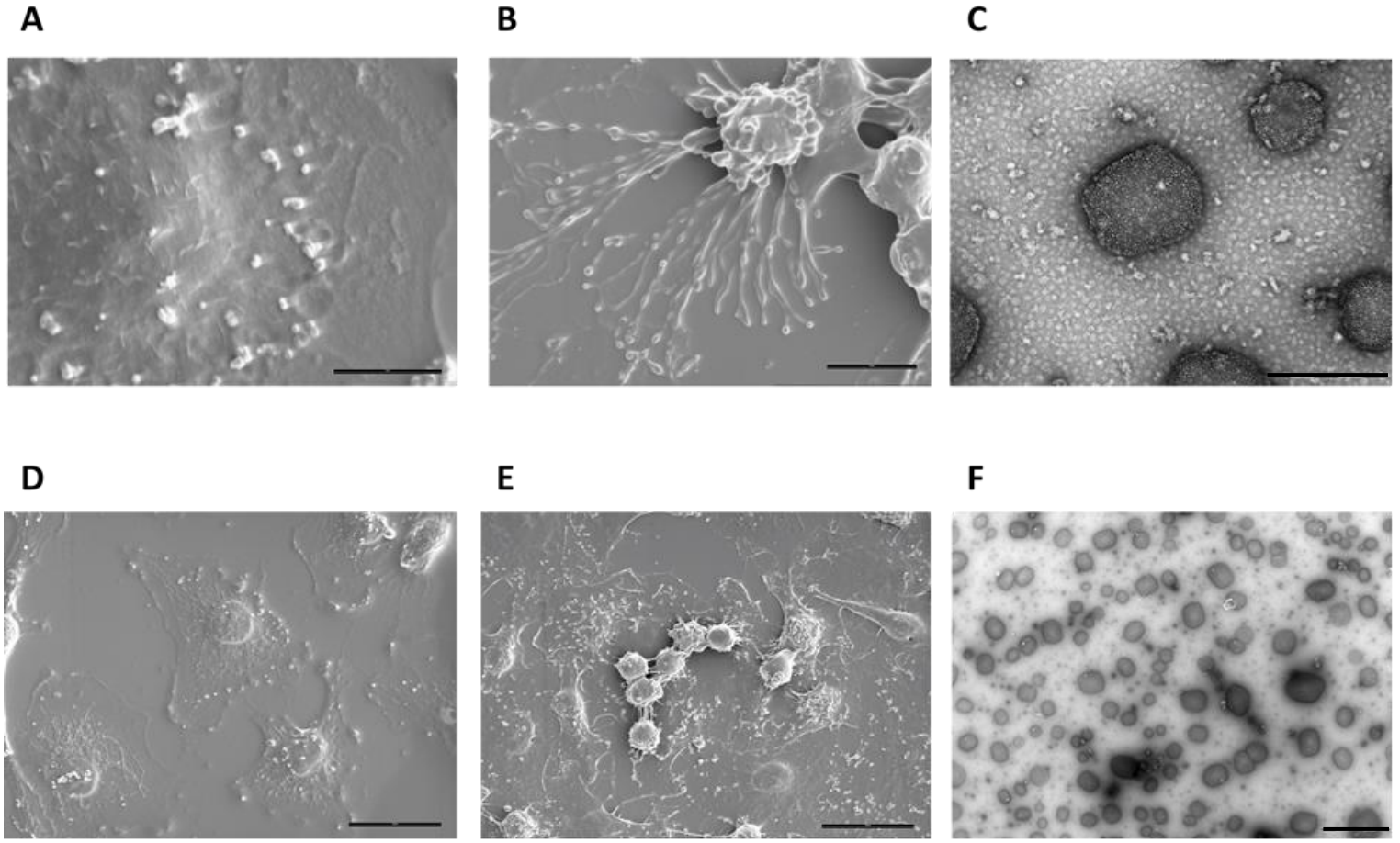

Figure 5.13 Morphology of HECV cells and HECV derived-microparticles. SEM images: MPs budding off non-stimulated (A, D) and H_2O_2 (10 mM) treated cells (B, E). MPs appear to be protruding from nanotubes/micro-spikes (B), from H_2O_2 (10 mM) treated HECV cells. Surface blebs and detached vesicles are visualised on non-stimulated and H_2O_2 treated HECV cells (A, D and B, E, respectively). Scale bars: 25 μm (D, E), 10 μm (B) and 5 μm (A). TEM images: submicron heterogeneous population of spherical MPs derived from un-stimulated HECV cells (C, F). MPs appear granular (C). Scale bars: 0.2 μm (C) and 2 μm (F).

5.4.7 Hypoxia mediated microparticle release

EPR – oximetry was used to confirm the O_2 concentration of cell culture medium surrounding HECV cells exposed to 1% or 21% O_2 (95% air) for 24 hrs (p = 0.003, figure 5.14). To examine the role of HIF-1α in the hypoxic enhancement of MP release, HECV cells were transfected with a siRNA targeting HIF-1α. Transfected cells (HIF-1α siRNA) failed to show an enhancement in MP release following hypoxia exposure compared to cells transfected with scrambled siRNA (control, p = 0.003, figure 5.15 A). Western blots confirmed that HIF-1α was induced at 1% O_2 in non-transfected cells. Cells transfected with HIF-1α siRNA inhibited HIF-1α expression, whilst the scrambled siRNA had no impact on HIF-1α expression (figure 5.15 B).

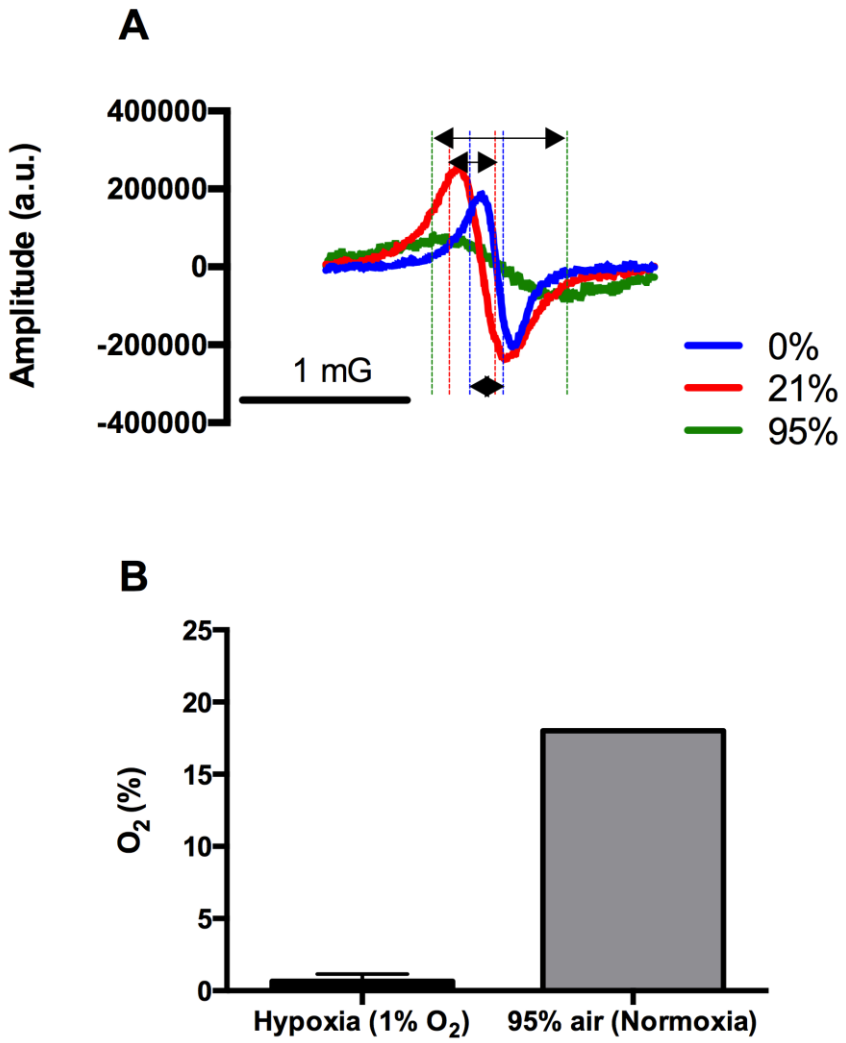

Figure 5.14. Oximetry. (A) Typical EPR spectra. (B) O_2 concentration (%) of the cell culture medium. Cells were maintained in an incubator at 37 °C and 5% CO_2. [Hypoxia: n = 3] and [normoxia: n = 1]. Results are expressed as mean ± SEM.

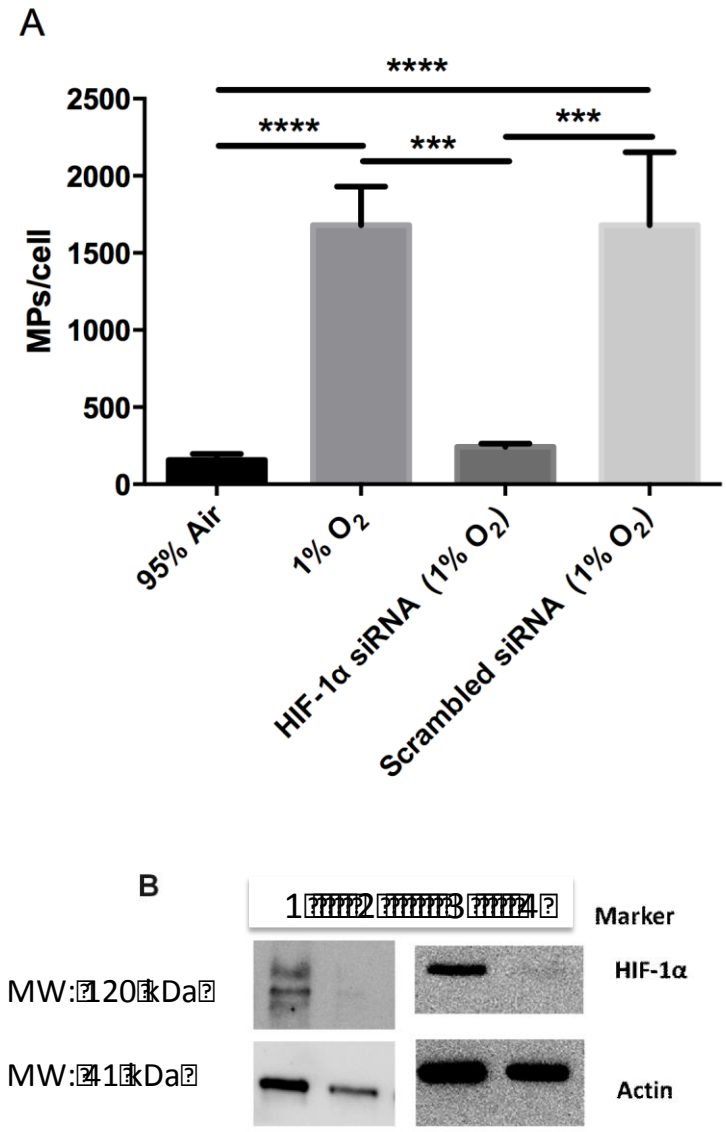

Figure 5.15. Hypoxia mediated microparticle release. Experiments were conducted on HECV cells at passage 14. Results represent [n = 3] mean ± SEM. * reflects $p < 0.05$, respectively. (A) MPs produced per viable cell. (B). Western blots sections showing relevant showing HIF-1α expression. Control refers to cells grown in 95% Air. (B) Lane 1, scrambled siRNA at 1% O_2. Lane 2: HIF-1α targeted siRNA, 1% O_2. Lane 3: 1% O_2. Lane 4: 95% air (normoxia). Cells were maintained in an incubator at 37 °C and 5% CO_2.

5.4.8 Microparticle coagulability

Annexin V positivity was measured by flow cytometry as described in section 2.23.4 (general methods). A greater proportion of MPs were derived from HECV cells exposed to H_2O_2 (10 mM), testosterone (1 μM), glucose depletion and insulin (2.5 nM) compared to control MPs. Hypoxia had no effect on annexin V MP positivity ($p = 0.0002$, figure 5.16 A). As an indication of MP coagulability, electrical impedance aggregometry was employed to investigate the ability of MPs to adhere to an electrode surface. MPs did not show a tendency to adhere to the artificial electrode within a 6-minute time scale. All MPs derived from HECV cells exposed to pathological stressors did not adhere to the surface apart from MPs derived from HECVs stimulated with H_2O_2 (10 mM, 20 ± 10 au, $p < 0.0001$). Thus, in order to provoke adhesion, MPs were primed with an acute oxidative insult, H_2O_2 (10 mM). Following this, MPs derived from HECV cells post glucose depletion and hypoxia (1% O_2) demonstrated enhanced adherence to the electrode [glucose-depleted: 711 ± 184, au. $p < 0.01$ and hypoxia (1 % O_2): 936 ± 339, $p < 0.01$]. No difference was found with H_2O_2 (10 mM) [455 ± 189 au], testosterone (1 μM) [150 ± 96 au] and insulin (2.5 nM) [142 ± 30 au] ($p > 0.05$, figure 5.16 B). H_2O_2 (10 mM) in saline buffer alone and the supernatant from the last wash step of MP isolation was used as controls and did not alter or affect the electrical impedance recordings.

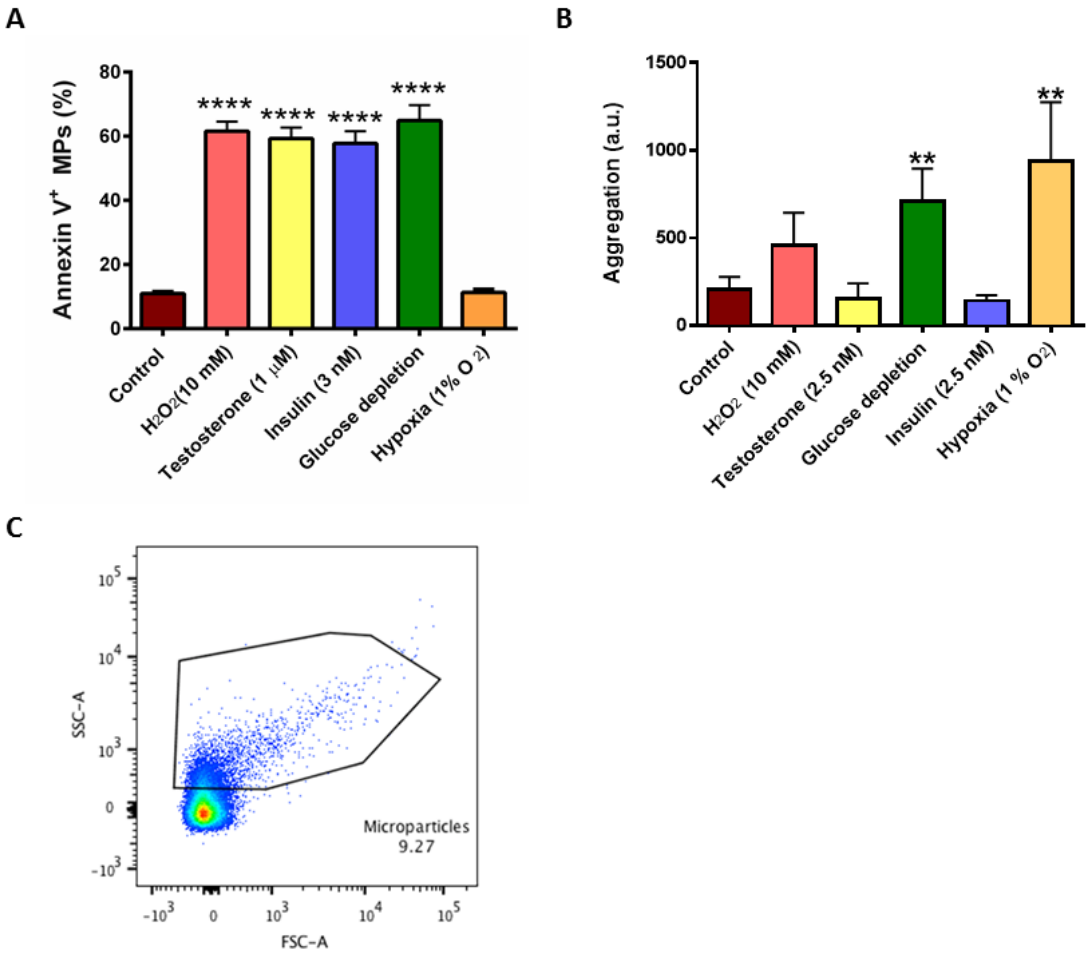

Figure 5.16 MP coagulability. (A) The extent of annexin V binding, expressed as a percentage (%) of annexin V^+ MPs. [n = 4]. Data is expressed as the group mean ± SEM. (B) The ability of HECV-derived MPs to adhere to an artificial electrode following acute exposure to H_2O_2 (10 mM). [n = 4]. Each sample was analysed in duplicate and the mean was used in further analysis. Data is expressed as the group mean ± SEM. The intra-assay coefficient of variation was <5%. (C) MP gate (flow cytometry). A.U: arbitrary units. p values reflect one-way ANOVA analysis, ** and **** reflect post-hoc analysis (Dunnetts multi-comparisons), p <0.05 and p <0.0001, respectively.

Characterisation of surface adhesion molecule profiles

Cellular activation may promote EC interactions with circulating cells by elevated expression of surface adhesion molecules. Antibody enabled flow cytometry was employed to investigate the impact of the pathological stressors on the expression of surface adhesion molecules.

Antibody binding may be expressed as median fluorescence intensity (MFI) or percentage of immunopositive cells/MPs. Both MFI and percent of immunopositive cells/MPs have biological relevance. In contrast to MFI, percent of antigen presenting cells/MPs is independent of signal amplitude. However, it is reasonable to postulate that although a cell/MP may be positive for a specific antigen, the amount of antigen present may be considerably different. Thus, results are expressed as both MFI and percent of antigen presenting cells/MPs.

The effect of metabolic stressors on HECV surface adhesion expression. MFI and percent of immunopositive HECV cells are summarised in table 5.2. Cellular stressors had no effect on VCAM-1, ICAM-1, or E-selectin expression. Glucose depletion decreased the percentage of PE-CAM-1 positive cells ($p < 0.0005$), but no difference was observed in MFI for PECAM-1 expression in HECV cells following exposure to metabolic stressors ($p > 0.05$). H_2O_2 (10 mM); Testosterone (1 μM); glucose depletion and Hypoxia (1 % O_2) decreased P-selectin MFI ($p < 0.001$, $p < 0.0001$, $p < 0.05$, $p < 0.01$, respectively). Insulin (2.5 nM) had no effect on P-selectin MFI ($p > 0.05$). The percentage of P-selectin positive cells was not affected by cellular insults ($p > 0.05$).

Treating HECV cells with metabolic stressors: the effect on MP surface adhesion expression. Data are summarised in table 5.3. The surface adhesion molecule profiles of MPs produced from treated cells were compared to MPs from unstimulated HECV cells. Cellular stressors had no effect on MP ICAM-1, PECAM-1, P-selectin or E-selectin expression. Glucose depletion resulted in an elevated percentage of VCAM-1 positive MPs ($p < 0.05$), but H_2O_2 (10 mM); testosterone (1 μM); insulin (2.5 nM) and hypoxia (1 % O_2) did not affect VCAM-1 expression ($p > 0.05$).

The effect of MP treatment (MPs derived from HECV cells treated with stressors) on HECV cell surface adhesion expression. Results are summarised in table 5.4. The surface adhesion molecule profile of HECVs was assessed after a 24 hr incubation with MPs (1 x

10^9/ml) produced from stimulated cells (including unstimulated cell-derived MPs), and profiles were compared to HECV which received no MP treatment. MP treatment had no effect on VCAM-1, ICAM-1 or E-selectin expression. HECV cells treated with unstimulated MPs decreased the percentage of PE-CAM-1 positive cells ($p < 0.0009$), but treatment of MPs obtained following H_2O_2 (10 mM); testosterone (1 μM); insulin (2.5 nM), glucose depletion or hypoxia (1 % O_2) stressors had no effect on PECAM-1 expression ($p > 0.05$). HECV cells treated with MPs, (irrespective of MP origin) decreased P-selectin expression (MFI) in HECV cells ($p < 0.0001$).

Table 5.2 **The effect of pathologically relevant stressors on HECV cell surface adhesion molecule expression**

	Control	H_2O_2 (10 mM)	Testosterone (1 µM)	Glucose depleted	Insulin (2.5 nM)	Hypoxia (1% O_2)	*p*
VCAM-1 expression							
Immunopositive cells (%)	90 ± 9	67 ± 35	97 ±2	80 ± 15	94 ± 6	85 ± 14	0.12
Median fluorescence intensity	580 ± 193	486 ± 318	800 ± 156	459 ± 196	791 ± 437	422 ± 135	0.1
ICAM-1 expression							
Immunopositive cells (%)	99 ± 0.1	100 ± 0	100 ± 0	99 ± 0.1	100 ± 0	99 ± 0.5	0.1
Median fluorescence intensity	7688 ± 458	8271 ± 424	7247 ± 118	8653 ± 1051	7402 ± 281	8207 ± 591	0.09
PECAM-1 expression							
Immunopositive cells (%)	84 ± 9	76 ± 26	80 ± 5	33 ± 23 ***	79 ± 6	82 ± 17	0.0005
Median fluorescence intensity	362 ± 70	440 ± 222	304 ± 6	218 ± 43	340 ± 40	433 ± 171	0.08
P-Selectin							
Immunopositive cells (%)	99 ± 2	90 ± 18	84 ± 14	92 ± 7	99 ± 2	93 ± 4	0.3
Median fluorescence intensity	1243 ± 31	380.0 ± 9***	435.5 ± 159***	760.2 ± 280*	821 ± 308	560.0 ± 27**	0.0004
E-Selectin							
Immunopositive cells (%)	74 ± 33	85 ±14	51 ± 45	73 ± 20	86 ± 9	96 ± 14	0.2
Median fluorescence intensity	369 ± 154	388 ± 73	326 ± 172	257 ± 6	491 ± 114	422 ± 118	0.3

Results were obtained from four experiments ($n = 4$). Results are expressed as mean ± SD. $p < 0.05$ was deemed significant. * equates to $p < 0.05$, ** equates to $p < 0.01$, *** equates to $p < 0.001$.

Table 5.3 **The effect of pathologically relevant stressors on microparticle surface adhesion molecule expression**

	Control	H_2O_2 (10 mM)	Testosterone (1 µM)	Glucose depleted	Insulin (2.5 nM)	Hypoxia (1% O_2)	*p*
VCAM-1 expression							
Immunopositive cells (%)	20 ±17	11 ± 13	14 ± 8	46 ± 27*	21 ± 6	23 ± 5	0.02
Median fluorescence intensity	213 ± 66	208 ± 32	192 ± 0	224 ±37	208 ± 32	195 ± 6	0.49
ICAM-1 expression							
Immunopositive cells (%)	23 ±18	17 ±13	23 ±14	18 ±14	27 ± 2	33 ± 4	0.49
Median fluorescence intensity	224 ±35	179 ±29	239 ±27	224 ±83	240 ±32	240 ±32	0.22
PECAM-1 expression							
Immunopositive cells (%)	15 ±13	14 ±11	11 ± 9	18 ±14	25 ± 25	26 ± 7	0.77
Median fluorescence intensity	181 ± 48	179 ± 29	192 ±40	191 ± 42	208 ± 32	217 ± 32	0.49
P-Selectin							
Immunopositive cells (%)	29 ± 13	11 ± 15	16 ± 7	33 ± 11	37 ± 5	34 ± 11	0.04
Median fluorescence intensity	288 ± 67	208 ± 61	192 ± 64	288 ± 153	320 ± 52	336 ± 160	0.29
E-Selectin							
Immunopositive cells (%)	23 ± 14	16 ± 16	18 ± 11	17 ± 11	24 ± 9	23 ± 12	0.77
Median fluorescence intensity	192 ± 52	256 ± 91	203 ± 26	256 ± 45	208 ± 32	256 ± 78	0.29

Results were obtained from four experiments ($n = 4$). Results are expressed as mean ± SD. * equates to $p < 0.05$.

Table 5.4 **The effect of microparticles on HECV cell surface adhesion expression**

	Control	Un-stimulated	H_2O_2 (10 mM)	Testosterone (1 µM)	Glucose depleted	Insulin (2.5 nM)	Hypoxia (1% O_2)	*p*
VCAM-1 expression								
Immunopositive cells (%)	90 ± 9	76 ± 14	85 ± 13	81 ± 21	65 ± 14	85 ± 13	81 ± 21	0.3
Median fluorescence intensity	580 ± 194	375 ± 181	369 ± 107	535 ± 308	293 ± 53	326 ± 66	540 ± 372	0.3
ICAM-1 expression								
Immunopositive cells (%)	100 ± 0.1	100 ± 0	100 ± 0	100 ± 0	100 ± 0	100 ± 0.5	100 ± 0.01	0.46
Median fluorescence intensity	7688 ± 484	10915 ± 3462	8438 ± 1071	10415 ± 1628	8894 ± 1150	8970 ± 513	8404 ± 251	0.2
PECAM-1 expression								
Immunopositive cells (%)	83.74 ± 9	65.48 ± 10*	98.53 ± 2	72.04 ± 18	63.97 ± 20	84.53 ± 8	68.00 ± 0	0.0009
Median fluorescence intensity	361.8 ±70	298.0 ± 40	4258 ± 5044	339.8 ± 86	289.7 ± 17	389.0 ± 166	326.5 ± 108	0.09
P-Selectin								
Immunopositive cells (%)	99 ± 1	78 ± 11	80 ± 18	65 ± 33	69 ± 15	68 ± 21	62 ± 34	0.2
Median fluorescence intensity	1243 ± 310	372 ± 82***	359 ± 125 ***	326 ± 132 ***	320 ± 97 ****	313 ± 82 ****	314 ± 117 ****	<0.0001
E-Selectin								
Immunopositive cells (%)	74 ± 33	75 ±26	82 ±13	76 ± 10	80 ± 5	46 ± 17	80 ± 1	0.52
Median fluorescence intensity	369 ± 154	555 ± 411	387 ± 146	347 ± 69	377 ± 47	241 ± 27	321 ± 32	0.54

Results were obtained from four experiments (n = 4). Results are expressed as mean ± SD. $p < 0.05$ was deemed significant. *** equates to $p < 0.001$, **** equates to $p < 0.0001$.

5.4.9 The effect of microparticles on platelet function

Eight healthy volunteers (n = 8) were recruited to assess the effect of EMPs on whole blood platelet aggregation as described in section 2.21. Briefly, blood was pre-incubated with control MPs (2 X 10^2/ml – 10 X 10^{10}/ml) prior to inducing platelet aggregation by ADP or TRAP agonists. Pre-conditioning whole blood with control MPs had no effect on ADP or TRAP induced platelet aggregation (figure 5.17 A, B, respectively), nor did MPs alone affect platelet aggregation (i.e. No ADP or TRAP p >0.05). MPs derived from metabolic stressors were compared to control MPs (normalised to 1 x 10^9 MPs/ml). MPs derived from different stressors did not alter ADP or TRAP induced platelet aggregation, p >0.05 (figure 5.17 C, D). Results were compared to control platelet aggregation values (i.e. no MP pre-conditioning), and expressed as a fold change.

Multiplate did not account for variability in platelet counts. Thus, antibody enabled flow cytometry was used to assess the effect of MPs on platelet activation (in whole blood) where blood was diluted in saline to normalise platelet levels (150 x 10^3 mm^3). Blood was collected from healthy volunteers (n = 4), as described in section 2.23.5. P-selectin expression was normalised to control levels (i.e. P-selectin expression with no MP pre-conditioning). Pre-conditioning whole blood with MPs had no effect on P-selectin expression induced by ADP or TRAP (B, C, respectively, figure 5.18), nor did MPs alone alter P-selectin expression (i.e. No ADP or TRAP, p >0.05).

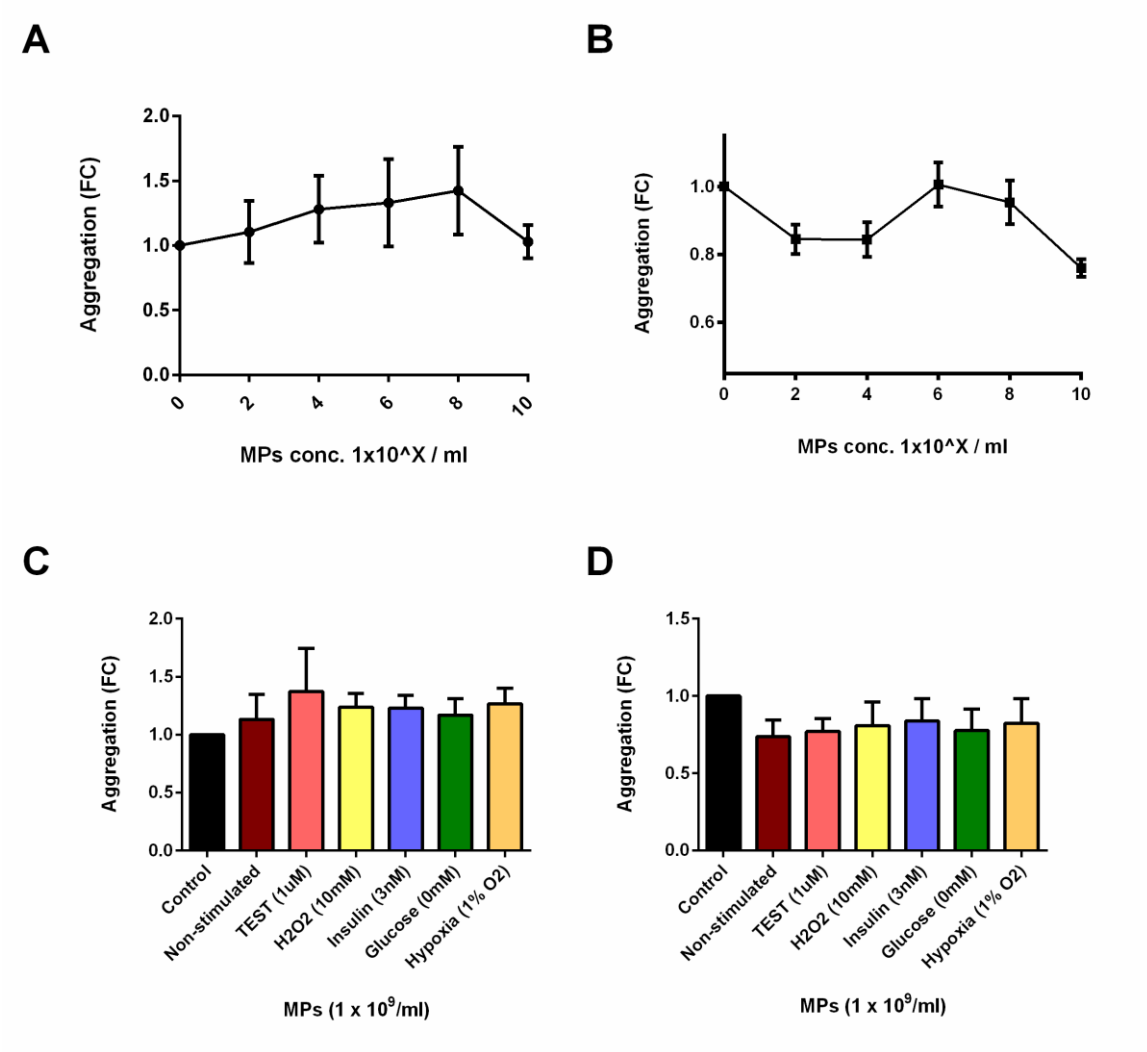

Figure 5.17. Multiplate – the effect of MPs on platelet aggregation. The effect of ADP (A) or TRAP (B) induced aggregation following pre-conditioning whole blood with control MPs. The effect of MP pre-conditioning (1 x 10^9 MPs/ml) on ADP (C) and TRAP (D) induced whole blood platelet aggregometry. X refers to the multiplying factor on the X axis. [*n* = 8]. Each sample was analysed in duplicate. The intra-assay coefficient of variation was <5%. Data reflects mean ± SEM.

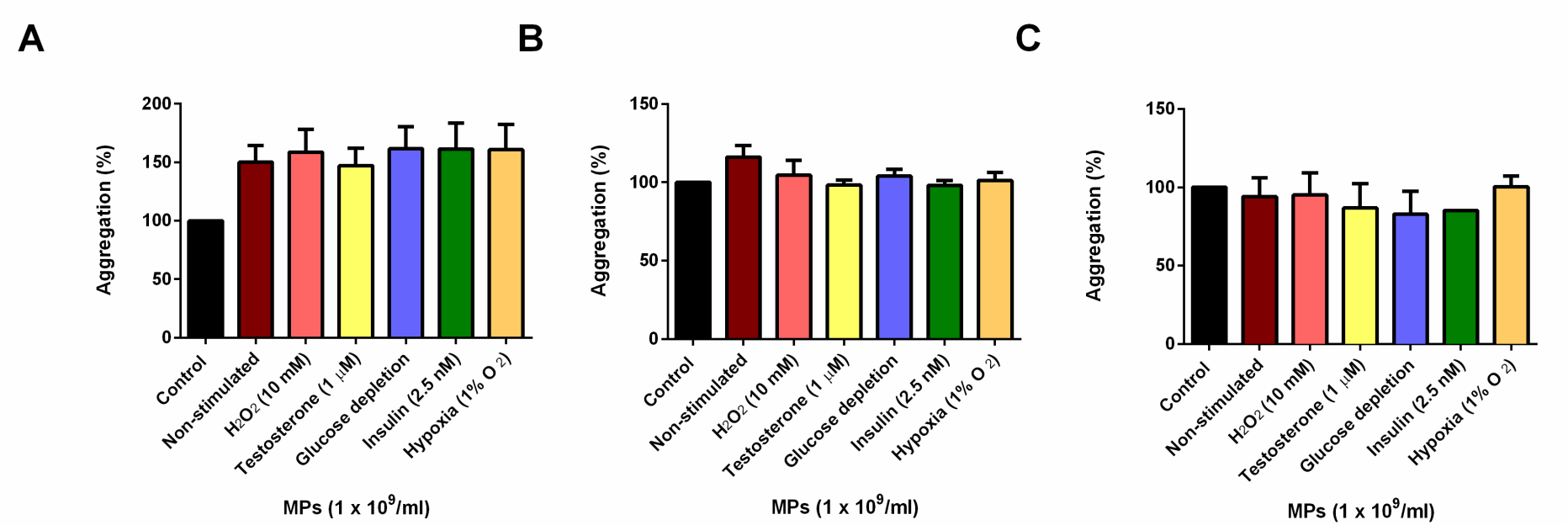

Figure 5.18. The effect of MPs on platelet activation (P-selectin). Whole blood was diluted in saline to normalise platelet levels (150 X 10^3 mm^3). To assess the effects of MPs, results are normalised to a whole blood sample control (i.e. No MP pre-conditioning). Results are expressed as a delta (%) in P-selectin expression compared to control ([black bar] control refers to whole blood sample not pre-conditioned with MPs). The effect of no-agonist (A), ADP (B) or TRAP (C) induced aggregation following pre-conditioning whole blood with MPs (1 x 10^9 MPs/ml). Results were obtained from four experiments (n = 4). Mean ± SEM.

5.5 Discussion

5.5.1 Main Findings

This study examined the effects of pathologically relevant stressors on MP size, concentration, surface adhesion molecule expression and function MPs generated by EC. H_2O_2 (10 mM), glucose depletion and hypoxia (1% O_2) increased MP production in ECs. The cellular stress condition is reflected in the MP characteristics, whereby each pathological stressor resulted in a unique MP phenotype. Notably, the induction of HIF-1α plays a central role in the hypoxic enhancement of MP release.

5.5.2 Interpretation

5.5.2.1 Hypoxia

During homeostasis or disease states, cellular O_2 levels are often insufficient to meet physiological demands, a state referred to as hypoxia. Hypoxia is an important feature of IHD, PAD, sleep apnoea and is associated with aggressive tumour phenotypes and poor patient outcomes (290). In this chapter, HECV cells exposed to hypoxia (1% O_2) for 24 hr resulted in increased MP production, a trend repeated in primary HUVECs. This increase in MP levels appeared to be non-selective, affecting both small MPs in the exosomal range and larger MPs. This is in accordance with previous studies which have demonstrated that hypoxia is associated with increased EMP production *in vitro* (291). Vince *et al*, (292) noted hypoxic breathing (15% O_2 for 80 minutes), resulted in a significantly elevated level of circulating EMPs, however this was measured by flow cytometry where only VCAM-1 expressing MPs were assessed.

Data in this chapter proves that HIF-1α is pivotal in the hypoxia-associated enhancement of MP release in HECV cells. To my knowledge, this is the first study to recognise that HIF-1α is involved in the hypoxia enhancement of MP release in ECs. This is in good accordance with previous reports that found that HIF-1α is central to hypoxia-mediated MP release in breast cancer cell lines (193). Thus, hypoxia-mediated MP release may share common cellular machinery regardless of the cell type. HIF-1α is a critical regulator of cellular and systemic responses to low O_2 levels. HIF-1α plays a critical protective role in the pathophysiology of

IHD. Future studies should explore potential cardio-protective and therapeutic implications of EMPs stimulated by hypoxia. I did not extend my work to identify the bioactive cargo and protein content of EMPs. A recent comparison of normoxic versus hypoxic EMPs (MPs derived from ECs exposed to 2% O_2 for 24 hours) identified that both protein and mRNA cargo is affected by hypoxia, although the functional characteristics of these MPs were not assessed (197).

The mechanisms by which HIF-1α mediates MP release remains relatively unclear, as does MP biogenesis in general. HIF-1α has been shown to induce apoptosis in neonatal rat brain (293). It is well established that apoptosis can induce MP formation (157); however there was no evidence to suggest that the hypoxic condition applied in this chapter induced apoptosis or altered cell viability. In line with this, it is noteworthy that 1% O_2 is equivalent to an O_2 concentration of 10 μM which is several orders of magnitude above that required to limit mitochondrial electron transport (0.1 μM) and is sufficient to maintain full eNOS function (6 – 9 μM). Moreover, atmospheric (sea level) oxygen (21% O_2) corresponds to a PO_2 of ~150 mmHg. Although difficult to accurately measure, the human body is exposed to much lower O_2 concentrations than this, ranging from 16% in the pulmonary alveoli, to 6% in exercised muscle tissues (290).

Previous reports have suggested that in relatively hypoxic conditions, oxygen-sensitive cells may elevate intracellular Ca^{2+} levels, which is known to initiate MP release. Recently, Zheng *et al*, (294) found that filamin A (FLNA), a large cytoskeletal actin-binding protein, interacts with HIF-1α. Moreover, hypoxia induces a calpain-dependent cleavage of FLNA to generate a naturally occurring C-terminal fragment that interacts with the N-terminal portion of HIF-1α, however MP formation was not assessed in that particular study. Nevertheless the mechanism linking HIF-1α to MP formation is still not fully elucidated.

MPs derived from hypoxia-treated HECV cells demonstrated an increased binding affinity to an electrode following an acute H_2O_2 insult compared to MPs derived from unstimulated HECV cells. The relevance of this in an *in vivo* setting is unclear. No difference was found in the proportion of annexin V positive MPs.

5.5.2.2 H_2O_2

H_2O_2 is less reactive and has a longer T½ in comparison to other ROS (such as $^{\cdot}OH$ or $^{\cdot}O_2^-$), and as such is arguably better-suited and more widely applied in *in vitro* settings. The physiological ranges for H_2O_2 vary amongst cell types/tissue. Reported intracellular H_2O_2 concentrations varies in the literature, ranging from 0.001 – 100 μM (295). Additionally, it is estimated that only 1- 15% of the H_2O_2 applied to the extracellular environment actually becomes biologically available in the cytosol, where glutathione peroxidase and catalase limit cytosolic H_2O_2 concentration (295, 296). Thus, *in vitro*, the concentration range of H_2O_2 is even more varied, ranging from nanomolar to millimolar concentrations. Previous studies have found that intracellular H_2O_2 concentration affects the biological activity of ECs, where millimolar concentrations induce apoptosis, micromolar concentrations affects cell growth and nanomolar concentrations affect cell proliferation (295, 296). Thus it was difficult to ascertain a suitable or physiologically pertinent concentration to use in my EC studies. In this chapter H_2O_2 was used to mimic oxidative stress because little is known about how an elevated oxidative burden affects MP production in ECs. HECV cells exposed to H_2O_2 (10 mM) for 24 hr resulted in increased MP production, a trend also seen in HUVECs. Specifically this increase was attributed to MPs with a diameter range of 50 – 300 nm. H_2O_2 significantly reduced cell viability based upon trypan blue exclusion, but did not alter caspase 3/7 acitivity or cell viability as assessed via the MTS assay. This is in accordance with previous reports that noted H_2O_2 increased MP release in ECs in a dose dependent manner, using H_2O_2 concentrations: 0.05 – 0.8 mM (297). Koga *et al*, (280) demonstrated a similar trend in endothelial progenitor cells treated with H_2O_2 (0.5 – 1 mM) for 24 hrs, where MP release was related to apoptosis. Jones and co-workers found that H_2O_2 induced apoptosis in a rat hepatocyte cell line RALA255-10G was associated with increased caspase activity (capase, 2, 3 and 7), where caspase inhibitors blocked H_2O_2-induced apoptosis (298). Thus, data in this chapter suggests that H_2O_2 enhancement of MP release maybe associated with cell death.

Several studies have previously shown that H_2O_2 induces concentration-dependent intracellular Ca^{2+} oscillations in human ECs, which result from the transient leakage of Ca^{2+} from endoplasmic reticulum Ca^{2+} stores (299). Interestingly, at low concentrations (1 - 10 μM), Hu and coworkers found H_2O_2 did not affect intracellular Ca^{2+} concentration. However, at higher concentrations (1 - 10 mM) intracellular Ca^{2+} concentration was increased (299). Thus, I speculate that the H_2O_2 enhancement of MP production by high (10 mM) concentrations may be related to intracellular Ca^{2+} concentration.

Additionally, an elevated proportion of MPs derived from H_2O_2 treated cells were annexin V positive. This increased exposure of PS may render such MPs more susceptible for target cell interaction as previous reports have shown PS exposure on the surface of PMPs, renders them 50 – 100 times more procoagulant than the surface of an activated platelet (180). However, this remains to be confirmed in further studies.

5.5.2.3 Insulin

As demonstrated in chapter 4, PCOS individuals with an elevated insulin response to a glucose challenge have elevated circulating MP levels. Insulin contributes to the metabolic and haemodynamic homeostasis of the vascular endothelium, however little is known about the direct effects of exogenous insulin on MP production.

In this study, insulin did not affect MP production in HECV or HUVEC cells. MP size, concentration and distribution did not alter. Moreover, insulin had no effect on MP annexin V positivity or coagulability. There was a modest increase in cell viability (assessed via CellTiter96® AQueous one solution cell proliferation assay) following exposure to exogenous insulin. This is in accordance with previous studies that found insulin exerts anti-apoptotic effects in neuronal and endothelial cells via a mechanism that is believed to involve PKB activation (300). The insulin concentration was chosen to reflect normal physiological levels as well as hyperinsulinaemic levels observed in PCOS patients described in chapter 3 and 4 (0.5 nM – 2.5 nM). Interestingly, Wang *et al*, (301) found the addition of insulin (50 nM) induces rapid actin cytoskeletal reorganisation in vascular ECs. This insulin-induced membrane cytoskeleton remodeling requires insulin signaling via the PI3K/PKB pathway. Although the exact mechanisms involved are unclear, cytoskeletal rearrangement is central to MP biogenesis. MP production was not assessed in this particular study, thus the direct effect of 'supra-physiological' insulin concentrations on MP production remains untested. However, my study shows that physiological concentrations of insulin do not appear to alter MP production, characteristics or function.

5.5.2.4 Glucose

Uncontrolled blood glucose levels in patients with diabetes may contribute to EC dysfunction. In this study, HECV cells were exposed to different glucose concentrations (0 - 20 mM).

Glucose depletion resulted in the greatest increase in MP production compared to unstimulated controls. Specifically this increase was attributed to MPs with a diameter range of 50 – 150 nm, suggesting non-selective MP production via both the exosomal classic pathway as well as membrane vesicle shedding *In vivo* evidence suggests type 2 diabetics (236) and subjects with IR have an elevated circulating level of MPs.

Wang and colleagues demonstrated that HUVECs exposed to low glucose conditions (0.2 - 0.4 μM) resulted in decreased NO bioavailability (assessed by OBC) coupled with a concomitant increase in mitochondrial $^{\cdot}O_2^-$ production (302). Moreover, intact human arterioles exposed to low glucose demonstrated marked endothelial dysfunction, a state linked to increased MP production (302). Paradoxically, high glucose conditions have been associated with increased intracellular Ca^{2+} levels and apoptosis. However, such effects often result from more chronic cell treatments, where HUVECs have been treated with 30 mM and 25 mM glucose for 90 and 75 hrs, respectively (303, 304). In comparison, data presented here reflects 24 hr treatments. No difference in caspase activity was noted, however glucose depletion did improve cell viability when assessed by the CellTiter96® AQueous one solution cell proliferation assay. This was not reflected in trypan blue exclusion. Interestingly, proof of principle confocal images demonstrated that HECV derived MPs interact and appear to internalise as intact MPs inside target HECV cells. Hempel and co-workers noted that 20 mM glucose medium conditions increased EC membrane permeability compared to lower (10 mM) glucose conditions (305). Thus, although membrane permeability was not assessed in this study, future studies could explore whether glucose depletion directly increases MP production per se rather than altering the membrane permeability and altering MP uptake (306).

In addition to enhancing MP production, a significant proportion of MPs produced in glucose naive conditions were VCAM-1 and annexin V positive and demonstrated an increased tendency to adhere to an electrode. Thus, hypoglycaemia may result in increased EMP production. Furthermore, these MPs appear to have increased PS and VCAM-1 exposure, are more coaguable and potentially more susceptible to cell interaction.

5.5.2.5 Testosterone

Previous studies have demonstrated that administration of testosterone increases plaque formation in monkeys (307). *In vitro* studies suggest that androgens may accelerate

atherosclerosis by stimulating the proliferation of VSMCs and increasing EC and monocyte VCAM- 1 expression (308). Previous studies have shown that circulating PMP levels are positively correlated with free androgen level in patients with PCOS (186), however little is known about the direct effect of testosterone on EC MP production. In this study, there was little evidence to suggest testosterone directly affected MP production in HECV or HUVEC cells. MP size, concentration and distribution did not alter. Testosterone had no effect on MP annexin V positivity or coagulability.

5.5.2.6 Surface adhesion molecule profiles

VCAM-1, ICAM-1, PECAM-1, P-selectin and E-selectin were detected on HECV cells and MPs. No difference was found in VCAM-1, ICAM-1, PECAM-1 or E-selectin expression on HECV cells treated with pathological stressors. A reduction in surface P-selectin expression (MFI) was noted in HECV cells following exposure to H_2O_2, hypoxia, testosterone and glucose depletion stressors but the mechanisms by which this occurs remains unclear. P-selectin is an adhesion molecule involved in the initial step of neutrophil recruitment. In contrast, previous studies have found that hypoxia (95% N_2, 5% CO_2) induces an increase in P-selectin expression in HUVEC (309). Additionally, other studies have shown that incubation of HUVECs with 25 mM glucose induced the expression of P-selectin, an effect reversed by the addition of 1 nM insulin (310). Numerous studies have shown that such pathological stressors also induce VCAM-1 and ICAM-1 expression in ECs (309). Notably, these studies used primary EC sources, where the biological relevance may be more apparent.

MPs harbour VCAM-1, ICAM-1, PECAM-1, P-selectin and E-selectin on their surface. Glucose depletion was linked to an increased proportion of VCAM-1 bearing MPs. This is in accordance with Joy and co-workers who found that hypoglycaemic conditions in patients with diabetes resulted in increased circulating VCAM-1 levels (311). Future studies can decipher if this increase in circulating VCAM-1 levels is attributed to any potential increase in VCAM-1 bearing EMPs. The other pathological stressors did not alter MP surface adhesion molecule profiles. Interestingly, all MPs (even control MPs isolated from HECV cells grown according to manufacturer's instructions) decreased P-selectin expression on HECV cells but the mechanisms by which this occurs remain unclear. Reduced vascular P-selectin expression has previously been observed in certain cancers and in patients undergoing immune-suppression. Although this is a novel finding with potential anti-thrombotic implications, further studies are needed for confirmation. These should include a primary cell model and explore whether MPs

interact with HECV cells via P-selectin, subsequently occupying the surface P-selectin antigen rendering it undetectable via flow cytometry.

5.5.2.7 The effect of microparticles on platelet function

Most of the literature focuses on MPs derived from platelets. Previous studies have shown that PMPs induce platelet activation and promote platelet aggregates via a glycoprotein IIb/IIIb dependent mechanism (312). However, the effects of EMPs on platelet aggregation remain untested. This study tested the hypothesis that EMP pre-conditioning would enhance platelet activation. There was little evidence to suggest that MPs altered whole blood platelet aggregometry or whole blood P-selectin expression.

5.5.3 Limitations

There are several potential limitations to this study. Firstly, HECV cells were used throughout this chapter. HECV is an established cell line. It is well recognised that although cell lines are convenient, their biology can become altered with time and may not truly reflect the primary cell. Furthermore, HECV cells were grown according to manufacturer's instructions in medium containing 22.5 mM glucose. Admittedly this reflects a hyperglycaemic environment *in vivo*. However, HUVECs were grown in 5 mM glucose (manufacturer's recommended medium). Notably, although similar trends were noted between both cell types, HUVECs produced fewer MPs per cell compared to HECV cells (~25 fold less). This may reflect cell culture medium conditions as well as possible differences in primary cells versus a cell line. On balance, future studies should build upon findings reported in this chapter with applications in primary ECs.

MPs are isolated from culture medium by differential ultra-centrifugation. Although this step-wise approach allows the removal of possible contaminants such as cells and cell debris, collecting MPs in the supernatant is based primarily on the assumption that MP production is increased/decreased rather than considering alterations in membrane permeability/MP uptake. Additionally, MPs were isolated from the cell culture medium, 24 hrs following exposure to the pathological stressors. It remains unclear if the increases in MP production are due to acute or chronic exposure. Thus, future studies should isolate MPs from culture medium at several time points to decipher the kinetics of MP release following stressor exposure.

Flow cytometry was used to determine annexin V positivity and to assess the surface adhesion molecule profiles of MPs and HECV cells. Typically, flow cytometry struggles to detect smaller MPs (<200 nm) and thus cannot observe the entire spectrum of MPs assessed using NTA. Previous studies have shown conflicting results regarding the extent of PS exposure on MPs. These studies often employ flow cytometry. Future studies should consider other methods of analysis, for example surface PS derivatisation and analysis via HPLC - mass spectroscopy, Western blot or ELISA for surface adhesion molecule profiling.

Apoptosis is known to induce MP formation (157). In this study, HECV cells were subjected to trypan blue exclusion, a caspase 3/7 assay and a CellTiter96® AQueous one solution cell proliferation assay to comprehensively assess the effect of each pathological stressor on cell viability. Results were often conflicting, however each method measures different aspects of cell viability and is subject to its own limitations and strengths.

In vivo the endothelium is not exposed to a single pathological stressor. Future work should explore how different *in vitro* conditions relevant to PCOS phenotypes might synergistically affect the endothelium.

5.5.4 Conclusion

A summary of the key findings are highlighted in table 6.4. In summary, this study demonstrates that H_2O_2, hypoxia and glucose depletion stressors enhance EC-derived MP release. HIF-1α induction plays an important role in the hypoxic enhancement of MP release, which was confirmed by manipulation of HIF-1α expression by siRNA interference. Although quantitative differences in MP release were not observed after exposure to every stressor assessed, several unique characteristics were observed. This would suggest that MP production and function reflects their environment/stimuli. Glucose deprived HECV cells produced PS exposing, procoagulant MPs. Although further studies are needed to determine the *in vivo* effect of these MPs, this would suggest that blood glucose regulation in patients with diabetes is important in perhaps limiting potentially damaging MP release. These MPs may be an appealing therapeutic target for future medicines but future work should confirm findings *in vivo* and explore the mechanism governing MP release.

Table 6.4	Summary: microparticle characteristics and function in comparison to the appropriate control(s)				
	H_2O_2 (10 mM)	**Testosterone (1 µM)**	**Glucose depleted**	**Insulin (2.5 nM)**	**Hypoxia (1% O_2)**
MP production	↑	–	↑	–	↑
Size distribution	↑ 50-300 nm	–	↑ 50-200 nm	–	–
Caspase 3/7 activity	–	–	–	↑	–
MTS assay	–	↑	↑	↑	–
Trypan blue exclusion	↓	–	–	–	–
MP annexin V positivity	↑	↑	↑	↑	–
Multiplate (MP adhesion)	–	–	↑	–	↑
HECV surface adhesion profile	↓ P-selectin (MFI)	↓ P-selectin (MFI)	↓ P-selectin (MFI)	–	↓ P-selectin (MFI)
MP surface adhesion profile	–	–	↑ VCAM-1 (%)	–	–
Effect of MPs on HECV surface adhesion profile	↓ P-selectin (MFI)	↓ P-selectin (MFI)	↓ P-selectin (MFI)	↓ P-selectin (MFI)	↓ P-selectin (MFI)

Arrow direction indicates an increase (↑), decrease (↓) or no change (−) in measurement. VCAM-1, vascular cell adhesion molecule-1; MFI, median fluorescence intensity.

5.6 Key findings

- Twenty-four hour exposure to H_2O_2 (10 mM), glucose depletion or hypoxia (1% O_2) enhanced MP production in ECs.
- Each pathological stressor affected MPs uniquely, suggesting MPs reflect their stimuli.
- MPs appear to internalise as intact vesicles in target cells.
- Not all MPs are annexin V positive.
- MPs possess an array of surface adhesion molecules.

6. RESULTS CHAPTER

The effect of lipoprotein-apheresis on circulating microparticles in individuals with familial hypercholesterolaemia

6.1 Introduction

Having previously shown that women with PCOS have an elevated concentration of circulating MPs, I chose to study an established CVD patient cohort, in which elevated MPs might be reduced by an extra-corporal intervention. Familial hypercholesterolaemia (FH) is a common genetic disorder that causes increased levels of atherogenic lipoproteins in the plasma, particularly LDL. Over 85% of FH cases are caused by mutations in the LDL receptor rendering these receptors unable to bind or internalise LDL, consequently leading to atherogenic lipoprotein accumulation in plasma (313). The disease follows an autosomal dominant pattern of inheritance and can result in heterozygote or homozygote forms (314). In severe forms of FH, diet alteration and lipid lowering medications are often insufficient to lower LDL levels enough to abate atherosclerotic plaque formation (315). Subsequently, these patients require frequent (bi-weekly) lipoprotein-apheresis (herein referred to as apheresis) treatments in combination with lifestyle modifications and pharmacological intervention to control LDL levels (316).

Apheresis is a well-established procedure for the extracorporeal removal of LDL. Briefly, blood is removed from one arm and passed through a column to remove atherogenic lipoproteins before being returned to the body via the other arm. Different apheresis techniques may be utilised, but all reduce LDL by approximately 70% immediately following treatment (317-320). However, post-treatment these reduced lipoprotein levels are not maintained with levels rising to 50% of pre-treatment values within 2-4 days (321). Despite this transiency, apheresis is associated with superior long-term cardiovascular benefits compared with alternative therapies (322-324). Apart from the physical removal of LDL, other cardio-protective mechanisms associated with apheresis remain unclear.

In addition to PCOS, increased numbers of MPs, particularly those derived from platelets, have been reported in many CVD entities (325, 326) though their function in both health and disease remains poorly understood. Previous studies have found that heterozygous FH patients have increased circulating levels of endothelial- and leukocyte-derived MPs compared to non-FH hypercholesterolaemia subjects (327). However, in this study MPs were quantified by flow cytometry. Cytometric analysis often struggles to detect MPs <200 nm. Little is known about the effects of apheresis on circulating MPs in individuals with FH, though other extracorporeal methods have been previously shown to remove MPs (328, 329).

6.2 Aims

The aim of this chapter was to characterise size, distribution, concentration, cellular origin, fatty acids and thrombin generation of MPs in FH patients undergoing apheresis, hypothesising that this treatment would reduce circulating MPs as well as LDL-cholesterol.

6.3 Methods

6.3.1 Ethical approval

The study was approved by Cardiff University (study sponsors), Cardiff & Vale University Health Board and the South East Wales research ethics committee. All subjects gave written informed consent before study commencement. Ethical approval was obtained by Prof Julian Halcox (Swansea University) as part of a study to assess vascular function in the setting of apheresis.

6.3.2 Subjects and protocol

Twelve patients with clinically significant dyslipidaemia undergoing fortnightly apheresis consented to take part in the study. For clinical reasons patients underwent treatment using three different techniques: polyacrylate whole blood adsorption (DALI®; n = 8), whole blood- (WB; n = 1), or plasma- (n = 3) dextran sulphate adsorption (DSA) as described previously (330). Patients attended the Lipid Unit at University Hospital Llandough, Cardiff for apheresis treatment as part of their normal clinical care. Patients fasted for at least 4 hours prior to attendance and took their prescribed medication for at least 1 hour prior to the study, excluding vasoactive medications from which patients were asked to refrain. Routine anthropometric measurements were carried out prior to apheresis treatment. After 15 minutes of rest, in a temperature controlled room vascular access was gained using 16 gauge 25 mm fistula needles into 2 anatomically distinct upper limb veins or by arterio-venous fistula. Blood samples were then drawn sequentially prior to and immediately after completion of apheresis, approximately 3 hours later. Seven healthy volunteers (no overt CVD or medication) were also recruited to compare baseline MP concentration, size distribution, cellular origin and fatty acid profiles with FH patients.

6.3.3 Biochemical Measurements

Blood samples were collected into EDTA and citrate vacutainers. Biochemical measurements were carried out by the Department of Medical Biochemistry - University Hospital Llandough, as described in section 2.4. BP measurements were taken using the Vicorder system (Skidmore Medical, UK).

6.3.4 Blood sampling, microparticle isolation and storage

Blood sampling is described in section 2.5. Plasma derived MPs were isolated by differential ultra-centrifugation as detailed in section 2.10, with modification. Briefly, blood was collected in citrate vacutainers and immediately centrifuged (1,509 x g, 10 mins, 4 °C) to obtain PPP. At the ISEV conference (2013) I learnt that citrate might prevent residual platelet activation during the pre-analytical protocol. Thus, unlike Chapter 3 where blood was collected in EDTA vacutainers, I choose to use citrate vacutainers in this chapter. Preliminary data from our research group has shown that MP cellular origin is not effected by the anticoagulant (EDTA or citrate) used for blood collection, however MPs derived from blood collected in citrate vacutainers appeared to have lower levels of MPs than blood collected using EDTA as an anticoagulant.

Citrate PPP was ultracentrifuged (100,000 x g, 1 hour, 4 °C) and the MP pellet was resuspended in either PBS or in PBS containing 0.05% (v/v) Tween 20 (for MP size and concentration). The latter was then passed through a 1 µm filter (Supelco, Sigma Aldrich, UK) and frozen overnight at -80 °C in a Mr Frosty (Nalgene, Thermo Scientific, UK). This forces a slow freeze (1 °C/minute). In pilot studies conducted in our research group, Connolly *et al*, (196) found that this freezing/storage protocol closely matched fresh MP samples (in regards to MP number and size).

6.3.5 Microparticle size, distribution and concentration

Two techniques were used to measure MP size and concentration: TRPS and NTA, as described in sections 2.12 and 2.11, respectively. Two nanopores (np100 and np200) were used for TRPS to detect the entire MP range (30-1000 nm). For NTA, 60-second videos were recorded in quintuplicate. Camera sensitivity and detection threshold were set to (14-16) and (5-6), respectively.

6.3.6 Microparticle cellular origin

Antibody enabled flow cytometry was used to determine the cellular origin and extent of annexin V positivity of plasma derived MPs, as described in section 2.23.3. Results are expressed as a percentage of total events (MPs).

6.3.7 Lipid extraction and fatty acid analysis

MP and plasma lipid extraction details are described in section 2.13. GC-FID was used to generate detailed fatty acid profiles of plasma and plasma-derived MPs, as noted in section 2.13.

6.3.8 Microparticle thrombin generation

Calibrated automated thrombography was used to assess MP thrombin generation, as described in section 2.24.

6.3.9 Statistical Analysis

Data were analysed using GraphPad Prism version 6.0 (GraphPad Software, San Diego, CA, USA). D'Agostino's K-squared test was used to check data for normality. Results are expressed as mean ± SD unless indicated. A paired *t-test* (two-tailed) or a Wilcoxon matched pairs test was used for parametric and non-parametric data, respectively. A p value <0.05 was deemed statistically significant.

6.4 Results

6.4.1 Subject characteristics and biochemical data

Demographic and biochemical measurements are summarised in Table 6.1. Apheresis reduced TC, triglycerides, HDL, LDL hsCRP and systolic BP. No changes were observed in glucose levels or diastolic BP.

Table 6.1 **Demographic and biochemical data**

n	12 (9 male, 3 female)
Age (years)	57.9 ± 10.3
BMI kg / m²	30 ± 4

	Pre-Apheresis	**Post-Apheresis**	***p value***
TC (mmol/L)	6.1 ± 0.5	2.7 ± 0.2	<0.0001
HDL (mmol/L)	1.1 (0.4-2.3)	0.9 (0.2-2.1)	0.003
Triglycerides (mmol/L)	1.8 ± 0.2	0.9 ± 0.1	<0.0001
LDL (mmol/L)	4.1 ± 0.4	1.4 ± 0.2	<0.0001
Glucose (mmol/L)	5.7 ± 0.3	6.1 ± 0.3	0.07
hsCRP (mg/L)	0.8 (0.2-16.9)	0.6 (0.2-13.8)	0.003
Systolic BP (mmHg)	140 ± 5	148 ± 6	0.02
Diastolic BP (mmHg)	81.8 ± 2.8	82.8 ± 2.7	0.45

BP: blood pressure. hsCRP: high sensitivity C-reactive protein. TC: total cholesterol. HDL: high density lipoprotein. LDL: low density lipoprotein. Results reflect mean ± SD or median (range).

Additionally, FH patient baseline measurements were compared to non-FH healthy volunteer basal measurements (Healthy volunteers: n = 7, 34 ± 8 years and 25 ± 3 kg / m^2) (33).

6.4.2 Microparticle size and concentration: Pre - versus post – apheresis

Two techniques, TRPS (np100 and np200) and NTA were used to analyse MP size, distribution and concentration. TRPS (np100) measured no difference in concentration pre- to post-apheresis ($4.6 \times 10^{11} \pm 1.3 \times 10^{11}$ to $3.1 \times 10^{11} \pm 1.0 \times 10^{11}$: $p = 0.18$; figure 6.1 A). However, TRPS (np200) and NTA both measured a decrease in MPs pre- vs. post-apheresis ($4.7 \times 10^{10} \pm 8.8 \times 10^{9}$ to $3.1 \times 10^{10} \pm 5.6 \times 10^{9}$, and $1.9 \times 10^{12} \pm 2.4 \times 10^{11}$ to $1.5 \times 10^{12} \pm 2.4 \times 10^{11}$ MPs/ml: $p = 0.013$ and $p = 0.025$; for TRPS (np200) and NTA, respectively, figure 6.1 C and E).

On assessment of MP distribution, TRPS (np100) and NTA showed no preferential reduction according to MP size (figure 6.1 B, F) whereas TRPS (np200) demonstrates a reduction in MPs between 200-249 nm (figure 6.1 D, $p = 0.01$). Plasma derived MP levels in FH patients showed a trend (non-significant) towards an increase in total concentration compared to healthy volunteers however, the size distribution showed subjects with FH had increased concentrations of MPs between 50-100 nm ($p < 0.05$, figure 6.2).

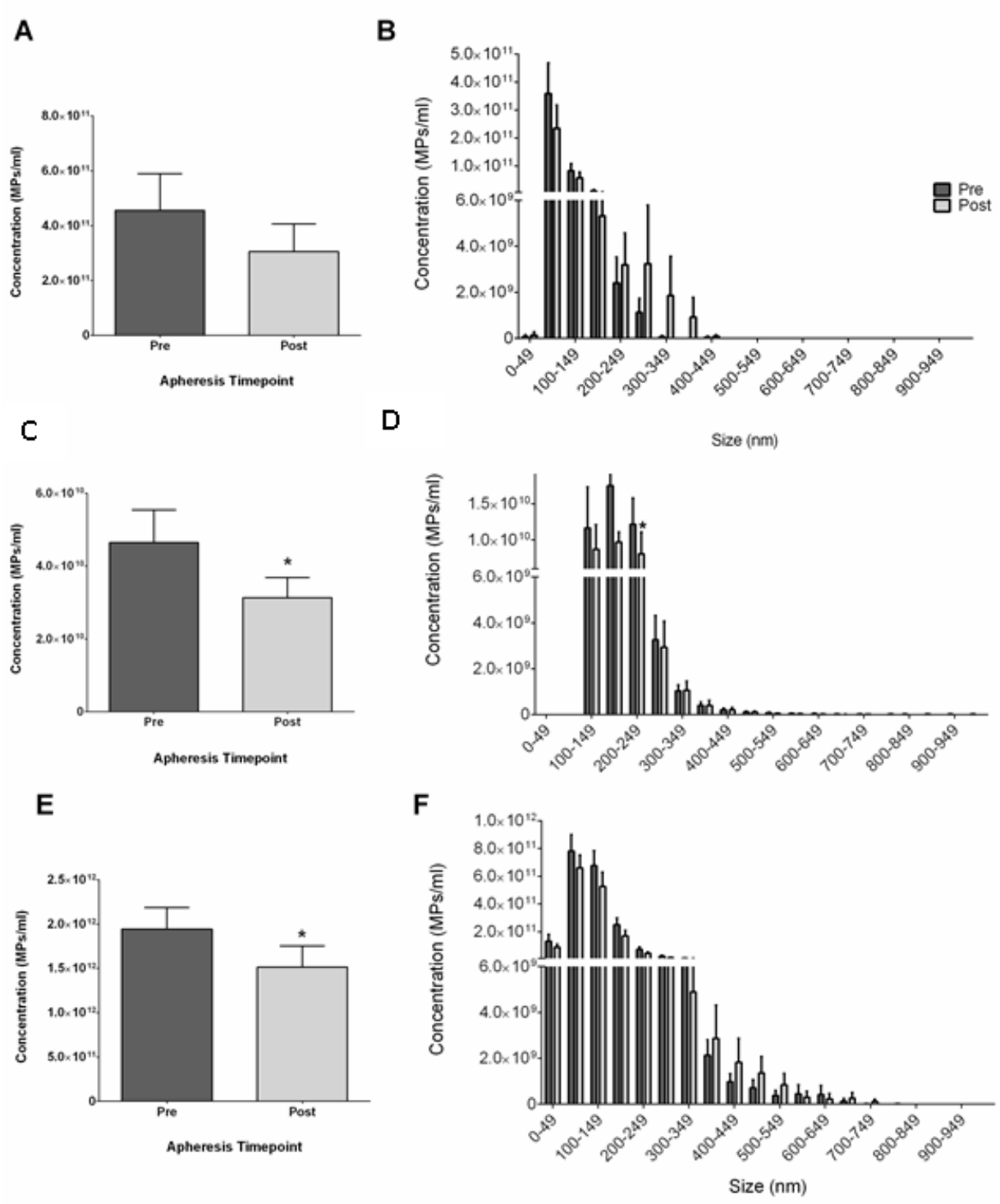

Figure 6.1. Microparticle concentration and size distributions pre- and post-apheresis. MP size and concentration was measured in pre- and post-apheresis samples using TRPS (np100 and np200) and NTA. Mean concentration of MPs pre- and post-apheresis is shown for TRPS np100 (A), np200 (C) and NTA (E). Size/concentration distribution of MPs pre- and post-apheresis is shown for TRPS np100 (B), TRPS np200 (D) and NTA (F). Concentrations are given in particles/mL of plasma. [n = 12, paired-samples, pre versus post apheresis]. Each sample was analysed in quintuplicate and the mean was used in further analysis. Data is expressed as the group mean ± SEM. * represents p <0.05.

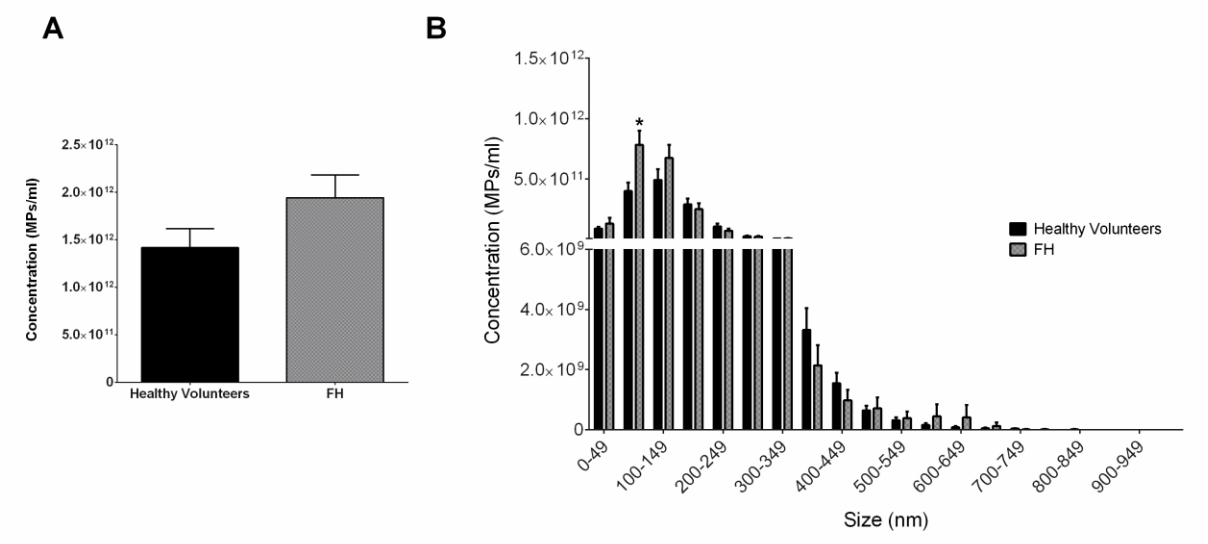

Figure 6.2. Comparison of the total microparticle concentration: Healthy volunteer versus FH patients. (A) Plasma derived MP concentrations – baseline measurements (B) Size/concentration distribution of plasma derived-MPs. NTA was used for comparison measurements. . [FH patients (n = 12), healthy volunteers (n = 7)]. Each sample was analysed in quintuplicate and the mean was used in further analysis. Data is expressed as the group mean ± SEM * represents p <0.05.

Total cholesterol was measured in the MP fraction and was below the detectability of the assay (<0.01 mM). Size/concentration distributions of MPs are shown pre- to post-apheresis for each technique. In addition to assessing the effect of apheresis on MP populations, I also compared each technique pre- and post-apheresis (figure 6.3). The size distribution of MPs was similar for TRPS (np100 and np200) and NTA though the measured concentration varied greatly between the two techniques. MP size did not change following apheresis by any technique (81.1 ± 19.6 to 78.4 ± 16.7, $p = 0.3$ for TRPS (np100), 170.3 ± 40.6 to 163.6 ± 29.2, $p = 0.18$ for TRPS (np200) and 93.3 ± 21 to 88.2 ± 14.7 nm, $p = 0.32$ for NTA).

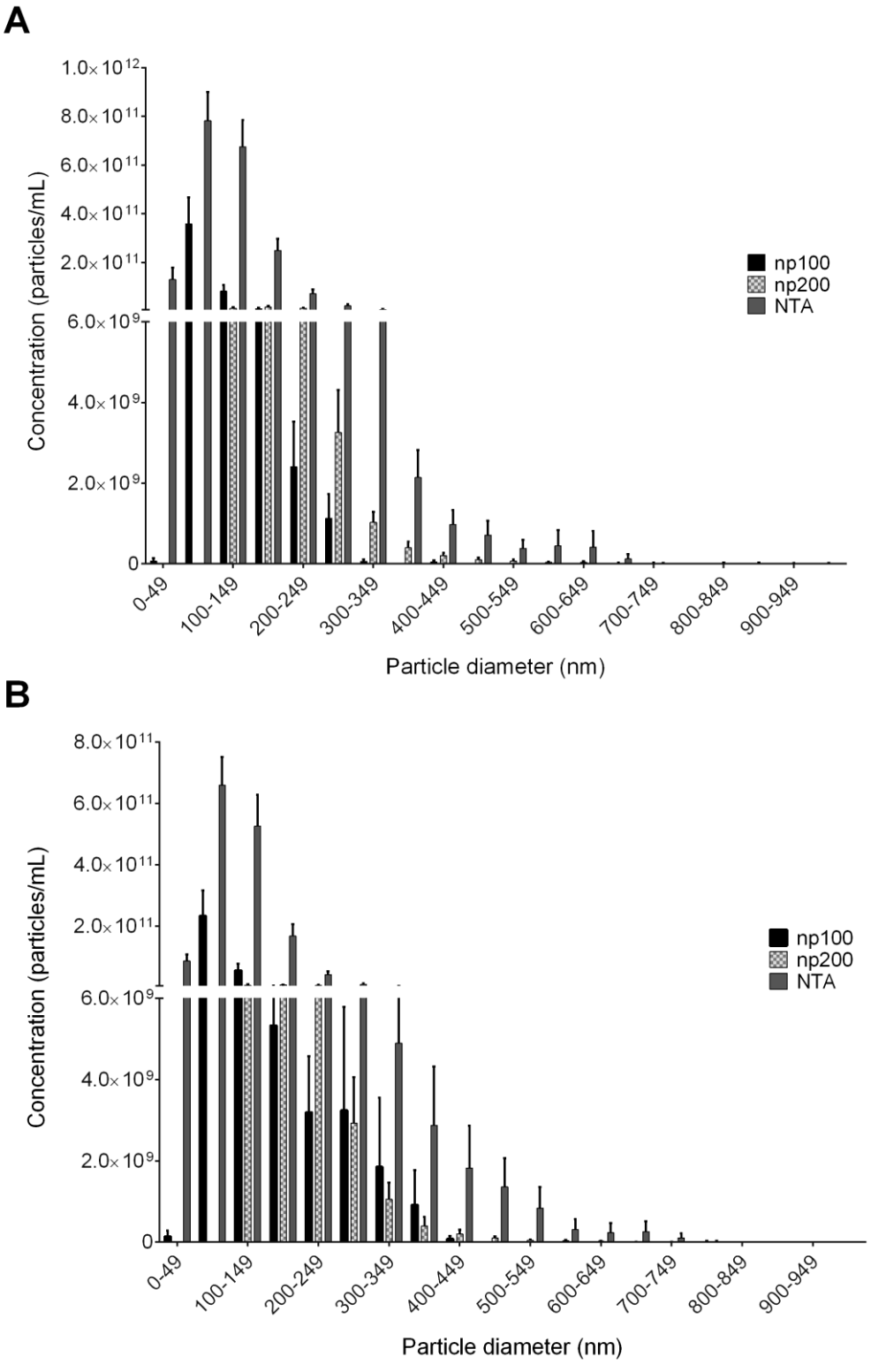

Figure 6.3. Range of microparticle sizes detected by each technique. A comparison of the spectrum of MPs measured by TRPS (np100 and np200) and NTA pre- (A) and post-apheresis (B). 50 nm bin sizes. Results reflect MPs per ml of plasma. [*n* = 12, paired-samples, pre versus post apheresis]. Each sample was analysed in quintuplicate for NTA measurements and the mean was used in further analysis. Data is expressed as the group mean ± SEM.

6.4.3 The effect of apheresis on microparticle cellular origin

MP cellular origin was determined by antibody enabled flow cytometry using CD41, CD144, CD235a and CD11b. No change in the proportion of annexin V positive MPs was found following apheresis (89 ± 12 % vs. 88 ± 17 %, respectively; p = 0.7, figure 6.4 A). Of these annexin V positive MPs, there were also no changes in the proportions derived from platelets, ECs, monocytes or erythrocytes (figure 6.4 B). MPs positive for both annexin V and CD41 accounted for the majority (~ 90%) of MPs measured, whilst erythrocyte, EC and monocyte derived MPs were infrequent. A similar trend was found for MPs in healthy volunteers. However, there was an increase in the proportion of EMPs in individuals with FH compared to healthy volunteers (p = 0.03, figure 6.5).

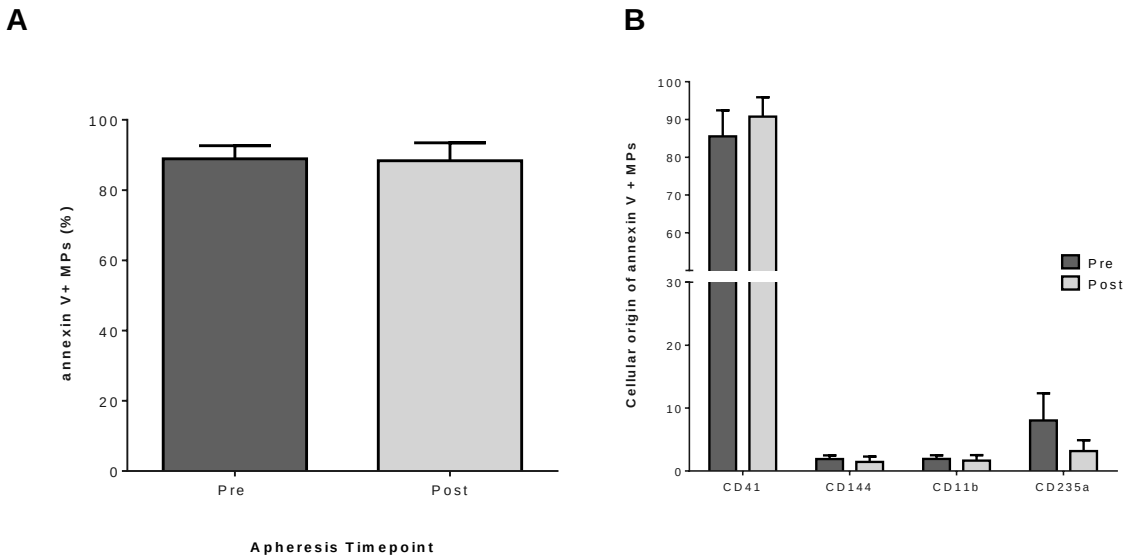

Figure 6.4. Microparticle origin. MPs from pre and post-apheresis samples were analyzed by flow cytometry to determine cellular origin. Forward and side scatter areas (FSC-A and SSC-A respectively) of platelets from fresh plasma were used to determine a sub-micron gate where only annexin V positive MPs were analysed. Samples were stained with annexin V (A), CD41, CD144, CD235a and CD11b to identify the proportion derived from platelets, endothelial cells, erythrocytes and monocytes respectively (B). [n = 12, paired-samples, pre versus post apheresis]. Data are presented as mean ± SEM.

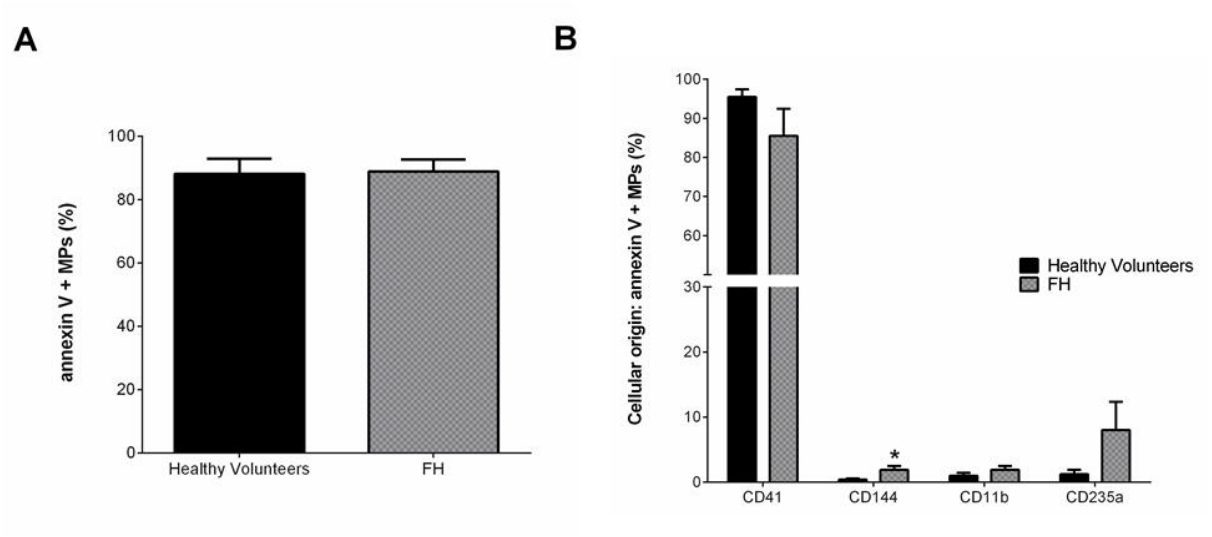

Figure 6.5. Microparticle: Healthy volunteers versus FH patients. Comparison of the MP annexin V positivity (A) and cellular origin (B) of MPs from healthy volunteers compared to individuals with FH. [FH patients (n = 12), healthy volunteers (n = 7)]. Data are presented as mean ± SEM. * Represents p <0.05.

6.4.4 Fatty acid analysis: pre - versus post - apheresis

Little is known about the lipid concentration of MPs, thus an aim of this chapter was to determine the fatty acid concentration and profile of MPs compared with that of the corresponding plasma and to observe the effect of apheresis. Total plasma fatty acid concentration decreased following apheresis (472 ± 262 to 268 ± 161 mg/200 µl plasma; p = 0.01) though this was not mirrored in the MP fraction (figure 6.6). Five individual fatty acids were altered in the plasma following apheresis (p <0.05): C14:0 (myristic acid); C18:0 (steric acid); C18:1n7 (cis-vaccenic acid); C20:5n3 (eicosapentaenoic acid) and C22:3n3 (docosatrienoic acid), the former three also being altered in the MP fraction (p <0.05, figure 6.6). Interestingly, comparison of plasma and MP compartments revealed that 10 fatty acids differed in composition (p <0.05). This was true in pre- and post-apheresis samples however the ten fatty acids were not the same (table 6.2).

Comparing FH subjects to healthy volunteers, both plasma and MP fatty acid levels were elevated in FH patients (p = 0.02 and p = 0.01, figure 6.7 A and C). Eight fatty acids were different in plasma and nine were different in MPs comparing healthy volunteers and individuals with FH (p <0.05, figure 6.7. B and D); apheresis had a similar effect on fatty acids in both compartments.

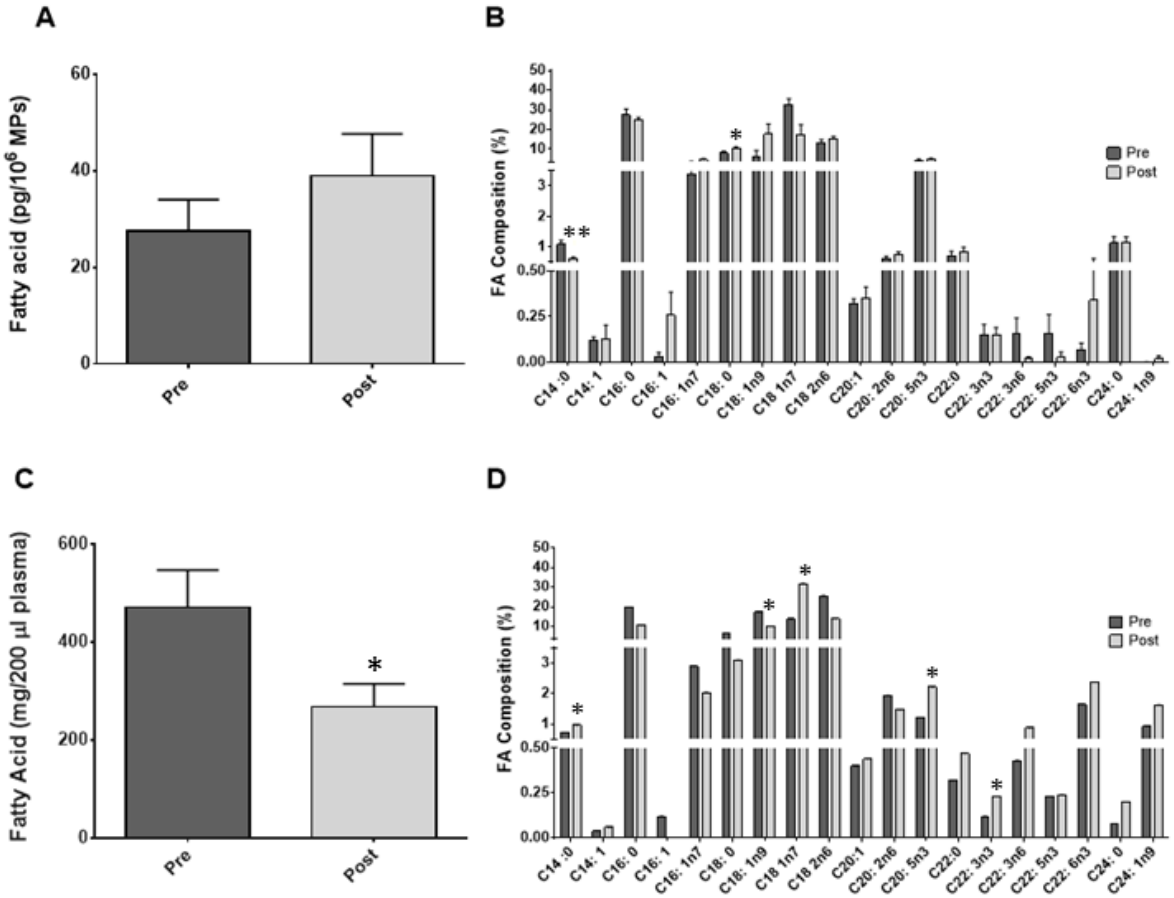

Figure 6.6. Fatty acid profiling. Total fatty acid concentration of plasma and MPs (A and C, respectively) followed by fatty acid profiling to determine compositional changes pre- to post-apheresis (B and D, respectively). [n = 12, paired-samples, pre versus post apheresis]. Data are presented as mean ± SEM. * and ** represents $p < 0.05$ and $p < 0.01$, respectively.

Table 6.2 **Fatty acid composition: Pre versus post apheresis**

	Pre - Apheresis			Post - Apheresis		
Fatty acid	**Plasma (%)**	**MP (%)**	***p* value**	**Plasma (%)**	**MP (%)**	***p* value**
C14:0	0.6 ± 0.1	1.09 ± 0.1	0.04*	0.9 ± 0.1	0.6 ± 0.07	0.008
C14:1	0.04 ± 0.01	0.1 ± 0.02	0.006*	0.06 ± 0.1	0.1 ± 0.08	0.4
C16:0	15.7 ± 3.2	27.3 ± 3.2	0.07	10.5 ± 3.9	25.1 ± 1.2	0.002
C16:1n7	2.5 ± 0.6	3.4 ± 0.4	0.4	2.0 ± 0.8	4.6 ± 0.7	0.02
C18:0	5.0 ± 0.8	8.2 ± 0.9	0.07	3.1 ± 1.3	10.6 ± 0.6	<0.001
C18:1n9	15.0 ± 4.2	6.2 ± 3.3	0.04*	10.1 ± 6.0	17.7 ± 5.4	0.4
C18:1n7	11.3 ± 4.2	32.5 ± 3.4	0.003*	31.8 ± 7.0	17.4 ± 5.4	0.1
C18:2n6	22.2 ± 5.8	13.3 ± 1.7	0.03*	14.0 ± 3.6	15.3 ± 1.2	0.7
C20:1	0.4 ± 0.1	0.3 ± 0.03	0.6	0.4 ± 0.06	0.4 ± 0.07	0.3
C20:2n6	1.7 ± 1.0	0.6 ± 0.09	0.2	1.5 ± 0.1	0.8 ± 0.09	<0.001
C20:5n3	0.9 ± 0.2	0.7 ± 0.15	0.03*	2.2 ± 0.4	0.9 ± 0.15	0.002
C22:0	0.3 ± 0.05	0.14 ± 0.06	0.02*	0.5 ± 0.07	0.14 ± 0.04	0.001
C22:3n3	0.1 ± 0.03	0.15 ± 0.09	0.7	0.2 ± 0.04	0.02 ± 0.01	<0.001
C22:3n6	0.4 ± 0.1	0.2 ± 0.1	0.09	0.9 ± 0.4	0.03 ± 0.03	0.004
C22:5n3	0.2 ± 0.06	0.07 ± 0.04	0.04*	0.2 ± 0.1	0.3 ± 0.3	0.8
C22:6n3	1.2 ± 0.2	1.1 ± 0.2	0.09	2.4 ± 0.6	1.2 ± 0.2	0.09
C24:0	0.07 ± 0.03	0.002	0.009*	0.2 ± 0.05	0.02 ± 0.02	0.003
C24:1n9	0.9 ± 0.2	0.2 ± 0.1	0.006*	1.6 ± 0.7	0.04 ± 0.02	0.08

MP, microparticle. Data are presented as mean ± SEM, (n = 12, paired-samples).

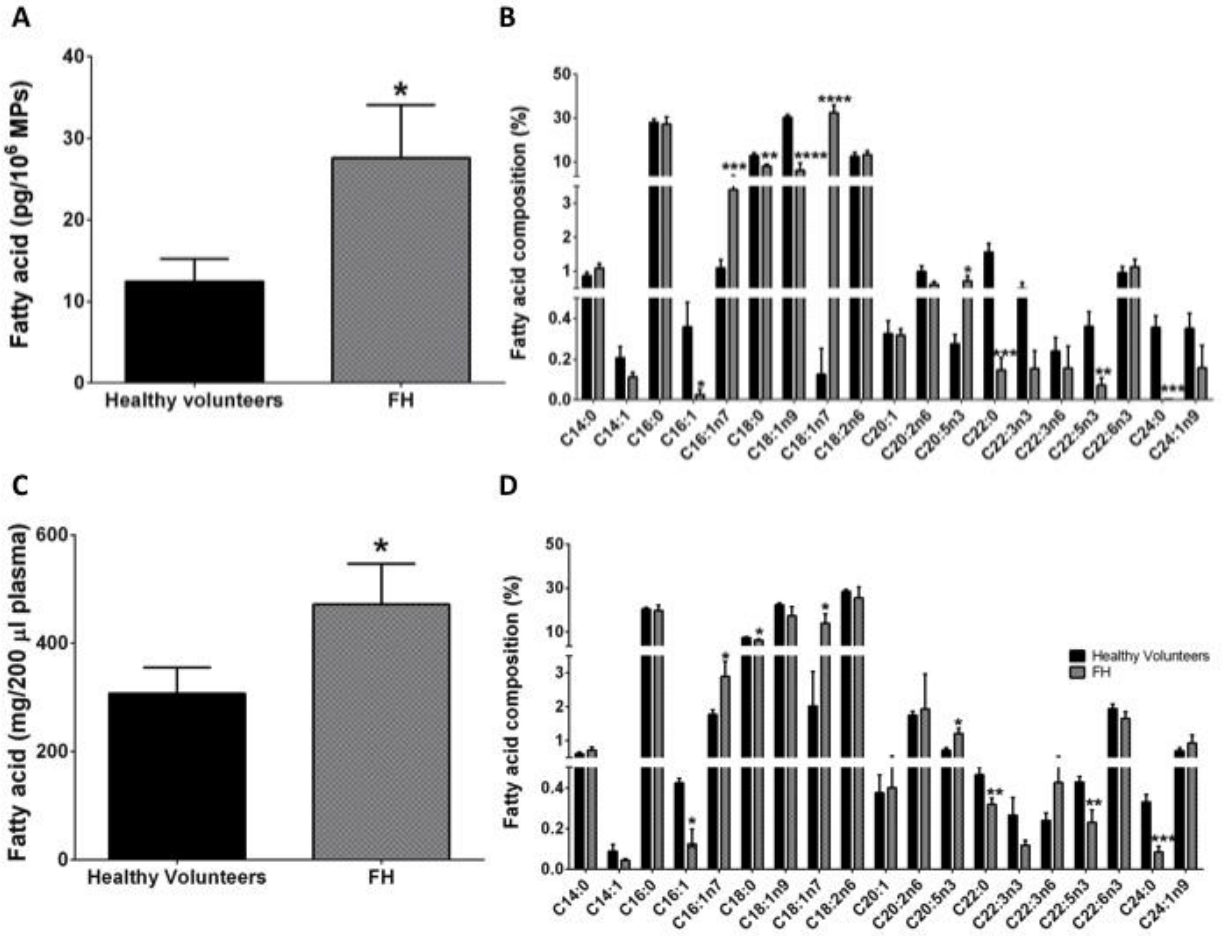

Figure 6.7: Plasma and microparticle fatty acid profiles: healthy volunteers versus FH patients (baseline measurements). Total fatty acid concentration of MPs (A) and plasma (C) was compared between healthy volunteers and individuals with FH. Individual fatty acid profiles of MPs (B) and plasma (D) were also compared between groups. [FH patients (n = 12), healthy volunteers (n = 7)]. Data are presented as mean ± SEM. *p <0.05, **p <0.01, ***p <0.001, ****p <0.0001.

6.4.5 Microparticle thrombin generation

Thrombin generation of MPs was compared pre- to post-apheresis and was also correlated with total MP concentrations. No change was observed in MP peak thrombin generation pre- to post-apheresis (14.8 ± 2.9 to 16.6 ± 4.1 nM, $p = 0.6$, figure 6.8). However, MP thrombin generation over time (AUC) was positively correlated with MP concentration measured by TRPS (np100) and NTA (r = 0.626, $p = 0.001$ and r = 0.424, $p = 0.04$ respectively). Thrombin AUC showed no correlation with MP concentration measured by TRPS (np200). Furthermore, when TF was added to MPs (to exogenously initiate maximum thrombin generation), thrombin AUC no longer correlated with MP concentration.

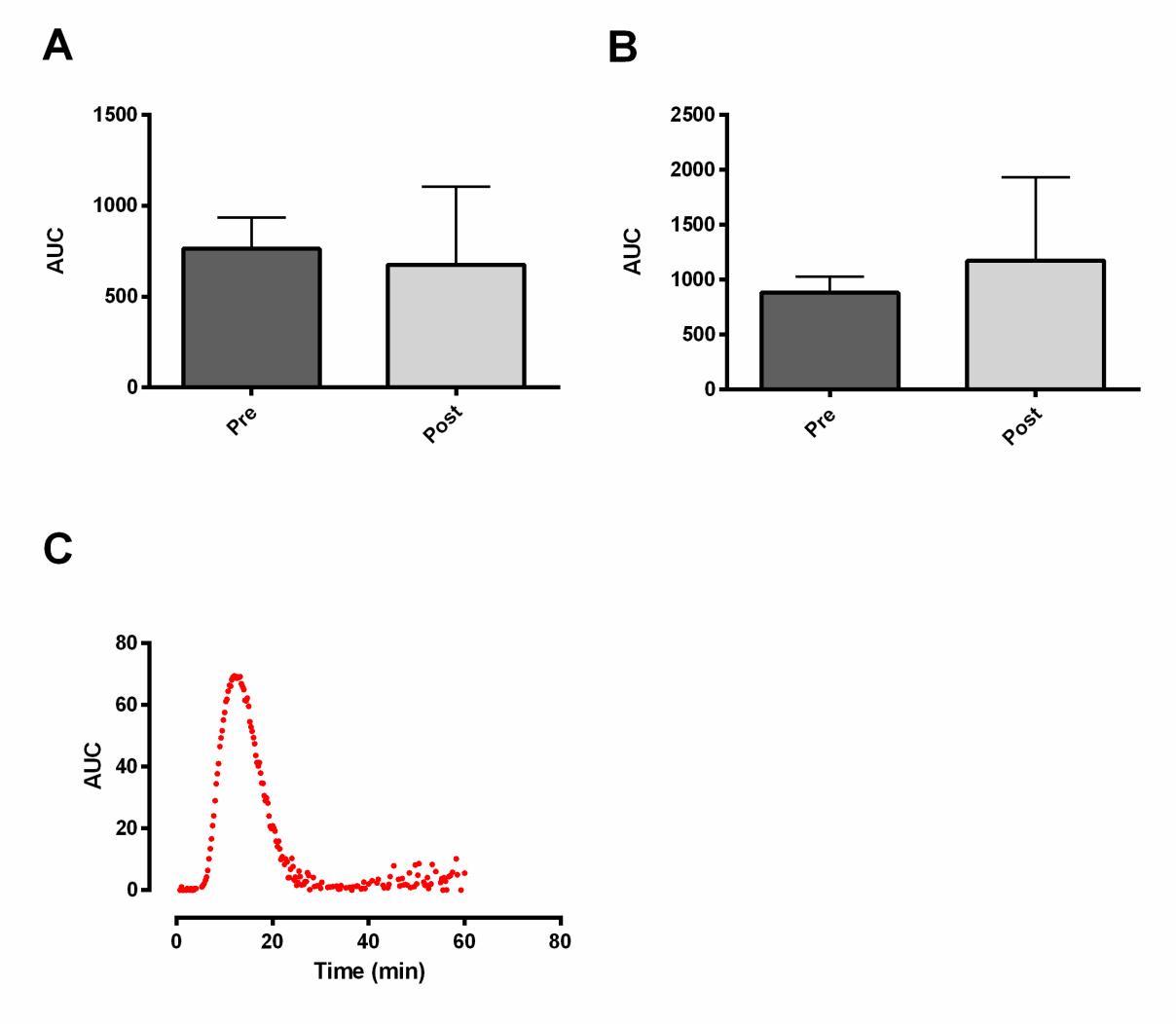

Figure 6.8. MP Thrombin generation: FH patients (pre versus post apheresis). (A) MP thrombin generation. (B) MP thrombin generation in the presence of exogenous tissue factor. Data are presented as mean ± SEM, (n = 12, paired-samples, pre versus post apheresis). (C) Typical calibrated automated thromborgam.

6.5 Discussion

6.5.1 Main findings

This study details the novel effects of apheresis on MP size, concentration, origin, fatty acid concentration and thrombin generation in FH patients. This study demonstrates that apheresis reduces circulating MP concentration, the majority of which were annexin V positive and derived from platelets.

6.5.2 Interpretation

There are numerous methods used to detect MPs, each exhibiting its own advantages/limitations. Often the technique employed is dictated by the specific research question. In this chapter, two well-established methods were used for MP measurement in order to capture the full spectrum of MP sizes. Moreover, TRPS and NTA have not previously been subjected to a direct comparison in biological samples. The data suggests the range of detectability of TRPS (np100 and np200) and NTA are similar, although they differ in reported MP concentration.

Both TRPS (np200) and NTA methods showed a decrease in MP concentration pre- versus post-apheresis. MPs within the range of 200-250 nm were reduced the most pre- versus post-apheresis which is much greater than the size of LDL particles (331), providing further evidence that the techniques are measuring a reduction in MPs and are not detecting LDL-cholesterol. Moreover, MPs were also shown to be elevated in the exosomal range in individuals with FH compared to healthy volunteers. This may suggest selective stimulation of the intracellular classical exosomal pathway compared to larger MPs formed via cell membrane shedding. Total MP concentration also appeared elevated in FH subjects compared to healthy volunteers, though overall this did not reach significance. Cytometric measurement of MPs revealed no changes in annexin V positivity or cellular origin following apheresis. In keeping with previous data (327, 332, 333) (and results found in PCOS patients/healthy volunteers detailed in chapter 4) PMPs occupied the majority of the MP population (88.9 ± 13%). Taken together with the fall in MP concentration this would suggest that apheresis non-selectively removes MPs, the majority of which are annexin V positive and derived from platelets. These MPs have not only been shown to be elevated in a variety of disease states (209, 237, 334-337) but also to promote coagulation

(180), atherosclerotic plaque formation (209) and to be associated with atherothrombotic events (336). Non-selective removal of these MPs by apheresis may reduce the risk of thrombus formation by slowing the progression of atherosclerotic lesions thereby complementing the effect of LDL removal. MPs in healthy volunteers were also found to be mainly annexin V positive and of platelet origin. It would appear that individuals with FH have a greater number of these circulating annexin V/platelet derived MPs. Interestingly, FH patients had a greater proportion of EMPs, perhaps suggesting a greater level of endothelial activation compared to healthy volunteers, although the percentage of the total was still low (<2%). This trend is in accordance with a recent meta-analysis that demonstrated that FH patients display an increased carotid IMT and reduced FMD compared to their non-FH counterparts, and may be indicative of endothelial dysfunction in these FH patients. However, the cause of this elevation in EMPs remains unclear.

The atheroprotective mechanisms of monousaturated fatty acid (MUFA) and PUFAs are well-documented (338), as are the data implicating saturated fatty acids in arterial wall lipid accumulation and atherosclerotic plaque formation (339). MPs have been shown to carry a specific cargo of proteins, genetic material and small molecules, including fatty acids (340) that can initiate a pro-inflammatory response in target cells (282). Total fatty acid concentration of plasma was decreased following apheresis, however MP fatty acid levels did not change following apheresis. Thus, although the overall number of MPs decreases post-apheresis, the fatty acid concentration per MP remains the same. Interestingly, apheresis seemed to affect individual fatty acids differently in plasma compared with the MP fraction; however the physiological relevance of this remains to be elucidated. Furthermore, when plasma was directly compared with the MP fraction, the proportion of fatty acids were found to be different between compartments. This suggests that the fatty acid composition of MPs is independent to that of surrounding plasma, a concept in keeping with the findings in chapter 4 in PCOS patients. Several fatty acids were different in individuals with FH compared to healthy volunteers in both plasma and MPs, however the affected fatty acids and the trends (i.e. increase or decrease) were the same. Similarly to the findings in FH, in healthy volunteers the fatty acid composition of MPs did not reflect that of plasma.

Although no change was observed in MP peak thrombin generation pre- versus post-apheresis, total MP concentration measured by either TRPS (np100) or NTA was positively correlated with thrombin AUC. MP concentration measured by TRPS (np200) showed no correlation. Taken together, this suggests that a reduction in MPs is associated with decreased thrombin

generation capacity and that smaller MPs, particularly exosomes, are associated with an increased total thrombin generation over time. This is on the basis that both TRPS (np100) and NTA have an increased sensitivity for MPs in the exosomal range compared to TRPS (np200). Additionally, FH patients were shown to have an increased circulating population of smaller MPs compared with healthy individuals. Both TRPS (np100) and NTA showed a trend towards reduction in exosomal populations of MPs following apheresis, though this did not reach significance. This could suggest that the increased circulating population of exosomes in individuals with FH makes their MP fraction more procoagulant. Apheresis treatment non-selectively removes MPs and could potentially reduce the procoagulant potential of exosomes and smaller MPs. Also, in accordance with previous studies, these findings confirm MPs have endogenous TF activity and can stimulate thrombin generation (341, 342). When exogenous TF was added to MPs to stimulate thrombin generation, the correlation between MP concentration and AUC was lost reflecting maximum thrombin generation.

6.5.3 Limitations

There are a number of potential limitations to this study. Patients in this study received apheresis based on individual clinical requirements resulting in the use of three different types of apheresis treatment. Though there was no observable difference between apheresis technique and MP concentration, the current study was not designed to assess this. *In vitro* studies have shown that the surface morphology of the adsorbent polymer may affect MP production (342), though this requires confirmation *in vivo*. FH patients were studied as part of their routine clinical outpatient treatment. Clearly, having now established that apheresis directly influences MP concentration, longitudinal studies and comparisons of apheresis techniques will help to establish whether the reduction in atherogenic MPs is maintained whilst further exploring the physiological relevance this reduction in MPs has in regards to CVD pathology.

It is acknowledged that many flow cytometers have a practical lower limit of around 200 nm. Therefore smaller MPs (particularly exosomes) are below the detectability of conventional flow cytometers. Thus the fluorescence data obtained from a given sample does not completely reflect the full range of MP sizes observed by NTA and TRPS. Despite this, antibody enabled flow cytometry is arguably the most reliable technique to assess surface antigen expression of MPs. Importantly, NTA and TRPS confirm MPs within the range of 200-250 nm were reduced the most pre- versus post-apheresis and are likely reflected by the flow cytometric results. The use of annexin V positivity to identify MP populations is used widely (332, 343, 344) but has

recently been questioned (176). As the majority (~90%) of MPs here were annexin V positive, I chose to accept this as the MP population for subsequent staining. This rationale was based on the fact that despite not all MPs binding to annexin V, only annexin V positive MPs have been shown to possess procoagulant activity (176).

The thrombin generation of patient MP samples was measured in the presence of pooled, healthy plasma (PPP) to specifically test the activity of MPs as opposed to whole patient plasma (that would likely reflect the total influence of apheresis). Future studies should firstly normalise MP thrombin generation to MP number. Secondly, studies should assess the procoagulant activity of plasma pre- to post-apheresis to confirm the reduction in MPs is associated with a decrease in plasma thrombin generation.

6.5.4 Conclusion

In summary, apheresis reduces the concentration of circulating MPs in patients with FH, the majority of which are annexin V / platelet (CD41) positive. Though MP concentration is reduced, apheresis has no effect on the total fatty acid concentration of MPs. Fatty acid composition of MPs is unique and does not reflect that of surrounding plasma. MP concentration (particularly in the exosomal range) was found to positively correlate with total thrombin generation, suggesting that a reduction in MP concentration via apheresis in FH may reduce MP-initiated thrombin production. The removal of MPs that are predominantly annexin V positive and platelet-derived is a novel finding, supporting the notion that apheresis may have beneficial cardiovascular effects beyond lipoprotein removal. Future work should investigate whether the reduced MP levels are maintained between apheresis treatments and should aim to establish whether MP reduction during apheresis is associated with the longer-term benefits of this treatment.

6.6 Key findings

- Apheresis decreases circulating MP levels, the majority of which are annexin V / platelet (CD41) positive.
- Apheresis decreases plasma fatty acid concentration.
- Plasma and MP fatty acid composition is altered by apheresis.
- Thrombin generation of MPs correlated with total MP concentrations, suggesting that greater numbers of circulating MPs are associated with increased prothrombotic activity in FH patients.
- Apheresis may have beneficial cardiovascular effects beyond lipoprotein removal.

7. GENERAL DISCUSSION

7.1 Overview and conclusions

The main aim of this thesis was to provide a clearer understanding of mechanisms that may predispose patients to CVD. The initial focus was two-fold; to establish the role of nitro-oxidative stress early in the disease process and to investigate the occurrence and function of circulating MPs in mediating endothelial dysfunction. Women with PCOS were used as a model of predisposition to CVD. These patients were compared to healthy controls in an observational study, which involved a comprehensive assessment of indices of nitro-oxidative stress and a detailed characterisation of circulating MPs. The effect of pathological stressors (akin to those found in PCOS), on EC-MP production were assessed in an *in vitro* model using cultured ECs. In order to ascertain whether circulating MP levels could be modulated in a clinical cohort the effect of apheresis on circulating MP levels was investigated in patients with established CVD.

Patients with PCOS appear prone to developing numerous cardiovascular health problems including obesity (77), hypertension (78), IR (263) and dyslipidaemia (89), which may contribute to an increased prevalence of cardiac events in later life (152). Whilst efforts have been made to find candidate genes that might influence PCOS expression, the syndrome has an unknown aetiology and the mechanisms that govern cardiovascular risk remain unclear.

Uncertainty remains as to whether patients with PCOS are prone to endothelial dysfunction, a state associated with nitro-oxidative stress. Previous studies show conflicting results, often analysing aspects of this complex biochemistry in isolation (138, 139, 142, 266-269). In contrast to my original hypothesis, whereby PCOS patients were predicted to display an elevated oxidative burden, a comprehensive biochemical analysis found that there is little evidence to suggest that PCOS patients have increased oxidative stress. However, the PCOS patients recruited in this thesis were young, carefully matched for age and BMI controls, and were diagnosed using the Rotterdam criteria which is associated with a less severe metabolic phenotype than other diagnostic criteria (276). The low mean age (29 yrs) is in keeping with data from the British Heart Foundation who found that only 798 out of 179,078 CVD associated deaths (in the UK in 2013) were in the <35 yr age range (7). Therefore, it is unlikely that this mild PCOS phenotype would have established cardiovascular disorders but perhaps may exhibit early indices of endothelial dysfunction, a prerequisite to CVD. An additional study from our group, using a similar patient cohort found that there was no difference in arterial stiffness (assessed by PWV), carotid IMT or myocardial function between PCOS patients and healthy controls (96). Nevertheless there is a general view in the literature that women with PCOS are prone to developing CVD.

Even though there is little biochemical evidence for nitro-oxidative stress in this young PCOS cohort, data presented in chapter 4 showed that women with PCOS exhibit elevated levels of annexin V positive MPs that were predominantly derived from platelets. The clinical significance of this elevated MP population remains unknown. Although MP biogenesis represents a physiological phenomenon, multiple pathologies are associated with an increase in circulating MPs (157), including inflammatory diseases (210), atherosclerosis (244) and certain cancers (226). Interestingly, previous reports have shown that the presence of annexin V positive MPs independently predicts cardiovascular events in stable CAD patients (345).

Young women with PCOS did not display any indices of nitro-oxidative stress, but did present with an elevated concentration of circulating MPs. Previous studies have found increased markers of nitro-oxidative stress in subjects with established, chronic CVD compared to a healthy population. In contrast, the PCOS patients investigated in this thesis were young and had no overt CVD. Thus, on reflection it is fair to speculate that these patients would not present with vast differences in nitro-oxidative measures, but perhaps may exhibit subtle changes which may have not yet be physiologically manifested. To maximise my chance of observing any differences in oxidative burden, I undertook a comprehensive set of 'gold-standard' biochemical measurements (described in chapter 3) to capture lipid-derived radicals in circulation, as well as differentiate between plasma NO_x.

There are several explanations that may explain why no differences were found in nitro-oxidative stress indices between PCOS and healthy controls. Firstly, PCOS patients do not exhibit nitro-oxidative stress. Secondly, PCOS patients may indeed harbour subtle differences in localised nitro-oxidative stress indices, however these are not yet detectable systemically using current methods. With an incomplete outer electron shell, ROS including NO are exceptionally potent and difficult to detect. Data presented in chapter 5 demonstrates that MP production by ECs can be enhanced by metabolic and oxidative stressors, however until current techniques are able to accurately detect subtle differences in ROS, it will remain difficult to confirm the role of nitro-oxidative stress in MP production *in vivo*, specifically in disease states where individuals may be at a predisposition to CVD and only exhibit subtle redox alterations.

In an exploratory sub-population, novel data presented in chapter 4 found that circulating MPs in PCOS patients harbour differentially-expressed miRs. No other study to date has investigated the miR content of circulating MPs in PCOS patients. Notably, differentially expressed miRs targeted genes that affect insulin sensitivity, androgen and cortisol levels. This finding may be

of significant interest to the PCOS community and suggests a novel mechanism by which the syndrome may affect cardiometabolic risk and provides an exciting future research theme. If these findings are confirmed in a larger PCOS cohort, an elevated annexin V positive MP population which harbours differentially expressed (PCOS-specific) miRs could have implications for use as biomarkers, in diagnosis and therapeutics. Previous reports have shown that MPs can induce ROS formation in ECs and decrease NO production, however, there appears to be no association between the nitro-oxidative stress parameters presented in chapter 3 and MP levels or characteristics presented in chapter 4 in this PCOS cohort.

Some pathological conditions are associated with an increase in circulating MPs; novel data presented in chapter 6 provides evidence that reducing circulating MP levels may have potential cardio-protective effects. Apheresis decreased circulating levels of MPs and was associated with a decreased thrombin generation capacity in patients with established CVD. In addition to reducing lipoprotein levels, the non-selective removal of circulating MPs could be another beneficial outcome of apheresis. Potentially, similar procedures could be applied to other disease states where circulating MPs play a pivotal role in disease pathology. Current commercial ventures are investigating the efficacy of the extra-corporeal removal of MPs in HIV patients. In order to confirm this, further studies should (i) assess the effect of apheresis on MP levels over time and assess if this is associated with acute or long-term cardiovascular benefits (ii) determine a means of removing MPs without altering lipoprotein profiles in non-FH subjects. Furthermore, the effects of apheresis on circulating MPs in FH patients was undertaken as part of a larger clinical study to measure the influence of apheresis on vascular flow indices (undertaken by Ms Libby Ellins) and biochemical markers of endothelial function (our group). Interestingly, baseline (pre-apheresis) MP concentration was significantly associated with CRP levels ($p = 0.02$), which suggests that this enhancement in circulating MPs may in part be related to inflammatory status. However it remains unclear if inflammation is a cause or consequence of this elevated MP population. No correlation was found between MP concentration and measures of endothelial function.

In PCOS patients, circulating MP concentration was associated with HOMA-IR values, suggesting that the increase in MPs may in part be driven by IR. However, I did not find evidence of an effect of hyperglycaemia and supra-physiological insulin levels on MP formation when tested directly on HECV cells *in vitro*. Several pathological stressors akin to those found in PCOS were used in the *in vitro* model in an attempt to investigate the possible causes of an increased MP formation. HECV cells were exposed to oxidative, hypoxic, hyperandrogenic and metabolic stressors. Each pathological stressor affected MP generation uniquely. In accordance

with previous studies which have shown that MP protein and mRNA content reflects cellular stress conditions, MP characteristics might reflect their particular stimulus.

Cells grown in compliance with the manufacturers recommendations represent cellular homeostasis *in vitro*. However, HECV cells exposed to a glucose-deprived condition resulted in an enhanced production of annexin V positive and VCAM-1 expressing MPs, which were more procoagulant *in vitro*. The precise mechanism involved in this enhancement in MP production remains unclear. Further studies should attempt to replicate findings *in vivo* (hypoglycaemia vs. normoglycaemia MP production in animal models). Several studies have shown that hypoglycaemia is associated with an increased risk of cardiovascular events. In a study involving 29 patients with type 2 diabetes, Desouza *et al,* (346) found that of 54 hypoglycaemic episodes, 10 were associated with electrocardiographic evidence or symptoms of ischaemia. In contrast, only one episode of chest pain occurred during 59 episodes of hyperglycaemia. The data in this thesis suggest that transient hypoglycaemia induces the secretion of prothrombotic MPs which might propagate CVD development in patients with diabetes. Furthermore, data presented in chapter 5 are the first to show that the enhanced production of hypoxia-mediated MP release in ECs is related to HIF-1α. However, further studies are needed to confirm the biological effects of these MPs.

Several consistent themes arise from the results of my thesis. Firstly, although the biological significance of MPs are increasingly recognised, their isolation and detection has proven difficult. For example, with respect to clinical samples, differing pre-analytical protocols not only complicate inter-study comparisons but may also co-isolate non-MP plasma fractions. Consequently, in chapters 4 and 6, where plasma-derived MPs were isolated, it is probable that non-MP plasma fractions were also detected and greater care may be needed in ensuring complete removal of contaminating platelets.

The cellular origin of MPs was determined using a custom built BD Aria, whereas MP surface adhesion molecule expression was measured using a BD Canto. Different flow cytometers have different sensitivity and detection limits (347). For example, Chandler *et al, (348)* applied a gating strategy based upon polystyrene beads (Megamix beads, Biocytex, UK) for the detection of PMPs using a Apogee A40 flow cytometer and showed that the gate only detected platelets (with a diameter of 2 – 5 μM). In contrast, Mullier *et al,* (349) and Robert *et al,* (350) were able to distinguish between PMPs and platelets using a similar gating strategy based upon the Megamix polystyrene beads using different flow cytometers. The refractive index of carboxylated polystyrene beads is different to that of MPs. Refractive index can be described by Rayleigh approximation, Faunhofer diffraction or Mie theory. Using Mie calculations, Van der

Pol *et al*, (248) showed that even if 220 nm polystyrene beads are detectable by flow cytometry, the same gate equates to MPs with a diameter of 300-500 nm, due to different refractive index values. Because MPs have a lower refractive index than polystyrene beads, they scatter light approximately 10-fold less efficiently than polystyrene beads. Furthermore, MP detection by a regular flow cytometer is limited by swarm detection, whereby multiple MPs are simultaneously illuminated by the laser beam and counted as a single event (one MP). This would under-estimate the FFC and SSC light detection and may account for different fluorescence signals corresponding to a single event, where the signal may originate from multiple MPs. Moreover, previous reports have shown that the concentration of MPs determined by flow cytometry is more than 1000-fold lower than the actual concentration (248). With different instrumentation used to determine MP cellular origin and MP surface adhesion molecules, it is likely that the flow cytometers would have had different detection parameters, although this was not assessed. In spite of these limitations, flow cytometry is often considered the present method of choice for MP detection, and is currently the only widely used method for establishing surface characteristics/MP parentage. Current on-going experiments in our laboratory are trialling enhanced ELISA based methods using time resolved fluorescence for the detection and quantification of MP surface makers. This may offer the advantage of high-throughput analysis coupled with enhanced sensitivity, especially for smaller MPs.

There are numerous methods used to detect MPs, each exhibiting its own advantages/limitations. Often the technique employed is dictated by the specific research question. In chapter 6, two well-established methods were used for MP measurement (TRPS and NTA). Previous reports have compared different quantitative methods for MP measurements such as, TRPS, NTA, TEM, DLS and flow cytometry, however these studies all utilised polystyrene beads (which have a greater refractive index compared to biological MPs). To the best of my knowledge, the data presented in chapter 6 are the first to compare NTA and TRPS directly in the measurement of biological samples. The data suggest that the detection ranges of TRPS (np100 and np200) and NTA are similar, although they differ in reported MP concentration.

7.2 Future directions

MPs play an important role in both health and disease. Future research should build upon the data presented in this thesis and explore the role of MPs in CVD development. The prospect of using circulating MPs as biomarkers or therapeutic agents is an exciting challenge, with

potential implications across several disorders. However, standardisation of the pre-analytical procedures and overcoming methodological limitations requires addressing and delays the implementation of MPs being used as biomarkers in routine clinical practice.

MPs derived from platelets occupied the greatest proportion of plasma-derived MPs. There is much variability in the literature regarding the cellular origin of MPs. Often, there are two requirements when isolating MPs from blood. Firstly, the venepuncture procedure technique itself should minimise platelet activation and secondly, blood must be collected into an anti-coagulant that will not only prevent coagulation, but preserve the activation status of platelets until they have been analysed (or more specifically, until platelets have been removed by differential ultra-centrifugation). Interestingly, EDTA, citrate and hirudin anti-coagulants are not able to suppress total platelet activation and the extent to which pre-analytical activation occurs is markedly dependent on the anticoagulant used. Future efforts should harmonise current practices in pre-analytical isolation protocols. Recently, Koshiar *et al,* (351) used corn-trypsin inhibitor coupled with tri-sodium citrate as an anti-coagulant medium prior to differential ultra-centrifugation. Corn-tripsin inhibitor – trisodium citrate - has been shown to inhibit platelet activation until analysis. Although only erythrocyte-derived MPs were assessed in their study, future studies should assess and compare such pre-analytical protocols.

Although MP concentration was significantly associated with thrombin generation potential (shown in chapter 6), the clinical implications of an elevated annexin V positive MP population remain untested. In addition to a prospective follow-up study in these patients, future studies could determine the physiological effects of these MPs on isolated vessels (myography).

Additionally, *in vitro* experiments were predominantly carried out using HECV cells. Future studies should use primary cells and compare the effect of pathologically relevant insults to established positive controls such as TNFα, which has been shown to induce expression of surface adhesion molecules in HUVECs.

Future studies should also study the biological action of MPs on target cells/vessels. This thesis showed that MPs interact and appear to internalise as intact MPs. Although it is likely to be MP and cell specific, it remains unclear whether MPs fuse with target cells and offload their bioactive cargo or whether MPs mediate biological changes via surface/phospholipid interaction. Specifically, future studies should test if PS or specific surface adhesion molecules (e.g. P-selectin) mediate MP-target cell interactions. The pre-treatment of vessels with MPs would provide evidence for their effect on endothelial function as well as an insight into modes of action.

To a large extent the focus continues to be on the detrimental effects of MPs, whereas in reality MP generation may represent a novel homeostatic response or signalling mechanism. In this sense MPs do indeed represent a biomarker of stress conditions, but could also be used beneficially if their function and role were understood and manipulated in a protective capacity. Indeed, this is already the case where mesenchymal stromal cell-derived MPs stimulated under hypoxic conditions are currently being trialled for the treatment of pulmonary hypertension (personal communication – Professor Stella Kourembanas, Harvard University Medical School).

Reference list

1. Mendis S, Puska P, Norrving B. Global atlas on cardiovascular disease prevention and control. World Health Organization, Geneva: 2011.
2. Colin D, Mathers DL. Projections of global mortality and burden of disease from 2002 to 2030. PLOS medicine. 2006;3(11):e442.
3. Fuster V, Kelly BB, Vedanthan R. Promoting global cardiovascular health: Moving forward. Circulation. 2011;123(15):1671-8.
4. Fuster VK. Promoting Cardiovascular Health in the Developing World: A critical challenge to achieve global health. Washington (DC): 2010.
5. Cubbin C, Hadden WC, Winkleby MA. Neighborhood context and cardiovascular disease risk factors: the contribution of material deprivation. Ethnicity and Disease. 2001;11(4):687-700.
6. Mozaffarian D, Benjamin EJ, Go AS, Arnett DK, Blaha MJ, Cushman M, de Ferranti S, Després J, Fullerton HJ, Howard VJ, Huffman MD, Judd SE, Kissela BM, Lackland DT, Lichtman JH, Lisabeth LD, Liu S, Mackey RH, Matchar DB, McGuire DK, Mohler ER 3rd, Moy CS, Muntner P, Mussolino ME, Nasir K, Neumar RW, Nichol G, Palaniappan L, Pandey DK, Reeves MJ, Rodriguez CJ, Sorlie PD, Stein J, Towfighi A, Turan TN, Virani SS, Willey JZ, Woo D, Yeh RW, Turner MB. Heart disease and stroke statistics—2014 update: A report from the American heart association. Circulation. 2014;129(3):28-292.
7. Townsend NW, Bhatnagar K, Smolina P, Nichol K, Leal SM, Luengo-Fernandez J, Rayner RM. Coronary heart disease statistics. London: 2012.
8. Vane JR, Änggård EE, Botting RM. Regulatory functions of the vascular endothelium. New England Journal of Medicine. 1990;323(1):27-36.
9. Pober JS, Sessa WC. Evolving functions of endothelial cells in inflammation. Nature Review Immunology. 2007;7(10):803-15.
10. Russo G, Leopold JA, Loscalzo J. Vasoactive substances: Nitric oxide and endothelial dysfunction in atherosclerosis. Vascular Pharmacology. 2002;38(5):259-69.
11. Orio F, Palomba S, Cascella T, De Simone B, Di Biase S, Russo T, et al. Early impairment of endothelial structure and function in young normal-weight women with polycystic ovary syndrome. Journal of Clinical Endocrinology & Metabolism. 2004;89(9):4588-93.
12. Abeywardena MY, Head RJ. Longchain n−3 polyunsaturated fatty acids and blood vessel function. Cardiovascular Research. 2001;52(3):361-71.
13. Verma S, Anderson TJ. Fundamentals of endothelial function for the clinical cardiologist. circulation. 2002;105(5):546-9.
14. Cines DB, Pollak ES, Buck CA, Loscalzo J, Zimmerman GA, McEver RA, Pober JS, Wick TM, Konkle BA, Schwartz BS, Barnathan ES, McCrae KR, Hug BA, Schmidt A, Stern DM. Endothelial cells in physiology and in the pathophysiology of vascular disorders. Blood. 1998;91(10):3527-61.
15. Deanfield JE, Halcox JP, Rabelink TJ. Endothelial function and dysfunction: testing and clinical relevance. Circulation. 2007;115(10):1285-95.
16. Galle J, Quaschning T, Seibold S, Wanner C. Endothelial dysfunction and inflammation: What is the link? Kidney International. 2003;63(84):45-S9.
17. Davignon J, Ganz P. Role of Endothelial dysfunction in atherosclerosis. Circulation. 2004;109(23):327-332.
18. Kawashima S, Yokoyama M. Dysfunction of endothelial nitric oxide synthase and atherosclerosis. Arteriosclerosis, Thrombosis, and Vascular Biology. 2004;24(6):998-1005.
19. Nathan C, Xie Q-w. Nitric oxide synthases: Roles, tolls, and controls. Cell. 1994;78(6):915-918.

20. Förstermann U, Münzel T. Endothelial nitric oxide synthase in vascular disease: from marvel to menace. Circulation. 2006;113(13):1708-14.
21. Iwata M, Suzuki S, Asai Y, Inoue T, Takagi K. Involvement of nitric oxide in a rat model of carrageenin-induced pleurisy. Mediators of Inflammation. 2010.
22. Rang HP DM, Ritter JM, Moore PK. Pharmacology. London: 2003.
23. Yang J, Clark JW, Bryan RM, Robertson CS. Mathematical modeling of the nitric oxide/cGMP pathway in the vascular smooth muscle cell. American Journal of Physiology. 2005;289(2):886-97.
24. Lundberg JO, Weitzberg E, Gladwin MT. The nitrate-nitrite-nitric oxide pathway in physiology and therapeutics. Nature Reviews Drug Discovery. 2008;7(2):156-67.
25. Allen JD, Gow AJ. Nitrite, NO and hypoxic vasodilation. British Journal of Pharmacology. 2009;158(7):1653-4.
26. Duranski MR, Greer JJ, Dejam A, Jaganmohan S, Hogg N, Langston W, Patel RP, Yet SF, Wang X, Kevil CG, Gladwin MT, Lefer DJ. Cytoprotective effects of nitrite during in vivo ischemia-reperfusion of the heart and liver. Journal of Clinical Investigation. 2005;115(5):1232-40.
27. Furchgott RF, Bhadrakom S. Reactions of strips of rabbit aorta to epinephrine, isopropylarterenol, sodium nitrite and other drugs. Journal of Pharmacology and Experimental Therapeutics. 1953;108(2):129-43.
28. Pinder AG, Khalatbari A, Ingram TE, James PE. The measurement of nitric oxide and its metabolites in biological samples by ozone-based chemiluminescence. Methods in Molecular Biology. 2009;476:10-27.
29. Willis GR, Udiawar M, Evans WD, Blundell HL, James PE, Rees DA. Detailed characterisation of circulatory nitric oxide and free radical indices—is there evidence for abnormal cardiovascular homeostasis in young women with polycystic ovary syndrome? BJOG: An International Journal of Obstetrics & Gynaecology. 2014;121(13):1596-603.
30. Ingram TE, Fraser AG, Bleasdale RA, Ellins EA, Margulescu AD, Halcox JP, James PE. Low-dose sodium nitrite attenuates myocardial ischemia and vascular ischemia-reperfusion injury in human models. Journal of the American College of Cardiology. 2013;61(25):2534-41.
31. Modin A, Björne H, Herulf M, Alving K, Weitzberg E, Lundberg JON. Nitrite-derived nitric oxide: a possible mediator of 'acidic–metabolic' vasodilation. Acta Physiologica Scandinavica. 2001;171(1):9-16.
32. Gladwin MT, Shelhamer JH, Schechter AN, Pease-Fye ME, Waclawiw MA, Panza JA, Waclawiw MA, Panza JA, Ognibene FP, Cannon RO. Role of circulating nitrite and S-nitrosohemoglobin in the regulation of regional blood flow in humans. Proceedings of the National Academy of Sciences of the United States of America. 2000;97(21):11482-7.
33. Muggeridge DJ, Sculthorpe N, Grace FM, Willis G, Thornhill L, Weller RB, James PE, Easton C. Acute whole body UVA irradiation combined with nitrate ingestion enhances time trial performance in trained cyclists. Nitric Oxide. 2014.
34. Ysart G, Miller P, Barrett G, Farrington D, Lawrance P, Harrison N. Dietary exposures to nitrate in the UK. Food Additives & Contaminants. 1999;16(12):521-32.
35. Kapil V, Weitzberg E, Lundberg JO, Ahluwalia A. Clinical evidence demonstrating the utility of inorganic nitrate in cardiovascular health. Nitric Oxide. 2014;38(0):45-57.
36. Kapil V, Haydar SMA, Pearl V, Lundberg JO, Weitzberg E, Ahluwalia A. Physiological role for nitrate-reducing oral bacteria in blood pressure control. Free Radical Biology & Medicine. 2013;55(C):93-100.
37. Sobko T, Reinders CI, Jansson EÅ, Norin E, Midtvedt T, Lundberg JO. Gastrointestinal bacteria generate nitric oxide from nitrate and nitrite. Nitric Oxide. 2005;13(4):272-8.
38. Wylie LJ, Kelly J, Bailey SJ, Blackwell JR, Skiba PF, Winyard PG, Jeukendrup AE, Vanhatalo A, Jones AM. Beetroot juice and exercise: pharmacodynamic and dose-response relationships. Journal of Applied Physiology. 2013;1;115(3):325-36.
39. Larsen FJ, Ekblom B, Sahlin K, Lundberg JO, Weitzberg E. Effects of dietary nitrate on blood pressure in healthy volunteers. New England Journal of Medicine. 2006;355(26):2792-3.

40. Webb AJ, Patel N, Loukogeorgakis S, Okorie M, Aboud Z, Misra S, Miall P, Deanfield J, Benjamin N, MacAllister R, Hobbs AJ, Ahluwalia A. Acute Blood Pressure Lowering, Vasoprotective, and Antiplatelet Properties of Dietary Nitrate via Bioconversion to Nitrite. Hypertension. 2008;51(3):784-90.
41. Kleinbongard P, Dejam A, Lauer T, Jax T, Kerber S, Gharini P, Balzer J, Zotz RB, Scharf RE, Willers R, Schechter AN, Feelisch M, Kelm M. Plasma nitrite concentrations reflect the degree of endothelial dysfunction in humans. Free Radical Biology and Medicine. 2006;40(2):295-302.
42. Goldstein S, Merényi G. The chemistry of peroxynitrite: implications for biological activity. Methods enzymology. 2008;436:49-61.
43. 43. Förstermann U, Kleinert H. Nitric oxide synthase: expression and expressional control of the three isoforms. Naunyn-Schmiedeberg's Archives of Pharmacology. 1995;352(4):351-64.
44. 44. Rubbo H, O'Donnell V. Nitric oxide, peroxynitrite and lipoxygenase in atherogenesis: mechanistic insights. Toxicology. 2005;208(2):305-17.
45. Virdis A, Ghiadoni L, Pinto S, Lombardo M, Petraglia F, Gennazzani A, Buralli S. Mechanisms responsible for endothelial dysfunction associated with acute estrogen deprivation in normotensive women. Circulation. 2000;101(19):2258-63.
46. 46. Rogers SC, Khalatbari A, Datta BN, Ellery S, Paul V, Frenneaux MP, James PE. NO metabolite flux across the human coronary circulation. Cardiovascular Research. 2007;75: 434-41.
47. Lawrence T, Willoughby DA, Gilroy DW. Anti-inflammatory lipid mediators and insights into the resolution of inflammation. Nature Reviews Immunology. 2002;2(10):787-95.
48. Cai H, Harrison DG. Endothelial dysfunction in cardiovascular diseases: the role of oxidant stress. Circulation Research. 2000;87(10):840-4.
49. Montezano AC, Touyz RM. Reactive oxygen species and endothelial function – role of nitric oxide synthase uncoupling and nox family nicotinamide adenine dinucleotide phosphate oxidases. Basic & Clinical Pharmacology & Toxicology. 2012;110(1):87-94.
50. Tsutsui H, Kinugawa S, Matsushima S. Oxidative stress and heart failure. American Journal of Physiology. 2011;301(6):2181-90.
51. Xu S, Chamseddine AH, Carrell S, Miller FJ. Nox4 NADPH oxidase contributes to smooth muscle cell phenotypes associated with unstable atherosclerotic plaques. Redox Biology. 2014;2:642-50.
52. Ushio-Fukai M, Zafari AM, Fukui T, Ishizaka N, Griendling KK. P22phox is a critical component of the superoxide-generating nadh/nadph oxidase system and regulates angiotensin ii induced hypertrophy in vascular smooth muscle cells. Journal of Biological Chemistry. 1996;271(38):23317-21.
53. Kunsch C, Medford RM. Oxidative stress as a regulator of gene expression in the vasculature. Circulation Research. 1999;85(8):753-66.
54. Li H, Cybulsky MI, Gimbrone MA, Libby P. An atherogenic diet rapidly induces VCAM-1, a cytokine-regulatable mononuclear leukocyte adhesion molecule, in rabbit aortic endothelium. Arteriosclerosis, Thrombosis, and Vascular Biology. 1993;13(2):197-204.
55. Cardillo C, Kilcoyne CM, Cannon RO, Quyyumi AA, Panza JA. Xanthine Oxidase Inhibition with oxypurinol improves endothelial vasodilator function in hypercholesterolemic but not in hypertensive patients. Hypertension. 1997;30(1):57-63.
56. Desco M-C, Asensi M, Márquez R, Martínez-Valls J, Vento M, Pallardó FV, et al. Xanthine Oxidase Is Involved in Free Radical Production in Type 1 Diabetes: Protection by Allopurinol. Diabetes. 2002;51(4):1118-24.
57. Ohara Y, Peterson TE, Harrison DG. Hypercholesterolemia increases endothelial superoxide anion production. Journal of Clinical Investigation. 1993;91(6):2546-51.
58. O'Driscoll JG, Green DJ, Rankin JM, Taylor RR. Nitric oxide-dependent endothelial function is unaffected by allopurinol in hypercholesterolaemic subjects. Clinical and Experimental Pharmacology and Physiology. 1999;26(10):779-83.

59. Sies H. Strategies of antioxidant defense. Springer. Berlin; 1994.
60. Engler MM, Engler MB, Malloy MJ, Chiu EY, Schloetter MC, Paul SM, Stuehlinger M, Lin KY, Cooke JP, Morrow JD, Ridker PM, Rifai N, Miller E, Witztum JL, Mietus-Snyder M. Antioxidant vitamins c and e improve endothelial function in children with hyperlipidemia: endothelial assessment of risk from lipids in youth (EARLY) trial. Circulation. 2003;108(9):1059-63.
61. Vivekananthan DP, Penn MS, Sapp SK, Hsu A, Topol EJ. Use of antioxidant vitamins for the prevention of cardiovascular disease: meta-analysis of randomised trials. The Lancet. 2003;361(9374):2017-23.
62. Steinhubl SR. Why have antioxidants failed in clinical trials? The American Journal of Cardiology. 2008;101(10):14-19.
63. Dröge W. Free radicals in the physiological control of cell function. Physiological Reviews. 2002;82(1):47-95.
64. Radák Z, Kaneko T, Tahara S, Nakamoto H, Ohno H, Sasvári M, Nyakas C., Goto S. The effect of exercise training on oxidative damage of lipids, proteins, and DNA in rat skeletal muscle: evidence for beneficial outcomes. Free Radical Biology and Medicine. 1999;27(1–2):69-74.
65. Ji LL, Gomez-Cabrera MC, Vina J. Exercise and hormesis. Annals of the New York Academy of Sciences. 2006;1067(1):425-35.
66. Ristow M, Zarse K, Oberbach A, Klöting N, Birringer M, Kiehntopf M, Stumvoll M, Kahn CR, Blüher M. Antioxidants prevent health-promoting effects of physical exercise in humans. Proceedings of the National Academy of Sciences of the United States of America. 2009;106(21):8665-70.
67. Ross R. Atherosclerosis — An inflammatory disease. New England Journal of Medicine. 1999;340(2):115-26.
68. Homburg R. Polycystic ovary syndrome. Best Practice; Research Clinical Obstetrics & Gynaecology. 2008;22(2):261-74.
69. Kahsar-Miller MD, Nixon C, Boots LR, Go RC, Azziz R. Prevalence of polycystic ovary syndrome (PCOS) in first-degree relatives of patients with PCOS. Fertility and Sterility.75(1):53-8.
70. San Millán JL, Botella-Carretero JI, Alvarez-Blasco F, Luque-Ramírez M, Sancho J, Moghetti P, Escobar-Morreale HF. A study of the hexose-6-phosphate dehydrogenase gene r453q and 11β-hydroxysteroid dehydrogenase type 1 gene 83557insA polymorphisms in the polycystic ovary syndrome. The Journal of Clinical Endocrinology & Metabolism. 2005;90(7):4157-62.
71. Ehrmann DA. Polycystic ovary syndrome. New England Journal of Medicine. 2005;352(12):1223-36.
72. Stein IF, Leventhal LM. Amenorrhea associated with bilateral polycystic ovaries. Am J Obstet Gynecol. 1935;29:181-91.
73. Carmina E. Diagnosis of polycystic ovary syndrome: from NIH criteria to ESHRE-ASRM guidelines. Minerva Ginecol. 2004;56(1):1-6.
74. Frank S. Diagnosis of polycystic ovarian syndrome: in defense of the rotterdam criteria. The Journal of Clinical Endocrinology & Metabolism. 2006;91(3):786-9.
75. Azziz R, Carmina E, Dewailly D, Diamanti-Kandarakis E, Escobar-Morreale HF, Futterweit W, Janssen OE, Legro RS, Norman RS, Taylor AE, Witchel SF. The Androgen Excess and PCOS Society criteria for the polycystic ovary syndrome: the complete task force report. Fertility and Sterility. 2009;91(2):456-88.
76. Wild RA, Carmina E, Diamanti-Kandarakis E, Dokras A, Escobar-Morreale HF, Futterweit W, Lobo R, Norman RJ, Talbott E, Dumesic DA. Assessment of cardiovascular risk and prevention of cardiovascular disease in women with the polycystic ovary syndrome: a consensus statement by the Androgen Excess and Polycystic Ovary Syndrome (AE-PCOS) Society. The Journal of Clinical Endocrinology & Metabolism. 2010;95(5):2038-49.
77. Sam S. Obesity and Polycystic Ovary Syndrome. Obesity management. 2007;3(2):69-73.

78. Sampson M, Kong C, Patel A, Unwin R, Jacobs HS. Ambulatory blood pressure profiles and plasminogen activator inhibitor (PAI-1) activity in lean women with and without the polycystic ovary syndrome. Clinical Endocrinology. 1996;45(5):623-9.
79. Talbott E, Guzick D, Clerici A, Berga S, Detre K, Weimer K, Kuller L. Coronary heart disease risk factors in women with polycystic ovary syndrome. Arteriosclerosis, Thrombosis, and Vascular Biology. 1995;15(7):821-6.
80. Ehrmann DA, Sturis J, Byrne MM, Karrison T, Rosenfield RL, Polonsky KS. Insulin secretory defects in polycystic ovary syndrome. Relationship to insulin sensitivity and family history of non-insulin-dependent diabetes mellitus. The Journal of Clinical Investigation. 1995;96(1):520-7.
81. Bentley-Lewis R, Seely E, Dunaif A. Ovarian Hypertension: Polycystic ovary syndrome. endocrinology and metabolism clinics of North America. 2011;40(2):433-99.
82. Holte J, Gennarelli G, Berne C, Bergh T, Lithell H. Elevated ambulatory day-time blood pressure in women with polycystic ovary syndrome: a sign of a pre-hypertensive state? Human Reproduction. 1996;11(1):23-8.
83. Elting MW, Korsen TJM, Bezemer PD, Schoemaker J. Prevalence of diabetes mellitus, hypertension and cardiac complaints in a follow-up study of a Dutch PCOS population. Human Reproduction. 2001;16(3):556-60.
84. Polycystic ovary syndrome: lack of hypertension despite profound insulin resistance. The Journal of Clinical Endocrinology & Metabolism. 1992;75(2):508-13.
85. Wild SP, Pierpoint T, Jacobs H, McKeigue P. Long-term consequences of polycystic ovary syndrome: results of a 31 year follow-up study. Human Fertility. 2000;3(2):101-5.
86. Luque-Ramírez M, Mendieta-Azcona C, Álvarez-Blasco F, Escobar-Morreale HF. Androgen excess is associated with the increased carotid intima-media thickness observed in young women with polycystic ovary syndrome. Human Reproduction. 2007;22(12):3197-203.
87. Lundberg C, Hansen T, Ahlström H, Lind L, Wikström J, Johansson L. The relationship between carotid intima–media thickness and global atherosclerosis. Clinical Physiology and Functional Imaging. 2014;34(6):457-62.
88. Third report of the National Cholesterol Education Program (NCEP) expert panel on detection, evaluation, and treatment of high blood cholesterol in adults (Adult Treatment Panel III) final report. Circulation. 2002;106(25):3143.
89. Wild RA, Rizzo M, Clifton S, Carmina E. Lipid levels in polycystic ovary syndrome: systematic review and meta-analysis. Fertility and Sterility. 2011;95(3):1073-9.
90. Essah PA, Nestler JE, Carmina E. Differences in dyslipidemia between American and Italian women with polycystic ovary syndrome. Journal of Endocrinological Investigation. 2008;31(1):35-41.
91. Carmina E, Legro RS, Stamets K, Lowell J, Lobo RA. Difference in body weight between American and Italian women with polycystic ovary syndrome: influence of the diet. Human Reproduction. 2003;18(11):2289-93.
92. Wild RA. Dyslipidemia in PCOS. Steroids. 2012;77(4):295-9.
93. Roith DL. Current therapeutic algorithms for type 2 diabetes. Clinical Cornerstone. 2001;4(2):38-49.
94. Burghen GA, Givens JR, Kitabchi AE. Correlation of hyperandrogenism with hyperinsulinism in polycystic ovarian disease. The Journal of Clinical Endocrinology & Metabolism. 1980;50(1):113-6.
95. Metabolic features of polycystic ovary syndrome are found in adolescent girls with hyperandrogenism. The Journal of Clinical Endocrinology & Metabolism. 1995;80(10):2966-73.
96. Rees E, Coulson R, Dunstan F, Evans WD, Blundell HL, Luzio SD, Dunseath G, Halcox JP, Fraser AG, Rees DA. Central arterial stiffness and diastolic dysfunction are associated with insulin resistance and abdominal obesity in young women but polycystic ovary syndrome does not confer additional risk. Human Reproduction. 2014;29(9):2041-9.

97. Dunaif A, Segal KR, Futterweit W, Dobrjansky A. Profound Peripheral Insulin Resistance, Independent of Obesity, in Polycystic Ovary Syndrome. Diabetes. 1989;38(9):1165-74.
98. Carmina E, Koyama T, Chang L, Stanczyk FZ, Lobo RA. Does ethnicity influence the prevalence of adrenal hyperandrogenism and insulin resistance in polycystic ovary syndrome? American Journal of Obstetrics and Gynecology. 1992;167(6):1807-12.
99. Legro RS, Kunselman AR, Dodson WC, Dunaif A. Prevalence and predictors of risk for type 2 diabetes mellitus and impaired glucose tolerance in polycystic ovary syndrome: a prospective, controlled study in 254 affected women. Journal of Clinical Endocrinology & Metabolism. 1999;84(1):165-9.
100. Legro IS, Finegood D, Dunaif A. A fasting glucose to insulin ratio is a useful measure of insulin sensitivity in women with polycystic ovary syndrome. The Journal of Clinical Endocrinology & Metabolism. 1998;83(8):2694-8.
101. Legro RS. Polycystic ovary syndrome and cardiovascular disease: a premature association? Endocrine Reviews. 2003;24(3):302-12.
102. Christakou C, Diamanti-Kandarakis E. Structural, biochemical and non-traditional cardiovascular risk markers in PCOS. Current Pharmaceutical Design. 2013;19(32):5764-74.
103. Diamanti-Kandarakis E. Insulin resistance in PCOS. Endocrinolgy. 2006;30(1):13-7.
104. Dunaif A, Xia J, Book CB, Schenker E, Tang Z. Excessive insulin receptor serine phosphorylation in cultured fibroblasts and in skeletal muscle. A potential mechanism for insulin resistance in the polycystic ovary syndrome. Journal of Clinical Investigation. 1995;96(2):801-10.
105. Rosenbaum D HR, Dunaif A. Insulin resistance in polycystic ovary syndrome: decreased expression of GLUT-4 glucose transporters in adipocytes. American Journal of Physiology. 1993;264(2):197-202.
106. Nestler JE. Insulin regulation of human ovarian androgens. Human Reproduction. 1997;12:53-62.
107. Kelly C, Speirs A, Gould G, Petrie J, Lyall H, Connell J. Altered vascular function in young women with polycystic ovary syndrome. The Journal of Clinical Endocrinology & Metabolism. 2002;87(2):742-6.
108. Carmina E, Orio F, Palomba S, Longo RA, Cascella T, Colao A, Lombardi G, Rini GB, Lobo RA. Endothelial dysfunction in PCOS: role of obesity and adipose hormones. The American Journal of Medicine. 2006;119(4):356-62.
109. González F, Rote NS, Minium J, Kirwan JP. Evidence of proatherogenic inflammation in polycystic ovary syndrome. Metabolism: clinical and experimental. 2009;58(7):954-62.
110. Diamanti-Kandarakis E, Paterakis T, Alexandraki K, Piperi C, Aessopos A, Katsikis I, Katsilambros N, Kreatsas G, Panidis D. Indices of low-grade chronic inflammation in polycystic ovary syndrome and the beneficial effect of metformin. Human Reproduction. 2006;21(6):1426-31.
111. Tarkun İ, Arslan BnÇ, Cantürk Z, Türemen E, Şahin T, Duman C. Endothelial dysfunction in young women with polycystic ovary syndrome: relationship with insulin resistance and low-grade chronic inflammation. The Journal of Clinical Endocrinology & Metabolism. 2004;89(11):5592-6.
112. Nestler JE, Jakubowicz DJ, Evans WS, Pasquali R. Effects of metformin on spontaneous and clomiphene-induced ovulation in the polycystic ovary syndrome. New England Journal of Medicine. 1998;338(26):1876-80.
113. Mattu HS, Randeva HS. Role of adipokines in cardiovascular disease. Journal of Endocrinology. 2013;2(216):17-36.
114. Galic S, Oakhill JS, Steinberg GR. Adipose tissue as an endocrine organ. The Journal of Clinical Endocrinology & Metabolism. 2004;89(6):2548-56.
115. Huxley R, Mendis S, Zheleznyakov E, Reddy S, Chan J. Body mass index, waist circumference and waist:hip ratio as predictors of cardiovascular risk: A review of the literature. European Journal of Clinical Nutrition. 2009;64(1):16-22.

116. Matsuzawa Y, Nakamura T, Shimomura I, Kotani K. Visceral fat accumulation and cardiovascular disease. Obesity Research. 1995;3(S5):645-7.
117. Rosito GA, Massaro JM, Hoffmann U, Ruberg FL, Mahabadi AA, Vasan RS, O'Donnell CJ, Fox CS. Pericardial fat, visceral abdominal fat, cardiovascular disease risk factors, and vascular calcification in a community-based sample: The Framingham Heart Study. Circulation. 2008;117(5):605-13.
118. Panagiotakos DB, Pitsavos C, Yannakoulia M, Chrysohoou C, Stefanadis C. The implication of obesity and central fat on markers of chronic inflammation: The ATTICA study. Atherosclerosis. 2005;183(2):308-15.
119. Cascella T, Palomba S, De Sio I, Manguso F, Giallauria F, De Simone B, Tafuri D, Lombardi G, Colao A, Orio F. Visceral fat is associated with cardiovascular risk in women with polycystic ovary syndrome. Human Reproduction. 2008;23(1):153-9.
120. Kawamoto R, Kajiwara T, Oka Y, Takagi Y. Association between abdominal wall fat index and carotid atherosclerosis in women. Journal of Atherosclerosis and Thrombosis. 2002;9(5):213-8.
121. Liu KH, Chan YL, Chan JCN, Chan WB. Association of carotid intima-media thickness with mesenteric, preperitoneal and subcutaneous fat thickness. Atherosclerosis. 2005;179(2):299-304.
122. Clark AM, Ledger W, Galletly C, Tomlinson L, Blaney F, Wang X, Norman RJ. Weight loss results in significant improvement in pregnancy and ovulation rates in anovulatory obese women. Human Reproduction. 1995;10(10):2705-12.
123. Van Gaal LF, Mertens IL, De Block CE. Mechanisms linking obesity with cardiovascular disease. Nature. 2006;444(7121):875-80.
124. Sprung VS, Cuthbertson DJ, Pugh CJA, Daousi C, Atkinson G, Aziz NF, et al. Nitric oxide-mediated cutaneous microvascular function is impaired in polycystic ovary sydrome but can be improved by exercise training. The Journal of Physiology. 2013;591(6):1475-87.
125. Mather KJ, Verma S, Corenblum B, Anderson TJ. Normal endothelial function despite insulin resistance in healthy women with the polycystic ovary syndrome. The Journal of Clinical Endocrinology & Metabolism. 2000;85(5):1851-6.
126. Paradisi G, Steinberg HO, Hempfling A, Cronin J, Hook G, Shepard MK, Baron AD. Polycystic ovary syndrome is associated with endothelial dysfunction. Circulation. 2001;103(10):1410-5.
127. Worboys S, Kotsopoulos D, Teede H, McGrath B, Davis SR. Evidence That Parenteral Testosterone Therapy may improve endothelium-dependent and -independent vasodilation in postmenopausal women already receiving estrogen. The Journal of Clinical Endocrinology & Metabolism. 2001;86(1):158-61.
128. Paradisi G, Steinberg HO, Shepard MK, Hook G, Baron AD. Troglitazone therapy improves endothelial function to near normal levels in women with polycystic ovary syndrome. The Journal of Clinical Endocrinology & Metabolism. 2003;88(2):576-80.
129. Tarkun İ, Çetinarslan B, Türemen E, Şahin T, Cantürk Z, Komsuoğlu B. Effect of rosiglitazone on insulin resistance, C-reactive protein and endothelial function in non-obese young women with polycystic ovary syndrome. European Journal of Endocrinology. 2005;153(1):115-21.
130. Diamanti-Kandarakis E, Alexandraki K, Protogerou A, Piperi C, Papamichael C, Aessopos A, Lekakis J, Mavrikakis M. Metformin administration improves endothelial function in women with polycystic ovary syndrome. European Journal of Endocrinology. 2005;152(5):749-56.
131. Agarwal N, Rice SP, Bolusani H, Luzio SD, Dunseath G, Ludgate M, Rees DA. Metformin reduces arterial stiffness and improves endothelial function in young women with polycystic ovary syndrome: A randomized, placebo-controlled, crossover trial. The Journal of Clinical Endocrinology & Metabolism. 2010;95(2):722-30.
132. Naka KK, Kalantaridou SN, Kazakos N, Katsouras CS, Makrigiannakis A, Paraskevaidis EA, Chrousos GP, Tsatsoulis A, Michalis LK. Predictors of endothelial dysfunction in

young women with polycystic ovary syndrome. The Journal of Clinical Endocrinology & Metabolism. 2005;90(9):5088-95.
133. Rajendran S, Willoughby SR, Chan WP, Liberts EA, Heresztyn T, Saha M, Marber MS, Norman RJ, Horowitz JD. Polycystic ovary syndrome is associated with severe platelet and endothelial dysfunction in both obese and lean subjects. Atherosclerosis. 2009;204(2):509-14.
134. Sorensen MB, Franks S, Robertson C, Pennell DJ, Collins P. Severe endothelial dysfunction in young women with polycystic ovary syndrome is only partially explained by known cardiovascular risk factors. Clinical Endocrinology. 2006;65(5):655-9.
135. Meyer C, McGrath BP, Cameron J, Kotsopoulos D, Teede HJ. Vascular dysfunction and metabolic parameters in polycystic ovary syndrome. The Journal of Clinical Endocrinology & Metabolism. 2005;90(8):4630-5.
136. Diamanti-Kandarakis E, Alexandraki K, Piperi C, Protogerou A, Katsikis I, Paterakis T, Lekakis J, Panidis D. Inflammatory and endothelial markers in women with polycystic ovary syndrome. European Journal of Clinical Investigation. 2006;36(10):691-7.
137. Mohamadin AM, Habib FA, Al-Saggaf AA. Cardiovascular disease markers in women with polycystic ovary syndrome with emphasis on asymmetric dimethylarginine and homocysteine. Annals of Saudi Medicine. 2010;30(4):278-83.
138. Nácul AP, Andrade CD, Schwarz P, Bittencourt PIH, Spritzer PM. Nitric oxide and fibrinogen in polycystic ovary syndrome: Associations with insulin resistance and obesity. European Journal of Obstetrics & Gynecology and Reproductive Biology. 2007;133(2):191-6.
139. Kuşçu NK, Var A. Oxidative stress but not endothelial dysfunction exists in non-obese, young group of patients with polycystic ovary syndrome. Acta Obstetricia et Gynecologica Scandinavica. 2009;88(5):612-7.
140. Dursun E, Akalın FA, Güncü GN, Çınar N, Aksoy DY, Tözüm TF, Kılınc K, Yıldız BO. Periodontal disease in polycystic ovary syndrome. Fertility and Sterility. 2011;95(1):320-3.
141. Türkçüoğlu I, Engin-Üstün Y, Turan F, Kali Z, Karabulut A, Meydanli M, Kafkasli A. Evaluation of asymmetric dimethylarginine, nitric oxide levels and associated independent variables in obese and lean patients with polycystic ovarian syndrome. Gynecological Endocrinology. 2011;27:609-14.
142. Baskol G, Aygen E, Erdem F, Caniklioğlu A, Narin F, Sahin Y, Kaya T. Assessment of paraoxonase 1, xanthine oxidase and glutathione peroxidase activities, nitric oxide and thiol levels in women with polycystic ovary syndrome. Acta Obstetricia et Gynecologica Scandinavica. 2012;91(3):326-30.
143. Bayram F, Kocer D, Ozsan M, Muhtaroglu S. Evaluation of endothelial dysfunction, lipid metabolism in women with polycystic ovary syndrome: relationship of paraoxonase 1 activity, malondialdehyde levels, low-density lipoprotein subfractions, and endothelial dysfunction. Gynecological Endocrinology. 2012;28(7):497-501.
144. Bailey DM, Davies B, Young IS, Jackson MJ, Davison GW, Isaacson R, Isaacson R, Richardson RS. EPR spectroscopic detection of free radical outflow from an isolated muscle bed in exercising humans. Journal of applied physiology. 2003;94(5):1714-8.
145. Murri M, Luque-Ramírez M, Insenser M, Ojeda-Ojeda M, Escobar-Morreale HF. Circulating markers of oxidative stress and polycystic ovary syndrome (PCOS): a systematic review and meta-analysis. Human Reproduction Update. 2013.
146. Sabuncu T, Vural Hs, Harma Mg, Harma M. Oxidative stress in polycystic ovary syndrome and its contribution to the risk of cardiovascular disease. Clinical Biochemistry. 2001;34(5):407-13.
147. González F, Rote NS, Minium J, Kirwan JP. Reactive oxygen species-induced oxidative stress in the development of insulin resistance and hyperandrogenism in polycystic ovary syndrome. The Journal of Clinical Endocrinology & Metabolism. 2006;91(1):336-40.
148. Macut D ST, Lissounov A, Pljesa-Ercegovac M, Bozic I, Djukic T, Bjekic-Macut J, Matic M, Petakov M, Suvakov S. Insulin resistance in non-obese women with polycystic

ovary syndrome: relation to byproducts of oxidative stress. Experimental Clinical Endocrinology and Diabetes. 2011;119(7):451-5.
149. Kurdoglu Z, Ozkol H, Tuluce Y, Koyuncu I. Oxidative status and its relation with insulin resistance in young non-obese women with polycystic ovary syndrome. Journal of Endocrinological Investigation. 2012;35(3):317-21.
150. Mohan SKP. Lipid peroxidation, glutathione, ascorbic acid, vitamin E, antioxidant enzyme and serum homocysteine status in patients with polycystic ovary syndrome. Biology and Medicine. 2009;l1(3):44-9.
151. Fenkci V, Fenkci S, Yilmazer M, Serteser M. Decreased total antioxidant status and increased oxidative stress in women with polycystic ovary syndrome may contribute to the risk of cardiovascular disease. Fertility and Sterility. 2003;80(1):123-7.
152. Solomon CG, Hu FB, Dunaif A, Rich-Edwards JE, Stampfer MJ, Willett WC, Speizer FE, Manson JE. Menstrual cycle irregularity and risk for future cardiovascular disease. Journal of Clinical Endocrinology and Metabolism. 2002; 87(5):2013-7.
153. Morgan CL, Jenkins-Jones S, Currie CJ, Rees DA. Evaluation of adverse outcome in young women with polycystic ovary syndrome versus matched, reference controls: A Retrospective, observational study. Journal of Clinical Endocrinology & Metabolism. 2012;97(9):3251-60.
154. van der Pol E, Böing AN, Harrison P, Sturk A, Nieuwland R. Classification, functions, and clinical relevance of extracellular vesicles. Pharmacological Reviews. 2012;64(3):676-705.
155. Chargaff E, West R. The biological significance of the thromboplastic protein of blood. Journal of Biological Chemistry. 1946;166(1):189-97.
156. Wolf P. The Nature and Significance of Platelet Products in Human Plasma. British Journal of Haematology. 1967;13(3):269-88.
157. VanWijk MJ, VanBavel E, Sturk A, Nieuwland R. Microparticles in cardiovascular diseases. Journal of Clinical Endocrinology and Metabolism. 2006;91(1):336-40.
158. Iero M, Valenti R, Huber V, Filipazzi P, Parmiani G, Fais S, Rivoltini L. Tumour-released exosomes and their implications in cancer immunity. Cell Death Differ. 2007;15(1):80-8.
159. Théry C, Boussac M, Véron P, Ricciardi-Castagnoli P, Raposo G, Garin J, Amigorena S. Proteomic Analysis of dendritic cell-derived exosomes: A secreted subcellular compartment distinct from apoptotic vesicles. The Journal of Immunology. 2001;166(12):7309-18.
160. 159. Trajkovic K, Hsu C, Chiantia S, Rajendran L, Wenzel D, Wieland F, Schwille P, Brügger B, Simons M. Ceramide triggers budding of exosome vesicles into multivesicular endosomes. Science. 2008;319(5867):1244-7.
161. Bobrie A, Colombo M, Raposo G, Théry C. Exosome secretion: Molecular mechanisms and roles in immune responses. Traffic. 2011;12(12):1659-68.
162. Buschow SI, Nolte-‘t Hoen ENM, Van Niel G, Pols MS, Ten Broeke T, Lauwen M, Ossendorp F, Melief CJ, Raposo G, Wubbolts R, Wauben MH, Stoorvogel W. MHC II in dendritic cells is targeted to lysosomes or t cell-induced exosomes via distinct multivesicular body pathways. Traffic. 2009;10(10):1528-42.
163. Savina A, Vidal M, Colombo MI. The exosome pathway in K562 cells is regulated by Rab11. Journal of Cell Science. 2002;115(12):2505-15.
164. 1Rao SK, Huynh C, Proux-Gillardeaux V, Galli T, Andrews NW. Identification of SNAREs Involved in synaptotagmin VII-regulated lysosomal exocytosis. Journal of Biological Chemistry. 2004;279(19):20471-9.
165. Bitbol M, Devaux PF. Measurement of outward translocation of phospholipids across human erythrocyte membrane. Proceedings of the National Academy of Sciences. 1988;85(18):6783-7.
166. Bevers EM, Comfurius P, Dekkers DWC, Zwaal RFA. Lipid translocation across the plasma membrane of mammalian cells. Biochimica et Biophysica Acta (BBA) - Molecular and Cell Biology of Lipids. 1999;1439(3):317-30.

167. Dignat-George F, Boulanger CM. The many faces of endothelial microparticles. Arteriosclerosis, Thrombosis, and Vascular Biology. 2011;31(1):27-33.
168. Morel O, Jesel L, Freyssinet J-M, Toti F. Cellular mechanisms underlying the formation of circulating microparticles. Arteriosclerosis, Thrombosis, and Vascular Biology. 2011;31(1):15-26.
169. Burger D, Schock S, Thompson CS, Montezano AC, Hakim AM, Touyz RM. Microparticles: biomarkers and beyond. Clinical Science. 2013;124:423-41.
170. Yano Y, Shiba E, Kambayashi J-i, Sakon M, Kawasaki T, Fujitani K, Kang J, Mori T. The effects of calpeptin (a calpain specific inhibitor) on agonist induced microparticle formation from the platelet plasma membrane. Thrombosis Research. 1993;71(5):385-96.
171. Wiedmer T, Esmon CT, Sims PJ. On the mechanism by which complement proteins C5b-9 increase platelet prothrombinase activity. Journal of Biological Chemistry. 1986;261(31):14587-92.
172. Gemmell CH, Sefton MV, Yeo EL. Platelet-derived microparticle formation involves glycoprotein IIb-IIIa. Inhibition by RGDS and a Glanzmann's thrombasthenia defect. Journal of Biological Chemistry. 1993;268(20):14586-9.
173. Sebbagh M, Renvoize C, Hamelin J, Riche N, Bertoglio J, Breard J. Caspase-3-mediated cleavage of ROCK I induces MLC phosphorylation and apoptotic membrane blebbing. Nat Cell Biol. 2001;3(4):346-52.
174. Sapet C, Simoncini S, Loriod B, Puthier D, Sampol J, Nguyen C, Dignat-George F, Anfosso F. Thrombin-induced endothelial microparticle generation: identification of a novel pathway involving ROCK-II activation by caspase. Blood. 2006;108(6):1868-76.
175. Tramontano AF, Lyubarova R, Tsiakos J, Palaia T, DeLeon JR, Ragolia L. Circulating Endothelial Microparticles in Diabetes Mellitus. Mediators of Inflammation. 2010.
176. Connor DE, Exner T, Ma DDF, Joseph JE. The majority of circulating platelet-derived microparticles fail to bind annexin V, lack phospholipid-dependent procoagulant activity and demonstrate greater expression of glycoprotein Ib. Thrombosis and Haemostasis. 2010;103(5):1044-52.
177. Fink K, Feldbrügge L, Schwarz M, Bourgeois N, Helbing T, Bode C, Schwab T, Busch HJ. Circulating annexin V positive microparticles in patients after successful cardiopulmonary resuscitation. Critical Care. 2011;15(5):251-264.
178. Harry FG, Heijnen AES, Fijnheer R, Geuze HJ, Sixma JJ. Activated Platelets Release Two Types of Membrane Vesicles: Microvesicles by Surface Shedding and Exosomes Derived From Exocytosis of Multivesicular Bodies and -Granules. Blood. 1999;94(11).
179. Meckes DG, Shair KHY, Marquitz AR, Kung C-P, Edwards RH, Raab-Traub N. Human tumor virus utilizes exosomes for intercellular communication. Proceedings of the National Academy of Sciences. 2010;107(47):20370-5.
180. Sinauridze EI, Kireev DA, Popenko NY, Pichugin AV, P Panteleev MA, Krymskaya OV, Ataullakhanov FI. Platelet microparticle membranes have 50- to 100-fold higher specific procoagulant activity than activated platelets. Thrombosis and Haemostasis. 2007;97(3):425-34.
181. Théry C, Amigorena S, Raposo G, Clayton A. Isolation and Characterization of Exosomes from Cell Culture Supernatants and Biological Fluids. Current Protocols in Cell Biology. 2006.
182. Webber J, Clayton A. How pure are your vesicles? Journal of Extracellular Vesicles. 2013;2:19861.
183. Böing AN, van der Pol E, Grootemaat AE, Coumans FAW, Sturk A, Nieuwland R. Single-step isolation of extracellular vesicles by size-exclusion chromatography. Journal of Extracellular Vesicles. 2014;3:10.
184. Aras O, Shet A, Bach RR, Hysjulien JL, Slungaard A, Hebbel RP, Escolar G, Jilma B, Key NS. Induction of microparticle- and cell-associated intravascular tissue factor in human endotoxemia. Blood. 2004;103(12):4545-53.
185. Nieuwland R, Berckmans RJ, Rotteveel-Eijkman RC, Maquelin KN, Roozendaal KJ, Jansen PG, ten Have K, Eijsman L, Hack CE, Sturk A. Cell-derived microparticles

generated in patients during cardiopulmonary bypass are highly procoagulant. Circulation. 1997;96(10):3534-41.
186. Koiou E, Tziomalos K, Katsikis I, Kalaitzakis E, Kandaraki EA, Tsourdi EA, Delkos D, Papadakis E, Panidis D. Circulating platelet-derived microparticles are elevated in women with polycystic ovary syndrome diagnosed with the 1990 criteria and correlate with serum testosterone levels. European Journal of Endocrinology. 2011;165(1):63-8.
187. Combes V, Simon AC, Grau GE, Arnoux D, Camoin L, Sabatier F, Mutin M, Sanmarco M, Sampol J, Dignat-George F. In vitro generation of endothelial microparticles and possible prothrombotic activity in patients with lupus anticoagulant. The Journal of Clinical Investigation. 1999;104(1):93-102.
188. Nieuwland R, Berckmans RJ, McGregor S, Böing AN, Romijn FP, Westendorp RG, Hack CE, Sturk A. Cellular origin and procoagulant properties of microparticles in meningococcal sepsis. Blood. 2000;95(3):930-5.
189. Ay C, Freyssinet J-M, Sailer T, Vormittag R, Pabinger I. Circulating procoagulant microparticles in patients with venous thromboembolism. Thrombosis Research. 2009;123(5):724-6.
190. Agouni A, Ducluzeau P-H, Benameur T, Faure S, Sladkova M, Duluc L, Leftheriotis G, Pechanova O, Delibegovic M, Martinez MC, Andriantsitohaina R. Microparticles from patients with metabolic syndrome induce vascular hypo-reactivity via fas/fas-ligand pathway in mice. PLoS ONE. 2011;6(11).
191. Boulanger CM, Scoazec A, Ebrahimian T, Henry P, Mathieu E, Tedgui A, Mallat Z. Circulating microparticles from patients with myocardial infarction cause endothelial dysfunction. Circulation. 2001;104(22):2649-52.
192. Mezentsev A, Merks RM, O'Riordan E, Chen J, Mendelev N, Goligorsky MS, Brodsky SV. Endothelial microparticles affect angiogenesis in vitro: role of oxidative stress. Amewrican Journal of Physiology. 2005;289(3):1106-14.
193. King HW, Michael MZ, Gleadle JM. Hypoxic enhancement of exosome release by breast cancer cells. BMC Cancer. 2012;12:421-.
194. Mobarrez F, Antovic J, Egberg N, Hansson M, Jörneskog G, Hultenby K, Wallén H. A multicolor flow cytometric assay for measurement of platelet-derived microparticles. Thrombosis Research. 2010;125(3):110-16.
195. Weber HKM, Kyrle PA. Comparison of different methods for isolation and storage of microparticles from human blood. Journal of Thrombosis and Haemostasis. 2007;5(2):445.
196. Abstracts from the Third International Meeting of ISEV 2014 Rotterdam, The Netherlands, April 30th – May 3rd, 2014. Journal of Extracellular Vesicles. 2014;3:24214.
197. de Jong OG, Verhaar MC, Chen Y, Vader P, Gremmels H, Posthuma G, Schiffelers RM, Gucek M, van Balkom BW. Cellular stress conditions are reflected in the protein and RNA content of endothelial cell-derived exosomes. Journal of Extracellular Vesicles. 2012.
198. Camussi G, Deregibus MC. Extracellular vesicle-mediated epigenetic reprogamming of cells. Extracellular vesicles in health and disease. Singapore; 2014.
199. Jimenez JJ, Jy W, Mauro LM, Soderland C, Horstman LL, Ahn YS. Endothelial cells release phenotypically and quantitatively distinct microparticles in activation and apoptosis. Thrombosis Research. 2003;109(4):175-80.
200. Terrisse AD, Puech N, Allart S, Gourdy P, Xuereb JM, Payrastre B, Sié P. Internalization of microparticles by endothelial cells promotes platelet/endothelial cell interaction under flow. Journal of Thrombosis and Haemostasis. 2010;8(12):2810-9.
201. Diehl P, Fricke A, Sander L, Stamm J, Bassler N, Htun N, Ziemann M, Helbing T, El-Osta A, Jowett JB, Peter K. Microparticles: major transport vehicles for distinct microRNAs in circulation. Cardiovascular Research. 2012;93(4):633-44.
202. Hergenreider E, Heydt S, Tréguer K, Boettger T, Horrevoets AJ, Zeiher AM, Scheffer MP, Frangakis AS, Yin X, Mayr M, Braun T, Urbich C, Boon RA, Dimmeler S.

Atheroprotective communication between endothelial cells and smooth muscle cells through miRNAs. Nature Cell Biology. 2012;14(3):249-56.
203. Burger D, Montezano AC, Nishigaki N, He Y, Carter A, Touyz RM. Endothelial microparticle formation by angiotensin II is mediated via Ang II receptor type I/NADPH oxidase/ rho kinase pathways targeted to lipid rafts. Arteriosclerosis, Thrombosis, and Vascular Biology. 2011;31(8):1898-907.
204. Distler JHW, Huber LC, Hueber AJ, Reich CF 3rd, Gay S, Distler O, Pisetsky DS. The release of microparticles by apoptotic cells and their effects on macrophages. Apoptosis. 2005;10(4):731-41.
205. Willekens FLA, Werre JM, Kruijt JK, Roerdinkholder-Stoelwinder B, Groenen-Döpp YA, van den Bos AG, Bosman GJ, van Berkel TJ. Liver kupffer cells rapidly remove red blood cell–derived vesicles from the circulation by scavenger receptors. Blood. 2005;105(5):2141-5.
206. Faille D, El-Assaad F, Mitchell AJ, Alessi MC, Chimini G, Fusai T, Grau GE, Combes V. Endocytosis and intracellular processing of platelet microparticles by brain endothelial cells. Journal of Cellular and Molecular Medicine. 2012;16(8):1731-8.
207. Dasgupta SK, Le A, Chavakis T, Rumbaut RE, Thiagarajan P. Developmental endothelial locus-1 (Del-1) mediates clearance of platelet microparticles by the endothelium. Circulation. 2012;125(13):1664-72.
208. Mesri M, Altieri DC. Endothelial cell activation by leukocyte microparticles. The Journal of Immunology. 1998;161(8):4382-7.
209. Nomura S, Tandon NN, Nakamura T, Cone J, Fukuhara S, Kambayashi J. High-shear-stress-induced activation of platelets and microparticles enhances expression of cell adhesion molecules in THP-1 and endothelial cells. Atherosclerosis. 2001;158(2):277-87.
210. Distler JHW, Pisetsky DS, Huber LC, Kalden JR, Gay S, Distler O. Microparticles as regulators of inflammation: Novel players of cellular crosstalk in the rheumatic diseases. Arthritis & Rheumatism. 2005;52(11):3337-48.
211. Barry OP, Praticò D, Savani RC, FitzGerald GA. Modulation of monocyte-endothelial cell interactions by platelet microparticles. Journal of Clinical Investigation. 1998;102(1):136-44.
212. Forlow SB, McEver RP, Nollert MU. Leukocyte-leukocyte interactions mediated by platelet microparticles under flow. Blood. 2000;95(4):1317-23.
213. Barry OP, FitzGerald GA. Mechanisms of cellular activation by platelet microparticles. Journal of Thrombosis and Haemostasis. 1999;82(2):794-800.
214. Fourcade O, Simon MF, Viodé C, Rugani N, Leballe F, Ragab A, Fournié B, Sarda L, Chap H. Secretory phospholipase A2 generates the novel lipid mediator lysophosphatidic acid in membrane microvesicles shed from activated cells. Cell. 1995;80(6):919-27.
215. Abid Hussein MN, Böing AN, Biró E, Hoek FJ, Vogel GM, Meuleman DG, Sturk A, Nieuwland R. Phospholipid composition of in vitro endothelial microparticles and their in vivo thrombogenic properties. Thrombosis Research. 2008;121(6):865-71.
216. Sabatier F, Roux V, Anfosso F, Camoin L, Sampol J, Dignat-George F. Interaction of endothelial microparticles with monocytic cells in vitro induces tissue factor–dependent procoagulant activity. Blood. 2002;99(11):3962-70.
217. Curtis AM, Wilkinson PF, Gui M, Gales TL, Hu E, Edelberg JM. p38 mitogen-activated protein kinase targets the production of proinflammatory endothelial microparticles. Journal of Thrombosis and Haemostasis. 2009;7(4):701-9.
218. Gasser O, Schifferli JA. Activated polymorphonuclear neutrophils disseminate anti-inflammatory microparticles by ectocytosis. Blood. 2004;104(8):2543-8.
219. Brodsky SV, Zhang F, Nasjletti A, Goligorsky MS. Endothelium-derived microparticles impair endothelial function in vitro. American Journal of Physilogy. 2004;286(5):1910-15.
220. Agouni A, Lagrue-Lak-Hal AH, Ducluzeau PH, Mostefai HA, Draunet-Busson C, Leftheriotis G, Heymes C, Martinez MC, Andriantsitohaina R. Endothelial dysfunction caused by circulating microparticles from patients with metabolic syndrome. The American Journal of Pathology. 2008;173(4):1210-9.

221. Agouni A, Mostefai HA, Porro C, Carusio N, Favre J, Richard V, Henrion D, Martínez MC, Andriantsitohaina R. Sonic hedgehog carried by microparticles corrects endothelial injury through nitric oxide release. The Federation of American Societies for Experimental Biology Journal. 2007;21(11):2735-41.
222. Benameur T, Soleti R, Porro C, Andriantsitohaina R, Martínez MC. Microparticles carrying sonic hedgehog favor neovascularization through the activation of nitric oxide pathway in mice. PLoS ONE. 2010;5(9):e12688.
223. Mostefai HA, A Agouni A, Carusio N, Mastronardi ML, Heymes C, Henrion D, Andriantsitohaina R, Martinez MC. Phosphatidylinositol 3-kinase and xanthine oxidase regulate nitric oxide and reactive oxygen species productions by apoptotic lymphocyte microparticles in endothelial cells. The Journal of Immunology. 2008;180(7):5028-35.
224. Headland SE, Jones HR, D'Sa ASV, Perretti M, Norling LV. Cutting-edge analysis of extracellular microparticles using imagestreamx imaging flow cytometry. Sci Rep. 2014;4.
225. Shah D MBL, Angela. Dong, Jing-Feir. López A, José. Flow cytometric measurement of microparticles: Pitfalls and protocol modifications. Platelets. 2008;30(5):365-72.
226. Amin C, Mackman N, Key NS. Microparticles and cancer. Pathophysiology of Haemostasis and Thrombosis. 2008;36(3-4):177-83.
227. Minagar A, Jy W, Jimenez JJ, Sheremata WA, Mauro LM, Mao WW, Horstman LL, Ahn YS. Elevated plasma endothelial microparticles in multiple sclerosis. Neurology. 2001;56(10):1319-24.
228. Geisbert TW, Young HA, Jahrling PB, Davis KJ, Kagan E, Hensley LE. Mechanisms underlying coagulation abnormalities in ebola hemorrhagic fever: overexpression of tissue factor in primate monocytes/macrophages is a key event. Journal of Infectious Diseases. 2003;188(11):1618-29.
229. Mayne E, Funderburg NT, Sieg SF, Asaad R, Kalinowska M, Rodriguez B, Schmaier AH, Stevens W, Lederman MM. Increased platelet and microparticle activation in HIV infection: upregulation of P-selectin and tissue factor expression. Journal of Acquired Immune Deficiency Syndromes. 2012;59(4):340-6.
230. Delabranche X, Berger A, Boisramé-Helms J, Meziani F. Microparticles and infectious diseases. Médecine et Maladies Infectieuses. 2012;42(8):335-43.
231. Combes V, Coltel N, Alibert M, van Eck M, Raymond C, Juhan-Vague I, Grau GE, Chimini G. ABCA1 Gene Deletion Protects against Cerebral Malaria: Potential pathogenic role of microparticles in neuropathology. The American Journal of Pathology. 2005;166(1):295-302.
232. Mallat Z, Hugel B, Ohan J, Lesèche G, Freyssinet J-M, Tedgui A. Shed membrane microparticles with procoagulant potential in human atherosclerotic plaques: A role for apoptosis in plaque thrombogenicity. Circulation. 1999;99(3):348-53.
233. Mallat Z, Benamer H, Hugel B, Benessiano J, Steg PG, Freyssinet JM, Tedgui A. Elevated levels of shed membrane microparticles with procoagulant potential in the peripheral circulating blood of patients with acute coronary syndromes. Circulation. 2000;101(8):841-3.
234. Koga H SS, Kugiyama K. Elevated levels of ve-cadherin-positive endothelial microparticles in patients with type 2 diabetes mellitus and coronary artery disease. Journal of the American College of Cardiology. 2005;45(10):1622-30.
235. Preston RA, Jy W, Jimenez JJ, Mauro LM, Horstman LL, Valle M, Aime G, Ahn YS. Effects of severe hypertension on endothelial and platelet microparticles. Hypertension. 2003;41(2):211-7.
236. Bernard S, Loffroy R, Sérusclat A, Boussel L, Bonnefoy E, Thévenon C, Rabilloud M, Revel D, Moulin P, Douek P. Increased levels of endothelial microparticles CD144 (VE-Cadherin) positives in type 2 diabetic patients with coronary noncalcified plaques evaluated by multidetector computed tomography (MDCT). Atherosclerosis. 2009;203(2):429-35.

237. Sabatier F, Darmon P, Hugel B, Combes V, Sanmarco M, Velut JG, Arnoux D, Charpiot P, Freyssinet JM, Oliver C, Sampol J, Dignat-George F. Type 1 And Type 2 diabetic patients display different patterns of cellular microparticles. Diabetes. 2002;51(9):2840-5.
238. Wang JM, Su C, Wang Y, Huang YJ, Yang Z, Chen L, Wu F, Xu SY, Tao J.. Elevated circulating endothelial microparticles and brachial-ankle pulse wave velocity in well-controlled hypertensive patients. Journal of Human Hypertension. 2008;23(5):307-15.
239. Boulanger CM. Microparticles, vascular function and hypertension. Current Opinion in Nephrology and Hypertension. 2010;19(2):177-80.
240. Puddu P, Puddu GM, Cravero E, Muscari S, Muscari A. The involvement of circulating microparticles in inflammation, coagulation and cardiovascular diseases. The Canadian Journal of Cardiology. 2010;26(4):e140-e5.
241. Amabile N, H Heiss C, Chang V, Angeli FS, Damon L, Rame EJ, McGlothlin D, Grossman W, De Marco T, Yeghiazarians Y. Increased CD62e+ endothelial microparticle levels predict poor outcome in pulmonary hypertension patients. The Journal of Heart and Lung Transplantation. 2009;28(10):1081-6.
242. Choudhury A, Chung I, Blann AD, Lip GYH. Elevated platelet microparticle levels in nonvalvular atrial fibrillation: Relationship to p-selectin and antithrombotic therapy. Chest. 2007;131(3):809-15.
243. Biasucci L. Study of Effects of Ticagrelor on Microparticles and Micro-RNA in NSTE-ACS (TIGER-M) 2014. Available from: https://clinicaltrials.gov/show/NCT02071966.
244. Horn P, Cortese-Krott MM, Amabile N, Hundsdörfer C, Kröncke KD, Kelm M, Heiss C. Circulating microparticles carry a functional endothelial nitric oxide synthase that is decreased in patients with endothelial dysfunction. Journal of the American Heart Association. 2013;2(1).
245. Amabile N, Guérin AP, Leroyer A, Mallat Z, Nguyen C, Boddaert J, London GM, Tedgui A, Boulanger CM. Circulating endothelial microparticles are associated with vascular dysfunction in patients with end-stage renal failure. Journal of the American Society of Nephrology. 2005;16(11):3381-8.
246. Werner N, Wassmann S, Ahlers P, Kosiol S, Nickenig G. Circulating CD31+/Annexin V+ apoptotic microparticles correlate with coronary endothelial function in patients with coronary artery disease. Arteriosclerosis, Thrombosis, and Vascular Biology. 2006;26(1):112-6.
247. El Btaouri H, Morjani H, Greffe Y, Charpentier E, Martiny L. Role of JNK/ATF-2 pathway in inhibition of thrombospondin-1 (TSP-1) expression and apoptosis mediated by doxorubicin and camptothecin in FTC-133 cells. Biochim Biophys Acta. 2011;1813(5):695-703.
248. Van Der Pol E, Van Gemert MJC, Sturk A, Nieuwland R, Van Leeuwen TG. Single vs. swarm detection of microparticles and exosomes by flow cytometry. Journal of Thrombosis and Haemostasis. 2012;10(5):919-30.
249. Ekaterini KK, TziomalosI, Efstathios K, Eleni PA, Dimitrios KP. Flow cytometric measurement of microparticles: Pitfalls and protocol modifications. Gynecological Endocrinology. 2013;9(3):250-3.
250. Nozaki T, Sugiyama S, Sugamura K, Ohba K, Matsuzawa Y, Konishi M, Matsubara J, Akiyama E, Sumida H, Matsui K, Jinnouchi H, Ogawa H. Prognostic value of endothelial microparticles in patients with heart failure. European Journal of Heart Failure. 2010;12(11):1223-8.
251. Berezin AAK, Samura TA, Martovitskaya YV. Predictive value of circulating apoptotic microparticles in patients with ischemic symptomatic moderate-to-severe chronic heart failure. Angiology. 2014;2(121).
252. Watson S, Blundell HL, Evans WD, Griffiths H, Newcombe RG, Rees DA. Can abdominal bioelectrical impedance refine the determination of visceral fat from waist circumference? Physiological Measurement. 2009;30(7):53-58.
253. Dada J, Pinder AG, Lang D, James PE. Oxygen mediates vascular smooth muscle relaxation in hypoxia. PLoS ONE. 2013;8(2).

254. Nourooz-Zadeh J, Tajaddini-Sarmadi J, McCarthy S, Betteridge DJ, Wolff SP. Elevated levels of authentic plasma hydroperoxides in NIDDM. Diabetes. 1995;44(9):1054-8.
255. Prior RL, Hoang H, Gu L, Wu X, Bacchiocca M, Howard L, Hampsch-Woodill M, Huang D, Ou B, Jacob R. Assays for hydrophilic and lipophilic antioxidant capacity (oxygen radical absorbance capacity (ORACFL)) of plasma and other biological and food samples. Journal of Agricultural and Food Chemistry. 2003;51(11):3273-9.
256. Bob Carr MW. Nanoparticle tracking analysis: A review of applications and usage 2011-2012. Wiltshire: 2011.
257. van der Pol EvLTNR. An overview of novel and conventional methods to detect extracellular vesicles. Extracellular vesicles in health and disease. Signapore: 2014.
258. Garaiova I, Guschina I, Plummer S, Tang J, Wang D, Plummer N. A randomised cross-over trial in healthy adults indicating improved absorption of omega-3 fatty acids by pre-emulsification. Nutrition Journal. 2007;6(1):4.
259. Garbus J, De Luca HF, Loomans ME, Strong FM. The rapid incorporation of phosphate into mitochondrial lipids. Journal of Biological Chemistry. 1963;238:59-63.
260. Isa SA, Ruffino JS, Ahluwalia M, Thomas AW, Morris K, Webb R. M2 macrophages exhibit higher sensitivity to oxLDL-induced lipotoxicity than other monocyte/macrophage subtypes. Lipids in Health and Disease. 2011;10:229.
261. Richardson K. Analysis of cell surface markers within immature bovine articular cartilage. Cardiff: Cardiff Univerisuty; 2011.
262. Collins PW, Macchiavello LI, Lewis SJ, Macartney NJ, Saayman AG, Luddington R, Baglin T, Findlay GP. Global tests of haemostasis in critically ill patients with severe sepsis syndrome compared to controls. British Journal of Haematology. 2006;135(2):220-7.
263. Ehrmann D, Sturis J, Byrne M, Rosenfield R, Polonsky K. Insulin secretory defects in polycystic ovary syndrome. Relationship to insulin sensitivity and family history of non-insulin dependent diabetes mellitus. Journal of Clinical Investigation. 1995;96:520–7.
264. Talbott EO, Guzick DS, Sutton-Tyrrell K, McHugh-Pemu KP, Zborowski JV, Remsberg KE, Kuller LH. Evidence for association between polycystic ovary syndrome and premature carotid atherosclerosis in middle-aged women. Arteriosclerosis, Thrombosis, and Vascular Biology. 2000;20(11):2414-21.
265. Sprung VS, Atkinson G, Cuthbertson DJ, Pugh CJA, Aziz N, Green DJ, Cable NT, Jones H. Endothelial function measured using flow-mediated dilation in polycystic ovary syndrome: a meta-analysis of the observational studies. Clinical Endocrinology. 2013;78(3):438-46.
266. Karadeniz M, Erdoğan M, Ayhan Z, Yalcin M, Olukman M, Cetinkalp S. Effect of G2706A and G1051A polymorphisms of the ABCA1 gene on the lipid, oxidative stress and homocystein levels in Turkish patients with polycystic ovary syndrome. Lipids in Health and Disease. 2011;10:193.
267. Türkçüoğlu I, Engin-Üstün Y, Turan F, Kali Z, Bay Karabulut A, Meydanli M, Kafkasli A. Evaluation of asymmetric dimethylarginine, nitric oxide levels and associated independent variables in obese and lean patients with polycystic ovarian syndrome. Gynecological Endocrinology. 2011;27(9):609-14.
268. Erdogan M, Karadeniz M, Berdeli A, Alper G, Caglayan O, Yilmaz C. The relationship of the interleukin-6 174G>C gene polymorphism with oxidative stress markers in Turkish polycystic ovary syndrome patients. Journal of Endocrinology Investigations. 2008;31:624-29.
269. Anderson RA, Evans ML, Ellis GR, Graham J, Morris K, Jackson SK, Lewis MJ, Rees A, Frenneaux MP. The relationships between post-prandial lipaemia, endothelial function and oxidative stress in healthy individuals and patients with type 2 diabetes. Atherosclerosis. 2001;154(2):475-83.
270. Lauer T, Preik M, Rassaf T, Strauer BE, Deussen A, Feelisch M, Kelm M. Plasma nitrite rather than nitrate reflects regional endothelial nitric oxide synthase activity but lacks intrinsic vasodilator action. Proceedings of the National Academy of Sciences of the United States of America. 2001;98(22):12814-9.

271. Bryan NS. Nitrite in nitric oxide biology: Cause or consequence?: A systems-based review. Free Radical Biology and Medicine. 2006;41(5):691-701.
272. Blair SA, Kyaw-Tun T, Young IS, Phelan NA, Gibney J, McEneny J. Oxidative stress and inflammation in lean and obese subjects with polycystic ovary syndrome. Journal of Reproductive Medicine. 2013;58(3-4):107-14.
273. Glintborg D, Højlund K, Andersen M, Henriksen JE, Beck-Nielsen H, Handberg A. Soluble cd36 and risk markers of insulin resistance and atherosclerosis are elevated in polycystic ovary syndrome and significantly reduced during pioglitazone treatment. Diabetes Care. 2008;31(2):328-34.
274. Demirel F, Bideci A, Cinaz P, Camurdan MO, Biberoğlu G, Yesilkaya E, Hasanoğlu A. Serum leptin, oxidized low density lipoprotein and plasma asymmetric dimethylarginine levels and their relationship with dyslipidaemia in adolescent girls with polycystic ovary syndrome. Clinical Endocrinology. 2007;67(1):129-34.
275. Carmina E, Longo MCCRA, Rini GB, Lobo RA. Phenotypic variation in hyperandrogenic women influences the findings of abnormal metabolic and cardiovascular risk parameters. Journal of Clinical Endocrinology & Metabolism. 2005;90(5):2545-9.
276. El-Kannishy G, Kamal S, Mousa A, Saleh O, Badrawy AE, Farahaty RE, Shokeir T. Endothelial function in young women with polycystic ovary syndrome (PCOS): Implications of body mass index (BMI) and insulin resistance. Obesity Research; Clinical Practice. 2010;4(1):49-56.
277. Gündüz Z, Dursun İ, Tülpar S, Baştuğ F, Baykan A, Yıkılmaz A, Patıroğlu T, Poyrazoglu HM, Akın L, Yel S, Düşünsel R. Increased endothelial microparticles in obese and overweight children. Journal of Pediatric Endocrinology and Metabolism. 2012;25(11-12):1111-7.
278. Kim HK, Song KS, Park YS, Kang YH, Lee YJ, Lee KR, Kim HK, Ryu KW, Bae JM, Kim S. Elevated levels of circulating platelet microparticles, VEGF, IL-6 and RANTES in patients with gastric cancer: possible role of a metastasis predictor. European Journal of Cancer. 2003;39(2):184-91.
279. Koga H, Sugiyama S, Kugiyama K, Watanabe K, Fukushima H, Tanaka T, Sakamoto T, Yoshimura M, Jinnouchi H, Ogawa H. Elevated levels of ve-cadherin-positive endothelial microparticles in patients with type 2 diabetes mellitus and coronary artery disease. Journal of the American College of Cardiology. 2005;45(10):1622-30.
280. Mause SF, Weber C. Microparticles: Protagonists of a novel communication network for intercellular information exchange. Circulation Research. 2010;107(9):1047-57.
281. Barry OP, Kazanietz MG, Praticò D, FitzGerald GA. Arachidonic acid in platelet microparticles up-regulates cyclooxygenase-2-dependent prostaglandin formation via a protein kinase c/mitogen-activated protein kinase-dependent pathway. Journal of Biological Chemistry. 1999;274(11):7545-56.
282. Barry OP, Pratico D, Lawson JA, FitzGerald GA. Transcellular activation of platelets and endothelial cells by bioactive lipids in platelet microparticles. The Journal of Clinical Investigation. 1997;99(9):2118-27.
283. Koiou ET, Tziomalos K, Katsikis I, Papadakis E, Kandaraki EA, Panidis D. Platelet-derived microparticles in overweight/obese women with polycystic ovary syndrome. Gynecological Endocrinology. 2013;29(3):250-3.
284. Omoto S, Nomura S, Shouzu A, Hayakawa T, Shimizu H, Miyake Y, Yonemoto T, Nishikawa M, Fukuhara S, Inada M. Significance of Platelet-Derived Microparticles and Activated Platelets in Diabetic Nephropathy. Nephron. 1999;81(3):271-7.
285. Arteaga RB, Chirinos JA, Soriano AO, Jy W, Horstman L, Jimenez JJ, Mendez A, Ferreira A, de Marchena E, Ahn YS. Endothelial Microparticles and Platelet and Leukocyte Activation in Patients With the Metabolic Syndrome. The American Journal of Cardiology. 2006;98(1):70-4.
286. Augustine D, Ayers LV, Lima E, Newton L, Lewandowski AJ, Davis EF, Ferry B, Leeson P. Dynamic release and clearance of circulating microparticles during cardiac stress. Circulation Research. 2014;114(1):109-13.

287. Martínez-García MA, San-Millán JL, Escobar-Morreale HF. The R453Q and D151A polymorphisms of hexose-6-phosphate dehydrogenase gene (H6PD) influence the polycystic ovary syndrome (PCOS) and obesity. Gene. 2012;497(1):38-44.
288. Sang Q, Yao Z, Wang H, Feng R, Wang H, Zhao X, Xing Q, Jin L, He L, Wu L, Wang L. Identification of microRNAs in human follicular fluid: characterization of microRNAs that govern steroidogenesis in vitro and are associated with polycystic ovary syndrome in vivo. Journal of Clinical Endocrinology & Metabolism. 2013;98(7):3068-79.
289. Semenza GL. Hypoxia-inducible factor 1: oxygen homeostasis and disease pathophysiology. Trends in Molecular Medicine. 2001;7(8):345-50.
290. Lichtenauer M, Goebel B, Fritzenwanger M, Förster M, Betge S, Lauten A, Figulla HR, Jung C. Simulated temporary hypoxia triggers the release of CD31+/Annexin+ endothelial microparticles: A prospective pilot study in humans. Clinical Hemorheology and Microcirculation. 2014.
291. Vince RV, Chrismas B, Midgley AW, McNaughton LR, Madden LA. Hypoxia mediated release of endothelial microparticles and increased association of S100A12 with circulating neutrophils. Oxidative Medicine and Cellular Longevity. 2009;2(1):2-6.
292. Sandau US, Handa RJ. Glucocorticoids exacerbate hypoxia induced expression of the pro-apoptotic gene Bnip3 in the developing cortex. Neuroscience. 2007;144(2):482-94.
293. Zheng X, Zhou AX, Rouhi P, Uramoto H, Borén J, Cao Y, Pereira T, Akyürek LM, Poellinger L. Hypoxia-induced and calpain-dependent cleavage of filamin A regulates the hypoxic response. Proceedings of the National Academy of Sciences of the United States of America. 2014;111(7):2560-5.
294. Giorgio M, Trinei M, Migliaccio E, Pelicci PG. Hydrogen peroxide: a metabolic by-product or a common mediator of ageing signals? Nature Reviews Molecular Cell Biology. 2007;8(9):722-8.
295. Stone JR, Yang S. Hydrogen Peroxide: A signaling messenger. Antioxidants & Redox Signaling. 2006;8(3-4):243-70.
296. Pirro M, Schillaci G, Bagaglia F, Menecali C, Paltriccia R, Mannarino MR, Capanni M, Velardi A, Mannarino E. Microparticles derived from endothelial progenitor cells in patients at different cardiovascular risk. Atherosclerosis. 2008;197(2):757-67.
297. Jones BE, Lo CR, Liu H, Pradhan Z, Garcia L, Srinivasan A, Valentino KL, Czaja MJ. Role of caspases and NF-κB signaling in hydrogen peroxide- and superoxide-induced hepatocyte apoptosis. American Journal of Physiology. 2000;278(5):693-9.
298. Hu Q, Corda S, Zweier JL, Capogrossi MC, Ziegelstein RC. Hydrogen Peroxide Induces Intracellular calcium oscillations in human aortic endothelial cells. Circulation. 1998;97(3):268-75.
299. Hermann C, Assmus B, Urbich C, Zeiher AM, Dimmeler S. Insulin-mediated stimulation of protein kinase Akt: A Potent survival signaling cascade for endothelial cells. Arteriosclerosis, Thrombosis, and Vascular Biology. 2000;20(2):402-9.
300. Wang H, Wang AX, Barrett EJ. Insulin-induced endothelial cell cortical actin filament remodeling: a requirement for trans-endothelial insulin transport. Molecular Endocrinology. 2012;26(8):1327-38.
301. Wang J, AAlexanian A, Ying R, Kizhakekuttu TJ, Dharmashankar K, Vasquez-Vivar J, Gutterman DD, Widlansky ME. Acute exposure to low glucose rapidly induces endothelial dysfunction and mitochondrial oxidative stress: Role for AMP kinase. Arteriosclerosis, Thrombosis, and Vascular Biology. 2012;32(3):712-20.
302. Tamareille S, Mignen O, Capiod T, Rücker-Martin C, Feuvray D. High glucose-induced apoptosis through store-operated calcium entry and calcineurin in human umbilical vein endothelial cells. Cell Calcium. 2006;39(1):47-55.
303. Bishara NB, Ding H. Glucose enhances expression of TRPC1 and calcium entry in endothelial cells. American Journal of Physiology. 2010;298(1):171-8.
304. Hempel A, Maasch C, Heintze U, Lindschau C, Dietz R, Luft FC, Haller H. High Glucose Concentrations increase endothelial cell permeability via activation of protein kinase Cα. Circulation Research. 1997;81(3):363-71.

305. Kemeny SF, Figueroa DS, Clyne AM. Hypo- and Hyperglycemia impair endothelial cell actin alignment and nitric oxide synthase activation in response to shear stress. PLoS ONE. 2013;8(6):e66176.
306. Adams MR, Williams JK, Kaplan JR. Effects of androgens on coronary artery atherosclerosis and atherosclerosis-related impairment of vascular responsiveness. Arteriosclerosis, Thrombosis, and Vascular Biology. 1995;15(5):562-70.
307. Nheu L, Nazareth L, Xu GY, Xiao FY, Luo RZ, Komesaroff P, Ling S. Physiological effects of androgens on human vascular endothelial and smooth muscle cells in culture. Steroids. 2011;76(14):1590-6.
308. Closse C, Seigneur M, Renard M, Pruvost A, Dumain P, Belloc F, Boisseau MR. Influence of hypoxia and hypoxia-reoxygenation on endothelial p-selectin expression. Thrombosis Research. 1997;85(2):159-64.
309. Puente Navazo MD, Chettab K, Duhault J, Koenig-Berard E, McGregor JL. Glucose and insulin modulate the capacity of endothelial cells (huvec) to express p-selectin and bind a monocytic cell line (U937). Thrombosis and Haemostasis. 2001;86(8):680-5.
310. Gogitidze Joy N, Hedrington MS, Briscoe VJ, Tate DB, Ertl AC, Davis SN. Effects of acute hypoglycemia on inflammatory and pro-atherothrombotic biomarkers in individuals with type 1 diabetes and healthy individuals. Diabetes Care. 2010;33(7):1529-35.
311. Merten M, Pakala R, Thiagarajan P, Benedict CR. Platelet microparticles promote platelet interaction with sub-endothelial matrix in a glycoprotein IIB/IIIA–dependent mechanism. Circulation. 1999;99(19):2577-82.
312. Goldstein JL. The LDL receptor locus and the genetics of familial hypercholesterolemia. Annual Review of Genetics. 1979;13:259-89.
313. Goldstein JL, Brown MS. Familial hypercholesterolemia. in the metabolic and molecular bases of inherited disease. New York: 2001.
314. Cheng AY, Leiter LA.Implications of recent clinical trials for the national cholesterol education program adult treatment panel III guidelines. Circulation. 2004;110(2):227-39.
315. Orsoni A, V Villard EF, Bruckert E, Robillard P, Carrie A, Bonnefont-Rousselot D, Chapman MJ, Dallinga-Thie GM, Le Goff W, Guerin M. Impact of LDL apheresis on atheroprotective reverse cholesterol transport pathway in familial hypercholesterolemia. Journal of Lipid Research. 2012;53(4):767-75.
316. Stoffel W, Borberg H, Greve V. Application of specific extracorporeal removal of low density lipoprotein in familial hypercholesterolaemia. The Lancet. 1981;318(8254):1005-7.
317. Yokoyama S, Hayashi R, Kikkawa T, Tani N, Takada S, Hatanaka K, Yamamoto A. Specific sorbent of apolipoprotein B-containing lipoproteins for plasmapheresis. Characterization and experimental use in hypercholesterolemic rabbits. Arteriosclerosis, Thrombosis, and Vascular Biology. 1984;4(3):276-82.
318. Eisenhauer T, Armstrong VW, Wieland H, Fuchs C, Scheler F, Seidel D. Selective removal of low density lipoproteins (LDL) by precipitation at low pH: First clinical application of the HELP system. Klin Wochenschr. 1987;65(4):161-8.
319. Otto C, Kern P, Bambauer R, Kallert S, Schwandt P, Parhofer KG. Efficacy and safety of a new whole-blood low-density lipoprotein apheresis system (liposorber D) in severe hypercholesterolemia. Artificial Organs. 2003;27(12):1116-22.
320. Kroon AA, van't Hof MA, Demacker PNM, Stalenhoef AFH. The rebound of lipoproteins after LDL-apheresis. Kinetics and estimation of mean lipoprotein levels. Atherosclerosis. 2000;152(2):519-26.
321. Kroon AA, Aengevaeren WR, van der Werf T, Uijen GJ, Reiber JH, Bruschke AV, Stalenhoef AF. LDL-Apheresis Atherosclerosis Regression Study (LAARS): Effect of aggressive versus conventional lipid lowering treatment on coronary atherosclerosis. Circulation. 1996;93(10):1826-35.
322. Thompson GR, Miller JP, Breslow JL. Improved survival of patients with homozygous familial hypercholesterolaemia treated with plasma exchange. British Medical Journal. 1985;14(291):1671-3.

323. Gordon BR, Kelsey SF, Dau PC, Gotto AM Jr, Graham K, Illingworth DR, Isaacsohn J, Jones PH, Leitman SF, Saal SD, Stein EA, Stern TN, Troendle A, Zwiener RJ. Long-term effects of low-density lipoprotein apheresis using an automated dextran sulfate cellulose adsorption system. The American Journal of Cardiology. 1998;81(4):407-11.
324. Katopodis JN, Kolodny L, Jy W, Horstman LL, De Marchena EJ, Tao JG, Haynes DH, Ahn YS. Platelet microparticles and calcium homeostasis in acute coronary ischemias. American Journal of Hematology. 1997;54(2):95-101.
325. Nomura S, Komiyama Y, Kagawa H, Iwasaka T, Takahashi H, Fukuhara S. Microparticles and coronary artery disease. American Journal of Hematology. 1997;56(4):296.
326. Suades R, Padró T, Alonso R, López-Miranda J, Mata P, Badimon L. Circulating CD45+/CD3+ lymphocyte-derived microparticles map lipid-rich atherosclerotic plaques in familial hypercholesterolaemia patients. Thrombosis and Haemostasis. 2014;111(1):111-21.
327. Abdelhafeez AH, Jeziorczak PM, Schaid TR, Hoefs SL, Kaul S, Nanchal R, Jacobs ER, Densmore JC. Clinical CVVH model removes endothelium-derived microparticles from circulation. Journal of Extracellular Vesicles. 2014;3:10.
328. Umekita K, Hidaka T, Ueno S, Takajo I, Kai Y, Nagatomo Y, Sawaguchi A, Suganuma T, Okayama A. Leukocytapheresis (LCAP) decreases the level of platelet-derived microparticles (MPs) and increases the level of granulocytes-derived MPs: a possible connection with the effect of LCAP on rheumatoid arthritis. Modern Rheumatology. 2009;19(3):265-72.
329. Lee W, Datta B, Ong B, Rees A, Halcox J. Defining the role of lipoprotein apheresis in the management of familial hypercholesterolemia. Americam Journal of Cardiovascular Drugs. 2011;11(6):363-70.
330. Krauss RM, Burke DJ. Identification of multiple subclasses of plasma low density lipoproteins in normal humans. Journal of Lipid Research. 1982;23(1):97-104.
331. Christersson C, Johnell M, Siegbahn A. Evaluation of microparticles in whole blood by multicolour flow cytometry assay. Scandinavian Journal of Clinical & Laboratory Investigation. 2013;73(3):229-39.
332. Robert S, Poncelet P, Lacroix R, Arnaud L, Giraudo L, Hauchard A, Sampol J, Dignat-George F. Standardization of platelet-derived microparticle counting using calibrated beads and a Cytomics FC500 routine flow cytometer: a first step towards multicenter studies? Journal of Thrombosis and Haemostasis. 2009;7(1):190-7.
333. Ichijo M, Ishibashi S, Ohkubo T, Nomura S, Sanjo N, Yokota T, Mizusawa H. Elevated Platelet microparticle levels after acute ischemic stroke with concurrent idiopathic thrombocytopenic purpura. Journal of Stroke and Cerebrovascular Diseases. 2014;23(3):587-9.
334. Pereira J, Alfaro G, Goycoolea M, Quiroga T, Ocqueteau M, Massardo L, Pérez C, Sáez C, Panes O, Matus V, Mezzano D. Circulating platelet-derived microparticles in systemic lupus erythematosus. Association with increased thrombin generation and procoagulant state. Thrombosis and Haemostasis. 2006;95(1):94-9.
335. Namba M, Tanaka A, Shimada K, Ozeki Y, Uehata S, Sakamoto T, Nishida Y, Nomura S, Yoshikawa J. Circulating platelet-derived microparticles are associated with atherothrombotic events. Arteriosclerosis, Thrombosis, and Vascular Biology. 2007;27(1):255-6.
336. Tan KT, Tayebjee MH, Lim HS, Lip GYH. Clinically apparent atherosclerotic disease in diabetes is associated with an increase in platelet microparticle levels. Diabetic Medicine. 2005;22(12):1657-62.
337. Hansen S, Harris W. New evidence for the cardiovascular benefits of long chain omega-3 fatty acids. Current Atherosclerosis Reports. 2007;9(6):434-40.
338. De Pascale C, Avella M, Perona JS, Ruiz-Gutierrez V, Wheeler-Jones CPD, Botham KM. Fatty acid composition of chylomicron remnant-like particles influences their uptake and induction of lipid accumulation in macrophages. Federation of European Biochemical Societies Journal. 2006;273(24):5632-40.

339. Deng Z-B, Zhuang X, Ju S, Xiang X, Mu J, Liu Y, Jiang H, Zhang L, Mobley J, McClain C, Feng W, Grizzle W, Yan J, Miller D, Kronenberg M, Zhang HG. Exosome-like Nanoparticles from Intestinal Mucosal Cells Carry Prostaglandin E2 and Suppress Activation of Liver NKT Cells. The Journal of Immunology. 2013;190(7):3579-89.
340. Nielsen MH, Beck-Nielsen H, Andersen MN, Handberg A. A flow cytometric method for characterization of circulating cell-derived microparticles in plasma. Journal of Extracellular Vesicles. 2014;3:10.
341. Weiss R, Spittler A, Schmitz G, Fischer MB, Weber V. Thrombocyte adhesion and release of extracellular microvesicles correlate with surface morphology of adsorbent polymers for lipid apheresis. Biomacromolecules. 2014;15(7):2648-55.
342. Larson MC, Woodliff JE, Hillery CA, Kearl TJ, Zhao M. Phosphatidylethanolamine is externalized at the surface of microparticles. Biochimica et Biophysica Acta (BBA) - Molecular and Cell Biology of Lipids. 2012;1821(12):1501-7.
343. Al Kaabi A, Traupe T, Stutz M, Buchs N, Heller M. Cause or effect of arteriogenesis: Compositional alterations of microparticles from CAD patients undergoing external counterpulsation therapy. PLoS ONE. 2012;7(10).
344. Sinning J-M, Losch J, Walenta K, Böhm M, Nickenig G, Werner N. Circulating CD31+/Annexin V+ microparticles correlate with cardiovascular outcomes. European Heart Jounral. 2011;32(16):2034-41.
345. Desouza CV, Bolli GB, Fonseca V. Hypoglycemia, diabetes, and cardiovascular events. Diabetes Care. 2010;33(6):1389-94.
346. van der Pol E, Coumans FA, Grootemaat AE, Gardiner C, Sargent IL, Harrison P, Sturk A, van Leeuwen TG, Nieuwland R. Particle size distribution of exosomes and microvesicles determined by transmission electron microscopy, flow cytometry, nanoparticle tracking analysis, and resistive pulse sensing. Journal of Thrombosis and Haemostasis. 2014;12(7):1182-92.
347. Chandler WL, Yeung W, Tait JF. A new microparticle size calibration standard for use in measuring smaller microparticles using a new flow cytometer. Journal of Thrombosis and Haemostasis. 2011;9(6):1216-24.
348. Mullier F, Bailly N, Chatelain C, DognÉ JM, Chatelain B. More on: calibration for the measurement of microparticles: needs, interests, and limitations of calibrated polystyrene beads for flow cytometry-based quantification of biological microparticles. Journal of Thrombosis and Haemostasis. 2011;9(8):1679-81.
349. Robert S, Poncelet P, Lacroix R, Raoult D, Dignat-George F. More on: calibration for the measurement of microparticles: value of calibrated polystyrene beads for flow cytometry-based sizing of biological microparticles. Journal of Thrombosis and Haemostasis. 2011;9(8):1676-8.
350. Livaja Koshiar R, Somajo S, Norström E, Dahlbäck B. Erythrocyte-derived microparticles supporting activated protein c-mediated regulation of blood coagulation. PLoS ONE. 2014;9(8):e104200.